MicroRNAs in the pathogenesis of cardiovascular disease in type 2 diabetes

Inaugural-Dissertation

zur Erlangung des Doktorgrades
der Mathematisch-Naturwissenschaftlichen Fakultät
der Heinrich-Heine-Universität Düsseldorf

vorgelegt von

Marcel Blumensatt

aus Simmern

Düsseldorf, September 2013

aus dem Institut für Klinische Biochemie und Pathobiochemie
Deutsches Diabetes-Zentrum

Leibniz-Zentrum für Diabetes-Forschung
an der Heinrich-Heine-Universität Düsseldorf

Gedruckt mit der Genehmigung der
Mathematisch-Naturwissenschaftlichen Fakultät der
Heinrich-Heine-Universität Düsseldorf

Referent:	Prof. Dr. Hadi Al-Hasani
Korreferent:	Prof. Dr. Michael Feldbrügge

Tag der mündlichen Prüfung: 11.12.2013

Für meinen ungeborenen Sohn

Zusammenfassung

Die Prävalenz des Diabetes hat weltweit epidemische Ausmaße angenommen. Gemäß der internationalen Diabetes Föderation (IDF) waren bereits im Jahr 2012 mehr als 371 Millionen Menschen an einem Diabetes erkrankt, von denen geschätzte 90% an einem Typ 2 Diabetes (T2D) leiden. Während des Verlaufs eines Diabetes kommt es zu diversen Folgekomplikationen. Hierzu gehören Erkrankungen des kardiovaskulären Systems wie etwa die diabetische Kardiomyopathie, oder aber auch eine Erkrankung der Herzkranzgefäße, die allesamt zum frühen Tod von Patienten mit einem Diabetes führen können. Fundierte Beweise unterlegen mittlerweile einen signifikanten und negativen Zusammenhang zwischen einer zunehmenden Fettmasse während einer krankhaften Fettleibigkeit und der Erkrankung peripherer Gewebe wie das Herz oder die vaskulären Gefäße. Hierbei spielen Faktoren, die vom Fettgewebe sekretiert werden und allgemein als Adipokine bekannt sind, eine bedeutende Rolle sowohl für die Regulation der Insulinsensitivität, die Kontraktion von Kardiomyozyten als auch für die Homeostasis von glatten Muskelzellen. Obwohl die Vergrößerung eines herzspezifischen Fettdepots, das epikardiale Fettgewebe, als Risikofaktor für kardiovaskuläre Komplikationen bei Patienten mit einem Type 2 Diabetes gilt, wurde der kausale Zusammenhang von epikardialen Adipokinen und der Pathogenese von kardiovaskulären Erkrankungen bisher nur unzureichend untersucht. Aus diesem Grund soll innerhalb dieser Arbeit zunächst das Sekretionsprofil von epikardialem Fettgewebe eines Patienten mit T2D zu dem eines Patienten ohne Diabetes bzw. zu anderen Fettdepots wie dem subkutanen oder dem perikardialen Fettgewebe abgegrenzt werden. Damit einhergehend soll der Einfluss von alternierenden Adipokinen auf die Kontraktilität, Insulinsensitivität und auf die Expression von microRNAs (miRNAs) in adulten Kardiomyozyten untersucht werden. Darüber hinaus soll die Beobachtung, dass konditionierte Medien (CM) von humanen Adipozyten mit subkutanem Ursprung atherosklerotische Veränderungen in glatten Muskelzellen hervorruft, erweitert werden. Hierzu soll der Einfluss von CM auf den Insulinsignalweg in glatten Muskelzellen untersucht werden und eine adipokinbedingte Veränderung der Insulinwirkung hinsichtlich der Expression von miRNAs und deren potentiellen Zielproteine analysiert werden.

Zunächst wurde CM mittels der Explantat-Technologie aus humanen Fettbiopsien des epikardialen (EAT), perikardialen (PAT) oder des subkutanen Fettgewebes (SAT) von Patienten mit (T2D) bzw. ohne (ND) Typ 2 Diabetes gewonnen. Die Behandlung von primären adulten Kardiomyozyten der Ratte (ARC) mit dem entsprechenden CMs sollte

Aufschluss über die Auswirkung von sekretierten Faktoren des Fettgewebes auf Kontraktilität, Insulinsensitivität und auf die Expression von miRNAs geben. Es zeigte sich, dass mit CM-EAT-T2D behandelte Kardiomyozyten eine verringerte Sarkomerverkürzung, eine reduzierte Expression von Serca2a, die wiederum mit einem reduzierten cytosolischen Abtransport von Kalzium nach erfolgter Kontraktion einhergeht, sowie eine reduzierte Insulinsensitivität aufweisen. Des Weiteren beeinflusste CM-EAT-T2D selektiv die Expression von acht miRNAs in ARC inklusive der Steigerung der Expression von miR-143 und miR-145. Die darauf folgende Analyse des CMs ergab, dass die Proteine Activin A, Angiopoietin-2 und CD14 in höheren Mengen von EAT-T2D im Vergleich zu anderen Depots oder zu Patienten, die nicht an einem Diabetes erkrankt waren, sekretiert werden. Durch die Verwendung eines Neutralisierungsantikörpers gegen Activin A konnte die nachteilige Wirkung von CM-EAT-T2D auf die Kontraktilität und die Insulinwirkung teilweise aufgehoben und die CM induzierte Expression von miR-143/145 vollständig geblockt werden. Im Anschluss führten funktionelle Untersuchungen zu der Erkenntnis, dass miR-143, jedoch nicht miR-145, zu einer verminderten Insulinsensitivität gefolgt von einer reduzierten Insulin stimulierten Aufnahme von Glucose in Kardiomyozyten führt. Diese Effekte konnten einer miR-143 vermittelten reduzierten Expression des Proteins „oxysterol binding protein-like 8“ (ORP8) zugeordnet werden. Mehr noch führte die Inkubation von humanen vaskulären glatten Muskelzellen (hVSMC) mit CMs von humanen Adipozyten ebenfalls zu einer erhöhten Expression von miR-143/145 und zu einer verminderten Insulin vermittelten Phosphorylierung der Proteinkinase B (Akt). Es zeigte sich, dass die verwendeten CMs die Aktivität der Signalmoleküle p38 und SMAD2 erhöht, die beide wiederum mit einer gesteigerten Expression von miR-143/145 in hVSMC assoziiert sind. Vergleichbar zu Kardiomyozyten, führte miR-143 in hVSMC ebenfalls zu einer verminderten Insulinsensitivität durch eine verringerte Expression von ORP8.

Zusammenfassend konnte in der vorliegenden Arbeit gezeigt werden, dass das epikardiale Fettgewebe von Patienten mit einem Typ 2 Diabetes durch die erhöhte Sekretion von Activin A und anderen Faktoren zu der Entstehung einer diabetischen Kardiomyopathie beitragen kann. Dies bewerkstelligt Activin A durch die Induzierung von miR-143, die wiederum für die Entstehung einer Insulinresistenz in Kardiomyozyten verantwortlich ist. Darüber hinaus konnte festgestellt werden, dass Adipokine von subkutanem Fettgewebe ebenfalls die Insulinsensitivität von hVSMC verringert indem sie die Expression von miR-143 steigert.

Summary

Diabetes is becoming a worldwide health problem more and more. According to the International Diabetes Federation (IDF), more than 371 million people have diabetes in 2012 of whom about 90% suffer from type 2 diabetes (T2D). In patients with T2D, diabetic cardiomyopathy, atherosclerosis, and coronary artery disease are common complications and a major cause of mortality. Profound evidence identified a negative crosstalk between increased adipose tissue mass in T2D and cardiovascular dysfunction. Accordingly, adipose tissue-derived factors have been associated with these cardiovascular complications by affecting insulin sensitivity and contractile function in cardiomyocytes and altering the homeostasis of smooth muscle cells. Although the expansion of a heart specific fat depot, the epicardial adipose tissue (EAT), has been identified as a risk factor for T2D, coronary artery disease and the metabolic syndrome, the contribution of EAT-derived factors to the pathogenesis of cardiac complications during T2D has not been investigated in detail. Therefore, this study was aimed to assess whether alterations in the secretory profile of EAT in patients with T2D affect contractile function and insulin action in cardiomyocytes and whether the detrimental effects of EAT-T2D-derived factors can be ascribed to alterations in microRNA (miRNA) expression. We also wanted to extend the observation that conditioned media (CM) generated from primary human subcutaneous adipocytes induce atherosclerotic changes in human vascular smooth muscle cells (hVSMC) by analysing the CM-induced effects on insulin action and whether this impairment can be ascribed to miRNA expression and their potential target genes.

Contractile function, insulin action and miRNA expression have been analysed in primary adult rat cardiomyocytes incubated with CM generated from explants of EAT biopsies obtained from patients without (ND) and with T2D. CM from subcutaneous (SAT) and pericardial adipose tissue (PAT) biopsies from the same patients served as control. Cardiomyocytes treated with CM-EAT-T2D showed reductions in sarcomere shortening, cytosolic Ca^{2+}-fluxes, expression of sarcoplasmic endoplasmic reticulum ATPase 2a (Serca2a), and decreased insulin-mediated Akt-phosphorylation as compared to CM from the other groups. Profiling miRNA expression in ARC incubated with CM-EAT-T2D identified alterations in the expression of eight miRNA species, including up-regulation of miR-143 and miR-145. Analysis of the CM revealed that activin A, angiopoietin-2 and CD14 were selectively accumulated in CM-EAT-T2D versus CM-EAT-ND and CM from the other fat depots. Accordingly, activin A neutralizing antibodies partially abolished the detrimental

effects of CM-EAT-T2D and completely prevented the CM-induced expression of the miR-143/145 cluster. Subsequently, overexpression of the miR-143/145 cluster revealed that miR-143, but not miR-145, blunted the insulin-mediated phosphorylation of Akt and reduced insulin-stimulated glucose uptake. In addition, the inhibition of miR-143 by locked nucleic acid (LNA)-anti-miR-143 restored the insulin stimulated Akt phosphorylation in ARC treated with CM-EAT-T2D. The CM-induced effects on insulin signaling were ascribed to down-regulation of the miR-143 target and regulator of insulin action, oxysterol binding protein-like 8 (ORP8).

Moreover, exposure of primary hVSMC to CM from human adipocytes increased the expression of the miR-143/145 cluster as well, but markedly impaired the insulin-mediated phosphorylation of Akt. Furthermore, CM promoted the phosphorylation of SMAD2 and p38, which have both been linked to the induction of miR-143/145 in hVSMC. Consistently, the up-regulation of miR-143/145 as well as the inhibition of insulin-mediated Akt-phosphorylation by CM was partially prevented in hVSMC pre-treated with an inhibitor either of SMAD-phosphorylation or for p38-activity. Similar to ARC, miR-143 blunted the insulin-mediated phosphorylation of Akt, and its substrate eNOS in hVSMC due to decreased expression of ORP8.

In conclusion, the present work demonstrates that secreted factors from adipose tissue or adipocytes severely impact the physiology of cardiomyocytes and smooth muscle cells. Specifically, epicardial adipokines induce contractile dysfunction, diminish insulin signaling, and alter the expression of miRNAs in cardiomyocytes. Particularly, contractile dysfunction, reduced sensitivity to insulin and expression of miR-143 and miR-145 in cardiomyocytes could be linked to a higher abundance of activin A in CM-EAT-T2D compared to CM generated from other fat depots from the same patients or from patients without diabetes. Moreover, adipocyte-derived CM has the ability to induce the expression of miR-143/145 in smooth muscle cells. In both cell types, cardiomyocytes and smooth muscle cells, a disturbed insulin action could be associated to higher levels of miR-143. Collectively, these findings provide important new insights how adipose tissue contributes to the pathophysiology of cardiovascular complications in diabetes.

Table of Contents

List of Figures

List of Tables

List of Abbreviations

AGO	argonaute
ALK	activin receptor-like kinase
AM	control adipocyte medium
ang2	angiopoietin-2
ARC	primary adult rat cardiomyocytes
ATP	adenosine triphosphate
BMI	body mass index
BMP	bone morphogenetic protein
CAD	coronary artery disease
CM	conditioned media
DCM	diabetic cardiomyopathy
EAT	epicardial adipose tissue
eNOS	endothelial NO-synthetase
ER	endoplasmic reticulum
GLUT4	glucose transporter 4
GSK3	glycogen synthase kinase-3
HDL	high density lipoprotein
hVSMC	human vascular smooth muscle cells
ICAM-1	intercellular adhesion molecule 1
IDF	International Diabetes Federation
IL-6	interleukin-6
IR	insulin receptor
IRS	insulin receptor substrate
LDL	low density lipoprotein
LNA	locked nucleic acid
LPS	lipopolysaccharides
LV	lentivirus
LVH	left ventricular hypertrophy
MAPK	mitogen-activated protein kinase
MCP-1	monocyte chemotactic protein
MCS	membrane contact sites
MED13	mediator complex subunit 13

miRNA	microRNA
MLC	myosin light chain
MOI	multiplicity of infection
mRNA	messenger RNA
Myh6	α-cardiac muscle myosin heavy chain gene
Myh7	β-cardiac muscle myosin heavy chain gene
ND	patients without diabetes
NO	nitric oxide
ORD	OSBP-related ligand binding domain
ORP8	oxysterol binding protein-like 8
OSBP	oxysterol binding protein
PAT	pericardial adipose tissue
PDK1	phosphoinositol dependent kinase
PH	pleckstrin homolog
PI3K	phosphatidylinositol 3-kinase
PIP3	phosphatidylinositol 3,4,5-trisphosphate
pre-miRNA	precursor-miRNA
pri-miRNA	primary-miRNA
PTB	phosphotyrosine-binding domain
PTP1B	phospho tyrosine phosphatase 1B
PVAT	perivascular adipose tissue
qRT-PCR	quantitative real-time PCR
RASMC	rat arterial smooth muscle cells
RISC	RNA-induced-silencing-complex
ROS	reactive oxygen species
SAT	subcutaneous adipose tissue
sCD14	soluble cluster of differentiation 14
Serca2a	sarcoplasmic endoplasmic reticulum ATPase 2a
SHC	Src homology 2 domain containing transforming protein
SIRT1	Sirtuin 1
SMC	smooth muscle cell
SNARE	soluble NSF attachment protein receptor
SR	sarcoplasmic reticulum
SRF	serum response factor

T1D	type 1 diabetes
T2D	type 2 diabetes
TBC1D1	Tre-2/USP6, BUB2, cdc16domain family member 1
TGF-β	transforming growth factor-β
TNF-α	tumor necrosis factor alpha
TβR-1	TGF-β type 1 receptor
TβR-2	TGF-β type 2 receptor
UTR	untranslated region
VCAM-1	vascular-cell adhesion molecule 1
WHR	waist-to-hip ratio
α-MHC	α-cardiac muscle myosin heavy chain
β-MHC	β-cardiac muscle myosin heavy chain

Chapter 1

General Introduction

1. General Introduction

1.1. Type 2 diabetes

1.1.1. Pathophysiology of type 2 diabetes

Diabetes mellitus describes a heterogeneous group of metabolic disorders. The expression "diabetes" originates from the ancient Greek and literally stands for "pass through" and the term "mellitus" comes from the Latin language and means "honey sweet".[1] Both terms implicate, that together with obvious symptoms, diabetes already has been recognized and illustrated in the ancient world. All diabetic patients have polyuria and in the early medicine diabetes mellitus was diagnosed through the taste of the urine which tasted "honey sweet". Nowadays we know that the sweet taste results from high glucose level within the blood or urine, respectively. The American Diabetes Association defines diabetes as a group of metabolic diseases characterized by hyperglycaemia caused by defects in insulin secretion, insulin action, or both.[2] Depending on the aetiology, diabetes can be divided into the subgroups type 1, type 2, gestational diabetes and others.[2]

The gestational diabetes occurs during pregnancy due to unknown reasons with a prevalence of up to 12% of all pregnancies.[3] However, the most prominent subgroups are type 1 (T1D) and type 2 diabetes (T2D). Previously, T1D, accounting for 5-10% of all diabetes cases today, was also referred to as insulin-dependent, juvenile-onset or immune-mediated diabetes due to the immune mediated destruction of insulin-producing pancreatic β-cells mostly at an early age.[4, 5] Since the β-cells are attacked and destroyed by autoreactive T-lymphocytes, autoantibody producing B lymphocytes and by activation of the innate immune system, T1D-patients have a lack of insulin and are therefore they depend on a life-long insulin treatment.[6-8] Although the pathophysiology of T1D has been investigated intensively for many years, the precise immunologic, genetic and physiologic events promoting disease progression are not fully understood. Some studies highlight that environmental factors modulate the onset of T1D in genetically susceptible individuals.[4, 9] In contrast to T1D or gestational diabetes, T2D is by far the most prevalent hyperglycaemic associated disorder.[10] This predominant isoform was formerly known as non-insulin-dependent diabetes mellitus and resulting from a combination of an inadequate response of peripheral tissues to insulin and an insufficient insulin secretion from the pancreatic β-cells.[11, 12] Both metabolic defects

lead to hyperglycaemia due to enhanced endogenous hepatic glucose production and insufficient glucose uptake primarily through the skeletal muscle.[12]

Worldwide diabetes becomes a health problem more and more. According to the International Diabetes Federation (IDF), more than 371 million people have diabetes in 2012, of whom about 90% suffer from T2D.[10] The IDF estimates that the current prevalence of 8.3% will rise to 9.9% of adults or to 552 million people by 2030 worldwide. This represents a global increase by approximately 50%, mostly due to a disproportional increase in low- and middle-income countries. In Africa alone, diabetic patients between 20 and 79 years will nearly double in numbers from 14.7 million people in 2011 to more than 28 million patients in 2030. Not only the still exploiting number of diabetic patients is alarming but, also the burden for the global and national healthcare systems. Already in 2011 more than 10% of global healthcare expenditures were spent to treat diabetes or to prevent diabetes-related complications. Currently, the IDF estimates that the current costs for diabetes of 465 billion US dollars in 2011 will increase to over 594 billion US dollars by 2030.

Table 1.1: Criteria for the metabolic syndrome.

Risk factor	Defining level
Obesity	BMI > 30 kg/m^2
raised Triglycerides	≥ 150 mg/dL (1.7 mmol/L)
reduced HDL-Cholesterol	
Men	< 40 mg/dL (1.03 mmol/L)
Women	< 50 mg/dL (1.29 mmol/L)
raised blood pressure	systolic ≥ 130 or diastolic ≥ 85 mm Hg
raised fasting plasma glucose	≥ 100 mg/dL (5.6 mmol/L)

Listed are criteria for the metabolic syndrome. A patient has the metabolic syndrome when 3 of the 5 listed criteria are fulfilled. In some cases the body mass index should be replaced by ethnic specific waist circumference. BMI, body mass index; HDL, high density lipoprotein

As mentioned above, T2D is the main isoform of all diabetes cases today. Besides a genetic predisposition, many studies implicate the human behaviour and lifestyle as well as the human environment together with escalating rates of obesity, particularly in low- and middle income countries, as the driving force of T2D.[13] However, prior to its manifestation, early events in the pathogenesis of T2D often remain undetected, since they occur without any clinical manifestations. In order to prevent the clinical manifestation and to determine the risk of diabetes, the metabolic syndrome coincides with diabetes and has been widely accepted as a tool for the detection of T2D. This is also known as syndrome x and refers to the clustering of the risk factors listed in table 1.1. If individuals fulfil three of the five risk

factors, they are considered to have the metabolic syndrome and hence a five-fold higher risk of T2D.[14-17]

1.1.2. Causal relationship between obesity and diabetes

Besides hypertension and dyslipidemia, obesity and a high plasma glucose level, particularly due to systemic insulin resistance, have evolved to be the central factor for the progression of T2D. Accordingly, the prevalence of T2D in obese adults is 3-7 times higher compared to normal-weight controls. Furthermore, morbidly obese patients with a BMI over 35 have a 20 fold higher risk to develop T2D than individuals with a normal BMI between 18 and 25.[18-20] Moreover, much evidence has accumulated that morbid enlargement of adipose tissue and especially the distribution of adipose tissue is highly associated with the development of T2D and cardiovascular diseases. Particularly, enlargement of abdominal or visceral adipose tissue seems to play a more crucial role for the progression of T2D compared to subcutaneous adipose tissue.[21] Studies have identified the waist circumference and/or the waist-to-hip ratio (WHR) as a crude marker for abdominal adiposity and highlighted that both parameters were strongly positively associated with T2D.[22] In a follow-up study, a higher WHR has clearly been associated with coronary artery diseases, even after adjustment for BMI, which rather is a correlate of total body fat mass.[23] Moreover, measurements of abdominal obesity using magnetic resonance and computed tomography have led to the conclusion that visceral adipose tissue is rather a key correlate of insulin resistance than subcutaneous adipose tissue.[24]

In recent years, evidence has emerged that obesity is linked to a chronic low grade inflammation of adipose tissue and is causally involved in the development of insulin resistance.[25] Usually, adipose tissue acts as a storage depot that control the energy supply due to the release and storage of energy rich substrates, but nowadays the endocrine function of this organ receives more and more attention. Through the release of several factors, adipose tissue is able to communicate with other tissues like liver, skeletal muscle, brain, vasculature and even the heart.[26-29] Adipocytes represent the major cell type of adipose tissue and since they are considered as endocrine cells they produce and release various proteins termed adipokines.[30] It could also be demonstrated that expression and secretion of adipo-, chemo- and cytokines is different between subcutaneous and visceral adipose tissue.[31, 32] Importantly, during obesity enlargement of adipose tissue occurs, and macrophages infiltrate in the adipose tissue. This alters the adipokine secretory profile, causes low-grade inflammation and promotes obesity-related metabolic complications.[33] Specifically, increased visceral adipose

tissue mass in obesity and T2D has been associated with an altered secretion profile of multiple adipokines, the most well-known being TNF-α, leptin or adiponectin.[34]

Besides adipocytes, adipose tissue contains preadipocytes, fibroblasts, vascular endothelial cells and macrophages. At least macrophages are also able to secret pro-inflammatory factors. Nevertheless, in a chronic state of low grade inflammation, a disturbed secretion of adipokines represents a link between obesity and insulin resistance, T2D or the metabolic syndrome.[25, 35, 36]

1.1.3. Epicardial adipose tissue and other fat depots

The development of cardiovascular diseases is highly associated with obesity, T2D and enlarged adipose tissue surrounding the heart and the coronary artery vessels. However, it is still incompletely understood how increased fat mass contributes to the pathogenesis of cardiovascular complications.[37-39] In recent years, the thickness of epicardial adipose tissue (EAT), a cardiac specific fat depot, has gained attention as a predictor for T2D, insulin resistance and the metabolic syndrome.[40] For instance, Cikim and colleagues described a correlation between the EAT-thickness and whole body fat mass, abdominal adiposity, insulin resistance, triglyceridemia, and waist circumference, respectively.[41] Moreover, a second study has confirmed that epicardial fat mass is higher in obese than in lean subjects.[42] EAT is a thoracic fat depot surrounding the aortic arch, the large coronary arteries, the ventricles, and the apex of the human heart.[43] In contrast to subcutaneous adipose tissue (SAT), the EAT and the anatomically related pericardial adipose tissue (PAT) are considered as true visceral adipose tissue. These fat depots cover approximately 80% of the heart is covered by either of the two fat depots. While EAT is located between the myocardium and the pericardium, PAT is located outside of the visceral pericardium.[39] Importantly, both fat depots differ in their embryologic origin and their blood supply. EAT and the underlying myocardium share the same coronary blood supply and they are not separated by a fascia whereas the blood supply to the PAT is not via the coronary arteries.[44] Consequently, secreted factors from EAT therefore may act more in a paracrine than in an endocrine way to affect the function of the underlying myocardium. So far, little is known about the expression and secretion of adipokines and related factors from EAT in T2D. Nevertheless, it seems likely that an altered secretory profile of EAT may contribute to the pathological progression of cardiovascular diseases in obesity.

1.2. Diabetic cardiomyopathy

1.2.1. Pathophysiology of diabetic cardiomyopathy

Corresponding to the IDF, diabetes and its complications are the major cause of death in most countries and approximately half of all diabetes patients die because of cardiovascular syndromes like coronary artery disease (CAD), hypertension or diabetic cardiomyopathy (DCM).[45] Already 40 years ago, Rubler and colleagues observed a cardiomyopathy characterized by left ventricular hypertrophy and cardiac fibrosis without a coronary artery disease.[46] Since the release of Rubler's publication, several independent epidemiological studies have confirmed the existence of a diabetic cardiomyopathy defined as diabetes-associated changes in myocardial structure and function with the exclusion of CAD or hypertension. In 1974, the Framingham study demonstrated that diabetic patients have a 2.4 and 5-fold higher risk for heart failure in men and women, respectively, than in patients without diabetes.[47] Even after adjustment for age, hypertension, obesity, CAD or dyslipidemia, the increase of heart failure in patients with diabetes still persist. Furthermore, the Cardiovascular Health study has revealed that elderly subjects with diabetes have an approximately 2-fold higher risk for heart failure than non-diabetics.[48] DCM is a disease characterized by multiple factors regarding changes in structure and function of the myocardium and calcium metabolism. However, one of the major contributing factors for the pathogenesis of DCM is the alteration of myocardial substrate supply and utilization caused by a disrupted insulin signaling.[49]

Even in asymptomatic diabetic patients the heart displays an increased higher left ventricular mass and wall thickness. Furthermore, it is assumed that the increased ventricular mass is a predictor of the progression of DCM.[50] Both the Framingham study as well as the Strong Heart Study reported a significant increase in left ventricular mass, which may contribute to reduced myocardial compliance. Interestingly, several studies have indicated that obesity is associated with left ventricular hypertrophy (LVH). Both cytokines, leptin and resistin, are linked to LVH and are released in higher levels by expanded adipose tissue. Furthermore, they induce cardiomyocyte hypertrophy *in vitro* via the production of reactive oxygen species and the activation of MAPK-signaling, respectively.[51, 52] Nevertheless, due to the overproduction of insulin to compensate insulin resistance in T2D, there is a possibility that hyperinsulinemia per se contributes to diabetes-related cardiac hypertrophy by IRS-1-mediated activation of the PI3K-signaling cascade (see section 1.2.2).[53] In addition, Karason

and colleagues have reported that body fat accumulation and insulin levels are associated with left ventricular geometry.[54, 55]

Besides LVH, myocardial fibrosis is another characteristic of the diabetic heart initially described by Rubler et al.[46] Fibrosis is a process where cardiac fibroblasts release a morbid excess of connective tissue within the myocardium. This is typically accompanied by a higher stiffness of the cardiac muscle and is further accelerated by increased proliferation of cardiac fibroblasts during DCM. Consistently, biopsies from patients with T2D showed an increased collagen deposition between myofibers of the heart.[56] Although the precise mechanisms for increased cardiac fibrosis are incompletely understood, some studies have suggested a role for diminished insulin action on diabetes-related fibrosis.[57]

The predominant characteristic of DCM is left ventricular diastolic dysfunction as illustrated by an impaired relaxation and decreased diastolic chamber compliance. The diastole is the relaxing and filling phase of the heart followed by complete contraction of the ventricle and output of the blood into the lung or body cycle. During diastole, the blood flow from the atria to the ventricle can be divided into two steps: a) the pressure within the atria exceeds the pressure in the relaxed ventricle and causes an opening of the valve trap doors between atria and ventricle. The speed of the blood flow between the heart chambers is called the early or “E” filling velocity. b) The speed of the blood flow in the second step is called the atrial or “A” filling velocity. In this step the atria contract and push the remaining blood from the atria to the ventricle. An indicator for diastolic dysfunction in diabetes patients is the reduced E/A-ratio, which can be assessed *in vivo* by Doppler echochardiography. In diabetic subjects, the prevalence of a diastolic dysfunction characterized amongst others by an impaired E/A-ratio is 40-75%.[58, 59] Similar results could be observed in the mouse model db/db *in vivo*, which exhibit T2D, obesity and insulin resistance without any obvious micro- and macro-vascular complications.[60] Accordingly, ob/ob mice and zucker diabetic fatty (ZDF) rats have an impaired cardiac function, which was supposed to be associated with an altered Ca^{2+}-homeostasis in cardiomyocytes.[61-63] As part of the electromechanical coupling of cardiomyocytes, activated ryanodine receptors, located at the sarcoplasmic reticulum (SR), release Ca^{2+} into the cytoplasm to trigger contraction. To sustain proper relaxation during myocardial diastole, SR Ca^{2+}-ATPase 2a (Serca2a) pump Ca^{2+} back to the SR in an energy-dependent process.[64] In ob/ob-mice, diastolic abnormalities were associated with an impaired Ca^{2+}-reuptake.[61, 62] Consistently, T2D-patients with diastolic dysfunction and isolated cardiomyocytes from db/db-mice exhibit an increased diastolic SR Ca^{2+} leak and a lower peak in systolic and diastolic Ca^{2+} release.[63] Finally, contractile dysfunction of the diabetic heart

can also be promoted by abnormalities in the protein levels and activities of myosin isoenzymes and regulatory proteins as well as myosin phosphorylation.[65]

As mentioned above, disturbed energy metabolism and impaired insulin signaling have detrimental effects on the cardiac performance. Therefore, a closer look at myocardial insulin action will be taken in the following section.

1.2.2. Myocardial energy metabolism and insulin resistance in diabetic cardiomyopathy

The insulin signaling pathway has important roles in normal physiology, whereas impaired insulin action is associated with diseases such as diabetes, obesity, the metabolic syndrome and diabetic cardiomyopathy.[66] Indeed, one of the major contributing factors to the pathogenesis of DCM is an altered myocardial substrate supply and utilization caused by a disturbed insulin signal transduction cascade.[67] In the heart, insulin enhances glucose uptake by promoting the translocation of the glucose transporter 4 (GLUT4) to the plasma membrane. In addition, insulin regulates the metabolism by promoting glycolysis, glycogen and protein synthesis, lipid metabolism as well as contractility, growth and apoptosis.[68] In order to sustain myocardial contraction, a constant supply of fuel and oxygen is required to maintain intracellular ATP-levels. In healthy conditions, 60-70% of the ATP consumption is derived from oxidative phosphorylation of long chain fatty acids within the mitochondria, whereas 20-30% and 10% of the energy demand is derived from oxidation of glucose or lactate, respectively.[68] Depending on the workload or even under hypoxic conditions, the heart is able to switch to glucose as the preferred substrate to produce ATP due to his anaerobic glycolytic conversion to lactate. This metabolic flexibility is supported by insulin in particular due to its key role in the events of glucose or fatty acid uptake within cardiomyocytes. In the context of obesity, T2D and insulin resistance, the heart is almost completely dependent on the oxidation of fatty acids. This represents the metabolic inflexibility of pathological myocardial states like DCM.[69] Since DCM is also characterized by increased uptake of circulating fatty acids, almost 80-90 % of the ATP is generated from lipid oxidation.[70, 71] Moreover, higher levels of intracellular fatty acids lead to lipotoxicity, which has also been linked to the development of cardiac dysfunction in DCM.[49] Oxidation of fatty acids further inhibits glucose oxidation via the Randle cycle.[72]

Hence, a closer look at the insulin-stimulated signal transduction cascade is worthwhile to understand the importance of insulin action and insulin resistance in diabetes and

myocardial energy metabolism. The initial step is the binding of insulin to the insulin receptor (IR), a member of the tyrosine kinase receptor family. The insulin receptor is a heterotetrameric protein consisting of two extracellular α-subunits and two transmembrane β-subunits. Upon binding of insulin to both α-subunits, a conformational change towards the intracellular components occurs which causes activation of the tyrosine kinase activity of the β-subunits.[73] Autotransphosphorylation-events lead to the phosphorylation of several tyrosine residues of the β-subunits, which function as docking sites for phosphotyrosine-binding domains (PTB), such as insulin receptor substrate (IRS)- and Src homology 2 domain containing transforming protein (SHC)- proteins.[74] In addition, the IR phosphorylates bound IRS proteins on tyrosines. The IRS-proteins are linked to the activation of the canonical phosphatidylinositol-3-kinase (PI3K)-dependent signaling pathway. In contrast, the mitogen-activated protein kinase (MAPK)-dependent pathway is initiated by binding of the scaffold protein SHC to the phosphorylated IR and principally involved in cell growth and differentiation. The adapter protein growth factor receptor-bound protein 2 (GRB2) binds to SHC and activates the associated guanidine nucleotide exchange factor son of sevenless (SOS). Subsequently, SOS promotes MAPK-signaling via the small GTPase Ras.[75, 76]

With regard to the myocardial metabolic insulin action, IRS-1 seems to be the most relevant target of the IR.[77] After binding to phosphorylated IRS-1, PI3K is activated and generates phosphatidylinositol 3,4,5-trisphosphate (PIP3) from phosphatidylinositol 4,5-diphosphate.[78] Depending on the primary structure, regulation and *in vitro* lipid substrate specificity, the PI3K-family can be divided into three classes.[79] Members belonging to class I-PI3K-enzymes are heterodimers existing of a catalytic p110 and a regulatory p85 subunit, each of which occurs in several isoforms.[66] Due to the SH2-domain within the p85 subunit, PI3K can bind to phosphorylated tyrosine residues of IRS and this allosterically activates the pre-associated p110 catalytic subunit (Fig.1.1).[76, 80]

In order to bind the product of the activated PI3K, PIP3, proteins require the so-called pleckstrin homolog (PH) domain. Both the 3'phosphoinositol dependent kinase (PDK1) and protein kinase B (PKB or Akt) contain this domain and after binding to PIP3, the kinases are recruited to and co-localized at the plasma membrane, where PDK1 phosphorylates Akt at the threonine residue at position 308. However, for full activation of Akt a second phosphorylation step at the serine residue at position 473 is necessary, which is thought to depend on the mammalian target of rapamycin complex 2 (mTORC2).[81]

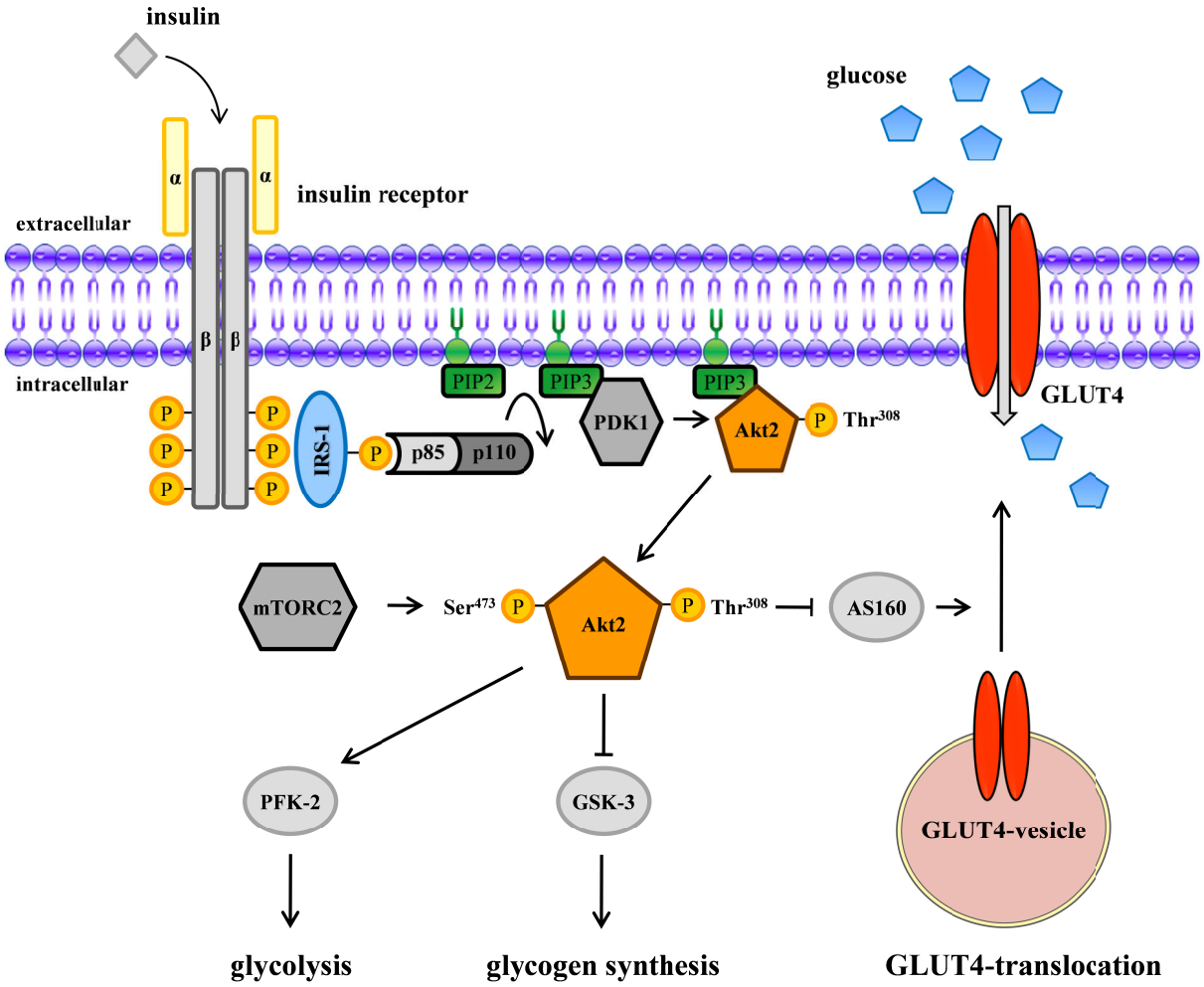

Figure 1.1: Insulin action regulates cardiac glucose metabolism. Upon binding of insulin to the insulin receptor (IR), one β-subunit autotransphosphorylates the other β-subunit at several tyrosine residues. Insulin receptor substrate (IRS-1) binds to the intrinsic PTB-domain at the IR and is phosphorylated by the β-subunit as well. Phosphatidylinositol-3-kinase (PI3K) consists of two subunits: a p110 catalytic subunit which is active upon binding of the p85 regulatory subunit to phosphorylated IRS-1. Subsequently, PI3K catalyses the transition of PIP2 to PIP3, to which PDK-1 and Akt can bind with their PH-domain. The co-localization of both serine/threonine-kinases to the plasma membrane leads to a phosphorylation of Akt at threonin 308. For full activation of Akt a second phosphorylation step at serine 473 by mTORC2 is necessary. Finally, active Akt phosphorylates downstream targets and initiates glucose uptake via the translocation of the vesicle-stored glucose transporter 4 (GLUT4) or increases glycolysis and glycogen synthesis.

Akt is a serine/threonine kinase and represents an important node in insulin-mediated regulation of metabolic actions by phosphorylation of critical downstream substrates.[66] In mammals, three different isoforms of Akt (Akt1-3) are described, which all share a highly conserved N-terminal PH-domain and a C-terminal catalytic domain. Despite their structural similarity, they are involved in the regulation of different biological processes due to differences in tissue and subcellular distribution as well as in the specific preference of different downstream targets.[66] The Akt1 and Akt2 isoforms are both widely expressed in nearly every tissue including the heart. In contrast, Akt3 expression and function seems to be restricted to the nervous system and testis and may therefore have a minor role regarding metabolic events.[82] Generally, Akt2 is more involved in metabolic issues such as glucose utilization, whereas Akt1 is responsible for growth and lifespan.[83]

Akt1-deficient mice exhibit normal glucose homeostasis, but their body and organ sizes are less than that of wild type (WT) littermates throughout their lifespan.[84] Akt1 is activated in rodent heart in response to pressure overload and short-term Akt1 activation promotes physiological hypertrophy, whereas long-term Akt1 activation is associated with pathological hypertrophy of the heart. [85, 86]

Akt2-deficient mice show diabetes and develop insulin resistance particularly due to the inability of insulin to induce glucose uptake and/or to inhibit hepatic glucose output.[87] One of the first identified targets of Akt was glycogen synthase kinase-3 (GSK3). After phosphorylation of GSK3 by Akt, the kinase remains inactive, which causes decreased phosphorylation of the GSK3-target, the glycogen synthase. This leads to a higher activation of the enzyme and therefore to an increased glycogen synthesis.[88]

In unstimulated cardiomyocytes, the GLUT4-transporter is stored in vesicles within the cytosol and after activation of the IRS-1-PI3K-Akt-pathway by insulin these vesicles are transported to the plasma membrane.[89, 90] Here, soluble N-ethylmaleimide-sensitive factor (NSF) attachment protein receptor (SNARE)-proteins control the fusion between the vesicles and plasma membrane to ensure the GLUT4-mediated uptake of glucose from the plasma into the cell. Multiple members of small GTPases belonging to the Rab-protein-family are also associated with GLUT4-containing vesicles and are implicated in cytoskeletal re-organization required for GLUT4-trafficking within cardiomyocytes.[91, 92] In response to insulin, Akt phosphorylates at multiple sites and inactivates the Rab-GTPase activating protein AS160.[93] AS160 is present in cardiomyocytes and is located at GLUT4-containing vesicles. Moreover, mutation of Akt phosphorylation sites within AS160 impairs GLUT4 translocation to the plasma membrane and reduced protein expression of AS160 leads to higher abundance of

GLUT4-protein at the plasma membrane.[94, 95] Accumulating evidence indicates that AS160 in its active form inhibits Rab-proteins and hence decreases GLUT4-trafficking. Tre-2/USP6, BUB2, cdc16domain family member 1 (TBC1D1) is a further Rab–GTPase-activating protein predominantly expressed in muscular tissues and closely related to the insulin signaling protein AS160.[96] Mice with a loss-of-function mutation in the gene coding for TBC1D1 exhibited a reduced body weight and are protected against adiposity.[97] Functional analysis of this protein revealed his involvement in insulin-stimulated glucose uptake and fatty acid oxidation.[98]

Once taken up by cardiomyocytes, glucose is either stored as glycogen or abolished via glycolysis.[68] Indeed, upon stimulation with insulin, Akt phosphorylates and activates the enzyme 6-phosphofructo-2-kinase (PFK-2), which generates fructose-2,6-bisphosphate. This is an allosteric activator of PFK-1, the rate limiting enzyme for glycolysis.[99]

In addition to the ability of insulin to initiate higher rates of glucose uptake, insulin-stimulated PI3K-activity is also associated with enhanced transport of fatty acids across the membrane of cardiomyocytes due to the translocation of the cluster of differentiation 36 (CD36)-protein.[100] So far, little is known about the exact mechanism how insulin regulates fatty acid uptake, but in the insulin resistant heart, a permanent presence of CD36 at the plasma membrane associated with higher rates of fatty acid uptake has been observed.[101] In the state when uptake of fatty acids exceeds β-oxidation within the mitochondria, lipotoxicity occurs, characterized by oxidative stress and accumulation of triacylglycerols and fatty acid intermediates within the cardiomyocytes. In addition, myocardial lipotoxicity has clearly been associated with contractile dysfunction in humans and rodents.[102-104]

1.3. Atherosclerosis in type 2 diabetes

1.3.1. Pathophysiology of Atherosclerosis

A key factor for the development of coronary artery disease, heart attack and stroke causing sudden death during diabetes and obesity is the development and progression of morbid thickening, hardening and narrowing of the artery wall, plaque formation and rupture, collectively also known as atherosclerosis.[10, 105] In this context, many studies have underlined the observation, that obesity-associated increased LDL-cholesterol plasma concentrations clearly and independently predicts cardiovascular events such as coronary artery disease and heart failure.[106, 107] Accumulating evidence further describes atherosclerosis as an inflammatory disease characterized by a series of highly specific cellular and molecular responses.[108] However, the exact and biologically complex interaction between the involved cells like endothelial cells, smooth muscle cells, leukocytes as well as thrombocytes in atherogenesis is incompletely understood. Nevertheless, various processes are suggested to be involved in the progression of atherosclerotic plaque formation and rupture such as activation of the coagulation cascade, the fibrinolytic system, smooth muscle cell (SMC) migration and proliferation, cellular inflammation as well as vascular insulin resistance.

Atherosclerosis principally occurs in large and medium-sized muscular arteries consist of three layers. The innermost layer, or tunica intima, predominantly consists of endothelial cells and is surrounded by the second layer, the tunica media, which is made up of SMC. The last layer consists of connective tissue and is known as the tunica adventitia. Several risk factors trigger the development of atherosclerosis, like diabetes, hypertension, dyslipidemia including high LDL and low HDL plasma levels, smoking and obesity. However, the biochemical cause is still under debate. There are two hypotheses trying to explain the initial phase of atherosclerosis: the “response-to-injury”- and the “lipoprotein-induced-atherosclerotic”-hypothesis. The first one emphasizes on endothelial injury, regardless of its origin, as a key event that initiates the inflammatory mechanisms associated with atherosclerosis.[108] Thus, the injury increases the adhesiveness of the endothelium for leukocytes or platelets as well as its permeability to lipoproteins and other plasma constituents. The higher permeability is mediated by the up-regulation of several leukocyte adhesion molecules like L-selectin, integrins, platelet-endothelial-cell adhesion molecule 1 and endothelial adhesion molecules like E-selectin, P-selectin, intercellular adhesion molecule 1 (ICAM-1) and vascular-cell adhesion molecule 1 (VCAM-1). In addition the secretion of

pro-inflammatory cytokines like monocyte chemotactic protein 1 (MCP-1) or interleukin-8 supports the migration of monocytes from the lumen across the intima to the media of the blood vessel.

According to the "lipoprotein-induced-atherosclerotic"-hypothesis, the endothelial dysfunction is not the initial cause but rather a consequence of the infiltration of the arterial wall by LDL in a chronic state of hypercholesterolemia and hypertension.[109] Studies underline this assumption that particularly lipoproteins containing apolipoprotein B can drive atherosclerosis even in the absence of other risk factors.[110] This is further supported by subendothelial proteoglycans and their affinity to retain LDLs within the tunica media.[111] Within this area, enzyme-dependent and -independent LDL oxidation leads to an activation of endothelial cells and thereby contributes to the above mentioned endothelial dysfunction, including the induction of expression of growth factors and pro-inflammatory cytokines and chemokines.[112]

Independently of its initiating trigger, the progression of atherosclerosis is consistent in both hypotheses. After adhesion to the endothelium, monocytes infiltrate the subendothelial space and differentiate in the present inflammatory milieu to macrophages, internalize oxidative LDL by scavenger receptors and become foam cells.[113, 114] Together with SMCs, the foam cells are the core of the fatty streak beyond the endothelium. The inflammatory milieu, triggered by oxidative LDL, T-Lymphocytes, foam cells and endothelial cells, induces on-going proliferation and migration of the SMCs within the lesion. During plaque formation, SMC migrate to the intima and are substantial for the fibrous cap covering the underlying and growing necrotic core of apoptotic macrophages, endothelial cells and SMC. At this stage, SMC synthesize essential extracellular matrix proteins, such as collagen and elastin, to maintain stability of the plaque. Activated T-cells within the fibrous cap inhibit this process by releasing interferon-γ. Furthermore, inflammatory macrophages, activated by amongst others TNF-α and MCP-1, promote tissue proteolysis by releasing matrix-degrading enzymes like metalloproteinases, which support breakdown of collagen and elastin.[115]

If the fibrous cap becomes thin, plaque rupture occurs and components of the lesion are released into the circulation, where they cause thrombus formation, narrowing and occlusion of the blood vessel, ischemia and infarction.[109]

1.3.2. Insulin signaling in the vasculature

Similarly to the described insulin signaling pathway in cardiomyocytes in section 1.2.2, a disturbed insulin-induced activation of the MAPK- and PI3K-pathway has major implications in the maintenance of SMC and endothelial cell homeostasis. A well described cardiovascular action of insulin is the stimulation of the production of the vasodilator nitric oxide (NO) in endothelial cells by the endothelial NO-synthetase (eNOS).[76] Classically, vasodilators like acetylcholine increase intracellular Ca^{2+}-concentrations, which activate eNOS-dependent NO-production.[116] Indeed, the insulin-dependent pathway has been considered as a completely calcium independent tool to regulate eNOS activity. This requires an insulin-stimulated phosphorylation of eNOS at Serine 1177 by the protein kinase Akt.[117] Available NO can passively diffuse from the cytosol of endothelial cells to SMC, activating guanylate cyclase to increase cyclic GMP levels. This inhibits contraction followed by vasodilation and reduced blood pressure. Nowadays, it is known, that besides blood pressure NO also regulates vascular remodeling and angiogenesis.[118, 119]

Nevertheless, it has also been shown that physiological concentrations of insulin induce NO-production in SMC by themselves by phosphorylating and activating eNOS.[120] Moreover, expression of all three isoforms of NOS (eNOS, inducible NOS and neuronal NOS) has been confirmed on the mRNA- as well as on the protein level, indicating a physiological role of SMC-derived NO.[121] This has also been demonstrated by Kahn and colleagues, who have correlated the insulin-induced inhibition of contraction to a NOS-dependent pathway within SMC.[122] However, the *in vivo* function of SMC-derived NO is still controversial and under debate.[121]

Insulin also attenuates the vascular tone by decreasing the contractility of SMC via the PI3K-Akt-pathway.[123] Normally, insulin-regulated contraction of SMC involves the small GTP-binding protein RhoA located at the plasma membrane. Here, RhoA promotes the activity of ROK-α, which phosphorylates and inactivates the myosin light chain (MLC) phosphatase. In turn, this leads to increasing levels of phosphorylated MLC and contraction. Insulin decreases the activity of RhoA by inhibitory phosphorylation and by delocalization of the protein from the plasma membrane, resulting in higher activity of the MLC-phosphatase and decreasing MLC-phosphorylation.[76] Moreover, insulin regulates Ca^{2+}-flux by inhibiting calcium influx through ion-channels along the plasma membrane as well as by supporting the efflux through Ca^{2+}-pumps at the plasma membrane and the sarcoplasmic reticulum, which results in a decreased vasoconstrictor tone.[124, 125]

1.4. MicroRNAs in diabetes and obesity

1.4.1. Biogenesis and function of microRNAs

A ground-breaking discovery in the scientific field of cell biology was made by Victor Ambros, Rosalind Lee and Rhonda Feinbaum with their report about the gene *lin-4* in *Caenorhabditis elegans* approximately two decades ago.[126] This gene, which is known to control early events in the larval development, does not code for a protein but rather for a small noncoding RNA with a length of approximately 22 nucleotides. In an earlier study by Whitmann and colleagues, the inhibitory effect of the gene product from *lin-4* to the gene *lin -14* was reported and they also proposed that the 3'UTR of *lin-14* mRNA had an eminent impact on the *lin-4* mediated repression.[127] It has been revealed that the *lin-4* RNA is antisense complementary to multiple sites within the 3'UTR of *lin-14* mRNA and that the base pairing of lin-4 with the mRNA is crucial for the reduction of lin-14 protein levels without any noticeable change in the amount of mRNA.[126, 127] Since this time, a first model has been developed in which a small RNA triggers the transition from the first larval stage to the second by 3'UTR-mediated repression of translation of the respective mRNA. For seven years it had seemed that this model was only restricted to nematodes and lin-4 and that there were no related pathways neither in *C. elegans* nor in other animals.[128] This changed with the discovery of a second small RNA, let-7, in *C. elegans* with comparable features and functions like lin-4.[129] In contrast to the *lin-4* gene, homologues of the *let-7* gene were soon detected in *Drosophila*, humans and other animals.[130] Only one year later, over hundreds of genes coding for small double stranded RNAs such as *lin-4* and *let-7* were cloned from cells from humans, flies and worms. This indicates a highly conserved mechanism throughout animal evolution how non-coding RNAs modulate posttranscriptional repression of protein synthesis [131-133]

Nowadays, the term microRNAs or miRNAs are used for this new class of 20-25 nucleotide long noncoding RNAs that modulate gene expression through canonical base pairing between the miRNA and its complementary match sequence within the mRNA.[134, 135] Since their discovery, the number of miRNAs has still been rising. At present, the miRNA database contains 2042 known miRNAs in humans, up to 1281 miRNAs in mice and at least 723 miRNAs in the rat (miRBASE, 2013). It is commonly accepted, that miRNAs modulate gene expression in nearly every important step within a cell, such as growth, differentiation, cell cycle and cell function as well as metabolic issues.

In consideration of the fact that miRNAs are encoded by nuclear DNA, the hypothesis of a

well regulated and balanced miRNome in a time and spatial specific manner developed. The let-7 family is also a good example for the structural organisation of some miRNA-genes and their regulation during differentiation. In the human genome there are at least 12 paralogues (isoforms) of let-7, indicated with a letter behind the name (let-7c for instance), which have probably been developed due to gene duplications. All sister miRNAs exhibit identical sequences from nucleotide 2 to 7 at their 5'end.[136] Due to their sequence homology in the so-called seed sequence, these miRNAs act redundantly at the same target. In most cases the expression of paralogues miRNA-genes is well controlled in a time specific manner, implicating their distinct role during differentiation and growth.

Normally, mammalian miRNA-genes are transcribed by RNA polymerase II (Pol II), whereas a small fraction of miRNAs are transcribed by Pol III, unless they are associated with Alu repeats.[137, 138] However, the transcription of miRNA-genes by Pol II provides the cell with an important tool for gene regulation. As required, the cell has the ability to control miRNA-expression with Pol II-associated transcription factors in a time and spatial dependent way. The organisation of miRNA-genes within the genome is very versatile.[137, 139] According to their genomic localization relative to exon or intron positions, miRNAs can be subdivided into four groups: intronic and exonic miRNAs in non-coding and coding transcripts, respectively.[136, 140, 141] Up to 48% of all existing miRNAs are in proximity to each other and are derived from polycistronic transcription units, which means that one transcription unit encodes two or even more miRNAs. This arrangement is known as clustered miRNAs and interestingly several clusters of miRNAs are highly conserved between species. However, miRNAs originating from the same transcription unit are co-regulated and obviously share related molecular processes.[139]

The first resulting transcript, the primary-miRNA (pri-miRNA), contains one or, if clustered miRNAs are present, several imperfect double stranded-like RNA (dsRNA)-hairpins. Depending on the nature of the miRNA-gene, pri-miRNAs often consist of 5'cap and a poly(A)-tail.[138] The hairpin structure includes the future mature miRNA and this steric conformation is absolutely essential for the nuclear processing step by Drosha, a RNase-III-type enzyme, existing as part of the microprocessor complex. This protein complex is responsible for the cleavage of the pri-miRNA to release a characteristic ~70nt long stem loop structure named precursor-miRNA (pre-miRNA).[142, 143] The cofactor of Drosha, DiGeorge syndrome critical region gene 8 (DGCR8), is also part of the microprocessor complex and recognizes the particular dsRNA hairpins within the pri-miRNA.[144]

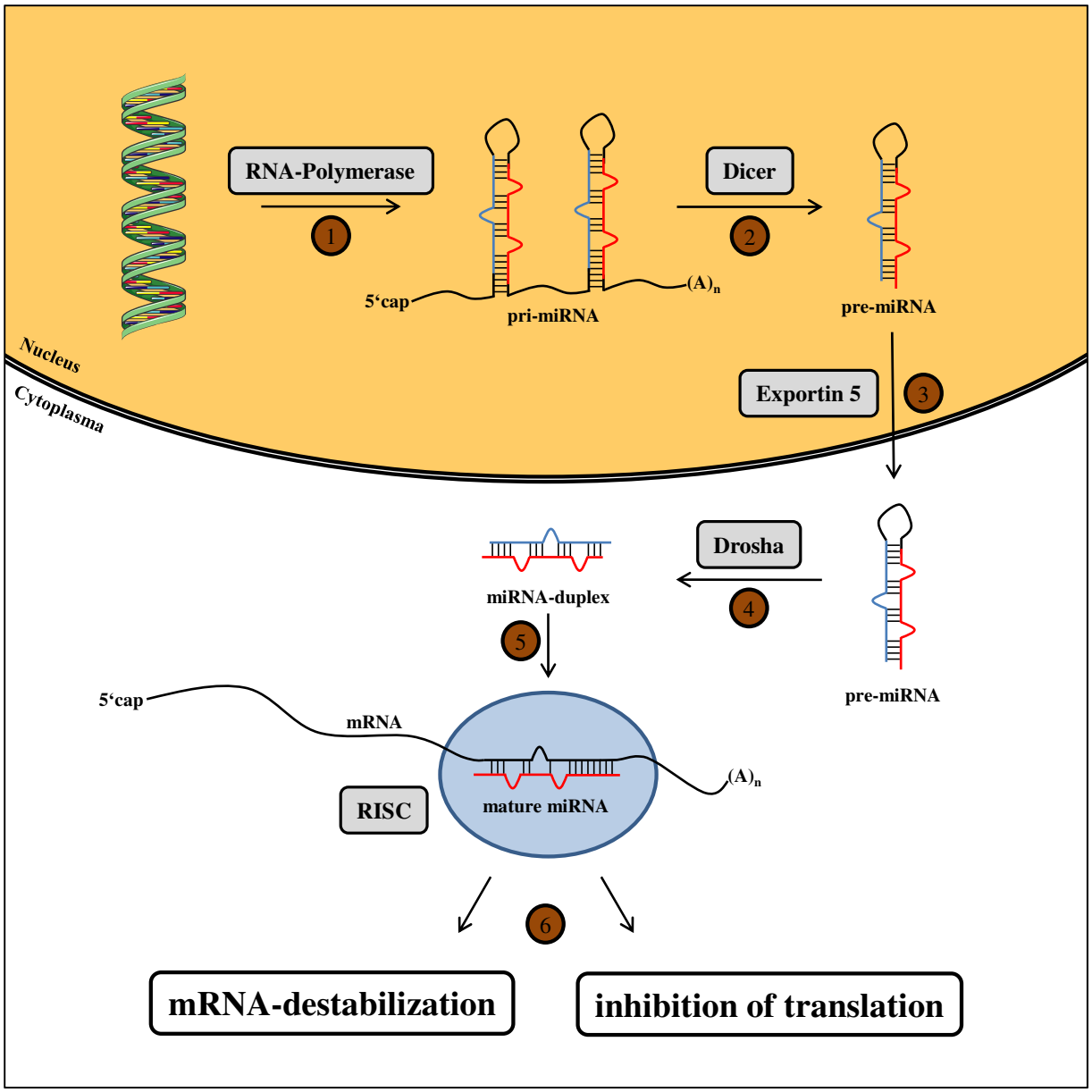

Figure 1.2: Simplified overview of the canonical biogenesis and function of microRNAs. (1) Genes are normally transcribed by RNA-Polymerase II with associated transcription factors resulting in a primary-miRNA (pri-miRNA) including the later mature miRNA (red, guided strand) and the minor miRNA (blue, passenger strand). **(2)** The locally existing hairpin structures are recognized and cleaved by Dicer into precursor-miRNAs (pre-miRNAs) with a characteristic and indispensable 3'-overhang of two nucleotides. **(3)** Exportin5 and the associated GTPase Ran translocate the pre-miRNA from the nucleus to the cytoplasm. **(4)** Here, a second RNase, Drosha, cleaves the pre-miRNA, resulting in a double stranded miRNA-duplex. **(5)** Among others, Argonaute proteins assemble with the mature miRNA to form the so called RNA-induced-Silencing-Complex (RISC). **(6)** Imperfect base pairing between the miRNA and mostly the 3'-Untranslated-Region (-UTR) of the protein-coding messenger-RNAs (mRNA) leads to either RISC-induced destabilization or inhibition of translation of the respective mRNA.

The next step of miRNA-biogenesis is the specific and energy-dependent translocation of the pre-miRNA from the nucleus to the cytosol by Exportin5 in cooperation with the GTPase Ran.[145] Within the cytosol, the pre-miRNA is cleaved by a second III-type-RNase, Dicer, resulting in an approximately 22-nt long ds miRNA duplex with a protruding 2-nucleotide overhang at its 3'end, similar to small interfering RNAs operating in RNA interference.[146] Together with several Argonaute (Ago) proteins and others, the miRNA-duplex is incorporated into the RNA-induced-silencing-complex (RISC), a micro-ribonucleoprotein, in which one of the strands (passenger strand) is degraded by the intrinsic endonucleolytic enzymatic activity. The second strand remains as the guided strand or mature miRNA within the RISC to fulfil its function. Mostly, there is only one mature miRNA from one miRNA duplex, but in some cases the minor miRNA (indicated with an asterisk behind its name, e.g. miR-26a*) retains in small or even equal amounts within a cell and functions as miRNA as well.

A further aspect underlying the versatility of miRNA biogenesis is the observation that some pre-miRNAs undergo RNA editing and processing, whereas adenosine is edited to inosine by adenosine deaminases acting on RNA (ADAR) proteins. This leads to an inhibition of Dicer-mediated processing of pre-miRNAs.[147] In addition, it has been reported that ADAR influences mature miRNA sequences, causing impaired miRNA-mediated target recognition. For instance the edited miR-376 interacts with a unique set of mRNAs compared to the unedited form.[148, 149]

Once loaded with RISC and argonaute proteins, the miRNA can directly induce the posttranscriptional repression of mRNAs.[150-152] Generally, metazoan miRNAs pair imperfectly with their targets following a set of rules. The most important rule includes the perfect binding of nucleotide 2 to 7, representing the seed region of the miRNA. Mismatches along the seed region have severe restrictions to the degree of repression. Interestingly, an adenine at position 1 and an adenine or uracil at position 9 of the mRNA improves miRNA-induced repression, although they do not need to pair with the nucleotides of the miRNA.[153] The seed region is often followed by a bulge, compensating mismatches between miRNAs and mRNAs, whereas good base pairing at the 3'end of miRNA (nucleotide 13-16) becomes even more important when the base pairing within the seed region is suboptimal.[154, 155] Multiple binding sites of a miRNA often coexist in a 3'UTR of a target mRNA, improving the effectiveness of repression. In few exceptions, miRNA-bindings sites are also found in coding regions or in 5'UTRs, although their physiological prevalence is still under debate.[156] Another factor for miRNA-mediated repression is the accessibility of the binding sites to RISC.[157]

Besides the nature and number of miRNA-binding sites, the influence of the UTR context seems to be important for miRNA function, because identical binding sites can mediate repression in some UTRs but not in others.[135, 154] A lot of sequence based computational methods explored during the last few years have tried to predict putative targets of a certain miRNA, but due to the complexity of miRNA-mediated repression a predicted target still has to be confirmed experimentally.[135]

Today, it is well known that ribonucleoprotein complexes loaded with miRNAs reduce protein levels by translational repression via mRNA cleavage and mRNA destabilization, which includes inhibition of translation and poly(A)-shortening or decapping.[135] Details concerning the exact mechanism how RISC represses protein synthesis are still poorly understood.[146] Kiriakidou and colleagues have reported that human Argonaute protein 2 has the ability to bind m^7G cap and its therefore able to compete with the eukaryotic translation initiation factor 4E for cap binding and proper promoting of translation, but many other models for translational inhibition during initiation or elongation processes exist.[146, 158] Concerning the destabilization of the mRNA, it is assumed that RISC recruits decay machinery components located within P-bodies. The latter are cellular structures that are enriched with mRNA catabolizing enzymes.[159]

1.4.2. microRNAs in diabetes and obesity

Because of their involvement in many relevant biological processes, miRNAs have also received attention in the field of diabetes- and obesity-related research. In order to maintain appropriate blood glucose levels, a precise regulation of insulin release from the pancreatic β-cells is necessary and thus the pancreatic islet-specific miR-375 plays a key role in blood glucose homeostasis via the regulation of β-cell function. By impairing the expression of myotrophin, a regulator of cytoskeleton formation and vesicle fusion, miR-375 suppresses insulin release.[160] Conversely, miR-375-knockout-mice develop hyperglycaemia even though plasma insulin levels remained unchanged compared with wild type littermates. Further analysis of this model revealed a change in pancreatic mass composition due to a decreased β-cell mass and number with a simultaneous increase in α-cell mass. This is accompanied by elevated levels of plasma glucagon, higher rates of gluconeogenesis and liver dependent release of glucose, which leads to the described hyperglycaemic phenotype.[161] Since the discovery of miR-375 as a regulator of β-cell biology, many other miRNAs such as miR-124a, miR-9 or let-7b have been found to regulate pancreatic homeostasis.[162]

Furthermore, miRNAs in cardiovascular disease, T2D or during the differentiation of adipocytes have been investigated in detail. Esau and colleagues have described that several miRNAs are regulated during adipogenesis and have characterized miR-143 as a highly up-regulated miRNA. Inhibition of miR-143 in pre-adipocytes leads to repression of differentiation, illustrated by inhibition of five markers such as Glut4, HSL, fatty acid-binding protein ap2, PPAR-γ2 and triglyceride accumulation.[163] Simultaneously, expression of miR-143 in adipose tissue has been elevated in mice fed a high fat diet.[164] Interestingly, miRNA expression can differ between fat depots. In 2009, Klöting and colleagues have compared the expression of 106 miRNAs in human abdominal subcutaneous and intra-abdominal omental adipose tissue and have found that 16 miRNAs exhibit a depot specific expression pattern. In addition, they described differences in miRNA-expression between subjects with normal glucose tolerance and patients suffering from T2D. Expression of several miRNAs in this study were found to correlate with parameters for glucose and lipid metabolism as well as for circulating leptin, adiponectin and interleukin-6 levels.[165]

The expression of miRNAs in other tissues like liver has also been analysed in the context of diabetes and obesity.[166] Recently, Kornfeld and colleagues have profiled the expression of miRNAs in the liver of mice fed a high fat diet and mice fed a normal chow diet and have identified, amongst others, miR-802 as an obesity-induced regulator of body glucose metabolism. Liver specific overexpression of miR-802 influences insulin action in the liver and causes systemic insulin resistance assessed by HOMA-index as well as disturbed glucose tolerance compared to control littermates.[167] Besides glucose metabolism, cholesterol biosynthesis has been affected by liver specific miR-122. Indeed, this miRNA is considered to be a key regulator of the cholesterol biosynthesis pathway because it affects at least 11 genes responsible for endogenous cholesterol production.[168] Effective silencing of miR-122 using systemic administration of locked nucleic acid (LNA) modified DNA against miR-122 (anti-miRs) has resulted in lower plasma cholesterol levels in mice and monkeys. The latter has demonstrated the pharmacological potential of LNAs to block the function of deregulated miRNAs *in vivo* and primates.[168]

1.5. Objectives

Diabetic cardiomyopathy and coronary artery disease are common complications and major causes of death in patients with type 2 diabetes (T2D). Profound evidence has identified a negative crosstalk between increased adipose tissue mass in obesity and peripheral tissues and organs such as the heart and the vasculature. Accordingly, adipose tissue-derived factors have been implicated in the regulation of insulin sensitivity and contractile function in cardiomyocytes as well as in the modulation of smooth muscle cells homeostasis. In this context, adipose tissue can be regarded as an endocrine organ secreting numerous adipokines, which are associated with inflammation, insulin resistance and atherosclerosis. Although expansion of a heart specific fat depot, the epicardial adipose tissue (EAT), has been identified as a risk factor for T2D, coronary artery disease and the metabolic syndrome, the contribution of EAT-derived factors to the pathogenesis of cardiac complications during T2D has not been investigated in detail. Identification of deregulated EAT-derived factors could lead to the discovery of new pharmacological treatments of cardiovascular complications or new biomarkers for an early detection of T2D.

Nowadays, microRNAs (miRNAs) as new modulators of mRNA translation have been implicated in several diverse biological processes. Moreover, accumulating evidence links miRNAs to the development of insulin resistance and to the pathogenesis of cardiovascular diseases. In this respect, modulation of miRNA expression via adipose tissue-derived factors could lead to the discovery of underlying mechanisms how enlarged and inflamed adipose tissue contributes to the development of cardiovascular diseases.

Consequently, the hypothesis of this work was that T2D-related alterations in the secretory profile of EAT affect myocardial function by modulating miRNA expression within cardiomyocytes. To address this hypothesis the following objectives were formulated:

- What are the effects of conditioned media generated from EAT from patients with T2D on determinants of contractile function, insulin signaling and miRNA expression in primary adult rat cardiomyocytes (ARC) and are they different as compared to conditioned media generated from biopsies from patients without T2D or other fat depots?

- Is the secretory profile from EAT from patients with T2D different from patients without diabetes and other fat depots? The antibody-array based profiling of the

factors released is expected to result in the recognition EAT-derived factors specifically released during T2D. In addition, we examined whether the factors with a deregulated secretion from EAT in patients with T2D have the potential to mimic the CM-induced effects.

- Can the CM-induced effects be ascribed to alterations in miRNA-expression and their potential target genes in ARC and can these detrimental and miRNA-triggered effects be linked to specific epicardial adipokines? In this case the exact pathway how adipokines regulate miRNA-expression and how miRNA modulate cardiac function will be analyzed in detail.

- What is the impact of adipokines on insulin action in human vascular smooth muscle cells (hVSMC) and can the detrimental effects on insulin signaling be ascribed to alterations in miRNA-expression? In this context a further aim was to determine the underlying pathway how CM modulate the expression of miRNAs in hVSMC.

Chapter 2

Study 1

Secretory products from epicardial adipose tissue of patients with type 2 diabetes induce cardiomyocyte dysfunction

Sabrina Greulich[1], Bujar Maxhera[2], Guy van de nPlas[3], Daniella Herzfeld de Wiza[1], Konstantinos Smiris[3], Heidi Mueller[1], Jessica Heinrichs[1], Marcel Blumensatt[1], Claude Cuvelier[4], Payam Akhyari[2], Johannes B. Ruige[5], D. Margriet Ouwens[1,7], and Juergen Eckel PhD[6,7]

published in Circulation, 2012

[1]Institute of Clinical Biochemistry and Pathobiochemistry, German Diabetes Center, Duesseldorf, Germany

[2]Department of Cardiovascular Surgery, Medical Faculty, Heinrich-Heine-University Duesseldorf, Duesseldorf, Germany

[3]Heart Centre, Ghent University Hospital, Ghent, Belgium

[4]Department of Pathology, Ghent University Hospital, Ghent, Belgium

[5]Department of Endocrinology, Ghent University Hospital, Ghent, Belgium

[6]Paul Langerhans Group – Integrative Physiology, German Diabetes Center, Duesseldorf, Germany

[7]JE and DMO equally contributed to this paper

Abbreviations

AgRP – Agouti-related protein, ANP – atrial natriuretic peptide, AM – control adipocyte medium, BNP – brain natriuretic peptide, CAD – coronary artery disease, CD14 – cluster of differentiation 14, CCL – Chemokine (C-C motif) ligand, CM – conditioned medium, T2D – type 2 diabetes, EAT – epicardial adipose tissue, FABP4 - adipocyte fatty acid binding protein 4, HGF – hepatocyte growth factor, IL- interleukin, MCP1 – monocyte chemoattractive protein-1, MMP – matrix metalloproteinase, ND – non-diabetics, PAI-1 – plasminogen activator inhibitor-1, PAT – pericardial adipose tissue, SAT – subcutaneous adipose tissue, SERCA2a – sarcoplasmic endoplasmic reticulum ATPase 2a, TGF – transforming growth factor, TIMP1 – tissue inhibitor of metalloproteinases, TNFα – tumour necrosis factor α, TRAILR – TRAIL receptor

Key Words

activins, adipose tissue, angiopoietin-2, insulin resistance, type 2 diabetes mellitus

Abstract

Background

Secreted factors from epicardial adipose tissue (EAT) have been implicated in the development of cardiomyocyte dysfunction. This study was aimed to assess whether alterations in the secretory profile of EAT in patients with type 2 diabetes (T2D) affect contractile function and insulin action in cardiomyocytes.

Methods and results

Contractile function and insulin action was analyzed in primary adult rat cardiomyocytes incubated with conditioned media (CM) generated from explants of EAT biopsies obtained from patients without (ND) and with T2D. CM from subcutaneous (SAT) and pericardial adipose tissue (PAT) biopsies from the same patients served as control. Cardiomyocytes treated with CM (EAT) from T2D-patients showed reductions in sarcomere shortening, cytosolic Ca^{2+}-fluxes, expression of sarcoplasmic endoplasmic reticulum ATPase 2a (SERCA2a), and decreased insulin-mediated Akt-Ser473-phosphorylation as compared to CM from the other groups. Profiling of the CM showed that activinA, angiopoietin-2 and CD14 selectively accumulated in CM-EAT-T2D versus CM-EAT-ND and CM from the other fat depots. Accordingly, EAT-biopsies from T2D-patients were characterized by clusters of CD14-positive monocytes. Furthermore, SMAD2-phosphorylation, a downstream target of activin A signaling was elevated in cardiomyocytes treated with CM (EAT) from T2D-patients, and the detrimental effects of CM (EAT) from T2D-patients were partially abolished in cardiomyocytes pretreated with a neutralizing antibody against activin A. Finally, both recombinant activin A and angiopoietin-2 reduced cardiomyocyte contractile function, but only activin A reduced the expression of SERCA2a.

Conclusions

Collectively, our data implicate T2D-related alterations in the secretory profile of EAT, in the pathogenesis of diabetes-related heart disease.

Introduction

Cardiac contractile dysfunction and myocardial insulin resistance frequently occur in patients with type 2 diabetes (T2D) and the metabolic syndrome.[1] Risk factors for diabetes-related heart disease, like hypertension, dyslipidemia, increased visceral adipose tissue mass, and insulin resistance, also associate with expansion of the epicardial adipose tissue (EAT).[2-5] EAT is a visceral thoracic fat depot, surrounding the aortic arch, the large coronary arteries, the ventricles and the apex of the human heart.[6] Because EAT shares the coronary blood supply with the myocardium, and no structures resembling a fascia separate the adipose and myocardial layers, factors released from EAT may directly affect the underlying tissues.[2, 6, 7]

Like other adipose tissue depots, EAT is a source of pro-inflammatory adipokines, like interleukin (IL) 1, IL6, IL8, monocyte chemoattractive protein-1 (MCP1), leptin, plasminogen activator inhibitor 1 (PAI-1), resistin, RANTES, and tumor necrosis factor α (TNFα), as well as potential protective factors, like adiponectin and omentin.[5, 8-16] Patients with coronary artery disease (CAD) show a deregulated expression and release of these factors by EAT.[7, 11, 15] For example, expression and intracoronary levels of adiponectin are lower in patients with CAD.[17] Furthermore, conditioned media (CM) from EAT from patients with CAD show an enhanced potential to induce atherogenic changes in monocytes and endothelial cells.[15] While these data implicate secretory products from EAT in the pathogenesis of CAD, studies toward the interaction between EAT and myocardial function in T2D are limited.

Since adipose tissue of patients with T2D is characterized by a state of low-grade inflammation, we propose that T2D-related alterations in the secretory profile of EAT may affect myocardial function. In the present study, we analyzed contractile function and insulin action in primary rat cardiomyocytes following exposure to CM generated from explants of EAT biopsies obtained from patients without (ND) and with T2D. CM from subcutaneous (SAT) and pericardial adipose tissue (PAT) biopsies from the same patients served as control. In addition, we used antibody arrays to profile the CM from the various experimental groups for changes in adipokine secretion. Our data provide evidence for a cardiodepressant activity in CM derived from EAT from patients with T2D, and implicate T2D-related alterations in the secretory profile of EAT in the pathogenesis of diabetes-related heart disease.

Methods

Adipose tissue biopsies

Patients with or without type 2 diabetes (T2D) undergoing open heart surgery (coronary artery bypass or valve replacement) were enrolled into this study with written informed consent. The procedure to obtain adipose tissue samples was approved by the ethical committee of the Heinrich-Heine-University (Duesseldorf, Germany). In this study, males of Caucasian origin were recruited and distributed into the two groups, non-diabetics (ND) or T2D, on the basis of the diagnosis T2D in the medical records of the patient. Patients of other ethnic origins, diagnosed as having HIV infection, lipodystrophy or chronic coexistent inflammatory disease were excluded.

Immunohistochemistry

Adipose tissue biopsies were immediately fixed in 4% buffered formalin, processed for paraffin embedding, cut into 5 µm thick sections and routinely stained with haematoxylin-eosin. Standard immunohistochemistry was applied to 5 µm thick sections after deparaffinising, antigen retrieval and blocking. Primary antibodies anti-CD8 (Thermo Scientific, Cheshire, UK) and anti-CD68 (DAKO M0814, Glostrup, DK) were applied for 32 min in a Benchmark® XT IHC/ISH Staining Module, followed by HRP-conjugated streptavidin (DAKO) for 30 minutes. The anti-human monoclonal antibody CD14 (Abcam, ab49755, Cambridge UK) was applied overnight after EDTA pre-treatment and blocking with 0.3% H_2O_2. After incubation, slides were treated with HRP-conjugated streptavidin (DAKO) for 30 minutes. Next, DAB (3,3diaminobenzidine) was used as chromogenic enzyme substrate before counterstaining with haematoxylin.

Preparation and characterization of conditioned media (CM)

Adipose tissue biopsies were used to generate conditioned media (CM) as previously described.[16, 18, 19] Antibody arrays (RayBio human cytokine antibody G series 2000; Ray Biotech, Inc., Norcross GA, USA) were used to determine the secretory profile of the CM.[16]

Effects of conditioned media on contractile function in primary adult rat cardiomyocytes

Cardiomyocytes were isolated from Lewis rats (Lew/Crl) as described,[20] and cultured for 24 h on laminin-coated dishes (ibidi GmbH, Martinsried, Germany) before exposure to

CM, recombinant human activin A (Biozol, Eching, Germany), or recombinant human angiopoietin-2 (R&D systems, Wiesbaden-Nordenstadt, Germany).[16] For inhibition of activinA signaling, CM was incubated for 60 min with 100 ng activin A βA subunit antibody, or 100 ng/ml recombinant follistatin (both from R&D systems, Wiesbaden-Nordenstadt, Germany) before addition to the cardiomyocytes. In addition, cardiomyocytes were preincubated with the activin A receptor like kinase SB431542 (10µmol/l, Sigma Aldrich, St. Louis, USA) for 60 min before addition of CM. The effects of CM, activin A, or angiopoietin-2 on sarcomere shortening and cytosolic Ca^{2+}-fluxes were determined following electric stimulation of the cells with 1 Hz on a contractility and fluorescence system from IonOptix (Dublin, Ireland) using Fura-2 AM (Merck chemicals, Darmstadt, Germany) as Ca^{2+}-indicator. Cells were preloaded with Fura-2 AM for 25 min at 37°C, washed twice with control adipocyte media (AM) (DMEM F12 containing 10% fetal calf serum, 33 µmol/l biotin, 17 µmol/l panthothenate (all from Invitrogen, Carlsbad, CA, USA)) and then incubated for 30 min with CM (diluted 1:4 with AM), AM, activin A, or angiopoietin-2. Trypan bleu staining following exposure to the various stimuli indicated no differences in cell mortality. Contractile function and Ca^{2+}-transients were analyzed in cells showing an intact rod-shaped morphology and sarcomere length >1.6 µm. Before measurement was started, cells were electrically pre-stimulated for 5 min with 1 Hz to reach a steady-state level for sarcomere shortening and Fura-2 fluorescence. Then, cells were paced with bipolar pulses of 5 ms duration at 1 Hz. The cytosolic Ca^{2+}-concentration was monitored as a ratio of the fluorescence emission peaks at 340 and 380 nm. In each experimental condition, data files were recorded of 10 consecutive beats for at least 10 different cells. Sarcomere shortening and Ca^{2}-transients were calculated using IonWizard (IonOptix).

Western blot analysis

Cardiomyocytes were isolated from Lewis rats (Lew/Crl) as described,[20] and incubated with CM (diluted 1:6 with AM), AM, human recombinant activin A, or angiopoietin-2, and insulin as indicated in the figure legends. Trypan bleu staining following exposure to the various stimuli indicated no differences in cell mortality. After exposure to the various stimuli, cells were washed twice with ice-cold PBS and lysed for 2h at 4°C in Triton X-100 lysis buffer, containing 50mM Tris.HCl [pH 7.5]; 150 mMNaCl; 0.5 % Triton X-100; 1 mMNaF; 1 mM Na_3VO_4; 2 mM $MgCl_2$, 1 mM DTT; and protease inhibitors (Complete, Roche Diagnostics, Mannheim, Germany) under gentle rotation. For protein expression of activin A in human adipose tissue, biopsies were homogenized for 2 h at 4°C in Triton X-100

lysis buffer. Lysates were cleared by centrifugation (15 min; 12.000 rpm; 4°C), and protein content was determined using Bradford reagent (Biorad Laboratories, München, Germany). Ten microgram of protein was loaded onto 10% SDS-Page gels, and transferred to polyvinylidenedifluoride (PVDF) membranes. After blotting, membranes were blocked with Tris-buffered saline (TBS), containing 0.1 % Tween 20 and 5 % non fat dry milk for 2 h at room temperature and then incubated overnight at 4°C with primary antibodies for Akt, phospho-Akt-Ser473, phospho-SMAD2-Ser465/467 (all Cell Signalling Technology, Danvers, MA, USA), SMAD2/3 (B&D Bioscience, Franklin Lakes, NJ, USA), sarcoplasmic endoplasmic reticulum ATPase 2a (SERCA2a), activin A βA subunit antibody (R&D systems) and GAPDH (both from Abcam, Cambridge, UK). After washing, membranes were incubated with appropriate secondary HRP-conjugated antibody for 2 h at room temperature and washed again. Bound antibodies were visualized using enhanced chemiluminescence and quantified using a LUMI Imager system (Roche Diagnostics, Mannheim, Germany).

Data analysis

Data are presented as mean ± standard error of the mean. Significant differences between experimental conditions were evaluated using Kruskall Wallis followed by a Dunns test for multiple comparisons or by a Mann Whitney U-test using Graphpad Prism software (version 5) as indicated in the legends to the Figures and tables. A value of $P<0.05$ was considered as statistically significant.

Results

Patient characteristics

Adipose tissue biopsies to generate CM were collected from males of Caucasian origin with or without T2D undergoing open heart surgery. The anthropometric characteristics and medication use of the subjects are listed in Table 1. Briefly, T2D-patients had elevated blood glucose levels as compared to ND-patients, whereas age and BMI were similar between the two groups (Table 2.1).

Effect of conditioned media on sarcomere shortening and cytosolic Ca^{2+}-fluxes in cardiomyocytes

Compared to control adipocyte medium (AM) and CM-EAT from ND-patients (CM-EAT-ND), a 30 min exposure of primary rat cardiomyocytes to CM-EAT from patients with T2D (CM-EAT-T2D) markedly impaired contractile function, as illustrated by reductions in departure velocity of contraction, peak sarcomere shortening, and return velocity of contraction (Figure 2.1 A-C). CM-SAT and CM-PAT from T2D-patients induced minor reductions in cardiomyocyte function (Figure 2.1 A-C). Contractile parameters were not affected by CM generated from fat depots from ND-patients (Figure 2.1 A-C). Abrogation of cytosolic Ca^{2+}-transients, as illustrated by reductions in departure and return velocities and a lower peak Fura-2 fluorescence signal was only induced by CM-EAT-T2D (Figure 2.1 D-F).

Effect of conditioned media on insulin signaling in cardiomyocytes

Compared to AM and CM-EAT-ND, CM-EAT-T2D markedly blunted insulin-stimulated Akt-phosphorylation in adult rat cardiomyocytes (Figure 2.2). Also exposure of cardiomyocytes to CM-SAT-T2D led to abrogation of insulin-mediated Akt-phosphorylation (Figure 2.2). In contrast, CM-PAT-T2D or CM generated from fat depots from ND-patients had no inhibitory effect on insulin-stimulated Akt-phosphorylation (Figure 2.2).

Characterization of conditioned media

In order to identify the factor(s) responsible for the selective induction of cardiomyocyte dysfunction by CM-EAT-T2D, alterations in adipokine secretion by CM from the various groups were profiled using antibody arrays. The immunoreactivity of the 174 factors present on the array for CM-EAT, CM-SAT, and CM-PAT from patients with and without T2D is presented in Supplementary Tables 2.1-3. In CM-EAT-T2D, immunoreactivity of activin A,

agouti-related protein (AgRP), angiopoietin-2, cluster of differentiation 14 (CD14), eotaxin-2 (also known as CCL24 (chemokine C-C- motif ligand 24)), and TRAIL-receptor 4 (TRAILR4) was increased versus CM-EAT-ND (all $P<0.05$) (Supplementary Table 2.2, Figure 2.3). However, when compared to CM-SAT-T2D and CM-PAT-T2D only the immunoreactivity of activin A, angiopoietin-2 and CD14 was selectively increased in CM-EAT-T2D (Figure 2.3).

To substantiate these findings, we first examined biopsies from EAT by immunohistochemistry. In EAT-ND, there were no marked differences between biopsies collected from patients undergoing aortic valve replacement or coronary artery bypass surgery except for the infiltration of CD8-positive cytotoxic T-cells in the connective tissue (Supplementary Figure 2.1). However, EAT-T2D was characterized by infiltration of numerous inflammatory cells, including CD8-positive T-cells, and clusters of CD68-positive macrophages and CD14-positive monocytes (Supplementary Figure 2.1). In addition, using ELISA, the amounts of activin A and angiopoietin-2 in CM-EAT-T2D were determined at 2.4 ± 0.8 ng/ml and 2.7 ± 0.7 ng/ml, respectively. Finally, protein expression of activin A determined by western blotting was higher in EAT-T2D compared to EAT-ND (Figure 2.4).

Effects of recombinant angiopoietin-2 on cardiomyocyte function

Next, we assessed whether recombinant angiopoietin-2 could mimic the detrimental effects of CM-EAT-T2D in cardiomyocytes. A 30-min exposure of cardiomyocytes to angiopoietin-2 caused a dose-dependent reduction in the parameters of sarcomere shortening and cytosolic Ca^{2+}-fluxes, which became significant at a concentration of 2 ng/ml angiopoietin-2 (Figure 2.5 A/B, Supplementary Figure 2.2). In contrast, exposing cardiomyocytes to concentrations up to 200 ng/ml angiopoietin-2 for up to 24 h had no effect on insulin-mediated Akt-phosphorylation (Figure 2.5 C).

Activin A and cardiomyocyte function

To verify whether activin A in CM-EAT-T2D is biologically active, we analyzed cardiomyocytes incubated with CM for phosphorylation of SMAD2, a downstream target of activin A signaling.[21] As shown in Supplementary Figure 2.3 A, only primary rat cardiomyocytes exposed to CM-EAT-T2D showed a significantly increased SMAD2-phoshorylation. Accordingly, pretreating cardiomyocytes with the activin-receptor-like kinase inhibitor SB431542 prevented the increase in SMAD2-phosphorylation induced by CM-EAT-T2D and activinA (Supplementary Figure 2.3 B). Next, we evaluated whether activin A is

responsible for the detrimental effect induced by CM-EAT-T2D. Both pre-incubation of CM-EAT-T2D with a neutralizing activin A antibody and with the natural activin A antagonist follistatin, partially improved the reductions in sarcomere shortening and cytosolic Ca^{2+}-fluxes induced by CM-EAT-T2D (Figure 2.6 A-B, Supplementary Figures 2.4 and 2.5). Similar results were obtained when cardiomyocytes were treated with SB431542 prior to exposure to CM-EAT-T2D (Supplementary Figure 2.6). Also the inhibitory effect of CM-EAT-T2D on insulin-mediated Akt-phosphorylation was partially reversed by a neutralizing activinA antibody, follistatin or SB431542 (Figure 2.6 C, Supplementary Figure 2.7). In contrast, these inhibitors had no effect on parameters of contractile function and Akt-phosphorylation in cardiomyocytes incubated with AM or CM-EAT-ND (Figure 2.6 A-C, Supplementary Figure 2.4-7).

Next, we determined whether recombinant activin A could mimic the detrimental effects of CM-EAT-T2D in cardiomyocytes. A 30-min exposure of cardiomyocytes to recombinant activin A caused a dose-dependent reduction in the parameters of sarcomere shortening and cytosolic Ca^{2+}-fluxes, which for sarcomere shortening became significant at a concentration of 1 ng/ml activin A (Figure 2.7 A/B, Supplementary Figure 2.8 A-D). Exposing cardiomyocytes for up to 4h to activin A had no significant effect on insulin-mediated Akt-phosphorylation. However, in cells incubated overnight with activinA insulin-mediated Akt-phosphorylation was blunted in cardiomyocytes exposed to activin A (Figure 2.7 C). This effect became significant at a concentration of 1 ng/ml activin A (Figure 2.7 C).

Effect of conditioned media, angiopoietin-2 and activinA on sarcoplasmic endoplasmic reticulum ATPase 2a expression

Because of the rapid cardiodepressant actions of CM-EAT-T2D, angiopoietin-2 and activin A, we examined the protein expression of SERCA2a, a key regulator of cytosolic Ca^{2+}-metabolism, in cardiomyocytes exposed to these stimuli. Figure 2.8 shows that a 30 min exposure to CM-EAT-T2D led to a 50% reduction in SERCA2a protein expression versus cells exposed to AM or CM-EAT-ND. Furthermore, 10 ng/ml activin A induced a decrease in SERCA2a protein expression (Figure 2.8). Angiopoietin-2 reduced SERCA2a protein expression only in cardiomyocytes exposed to 200 ng/ml angiopoietin-2 (Figure 2.8).

Discussion

This study demonstrates that EAT from T2D-patients secretes factors that induce contractile dysfunction and insulin resistance in primary rat cardiomyocytes. Moreover, we show that the secretory profile of EAT from patients with T2D differs from that of SAT and PAT, and from EAT from ND-patients. Finally, we identified activin A and angiopoietin-2 as factors responsible for the detrimental effects on cardiomyocyte function induced by CM-EAT-T2D. Collectively, these findings implicate T2D-related alterations in the secretory profile of EAT in the pathogenesis of diabetes-related heart disease.

Multiple epidemiological studies have demonstrated associations between expansion of EAT and clinical markers of the metabolic syndrome, T2D, CAD, and cardiac function.[3, 5] Recently, we demonstrated that high-fat feeding of guinea pigs induces qualitative alterations in the secretory profile of EAT which contribute to the induction of cardiomyocyte dysfunction.[16] Also obesity and CAD have been associated with qualitative alterations in the secretory profile of EAT that underlie the induction of atherogenic changes in monocytes and endothelial cells.[15] Here, we extend these observations by showing that CM generated from EAT of T2D-patients exerts a strong cardiodepressant and negative inotropic effect on primary rat cardiomyocytes. The reductions in sarcomere shortening and cytosolic Ca^{2+}-fluxes were paralleled by a decreased protein expression of SERCA2a in cardiomyocytes incubated with CM-EAT from T2D-patients. SERCA2a is a key regulator of myocardial Ca^{2+} metabolism, and decreases in SERCA2a expression are a common characteristic of cardiopathological states in humans and rodents.[22, 23] Therefore, it seems likely that the reduction in SERCA2a expression could contribute to the reduction in Ca^{2+}-transients in cardiomyocytes treated with CM-EAT from patients with T2D. We also observed that CM from SAT and PAT of T2D-patients exhibited minor inhibitory effects on parameters of sarcomere shortening in the absence of significant effects on cytosolic Ca^{2+}-transients. Previous studies already reported cardiosuppressive effects induced by CM from human SAT in isolated cardiomyocytes and hearts under Langendorff perfusion.[24-26] These cardiosuppressive effects of adipose tissue have been ascribed to adipokines which are elevated in T2D, including fatty acid binding protein 4 (FABP4), IL1β and 6, and TNFα.[24, 27-30] However, the physiological relevance of the cardiodepressant factor(s) secreted by other adipose tissue depots remains to be elucidated since it may only affect cardiomyocyte function via the systemic circulation. In contrast, factors secreted from the EAT can directly

affect the function of the underlying myocardium because to the absence of fascial boundaries.[2, 4, 5]

In addition to the induction of cardiomyocyte contractile dysfunction, we observed that CM-EAT-T2D abrogates insulin-mediated phosphorylation of Akt, a key regulator of myocardial glucose uptake.[31] In patients with T2D, alterations in cardiac structure and function which are found even in the absence of hypertension and CAD are ascribed to diabetic cardiomyopathy. The latter syndrome often co-exists with alterations in myocardial substrate metabolism, such as decreased insulin stimulation of myocardial glucose uptake.[31, 32]Although our study provides strong evidence that secretory products of EAT from T2D-patients contribute to the induction of myocardial insulin resistance, it should be noted that the detrimental effects on insulin action could only be demonstrated upon prolonged incubation of the cardiomyocytes with CM. Since the effects on contractile function could already be observed within minutes after the addition of CM, it is likely that the induction of insulin resistance by CM-EAT-T2D is established through a distinct signaling pathway.

To identify factors responsible for the detrimental effect of CM-EAT-T2D, we characterized the secretory profile of CM-EAT as compared to CM from the other experimental groups. Using antibody arrays, we observed that the secretory profile of CM-EAT differs from CM-SAT and CM-PAT. Furthermore, we observed an EAT-specific accumulation of three factors, i.e. activin A, angiopoietin-2, and CD14 in CM-EAT-T2D versus CM-EAT-ND. Accumulation of activin A in CM-EAT was also observed in guinea pigs upon high-fat diet feeding versus animals fed a standard diet.[16] The alterations in activin A immunoreactivity were accompanied by biological activity of the CM, as illustrated by the induction of SMAD2-phosphorylation by CM-EAT-T2D only. Although other factors present on the arrays like tumor growth factor (TGF) β1, TGFβ2, TGFβ3, hepatocyte growth factor (HGF), and insulin-like growth factor binding protein (IGFBP) 3, are also capable to regulate SMAD2-phosphorylation, the immunoreactivity of these factors did not differ among the experimental groups. In line with this, we observed that incubation of primary adult rat cardiomyocytes with activin A at a concentration comparable to that found in CM-EAT-T2D reduced cardiomyocyte contractile parameters and insulin-mediated Akt phosphorylation up to 30-50% as compared to the inhibition caused by CM-EAT-T2D. Importantly, the cardiosuppressive effects of CM-EAT-T2D could be partially reversed by pharmacological inhibition of the activin A receptor, as well as by a physiological antagonist of activin A, follistatin and by a neutralizing antibody against activin A.

The identification of activin A as potential cardiodepressant factor is strongly supported by several independent clinical observations. Serum levels of activinA are significantly elevated in patients with heart failure versus control subjects as well as in patients with acute myocardial infarction and abnormal glucose regulation versus acute myocardial infarction and normal glucose regulation.[33, 34] Furthermore, analysis of circulating activin A levels in samples from a previously described study on males with uncomplicated T2D,[32] identified a positive relation between activin A levels and the left ventricular mass-to-volume ratio, and a negative association with the rate of myocardial glucose metabolism (Ouwens et al., manuscript in preparation). In contrast, systemic overexpression of activin A in mice protects the hearts from ischemia by protecting against apoptosis.[35] Therefore, further investigations are required to assess the precise function of activin A in the pathogenesis of cardiac disorders.

With the use of the antibody arrays, we could indeed identify additional factors that are selectively increased in CM-EAT-T2D, namely angiopoietin-2, and CD14. Although serum levels of these factors are raised in patients with T2D and cardiovascular dysfunction,[36, 37] the role of these factors in relation to myocardial function and insulin sensitivity remains to be clarified in clinical studies. *In vitro*, we showed that recombinant angiopoietin-2 reduced cardiomyocyte contractile function, but not insulin action, at concentrations comparable to that found in CM-EAT-T2D. Therefore, the possibility that the inhibitory effect of CM-EAT-T2D is caused by an adipokine not present on the array cannot be excluded. The antibody array used in this study allowed the profiling of 174 adipokines, while recent profiling studies of the adipokinome indicate the existence of up to 700 adipokines. In a separate study, we have analyzed an adipokine for this effect on insulin action in rat cardiomyocytes, namely omentin-1. This factor was found to be reduced in CM-EAT-T2D, and addition of recombinant omentin could prevent the inhibitory effect induced by CM on cardiomyocyte action (Greulich et al., submitted).

Another question that remains to be addressed is what underlies the alterations in the secretory profile of EAT from patients with T2D. In the present study, CM was generated from adipose tissue explants. In addition to adipocytes, adipose tissue also contains other cell types, like pre-adipocytes, macrophages, monocytes, endothelial cells and lymphocytes, which can release a variety of chemo-, cytokines and other factors.[38, 39] Hypertrophy of adipose tissue in obesity and T2D is closely linked to low-grade inflammation,[40] which can be ascribed to accumulation of immune cells in the adipose tissue, and secretion of pro-inflammatory cytokines.[38, 39] In line with previous reports, we found an infiltration of immune

cells in EAT from patients with CAD.[11, 41-43] Here, we extend these observations by showing a dramatic increase in macrophage and monocyte infiltration in EAT-T2D versus EAT-ND. Notably, it has been reported that activin A expression is markedly induced in monocytes as well as stromal fibroblasts by cognate interaction with activated T cells.[44] Furthermore, others demonstrated that activin A expression is elevated in adipose tissue from obese subjects, and dramatically increased by factors secreted by macrophages isolated from obese adipose tissue.[45] Therefore, it seems likely that at least the accumulation of activin A in CM-EAT-T2D can be ascribed to inflammation, and presumably monocyte infiltration into the EAT in T2D.

In conclusion, the present study indicates that CM-EAT from patients with T2D causes myocardial dysfunction and induces insulin resistance in primary rat cardiomyocytes. Our data also demonstrate that the secretory profile of EAT is considerably different from SAT and PAT and that this secretion pattern differs between ND- and T2D-patients. Furthermore, in this study we report for the first time that the release of activin A and angiopoietin-2 are elevated by EAT from T2D-patients and that these factors contribute to cardiomyocyte dysfunction. Therefore, the present study suggests that T2D-related alterations in the secretory profile of EAT could contribute to the pathogenesis of cardiac dysfunction in T2D.

Clinical Perspective

Cardiac contractile dysfunction and myocardial insulin resistance frequently occur in patients with type 2 diabetes mellitus. Recent studies link adipose tissue– derived factors, termed adipokines, to the pathogenesis of these cardiac alterations. Epicardial adipose tissue a visceral thoracic fat depot surrounding the aortic arch, the large coronary arteries, the ventricles, and the apex of the human heart. Because no fascial boundaries separate the epicardial adipose tissue from the myocardium, factors released from this fat depot may directly affect the underlying tissues. In patients with type 2 diabetes mellitus, the adipose tissue is characterized by a chronic state of inflammation, which results in alterations in adipokine secretion. The present studies investigated whether alterations in the secretory profile of epicardial adipose tissue in patients with type 2 diabetes mellitus occur, and whether these alterations affect contractile function and insulin sensitivity in rat cardiomyocytes. Epicardial biopsies of patients with type 2 diabetes mellitus were characterized by clusters of CD14-positive monocytes and CD68-positive macrophages, which are both indicative of inflammation. Exposing cardiomyocytes to conditioned media prepared from epicardial adipose tissue from patients with type 2 diabetes mellitus induced reductions in contractile function and insulin resistance. These effects could be ascribed to a selective accumulation of activin A and angiopoietin-2 in the conditioned media. Collectively, these data show that inflammation of epicardial adipose tissue in patients with type 2 diabetes mellitus is associated with alterations in adipokine secretion, which may contribute to the pathogenesis of type 2 diabetes mellitus–related heart disease.

Sources of funding

This work was supported by the Federal Ministry of Health, the Ministry of Innovation, Science, Research and Technology of the German State of North-Rhine Westphalia, and the Commission of the European Communities (Collaborative Project ADAPT, contract no. HEALTH-F2–2008–201100).

Acknowledgements

We thank Peter Roesen (German Diabetes Center, Duesseldorf, Germany), Artur Lichtenberg, Emmeran Gams (both Department of Cardiovascular Surgery, Heinrich Heine University, Duesseldorf, Germany), and Peter ten Dijke (Dept. Molecular Cell Biology, Leiden University Medical Center, Leiden, The Netherlands) for critical discussions.

Duality of interest

The authors have no conflicts of interest.

Table 2.1: Patient characteristics.

	ND (n=11)	T2D (n=11)	*P*
Age (years)	72.4 ± 1.7	72.8 ±2.3	0.898
Blood glucose level (mg/dL)	97.2 ± 3.9	173 ± 22	<0.001
BMI (kg/m^2)	29.0 ± 1.4	29.6 ± 1.2	0.699
Medication use			
Statins	7	7	1.000
ACE	7	6	1.000
β-blockers	7	5	0.670
diuretics	6	5	1.000
glucose lowering medication	0	9	<0.001

Anthropometric characteristics are expressed as mean ± standard error of the mean, and differences between the anthropometric parameters between the disease groups were evaluated using a Mann-Whitney U-test, while differences in medication use were determined using a Fisher's exact test.; ND, non-diabetic; T2D, type 2 diabetes; ACE, angiotensin-converting enzyme inhibitor; BMI, body mass index.

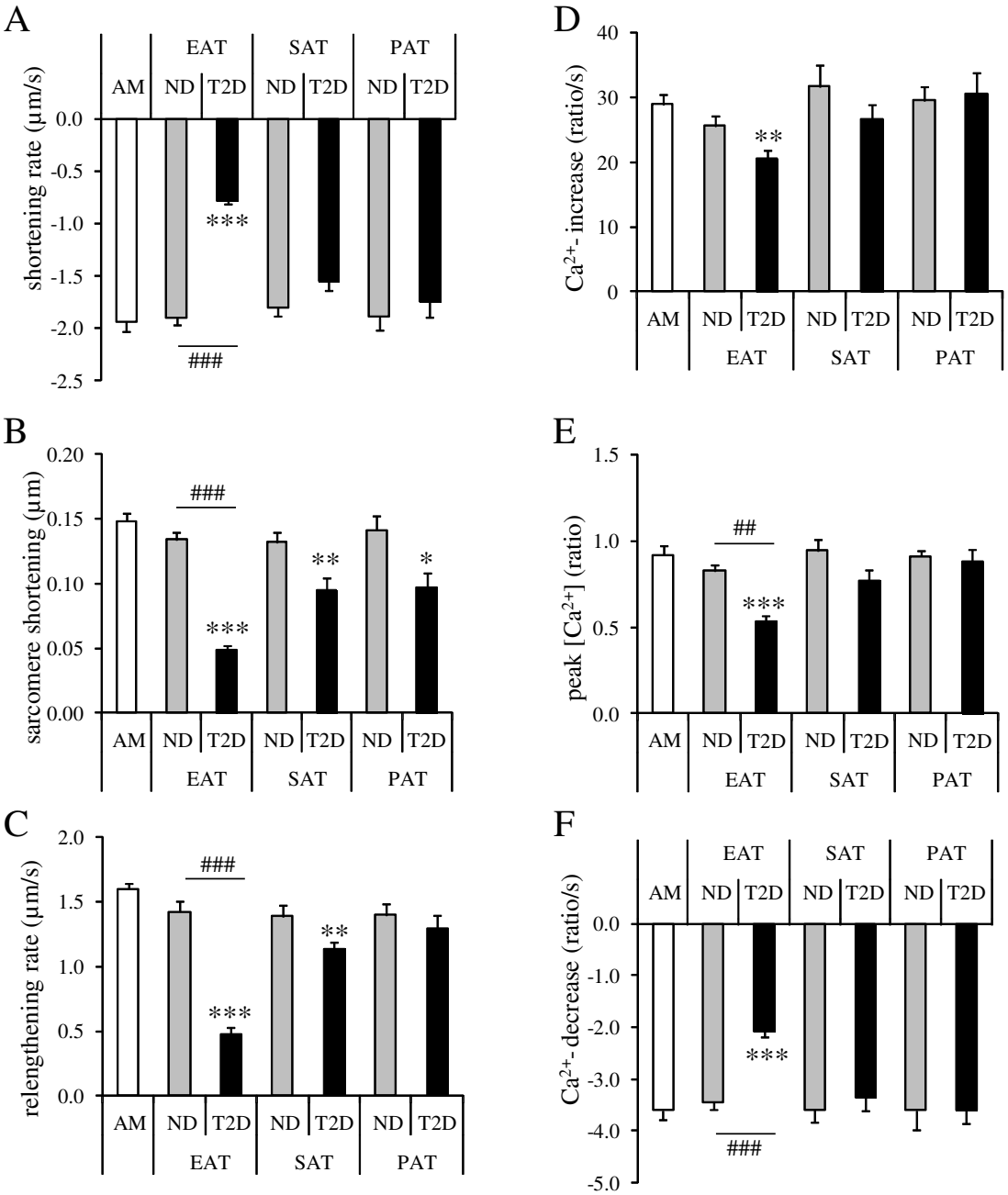

Figure 2.1: Effect of conditioned media from human epicardial (EAT), subcutaneous (SAT) and pericardial adipose tissue (PAT) on cardiomyocyte contractile function. Primary adult rat cardiomyocytes were exposed to control adipocyte medium (AM) or CM (diluted 1:4) from EAT, SAT, and PAT from patients with type 2 diabetes mellitus (T2D) and without (ND) for 30 minutes before analysis of sarcomere shortening and Ca^{2+} fluxes. Effect of AM or CM on departure velocity of contraction (A), peak sarcomere shortening (B), and return velocity of contraction (C). Response of cardiomyocytes to AM or CM on cytosolic [Ca^{2+}] increases (D), peak Fura-2 fluorescence signal (E), and cytosolic [Ca^{2+}] decreases (F). Open bars indicate AM; gray bars, CM from ND-patients; and black bars, CM from T2D patients. Data were collected during at least 8 independent experiments using cardiomyocyte preparations from different rats and CM from different donors, and are expressed as mean±SEM. Differences among the groups were evaluated using the Kruskal–Wallis method followed by a Dunns multiple comparison test. ***P<0.001, **P<0.01, *P<0.05 vs control AM, ###P<0.001 ND vs T2D.

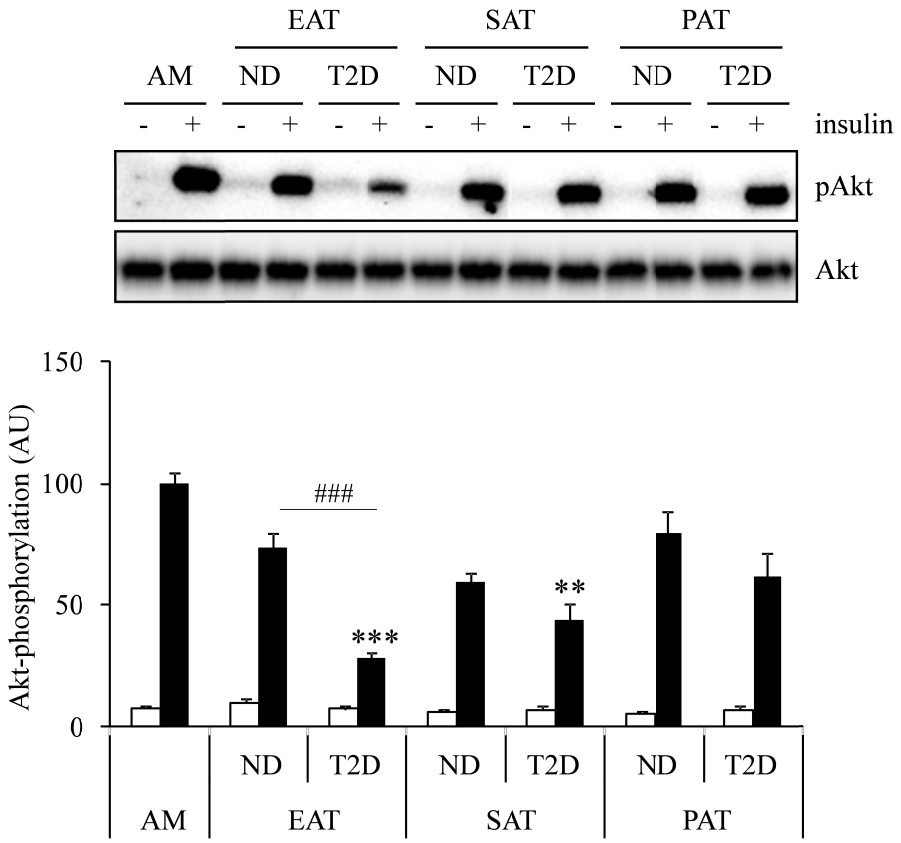

Figure 2.2: Effect of conditioned medium on insulin action in primary adult rat cardiomyocytes. Representative Western blots and quantification of insulin-induced Akt-Ser473 phosphorylation in cardiomyocytes treated with control adipocyte medium (AM) or conditioned media (CM, diluted 1:6) from epicardial (EAT), subcutaneous (SAT) and pericardial adipose tissue (PAT) from patients with type 2 diabetes (T2D) and without (ND) for 24 h. Data were collected during at least 6 independent experiments using cardiomyocyte preparations from different rats and CM from different donors, and are expressed as mean ± SEM. Open bars indicate basal; filled bars, insulin stimulated cells (10 minutes; 100 nmol/L). Differences among the groups were evaluated using the Kruskal-Wallis method followed by a Dunns multiple comparison test. ***P<0.001, **P<0.01, vs control AM; ###, P<0.001 ND versus T2D.

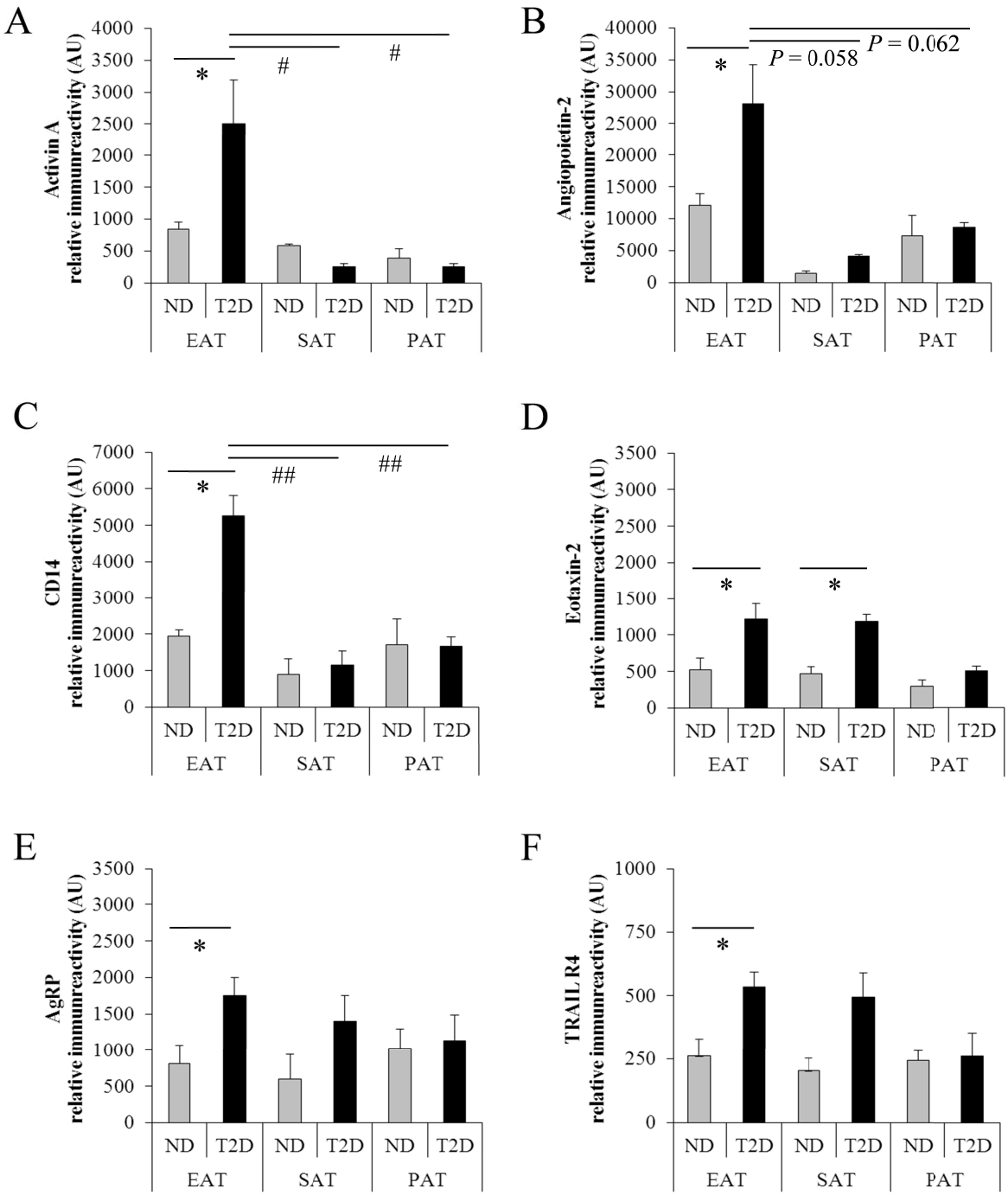

Figure 2.3: Adipokine immunoreactivity in conditioned media (CM) from epicardial (EAT), subcutaneous (SAT) and pericardial adipose tissue (PAT) from patients with type 2 diabetes (T2D) and without (ND). CM from EAT, SAT and PAT from ND- and T2D patients was profiled using antibody arrays. Shown is the immunoreactivity for activin A (A), angiopoietin-2 (B), CD14 (C), eotaxin-2 (D), AgRP (E), and TRAIL R4 (F). Gray bars indicate CM from ND-patients; black bars, CM from T2D-patients. Values are expressed as mean ± SEM (n=4 per group). Differences between ND and T2D for each depot were evaluated using a Mann-Whitney *U* test; **P*<0.05 ND vs T2D. Differences between the various depots were analyzed using a paired t-test; ##*P*<0.01, #*P*<0.05 for T2D-EAT vs T2D-SAT, and T2D-EAT vs T2D-PAT, respectively.

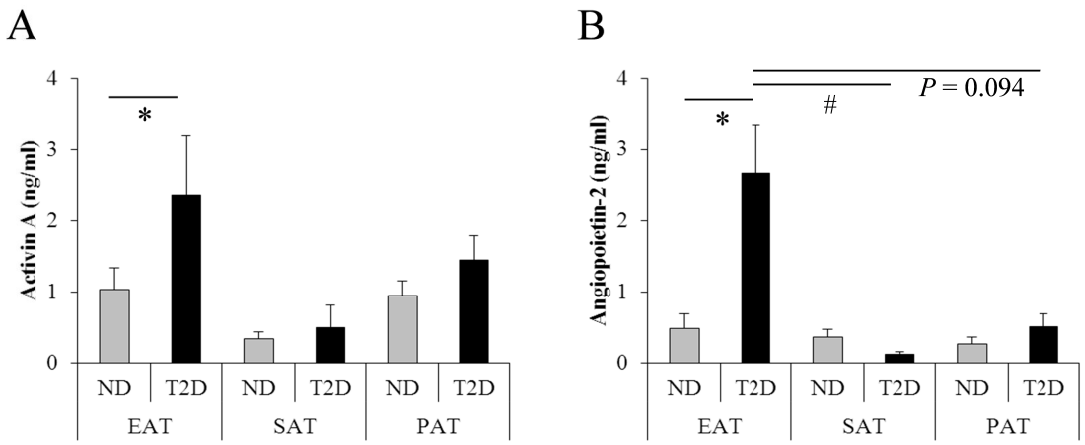

Figure 2.4: Activin A and angiopoietin-2 levels in conditioned media from epicardial (EAT), subcutaneous (SAT), and pericardial adipose tissue (PAT) from patients with type 2 diabetes mellitus (T2D) and without (ND). Activin A (A) and angiopoietin-2 (B) content was determined using enzyme-linked immunoabsorbent assays. Gray bars indicate CM from ND patients; black bars, CM from T2D patients. Values are expressed as mean ± SEM (n=6 per group). Differences between ND and T2D for each depot were evaluated using a Mann–Whitney *U* test; **P*<0.05 ND vs T2D. Differences between the various depots were analyzed using a paired t-test; #*P*<0.05 for T2D-EAT vs T2D-SAT.

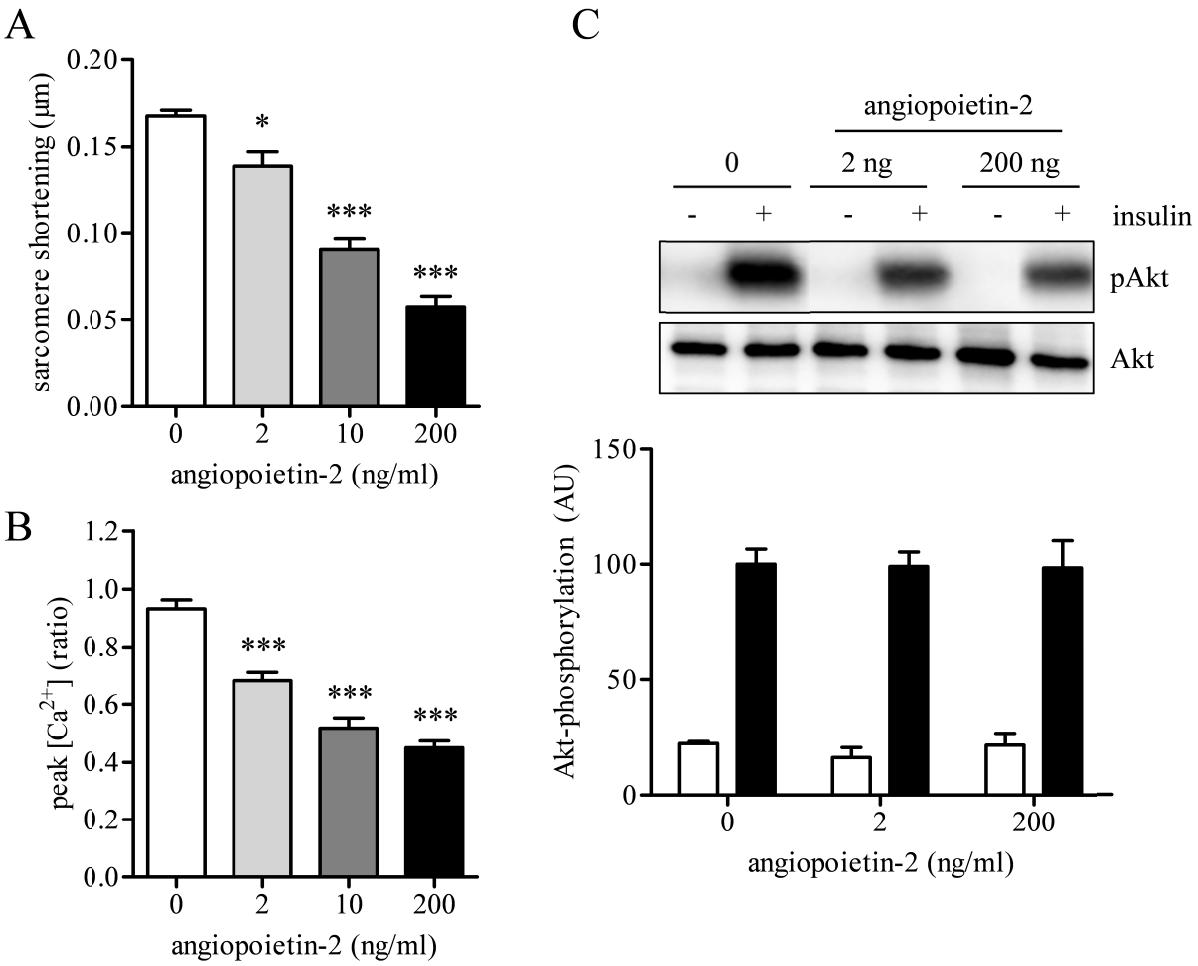

Figure 2.5: Effect of angiopoietin-2 on cardiomyocyte function. Dose-dependent effect of a 30 min exposure of primary adult rat cardiomyocytes to recombinant angiopoietin-2 on peak sarcomere shortening (A), and peak Fura-2 fluorescence signal (B). Data were collected in 4 independent experiments using cardiomyocyte preparations from different rats and are expressed as mean SEM. C. Effect of 24-h exposure to angiopoietin-2 of primary human adult cardiomyocytes on insulin-induced Akt-Ser473-phosphorylation. Data are presented as mean±SEM (n=5 per group). Open bars indicate basal; filled bars, insulin-stimulated cells (10 minutes; 100 nmol/L). The effect of the various angiopoietin-2 concentrations on cardiomyocyte function was evaluated using the Kruskal-Wallis method followed by a Dunns multiple comparison test. ***P<0.001, *P<0.05, vs control adipocyte medium (0) without angiopoietin-2.

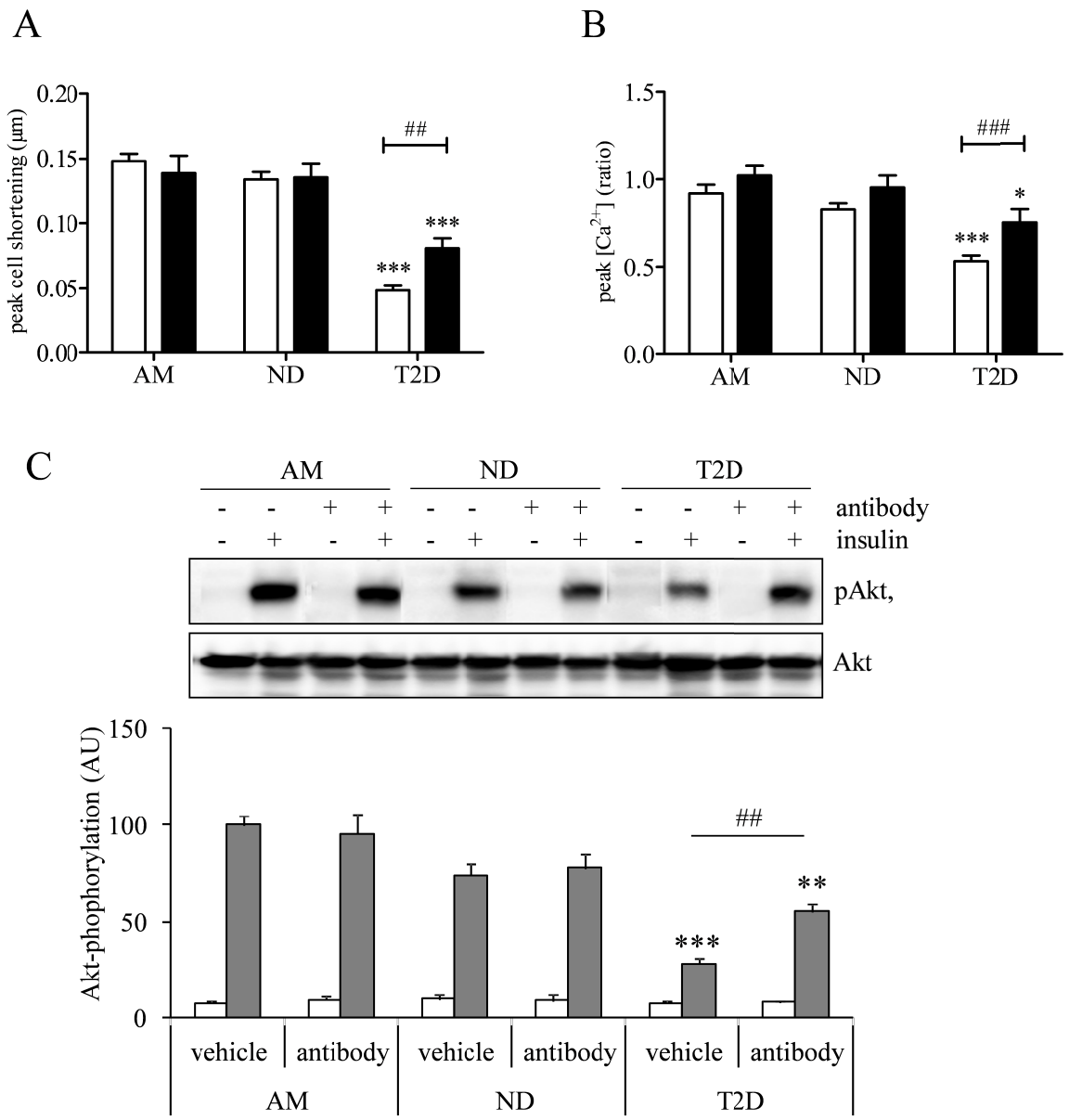

Figure 2.6: Effect of a neutralizing activin A antibody on the detrimental effects induced by CM-EAT in cardiomyocytes. Control adipocyte medium (AM), or conditioned media (CM) from epicardial adipose tissue (EAT) of patients with type 2 diabetes (T2D) or without (ND) were preincubated with an activin A neutralizing antibody before incubation with cardiomyocytes. Shown are the effects of activin A neutralizing antibody on peak sarcomere shortening (A), peak Fura-2 fluorescence signal (B), and insulin-mediated pAkt-Ser473-phosphorylation (C). For A and B, open bars indicate no antibody; black bars, neutralizing activin A antibody. For C, open bars indicate basal; gray bars, insulin-stimulated cells (10 minutes; 100 nmol/L). Values are expressed as mean±SEM of at least 4 independent experiments using cardiomyocyte preparations from different rats and CM from different donors. Differences among the groups were evaluated using the Kruskal–Wallis method followed by a Dunns multiple comparison test. ***P<0.001, *P<0.05, vs control AM; ###P<0.001, ##P<0.01, CM with or without neutralizing antibody.

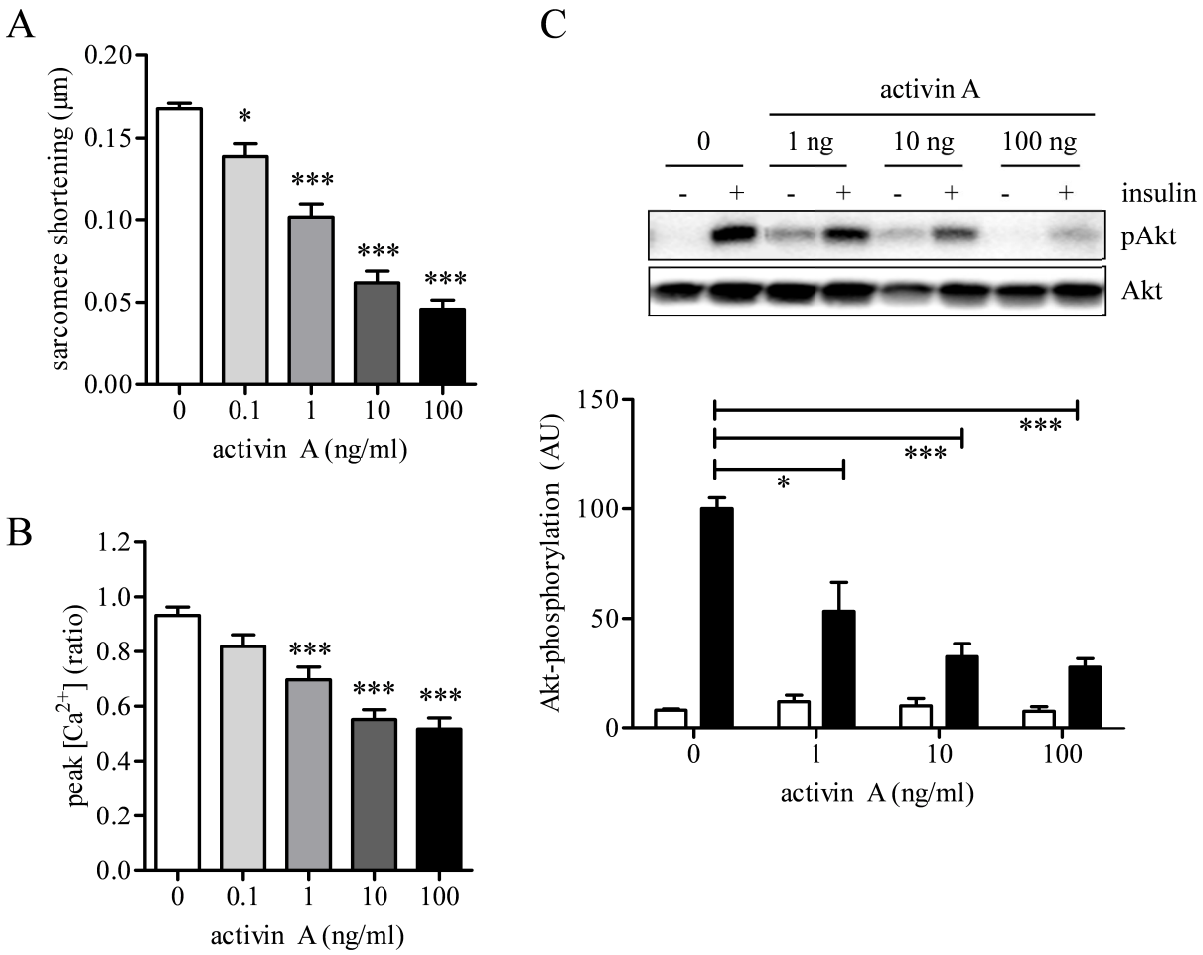

Figure 2.7: Effect of activin A on cardiomyocyte function. Dose-dependent effect of a 30-minute exposure of primary adult rat cardiomyocytes to recombinant activin A on peak sarcomere shortening (A) and peak Fura-2 fluorescence signal (B). Data were collected in 4 independent experiments using cardiomyocyte preparations from different rats and are expressed as mean±SEM. C, Effect of 24-hour exposure of primary rat adult cardiomyocytes to activin A on insulin-induced Akt-Ser473-phosphorylation. Data are presented as mean±SEM (n=6 per group). Open bars indicate basal; filled bars, insulin-stimulated cells (10 minutes; 100 nmol/L). The effect of the various activin A concentrations on cardiomyocyte function was evaluated using the Kruskal–Wallis method followed by a Dunns multiple comparison test. ***P<0.001, *P<0.05, vs control adipocyte medium (0) without activin A.

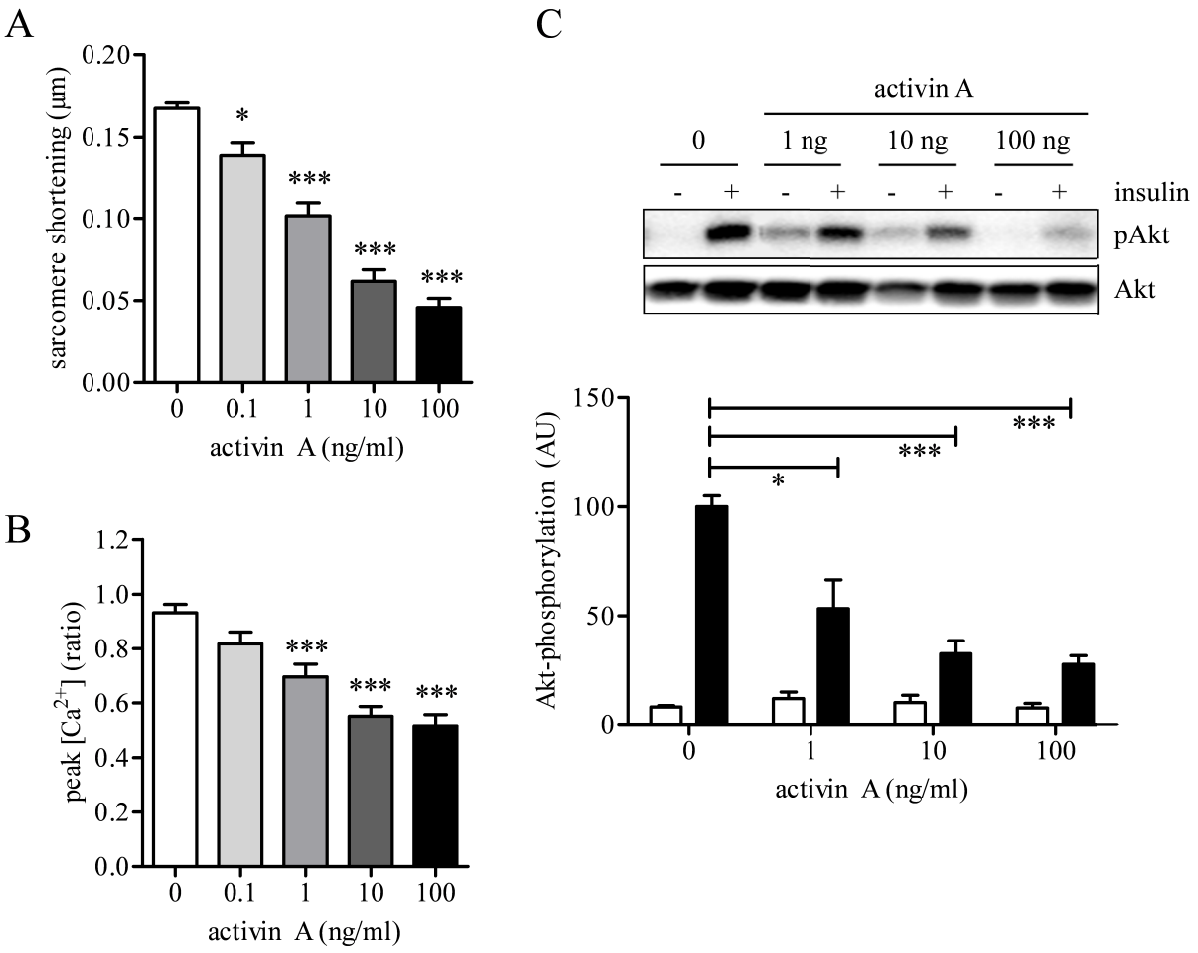

Figure 2.8: Effect of conditioned media (CM), activin A and angiopoietin-2 on SERCA2a expression. Representative Western blots and quantification of sarcoplasmic endoplasmic reticulum ATPase 2a protein expression in cardiomyocytes exposed for 30 minutes to control adipocyte medium (AM), CM from epicardial adipose tissue (EAT) from patients with type 2 diabetes (T2D) and without (ND), recombinant activin A, or recombinant angiopoietin-2. Data were collected in at least 4 independent experiments using cardiomyocyte preparations from different rats and CM from different donors and are expressed as mean±SEM. Differences among the groups were evaluated using the Kruskal–Wallis method followed by a Dunns multiple comparison test. $^{**}P<0.01$ vs control adipocyte medium (0).

References

[1] Boudina S, Abel ED (2010) Diabetic cardiomyopathy, causes and effects. Rev.Endocr.Metab Disord. 11: 31-39

[2] Sacks HS, Fain JN (2007) Human epicardial adipose tissue: a review. Am.Heart J. 153: 907-917

[3] Iacobellis G, Willens HJ (2009) Echocardiographic epicardial fat: a review of research and clinical applications. J.Am.Soc.Echocardiogr. 22: 1311-1319

[4] Rabkin SW (2007) Epicardial fat: properties, function and relationship to obesity. Obes.Rev. 8: 253-261

[5] Ouwens DM, Sell H, Greulich S, Eckel J (2010) The role of epicardial and perivascular adipose tissue in the pathophysiology of cardiovascular disease. J.Cell Mol.Med 14: 2223-2234

[6] Iacobellis G, Corradi D, Sharma AM (2005) Epicardial adipose tissue: anatomic, biomolecular and clinical relationships with the heart. Nat.Clin.Pract.Cardiovasc.Med. 2: 536-543

[7] Iacobellis G, Barbaro G (2008) The double role of epicardial adipose tissue as pro- and anti-inflammatory organ. Horm.Metab Res. 40: 442-445

[8] Baker AR, Silva NF, Quinn DW, et al (2006) Human epicardial adipose tissue expresses a pathogenic profile of adipocytokines in patients with cardiovascular disease. Cardiovasc.Diabetol. 5: 1

[9] Iacobellis G, Pistilli D, Gucciardo M, et al (2005) Adiponectin expression in human epicardial adipose tissue in vivo is lower in patients with coronary artery disease. Cytokine 29: 251-255

[10] Kremen J, Dolinkova M, Krajickova J, et al (2006) Increased subcutaneous and epicardial adipose tissue production of proinflammatory cytokines in cardiac surgery patients: possible role in postoperative insulin resistance. J.Clin.Endocrinol.Metab 91: 4620-4627

[11] Mazurek T, Zhang L, Zalewski A, et al (2003) Human epicardial adipose tissue is a source of inflammatory mediators. Circulation 108: 2460-2466

[12] Chaldakov GN, Fiore M, Stankulov IS, et al (2004) Neurotrophin presence in human coronary atherosclerosis and metabolic syndrome: a role for NGF and BDNF in cardiovascular disease? Prog.Brain Res. 146: 279-289

[13] Vural B, Atalar F, Ciftci C, et al (2008) Presence of fatty-acid-binding protein 4 expression in human epicardial adipose tissue in metabolic syndrome. Cardiovasc.Pathol. 17: 392-398

[14] Fain JN, Sacks HS, Buehrer B, et al (2008) Identification of omentin mRNA in human epicardial adipose tissue: comparison to omentin in subcutaneous, internal

mammary artery periadventitial and visceral abdominal depots. Int.J.Obes.(Lond) 32: 810-815

[15] Karastergiou K, Evans I, Ogston N, et al (2010) Epicardial adipokines in obesity and coronary artery disease induce atherogenic changes in monocytes and endothelial cells. Arterioscler.Thromb.Vasc.Biol. 30: 1340-1346

[16] Greulich S, De Wiza DH, Preilowksi S, et al (2011) Secretory products of guinea pig epicardial fat induce insulin resistance and impair primary adult rat cardiomyocyte function. J.Cell Mol.Med 15: 2399-2410

[17] Iacobellis G, di Gioia CR, Cotesta D, et al (2009) Epicardial adipose tissue adiponectin expression is related to intracoronary adiponectin levels. Horm.Metab Res. 41: 227-231

[18] Moro C, Klimcakova E, Lolmede K, et al (2007) Atrial natriuretic peptide inhibits the production of adipokines and cytokines linked to inflammation and insulin resistance in human subcutaneous adipose tissue. Diabetologia 50: 1038-1047

[19] Thalmann S, Juge-Aubry CE, Meier CA (2008) Explant cultures of white adipose tissue. Methods Mol.Biol. 456: 195-199

[20] Eckel J, Pandalis G, Reinauer H (1983) Insulin action on the glucose transport system in isolated cardiocytes from adult rat. Biochem.J. 212: 385-392

[21] ten Dijke P, Arthur HM (2007) Extracellular control of TGFbeta signalling in vascular development and disease. Nat.Rev.Mol.Cell Biol. 8: 857-869

[22] Lebeche D, Davidoff AJ, Hajjar RJ (2008) Interplay between impaired calcium regulation and insulin signaling abnormalities in diabetic cardiomyopathy. Nat.Clin.Pract.Cardiovasc.Med 5: 715-724

[23] Periasamy M, Bhupathy P, Babu GJ (2008) Regulation of sarcoplasmic reticulum Ca2+ ATPase pump expression and its relevance to cardiac muscle physiology and pathology. Cardiovasc.Res. 77: 265-273

[24] Lamounier-Zepter V, Look C, Alvarez J, et al (2009) Adipocyte fatty acid-binding protein suppresses cardiomyocyte contraction: a new link between obesity and heart disease. Circ.Res. 105: 326-334

[25] Look C, Morano I, Ehrhart-Bornstein M, Bornstein SR, Lamounier-Zepter V (2011) Adipocyte-derived factors suppress heart contraction. Int.J.Obes.(Lond) 35: 84-90

[26] Look C, Morano I, Lamounier-Zepter V (2008) Human adipocyte-derived factors directly inhibit cardiac contraction. J.Muscle Res.Cell Motil. 29: 181-184

[27] Maass DL, White J, Horton JW (2002) IL-1beta and IL-6 act synergistically with TNF-alpha to alter cardiac contractile function after burn trauma. Shock. 18: 360-366

[28] Kumar A, Thota V, Dee L, Olson J, Uretz E, Parrillo JE (1996) Tumor necrosis factor alpha and interleukin 1beta are responsible for in vitro myocardial cell depression induced by human septic shock serum. J.Exp.Med. 183: 949-958

[29] Weisensee D, Bereiter-Hahn J, Schoeppe W, Low-Friedrich I (1993) Effects of cytokines on the contractility of cultured cardiac myocytes. Int.J.Immunopharmacol. 15: 581-587

[30] Radin MJ, Holycross BJ, Dumitrescu C, Kelley R, Altschuld RA (2008) Leptin modulates the negative inotropic effect of interleukin-1beta in cardiac myocytes. Mol.Cell Biochem. 315: 179-184

[31] Ouwens DM, Diamant M (2007) Myocardial insulin action and the contribution of insulin resistance to the pathogenesis of diabetic cardiomyopathy. Arch Physiol Biochem. 113: 76-86

[32] Rijzewijk LJ, van der Meer RW, Lamb HJ, et al (2009) Altered myocardial substrate metabolism and decreased diastolic function in nonischemic human diabetic cardiomyopathy: studies with cardiac positron emission tomography and magnetic resonance imaging. J.Am.Coll.Cardiol. 54: 1524-1532

[33] Yndestad A, Ueland T, Oie E, et al (2004) Elevated levels of activin A in heart failure: potential role in myocardial remodeling. Circulation 109: 1379-1385

[34] Andersen GO, Ueland T, Knudsen EC, et al (2011) Activin A levels are associated with abnormal glucose regulation in patients with myocardial infarction: potential counteracting effects of activin A on inflammation. Diabetes 60: 1544-1551

[35] Oshima Y, Ouchi N, Shimano M, et al (2009) Activin A and follistatin-like 3 determine the susceptibility of heart to ischemic injury. Circulation 120: 1606-1615

[36] Mo H, Liu S, Zhou Z, et al (2010) Change of serum soluble CD14 level in newly diagnosed Type 2 diabetes and its significance. Zhong.Nan.Da.Xue.Xue.Bao.Yi.Xue.Ban. 35: 699-704

[37] Lieb W, Zachariah JP, Xanthakis V, et al (2010) Clinical and genetic correlates of circulating angiopoietin-2 and soluble Tie-2 in the community. Circ.Cardiovasc.Genet. 3: 300-306

[38] Bourlier V, Bouloumie A (2009) Role of macrophage tissue infiltration in obesity and insulin resistance. Diabetes Metab 35: 251-260

[39] Olefsky JM, Glass CK (2010) Macrophages, inflammation, and insulin resistance. Annu.Rev.Physiol 72: 219-246

[40] Bluher M (2009) Adipose tissue dysfunction in obesity. Exp.Clin.Endocrinol.Diabetes 117: 241-250

[41] Zhou Y, Wei Y, Wang L, et al (2011) Decreased adiponectin and increased inflammation expression in epicardial adipose tissue in coronary artery disease. Cardiovasc.Diabetol. 10: 2

[42] Hirata Y, Tabata M, Kurobe H, et al (2011) Coronary atherosclerosis is associated with macrophage polarization in epicardial adipose tissue. J.Am.Coll.Cardiol. 58: 248-255

[43] Hirata Y, Kurobe H, Akaike M, et al (2011) Enhanced inflammation in epicardial fat in patients with coronary artery disease. Int.Heart J. 52: 139-142

[44] Abe M, Shintani Y, Eto Y, Harada K, Kosaka M, Matsumoto T (2002) Potent induction of activin A secretion from monocytes and bone marrow stromal fibroblasts by cognate interaction with activated T cells. J.Leukoc.Biol. 72: 347-352

[45] Zaragosi LE, Wdziekonski B, Villageois P, et al (2010) Activin A Plays a Critical Role in Proliferation and Differentiation of Human Adipose Progenitors. Diabetes 59: 2513-2521

Supplementary Table 2.1: Immunoreactivity in conditioned media generated from epicardial adipose tissue explants from patients without (ND) and with type 2 diabetes (T2D).

Swiss Prot	Name on array	Symbol	ND (n=4)	T2D (n=4)	*P*
Q15848	Acrp30	ADIPOQ	103593 ± 36671	56030 ± 24285	0.386
P08476	Activin A	INHBA	842 ± 115	3023 ± 623	0.043
O00253	AgRP	AGRP	817 ± 248	1757 ± 245	0.043
Q13740	ALCAM	ALCAM	540 ± 116	536 ± 314	0.386
P15514	Amphiregulin	AREG	540 ± 202	677 ± 206	0.248
P03950	Angiogenin	ANG	3477 ± 1153	11415 ± 7505	0.564
O15123	Angiopoietin-2	ANGPT2	12111 ± 1819	28157 ± 6077	0.021
P30530	Axl	AXL	466 ± 254	610 ± 305	0.564
P33681	B7-1 (CD80)	CD80	795 ± 122	744 ± 321	0.773
P23560	BDNF	BDNF	246 ± 62	384 ± 153	0.564
P09038	bFGF	FGF2	1296 ± 220	854 ± 288	0.289
O43927	BLC	CXCL13	78 ± 29	76 ± 17	0.773
P12644	BMP-4	BMP4	291 ± 64	439 ± 211	0.773
P22003	BMP-5	BMP5	590 ± 77	408 ± 235	0.386
P22004	BMP-6	BMP6	482 ± 63	929 ± 427	0.564
P18075	BMP-7	BMP7	276 ± 56	316 ± 163	1.000
P01138	b-NGF	NGF	641 ± 444	257 ± 43	1.000
P35070	BTC	BTC	838 ± 496	799 ± 267	0.773
Q16619	Cardiotrophin-1	CTF1	530 ± 40	611 ±378	0.480
Q9NRJ3	CCL-28	CCL28	630 ± 541	251 ± 145	1.000
P08571	CD14	CD14	1952 ± 154	5260 ± 555	0.021
P55773	CK b 8-1	CCL23	363 ± 172	435 ± 152	0.386
P26441	CNTF	CNTF	164 ± 51	127 ± 44	0.724
Q9Y4X3	CTACK	CCL27	366 ± 103	122 ± 31	0.149
Q9H2A7	CXCL-16	CXCL16	631 ± 121	787 ± 184	0.386
O75509	DR6 (TNFRSF21)	TNFRSF21	283 ± 41	408 ± 222	0.724
Q06418	Dtk	TYRO3	240 ± 50	214 ± 41	0.724
P01133	EGF	EGF	772 ± 142	817 ± 205	0.773
P00533	EGF-R	EGFR	214 ± 71	379 ± 131	0.564
P42830	ENA-78	CXCL5	44663 ± 23528	9349 ± 6047	0.083
P17813	Endoglin	ENG	571 ± 108	338 ± 232	0.248
P51671	Eotaxin	CCL11	171 ± 36	80 ± 21	0.083
O00175	Eotaxin-2	CCL24	521 ± 158	1213 ± 221	0.043
Q9Y258	Eotaxin-3	CCL26	129 ± 39	207 ± 93	0.564
P21860	ErbB3	ERBB3	1001 ± 117	705 ± 428	0.248
P16581	E-Selectin	SELE	392 ± 84	252 ± 172	0.248
P48023	Fas Ligand	FASLG	393 ± 57	254 ± 122	0.386
Q549F0	Fas/TNFRSF6	FAF1	3542 ± 2478	3283 ± 2028	1.000
P08620	FGF-4	FGF4	7238 ± 2279	5411 ± 1856	0.386
P10767	FGF-6	FGF6	240 ± 101	288 ± 75	0.564
P21781	FGF-7	FGF7	188 ± 58	203 ± 73	1.000
P31371	FGF-9	FGF9	584 ± 126	579 ± 23	0.468
P49771	Fit-3 Ligand	FLT3LG	165 ± 34	97 ± 35	0.083
P78423	Fractalkine	CX3CL1	129 ± 18	72 ± 36	0.165
P80162	GCP-2	CXCL6	2709 ± 1182	2535 ± 1976	0.564
P09919	GCSF	CSF3	326 ± 122	434 ± 189	0.773
P39905	GDNF	GDNF	590 ± 79	823 ± 292	0.773
Q9Y5U5	GITR	TNFRSF18	3981 ± 1242	2204 ± 663	0.149
Q9UNG2	GITR-Ligand	TNFSF18	281 ± 105	343 ± 131	0.564
P04141	GM-CSF	CSF2	675 ± 107	2005 ± 1882	0.248
P09341	GRO	CXCL1	303092 ± 103372	199124 ± 49973	0.386
P09341	GROα	CXCL1	78485 ± 25344	23553 ± 14967	0.083

O15467	HCC-4	CCL16	455 ± 121	548 ± 195	0.773
P14210	HGF	HGF	36768 ± 11706	53397 ± 12016	0.248
P22362	I-309	CCL1	208 ± 77	174 ± 25	0.773
P05362	ICAM-1	ICAM1	4064 ± 1173	11417 ± 2852	0.149
P13598	ICAM-2	ICAM2	6275 ± 2610	4168 ± 1031	0.564
P32942	ICAM-3	ICAM3	335 ± 120	398 ± 153	0.564
P01343	IGF-1	IGF1	121 ± 30	322 ± 149	0.248
P08833	IGFBP-1	IGFBP1	235 ± 47	467 ± 97	0.083
P18065	IGFBP-2	IGFBP2	385 ± 69	485 ± 35	0.149
P17936	IGFBP-3	IGFBP3	602 ± 69	523 ± 153	0.773
P22692	IGFBP-4	IGFBP4	928 ± 48	1545 ± 665	1.000
P24592	IGFBP-6	IGFBP6	1318 ± 462	774 ± 333	0.564
P08069	IGF-I SR	IGF1R	153 ± 30	224 ± 104	0.772
P01344	IGF-II	IGF2	3045 ± 324	3978 ± 1184	1.000
P27930	IL-1 R II	IL1R2	7058 ± 1691	4856 ± 1553	0.248
Q01638	IL-1 RA/ST2	IL1RL1	1006 ± 272	545 ± 217	0.149
P14778	IL-1 RI	IL1R1	105 ± 24	115 ± 41	0.772
P22301	IL-10	IL10	1140 ± 491	3709 ± 3023	1.000
Q08334	IL-10 Rβ	IL10RB	409 ± 78	374 ± 254	0.309
P20809	IL-11	IL11	142 ± 61	151 ± 105	0.724
P29459	IL-12 p40	IL12A	1780 ± 869	1046 ± 210	0.564
P29460	IL-12 p70	IL12B	253 ± 44	156 ± 22	0.083
P35225	IL-13	IL13	150 ± 105	194 ± 82	0.564
Q14627	IL-13 Rα2	IL13RA2	1205 ± 444	1312 ± 1051	0.386
P40933	IL-15	IL15	99 ± 40	149 ± 133	0.480
Q14005	IL-16	IL16	236 ± 48	410 ± 127	0.289
Q16552	IL-17	IL17A	157 ± 51	648 ± 3121	0.386
Q13478	IL-18 BPα	IL18R1	377 ± 15	398 ± 297	0.480
O95256	IL-18 Rβ	IL18RAP	1168 ± 302	1024 ± 704	0.386
P01583	IL-1a	IL1A	479 ± 118	622 ± 189	0.564
P01584	IL-1b	IL1B	143 ± 29	277 ± 142	0.564
P18510	IL-1ra	IL1RN	310 ± 94	181 ± 22	0.386
P60568	IL-2	IL2	87 ± 24	39 ± 20	0.289
P31785	IL-2 Rg	IL2RG	545 ± 51	573 ± 354	1.000
P01589	IL-2 Rα	IL2RA	344 ± 53	425 ± 26	0.149
P14784	IL-2 Rβ	IL2RB	294 ± 108	436 ± 72	0.480
Q9HBE5	IL-21R	IL21R	522 ± 44	299 ± 166	0.248
P08700	IL-3	IL3	138 ± 36	55 ± 14	0.245
P05112	IL-4	IL4	259 ± 101	116 ± 5	0.289
P05113	IL-5	IL5	3714 ± 1001	2140 ± 481	0.149
Q01344	IL-5 Rα	IL5RA	624 ± 123	396 ± 264	0.248
P05231	IL-6	IL6	888441 ± 30874	605767 ± 177670	0.564
P08887	IL-6R	IL6R	9270 ± 3607	1949 ± 685	0.149
P13232	IL-7	IL7	345 ± 127	584 ± 335	0.773
P10145	IL-8	IL8	209915 ± 79553	74004 ± 33505	0.248
P15248	IL-9	IL9	434 ± 29	288 ± 158	0.248
P01579	INFg	IFNG	128 ± 24	143 ± 26	0.724
P02778	IP-10	CXCL10	2767 ± 517	1620 ± 733	0.149
O14625	I-TAC	CXCL11	201 ± 45	406 ± 177	0.386
P17676	LAP	CEBPB	979 ± 187	908 ± 410	0.564
P41159	Leptin	LEP	5657 ± 4143	39186 ± 38128	0.773
P48357	Leptin R	LEPR	461 ± 116	552 ± 336	1.000
P15018	LIF	LIF	1138 ± 356	777 ± 250	0.564
O43557	LIGHT	TNFSF14	936 ± 227	1295 ± 449	0.564
P14151	L-Selectin	SELL	331 ± 75	339 ± 180	0.564
P47992	Lymphotactin	XCL1	232 ± 83	424 ± 201	0.772

P13500	MCP-1	CCL2	291590 ± 94218	171828 ± 41996	0.386
P80075	MCP-2	CCL8	71914 ± 33617	54150 ± 32994	0.386
P80098	MCP-3	CCL7	4262 ± 2614	29015 ± 28278	0.289
Q99616	MCP-4	CCL13	210 ± 67	555 ± 364	0.564
P09603	M-CSF	CSF1	627 ± 58	726 ± 222	0.773
P07333	M-CSF R	CSF1R	558 ± 78	618 ± 336	0.386
O00626	MDC	CCL22	247 ± 115	301 ± 97	0.773
P14174	MIF	MIF	1475 ± 235	1648 ± 397	0.773
Q07325	MIG	CXCL9	256 ± 144	230 ± 105	0.773
P10147	MIP-1a	CCL3	40864 ± 9020	19817 ± 18123	0.248
P13236	MIP-1b	CCL4	64582 ± 17447	22821 ± 11863	0.083
Q16663	MIP-1d	CCL15	144 ± 62	319 ± 148	0.386
P78556	MIP-3a	CCL20	1067 ± 803	1207 ± 885	1.000
Q99731	MIP-3b	CCL19	2104 ± 925	765 ± 331	0.248
P03956	MMP-1	MMP1	4604 ± 750	5940 ± 3034	0.245
P45452	MMP-13	MMP13	627 ± 111	641 ± 365	0.386
P08254	MMP-3	MMP3	6138 ± 2079	2882 ± 497	0.248
P14780	MMP-9	MMP9	2292 ± 270	2672 ± 1774	0.248
P55773	MPIF-1	CCL23	394 ± 42	363 ± 236	0.248
P26927	MSPa	MST1	869 ± 135	662 ± 193	0.289
P02775	NAP-2	PPBP	5118 ± 1566	14235 ± 5364	0.083
P08138	NGF R	NGFR	277 ± 76	702 ± 518	0.724
P20783	NT-3	NTF3	476 ± 112	844 ± 224	0.149
P34130	NT-4	NTF4	290 ± 146	410 ± 160	0.480
P13725	Oncostatin	OSM	357 ± 82	272 ± 49	0.564
O00300	Osteoprotegerin	TNFRSF11B	829 ± 278	1502 ± 577	0.289
P55774	PARC	CCL18	129 ± 31	440 ± 208	0.480
P04085	PDGF AA	PDGFA	1500 ± 196	1443 ± 422	0.773
P16234	PDGF Rα	PDGFRA	302 ± 31	272 ± 155	0.480
P09619	PDGF Rβ	PDGFRB	178 ± 24	177 ± 81	0.480
na	PDGF-AB		605 ± 89	496 ± 250	0.724
P01127	PDGF-BB	PDGFB	353 ± 165	1278 ± 795	0.386
P16284	PECAM-1	PECAM1	218 ± 45	360 ± 187	0.773
Q07326	PIGF	PIGF	1789 ± 89	1166 ± 661	0.480
P01236	Prolactin	PRL	666 ± 102	607 ± 367	0.248
P13501	RANTES	CCL5	10758 ± 6352	38902 ± 32987	0.386
P21583	SCF	KITLG	396 ± 74	344 ± 81	0.564
P10721	SCF R	KIT	586 ± 64	590 ± 332	0.248
P48061	SDF-1	CXCL12	136 ± 36	290 ± 142	0.480
P48061	SDF-1β	CXCL12	428 ± 39	368 ± 261	0.248
P40189	sgp 130	IL6ST	928 ± 150	834 ± 193	0.564
O15389	Siglec-5	SIGLEC5	1205 ± 423	1608 ± 526	0.564
P19438	sTNFR I	TNFRSF1A	1239 ± 377	1153 ± 435	0.773
P20333	sTNFR II	TNFRSF1B	6406 ± 1612	3633 ± 1875	0.248
Q92583	TARC	CCL17	115 ± 45	182 ± 32	0.480
O15444	TECK	CCL25	235 ± 56	472 ± 279	1.000
P01135	TGFα	TGFA	521 ± 35	634 ± 348	0.593
P01137	TGFβ1	TGFB1	218 ± 21	306 ± 116	0.248
P61812	TGFβ2	TGFB2	95 ± 19	142 ± 29	0.773
P10600	TGFβ3	TGFB3	109 ± 24	119 ± 54	0.643
P40225	Thrombopoeitin	THPO	361 ± 83	397 ± 132	1.000
P35590	Tie-1	TIE1	508 ± 21	590 ± 343	0.248
Q02763	Tie-2	TEK	812 ± 64	1054 ± 720	0.480
P01033	TIMP-1	TIMP1	37154 ± 7877	21700 ± 6103	0.083
P16035	TIMP-2	TIMP2	13257 ± 2762	10736 ± 4371	0.773
Q99727	TIMP-4	TIMP4	1476 ± 635	1850 ± 750	1.000

P01375	TNFα	TNF	129 ± 14	189 ± 60	0.564
P01374	TNFβ	LTA	330 ± 103	593 ± 119	0.248
O14798	TRAIL R3	TNFRSF10C	251 ± 45	229 ± 47	0.724
Q9UBN6	TRAIL R4	TNFRSF10D	262 ± 69	533 ± 60	0.021
Q03405	uPAR	PLAUR	2996 ± 494	3330 ± 1237	1.000
P33151	VE-Cadherin	CDH5	379 ± 58	213 ± 140	0.289
P15692	VEGF	VEGFA	588 ± 184	951 ± 393	0.564
P35968	VEGF R2	KDR	677 ± 94	542 ± 274	0.724
P35916	VEGF R3	FLT4	1333 ± 11	1192 ± 506	0.248
O43915	VEGF-D	FIGF	392 ± 186	547 ± 24	0.248

Data are expressed as mean ± standard error of the mean. The P-values for the differences between ND and T2D were calculated using a Mann-Whitney test.

Supplementary Table 2.2: Immunoreactivity in conditioned media generated from subcutaneous adipose tissue explants from patients without (ND) and with type 2 diabetes (T2D).

Swiss Prot	Name on array	Symbol	ND (n=4)	T2D (n=4)	*P*
Q15848	Acrp30	ADIPOQ	95333 ± 41502	69382 ± 14531	0.773
P08476	Activin A	INHBA	595 ± 159	259 ± 47	0.083
O00253	AgRP	AGRP	955 ± 338	1405 ± 345	0.149
Q13740	ALCAM	ALCAM	573 ± 89	507 ± 338	0.480
P15514	Amphiregulin	AREG	276 ± 50	231 ± 78	0.773
P03950	Angiogenin	ANG	2840 ± 617	18859 ± 11868	0.083
O15123	Angiopoietin-2	ANGPT2	5448 ± 2559	6209 ± 3434	1.000
P30530	Axl	AXL	208 ± 46	376 ± 141	0.289
P33681	B7-1 (CD80)	CD80	944 ± 114	665 ± 274	0.248
P23560	BDNF	BDNF	240 ± 72	339 ± 127	0.386
P09038	bFGF	FGF2	2310 ± 988	604 ± 80	0.021
O43927	BLC	CXCL13	100 ± 25	115 ± 50	1.000
P12644	BMP-4	BMP4	239 ± 53	510 ± 177	0.083
P22003	BMP-5	BMP5	604 ± 134	475 ± 232	0.386
P22004	BMP-6	BMP6	406 ± 42	1296 ± 528	0.021
P18075	BMP-7	BMP7	320 ± 90	259 ± 124	0.564
P01138	b-NGF	NGF	254 ± 61	366 ± 69	0.149
P35070	BTC	BTC	336 ± 62	910 ± 133	0.034
Q16619	Cardiotrophin-1	CTF1	569 ± 41	708 ± 301	1.000
Q9NRJ3	CCL-28	CCL28	101 ± 25	345 ± 124	0.248
P08571	CD14	CD14	1591 ± 434	1163 ± 368	0.248
P55773	CK b 8-1	CCL23	351 ± 101	1068 ± 279	0.021
P26441	CNTF	CNTF	118 ± 29	196 ± 65	0.157
Q9Y4X3	CTACK	CCL27	369 ± 94	259 ± 98	0.773
Q9H2A7	CXCL-16	CXCL16	606 ± 119	650 ± 205	0.564
O75509	DR6 (TNFRSF21)	TNFRSF21	282 ± 74	405 ± 147	0.480
Q06418	Dtk	TYRO3	262 ± 52	200 ± 54	0.386
P01133	EGF	EGF	789 ± 151	729 ± 194	0.564
P00533	EGF-R	EGFR	251 ± 52	283 ± 99	0.564
P42830	ENA-78	CXCL5	57678 ± 19965	10323 ± 5692	0.083
P17813	Endoglin	ENG	569 ± 147	344 ± 230	0.564
P51671	Eotaxin	CCL11	160 ± 35	139 ± 10	0.643
O00175	Eotaxin-2	CCL24	580 ± 93	1186 ± 99	0.021
Q9Y258	Eotaxin-3	CCL26	161 ± 91	301 ± 91	0.149
P21860	ErbB3	ERBB3	1118 ± 225	626 ± 340	0.248
P16581	E-Selectin	SELE	449 ± 121	300 ± 118	0.386
P48023	Fas Ligand	FASLG	408 ± 71	328 ± 87	0.248
Q549F0	Fas/TNFRSF6	FAF1	3851 ± 2657	4641 ± 3041	0.773
P08620	FGF-4	FGF4	9438 ± 3044	9921 ± 4074	0.773
P10767	FGF-6	FGF6	272 ± 65	278 ± 99	0.724
P21781	FGF-7	FGF7	167 ± 27	434 ± 115	0.021
P31371	FGF-9	FGF9	745 ± 126	827 ± 121	0.773
P49771	Fit-3 Ligand	FLT3LG	121 ± 31	284 ± 152	1.000
P78423	Fractalkine	CX3CL1	85 ± 39	129 ± 38	0.248
P80162	GCP-2	CXCL6	817 ± 234	153 ± 65	0.021
P09919	GCSF	CSF3	407 ± 150	285 ± 126	0.248
P39905	GDNF	GDNF	801 ± 214	1011 ± 322	0.564
Q9Y5U5	GITR	TNFRSF18	2889 ± 1406	3954 ± 1619	0.564
Q9UNG2	GITR-Ligand	TNFSF18	321 ± 143	396 ± 112	0.386
P04141	GM-CSF	CSF2	13881 ± 12945	266 ± 136	0.083
P09341	GRO	CXCL1	332616 ± 98420	292569 ± 122638	0.773
P09341	GROα	CXCL1	91290 ± 35618	26283 ± 18289	0.149

O15467	HCC-4	CCL16	434 ± 94	637 ± 329	0.773
P14210	HGF	HGF	6064 ± 1808	7160 ± 3728	0.773
P22362	I-309	CCL1	370 ± 48	263 ± 49	0.248
P05362	ICAM-1	ICAM1	1689 ± 423	2435 ± 1189	0.773
P13598	ICAM-2	ICAM2	7481 ± 3073	9164 ± 4335	0.564
P32942	ICAM-3	ICAM3	325 ± 135	276 ± 85	1.000
P01343	IGF-1	IGF1	116 ± 33	159 ± 94	0.724
P08833	IGFBP-1	IGFBP1	252 ± 45	458 ± 119	0.149
P18065	IGFBP-2	IGFBP2	719 ± 399	851 ± 344	0.289
P17936	IGFBP-3	IGFBP3	492 ± 88	658 ± 126	0.386
P22692	IGFBP-4	IGFBP4	652 ± 237	554 ± 218	0.773
P24592	IGFBP-6	IGFBP6	936 ± 384	599 ± 119	0.564
P08069	IGF-I SR	IGF1R	235 ± 58	95 ± 12	0.077
P01344	IGF-II	IGF2	3388 ± 195	3482 ± 540	0.773
P27930	IL-1 R II	IL1R2	9732 ± 3008	9021 ± 2975	0.773
Q01638	IL-1 RA/ST2	IL1RL1	613 ± 118	544 ± 96	0.773
P14778	IL-1 RI	IL1R1	174 ± 43	206 ± 96	1.000
P22301	IL-10	IL10	1199 ± 378	593 ± 172	0.248
Q08334	IL-10 Rβ	IL10RB	463 ± 104	484 ± 198	0.773
P20809	IL-11	IL11	97 ± 40	47 ± 33	0.355
P29459	IL-12 p40	IL12A	936 ± 129	1575 ± 167	0.043
P29460	IL-12 p70	IL12B	284 ± 60	192 ± 67	0.149
P35225	IL-13	IL13	37 ± 10	201 ± 84	0.050
Q14627	IL-13 Rα2	IL13RA2	1353 ± 545	1280 ± 834	0.386
P40933	IL-15	IL15	49 ± 34	213 ± 127	0.275
Q14005	IL-16	IL16	215 ± 38	384 ± 35	0.021
Q16552	IL-17	IL17A	175 ± 34	530 ± 317	0.564
Q13478	IL-18 BPα	IL18R1	336 ± 45	322 ± 191	0.386
O95256	IL-18 Rβ	IL18RAP	1381 ± 439	1216 ± 388	0.773
P01583	IL-1a	IL1A	473 ± 116	771 ± 248	0.564
P01584	IL-1b	IL1B	218 ± 87	263 ± 86	0.564
P18510	IL-1ra	IL1RN	302 ± 89	380 ± 117	0.564
P60568	IL-2	IL2	221 ± 119	106 ± 25	0.513
P31785	IL-2 Rg	IL2RG	739 ± 98	596 ± 233	0.773
P01589	IL-2 Rα	IL2RA	351 ± 75	502 ± 198	0.083
P14784	IL-2 Rβ	IL2RB	301 ± 74	693 ± 142	0.564
Q9HBE5	IL-21R	IL21R	562 ± 118	431 ± 205	0.564
P08700	IL-3	IL3	171 ± 48	193 ± 28	0.643
P05112	IL-4	IL4	1266 ± 1107	112 ± 25	0.480
P05113	IL-5	IL5	4168 ± 788	477 ± 116	0.021
Q01344	IL-5 Rα	IL5RA	648 ± 142	560 ± 183	0.773
P05231	IL-6	IL6	882821 ± 284453	421784 ± 164289	0.149
P08887	IL-6R	IL6R	10350 ± 5159	3724 ± 1962	0.564
P13232	IL-7	IL7	805 ± 545	447 ± 218	0.564
P10145	IL-8	IL8	272132 ± 88962	136061 ± 75582	0.149
P15248	IL-9	IL9	462 ± 63	508 ± 232	1.000
P01579	INFg	IFNG	142 ± 43	381 ± 148	0.083
P02778	IP-10	CXCL10	2297 ± 501	1432 ± 376	0.149
O14625	I-TAC	CXCL11	243 ± 68	286 ± 74	0.564
P17676	LAP	CEBPB	1100 ± 211	701 ± 167	0.083
P41159	Leptin	LEP	6676 ± 5713	50476 ± 29321	0.773
P48357	Leptin R	LEPR	557 ± 88	401 ± 132	0.561
P15018	LIF	LIF	1047 ± 209	689 ± 102	0.149
O43557	LIGHT	TNFSF14	839 ± 159	1463 ± 555	0.564
P14151	L-Selectin	SELL	372 ± 77	415 ± 122	0.773
P47992	Lymphotactin	XCL1	231 ± 73	179 ± 82	0.593

P13500	MCP-1	CCL2	269756 ± 70361	243230 ± 88360	0.564
P80075	MCP-2	CCL8	33432 ± 13170	5828 ± 4041	0.083
P80098	MCP-3	CCL7	756 ± 516	84 ± 58	0.077
Q99616	MCP-4	CCL13	64 ± 19	282 ± 141	0.289
P09603	M-CSF	CSF1	526 ± 80	761 ± 262	0.885
P07333	M-CSF R	CSF1R	706 ± 111	562 ± 214	0.564
O00626	MDC	CCL22	272 ± 88	463 ± 182	0.386
P14174	MIF	MIF	1146 ± 130	1269 ± 387	0.564
Q07325	MIG	CXCL9	253 ± 105	94 ± 37	0.289
P10147	MIP-1a	CCL3	43463 ± 6153	6964 ± 4973	0.021
P13236	MIP-1b	CCL4	65757 ± 13625	19409 ± 13510	0.043
Q16663	MIP-1d	CCL15	245 ± 76	559 ± 197	0.149
P78556	MIP-3a	CCL20	334 ± 141	227 ± 127	0.724
Q99731	MIP-3b	CCL19	533 ± 107	298 ± 74	0.083
P03956	MMP-1	MMP1	5533 ± 789	4022 ± 484	0.149
P45452	MMP-13	MMP13	767 ± 146	617 ± 264	0.564
P08254	MMP-3	MMP3	11168 ± 4837	8236 ± 1689	0.773
P14780	MMP-9	MMP9	2884 ± 463	1631 ± 640	0.149
P55773	MPIF-1	CCL23	552 ± 47	439 ± 244	0.480
P26927	MSPa	MST1	829 ± 128	837 ± 140	0.773
P02775	NAP-2	PPBP	4860 ± 659	11159 ± 4175	0.043
P08138	NGF R	NGFR	346 ± 108	490 ± 322	0.773
P20783	NT-3	NTF3	572 ± 220	622 ± 55	1.000
P34130	NT-4	NTF4	372 ± 78	556 ± 101	0.289
P13725	Oncostatin	OSM	303 ± 57	369 ± 63	0.386
O00300	Osteoprotegerin	TNFRSF11B	714 ± 225	1340 ± 477	0.386
P55774	PARC	CCL18	166 ± 25	260 ± 114	0.386
P04085	PDGF AA	PDGFA	1515 ± 225	758 ± 106	0.021
P16234	PDGF Rα	PDGFRA	324 ± 50	342 ± 81	0.564
P09619	PDGF Rβ	PDGFRB	177 ± 26	236 ± 67	0.564
na	PDGF-AB		631 ± 56	412 ± 130	0.248
P01127	PDGF-BB	PDGFB	402 ± 124	545 ± 314	1.000
P16284	PECAM-1	PECAM1	210 ± 33	192 ± 91	0.724
Q07326	PIGF	PIGF	934 ± 246	720 ± 237	0.386
P01236	Prolactin	PRL	589 ± 83	548 ± 266	0.386
P13501	RANTES	CCL5	2321 ± 453	1922 ± 587	0.773
P21583	SCF	KITLG	405 ± 56	321 ± 46	0.149
P10721	SCF R	KIT	609 ± 90	508 ± 171	0.248
P48061	SDF-1	CXCL12	72 ± 15	165 ± 50	0.043
P48061	SDF-1β	CXCL12	478 ± 75	443 ± 254	0.724
P40189	sgp 130	IL6ST	686 ± 174	685 ± 167	0.773
O15389	Siglec-5	SIGLEC5	1129 ± 435	610 ± 162	0.248
P19438	sTNFR I	TNFRSF1A	723 ± 200	725 ± 188	0.773
P20333	sTNFR II	TNFRSF1B	2774 ± 333	1055 ± 306	0.021
Q92583	TARC	CCL17	107 ± 50	159 ± 41	0.285
O15444	TECK	CCL25	276 ± 58	490 ± 231	0.773
P01135	TGFα	TGFA	732 ± 168	609 ± 239	0.386
P01137	TGFβ1	TGFB1	252 ± 68	334 ± 82	0.083
P61812	TGFβ2	TGFB2	105 ± 26	192 ± 40	0.564
P10600	TGFβ3	TGFB3	106 ± 53	163 ± 42	0.386
P40225	Thrombopoeitin	THPO	338 ± 34	519 ± 76	0.773
P35590	Tie-1	TIE1	648 ± 41	597 ± 286	1.000
Q02763	Tie-2	TEK	845 ± 65	906 ± 382	0.289
P01033	TIMP-1	TIMP1	37022 ± 8654	20310 ± 8608	0.386
P16035	TIMP-2	TIMP2	9406 ± 3244	6152 ± 1949	0.386
Q99727	TIMP-4	TIMP4	1365 ± 257	1000 ± 357	0.386

P01375	TNFα	TNF	187 ± 68	244 ± 54	0.289
P01374	TNFβ	LTA	404 ± 123	929 ± 291	0.149
O14798	TRAIL R3	TNFRSF10C	157 ± 37	245 ± 105	0.564
Q9UBN6	TRAIL R4	TNFRSF10D	270 ± 51	494 ± 96	0.077
Q03405	uPAR	PLAUR	1396 ± 287	1097 ± 269	0.773
P33151	VE-Cadherin	CDH5	380 ± 69	255 ± 83	0.564
P15692	VEGF	VEGFA	492 ± 112	750 ± 224	0.386
P35968	VEGF R2	KDR	636 ± 39	461 ± 117	0.248
P35916	VEGF R3	FLT4	1497 ± 127	1115 ± 356	0.248
O43915	VEGF-D	FIGF	314 ± 62	608 ± 109	0.149

Data are expressed as mean ± standard error of the mean. The P-values for the differences between ND and T2D were calculated using a Mann-Whitney test.

Supplementary Table 2.3: Immunoreactivity in conditioned media generated from pericardial adipose tissue explants from patients without (ND) and with type 2 diabetes (T2D).

Swiss Prot	Name on array	Symbol	ND (n=4)	T2D (n=4)	*P*
Q15848	Acrp30	ADIPOQ	130014 ± 10123	168694 ± 22025	0.248
P08476	Activin A	INHBA	276 ± 151	260 ± 46	0.773
O00253	AgRP	AGRP	1171 ± 269	1138 ± 345	0.564
Q13740	ALCAM	ALCAM	118 ± 77	286 ± 154	0.773
P15514	Amphiregulin	AREG	372 ± 135	687 ± 181	0.157
P03950	Angiogenin	ANG	1472 ± 447	4058 ± 1713	0.083
O15123	Angiopoietin-2	ANGPT2	5147 ± 3218	8654 ± 802	1.000
P30530	Axl	AXL	484 ± 135	654 ± 344	0.773
P33681	B7-1 (CD80)	CD80	252 ± 216	459 ± 156	1.000
P23560	BDNF	BDNF	2471 ± 776	2608 ± 621	0.773
P09038	bFGF	FGF2	425 ± 127	270 ± 43	0.564
O43927	BLC	CXCL13	531 ± 252	390 ± 108	0.724
P12644	BMP-4	BMP4	1401 ± 656	266 ± 53	1.000
P22003	BMP-5	BMP5	123 ± 102	152 ± 53	1.000
P22004	BMP-6	BMP6	143 ± 140	368 ± 11	1.000
P18075	BMP-7	BMP7	39 ± 44	202 ± 28	0.050
P01138	b-NGF	NGF	650 ± 254	410 ± 135	1.000
P35070	BTC	BTC	709 ± 91	461 ± 154	0.149
Q16619	Cardiotrophin-1	CTF1	122 ± 103	249 ± 95	1.000
Q9NRJ3	CCL-28	CCL28	396 ± 262	305 ± 25	0.513
P08571	CD14	CD14	1044 ± 713	1657 ± 262	0.564
P55773	CK b 8-1	CCL23	1769 ± 381	2119 ± 372	0.773
P26441	CNTF	CNTF	440 ± 106	184 ± 24	0.127
Q9Y4X3	CTACK	CCL27	334 ± 75	313 ± 81	0.724
Q9H2A7	CXCL-16	CXCL16	345 ± 115	389 ± 44	0.386
O75509	DR6 (TNFRSF21)	TNFRSF21	120 ± 59	235 ± 82	0.386
Q06418	Dtk	TYRO3	360 ± 61	179 ± 95	0.289
P01133	EGF	EGF	4529 ± 1113	5890 ± 1659	0.664
P00533	EGF-R	EGFR	238 ± 87	793 ± 524	1.000
P42830	ENA-78	CXCL5	33743 ± 3333	39505 ± 14325	0.157
P17813	Endoglin	ENG	108 ± 47	236 ± 105	0.386
P51671	Eotaxin	CCL11	205 ± 20	403 ± 138	0.289
O00175	Eotaxin-2	CCL24	227 ± 87	503 ± 64	0.050
Q9Y258	Eotaxin-3	CCL26	223 ± 121	149 ± 64	0.083
P21860	ErbB3	ERBB3	302 ± 72	241 ± 88	0.827
P16581	E-Selectin	SELE	360 ± 187	79 ± 43	0.083
P48023	Fas Ligand	FASLG	155 ± 63	150 ± 34	0.564
Q549F0	Fas/TNFRSF6	FAF1	1127 ± 215	1747 ± 276	0.083
P08620	FGF-4	FGF4	3646 ± 590	6395 ± 762	0.083
P10767	FGF-6	FGF6	343 ± 154	108 ± 36	0.248
P21781	FGF-7	FGF7	309 ± 53	385 ± 158	0.773
P31371	FGF-9	FGF9	586 ± 117	884 ± 171	0.564
P49771	Fit-3 Ligand	FLT3LG	505 ± 282	303 ± 113	0.724
P78423	Fractalkine	CX3CL1	345 ± 176	204 ± 96	0.827
P80162	GCP-2	CXCL6	7401 ± 4171	6232 ± 2523	0.773
P09919	GCSF	CSF3	722 ± 186	332 ± 108	0.149
P39905	GDNF	GDNF	272 ± 115	317 ± 91	0.724
Q9Y5U5	GITR	TNFRSF18	1130 ± 233	2068 ± 643	0.248
Q9UNG2	GITR-Ligand	TNFSF18	170 ± 57	142 ± 41	0.724
P04141	GM-CSF	CSF2	61819 ± 24038	1225 ± 569	0.021
P09341	GRO	CXCL1	336964 ± 31090	486758 ± 110849	0.564
P09341	GROα	CXCL1	170027 ± 5231	179718 ± 58710	0.248

O15467	HCC-4	CCL16	666 ± 162	941 ± 416	1.000
P14210	HGF	HGF	5942 ± 1506	14079 ± 3337	0.083
P22362	I-309	CCL1	1228 ± 441	396 ± 173	0.149
P05362	ICAM-1	ICAM1	11840 ± 2404	25776 ± 9727	0.564
P13598	ICAM-2	ICAM2	4468 ± 1893	10211 ± 5120	0.773
P32942	ICAM-3	ICAM3	227 ± 50	336 ± 188	0.773
P01343	IGF-1	IGF1	787 ± 308	425 ± 211	0.248
P08833	IGFBP-1	IGFBP1	555 ± 154	140 ± 41	0.289
P18065	IGFBP-2	IGFBP2	1313 ± 688	547 ± 174	0.773
P17936	IGFBP-3	IGFBP3	322 ± 47	251 ± 78	0.724
P22692	IGFBP-4	IGFBP4	3310 ± 511	6531 ± 4166	0.773
P24592	IGFBP-6	IGFBP6	292 ± 38	1079 ± 321	0.021
P08069	IGF-I SR	IGF1R	229 ± 82	231 ± 94	0.564
P01344	IGF-II	IGF2	993 ± 515	1510 ± 525	1.000
P27930	IL-1 R II	IL1R2	13212 ± 7813	23770 ± 10652	0.386
Q01638	IL-1 RA/ST2	IL1RL1	303 ± 72	1333 ± 714	0.248
P14778	IL-1 RI	IL1R1	225 ± 41	nd	0.180
P22301	IL-10	IL10	8393 ± 4870	3325 ± 3094	0.386
Q08334	IL-10 Rβ	IL10RB	135 ± 75	208 ± 65	1.000
P20809	IL-11	IL11	390 ± 49	376 ± 142	0.593
P29459	IL-12 p40	IL12A	797 ± 247	1044 ± 194	0.773
P29460	IL-12 p70	IL12B	381 ± 118	311 ± 190	0.564
P35225	IL-13	IL13	413 ± 112	201 ± 30	0.480
Q14627	IL-13 Rα2	IL13RA2	260 ± 136	419 ± 85	0.564
P40933	IL-15	IL15	180 ± 54	166 ± 39	0.827
Q14005	IL-16	IL16	157 ± 49	1363 ± 1178	0.658
Q16552	IL-17	IL17A	278 ± 42	539 ± 266	0.248
Q13478	IL-18 BPα	IL18R1	42 ± 126	168 ± 25	0.513
O95256	IL-18 Rβ	IL18RAP	280 ± 158	351 ± 45	1.000
P01583	IL-1a	IL1A	1209 ± 621	312 ± 53	0.021
P01584	IL-1b	IL1B	1534 ± 750	Nd	Nd
P18510	IL-1ra	IL1RN	811 ± 156	404 ± 228	0.149
P60568	IL-2	IL2	447 ± 168	339 ± 144	0.724
P31785	IL-2 Rg	IL2RG	222 ± 128	353 ± 134	0.724
P01589	IL-2 Rα	IL2RA	124 ± 85	247 ± 50	1.000
P14784	IL-2 Rβ	IL2RB	514 ±88	841 ± 305	0.564
Q9HBE5	IL-21R	IL21R	218 ± 29	157 ± 68	0.386
P08700	IL-3	IL3	449 ± 134	288 ± 36	0.248
P05112	IL-4	IL4	353 ± 52	373 ± 31	1.000
P05113	IL-5	IL5	22659 ± 2526	19019 ± 4834	0.386
Q01344	IL-5 Rα	IL5RA	110 ± 72	153 ± 39	0.773
P05231	IL-6	IL6	1686235 ± 15412	1327246 ± 184207	0.083
P08887	IL-6R	IL6R	1459 ± 227	2502 ± 363	0.021
P13232	IL-7	IL7	5277 ± 1764	1336 ± 436	0.480
P10145	IL-8	IL8	125902 ± 17399	154422 ± 28483	0.386
P15248	IL-9	IL9	177 ± 102	223 ± 17	0.724
P01579	INFg	IFNG	102 ± 92	357 ± 119	0.480
P02778	IP-10	CXCL10	1328 ± 434	1010 ± 196	0.564
O14625	I-TAC	CXCL11	376 ± 140	353 ± 116	1.000
P17676	LAP	CEBPB	393 ± 196	790 ± 410	0.663
P41159	Leptin	LEP	312 ± 191	25095 ± 16215	0.043
P48357	Leptin R	LEPR	151 ± 78	234 ± 101	1.000
P15018	LIF	LIF	489 ± 191	521 ± 106	0.773
O43557	LIGHT	TNFSF14	1038 ± 577	1118 ± 274	0.724
P14151	L-Selectin	SELL	192 ± 56	281 ± 104	0.513
P47992	Lymphotactin	XCL1	469 ± 91	650 ± 225	0.372

P13500	MCP-1	CCL2	189247 ± 30326	151622 ± 31512	0.149
P80075	MCP-2	CCL8	105751 ± 27042	60654 ± 36043	0.248
P80098	MCP-3	CCL7	2415 ± 837	3517 ± 2020	0.564
Q99616	MCP-4	CCL13	320 ± 128	820 ± 434	0.355
P09603	M-CSF	CSF1	578 ± 115	320 ± 114	0.043
P07333	M-CSF R	CSF1R	163 ± 80	269 ± 69	0.564
O00626	MDC	CCL22	419 ± 165	514 ± 209	0.773
P14174	MIF	MIF	2137 ± 487	3057 ± 403	0.248
Q07325	MIG	CXCL9	691 ± 239	733 ± 398	0.564
P10147	MIP-1a	CCL3	93873 ± 18907	52233 ± 18051	0.149
P13236	MIP-1b	CCL4	92230 ± 29163	99980 ± 41775	0.773
Q16663	MIP-1d	CCL15	902 ± 426	209 ± 69	0.275
P78556	MIP-3a	CCL20	1983 ± 664	2111 ± 1191	0.564
Q99731	MIP-3b	CCL19	1715 ± 1243	4313 ± 2706	0.564
P03956	MMP-1	MMP1	3437 ± 1593	5001 ± 2555	0.773
P45452	MMP-13	MMP13	325 ± 108	464 ± 110	1.000
P08254	MMP-3	MMP3	3032 ± 1843	4921 ± 2493	0.773
P14780	MMP-9	MMP9	644 ± 573	1159 ± 341	1.000
P55773	MPIF-1	CCL23	149 ± 62	270 ± 119	1.000
P26927	MSPa	MST1	1063 ± 548	551 ± 119	0.773
P02775	NAP-2	PPBP	8060 ± 3152	6685 ± 1445	0.773
P08138	NGF R	NGFR	139 ± 35	214 ± 28	0.289
P20783	NT-3	NTF3	679 ± 216	438 ± 112	0.564
P34130	NT-4	NTF4	192 ± 83	415 ± 73	0.248
P13725	Oncostatin	OSM	416 ± 89	504 ± 75	0.564
O00300	Osteoprotegerin	TNFRSF11B	518 ± 137	2067 ± 697	0.149
P55774	PARC	CCL18	690 ± 437	284 ± 120	0.157
P04085	PDGF AA	PDGFA	506 ± 154	638 ± 59	1.000
P16234	PDGF Rα	PDGFRA	143 ± 49	111 ± 43	0.564
P09619	PDGF Rβ	PDGFRB	95 ± 51	114 ± 44	0.355
na	PDGF-AB		201 ± 107	342 ± 73	0.564
P01127	PDGF-BB	PDGFB	1405 ± 443	705 ± 208	0.077
P16284	PECAM-1	PECAM1	110 ± 10	150 ± 31	0.564
Q07326	PIGF	PIGF	2447 ± 1027	1641 ± 473	0.564
P01236	Prolactin	PRL	273 ± 122	417 ± 101	0.386
P13501	RANTES	CCL5	17286 ± 8828	13157 ± 11784	0.386
P21583	SCF	KITLG	302 ± 87	294 ± 42	0.773
P10721	SCF R	KIT	318 ± 42	171 ± 60	0.157
P48061	SDF-1	CXCL12	252 ± 70	339 ± 99	0.275
P48061	SDF-1β	CXCL12	182 ± 76	143 ± 40	0.724
P40189	sgp 130	IL6ST	1094 ± 157	1422 ± 134	0.149
O15389	Siglec-5	SIGLEC5	742 ± 328	1878 ± 827	0.386
P19438	sTNFR I	TNFRSF1A	1326 ± 146	2055 ± 449	0.248
P20333	sTNFR II	TNFRSF1B	7474 ± 549	8944 ± 3008	0.386
Q92583	TARC	CCL17	490 ± 272	302 ± 88	0.564
O15444	TECK	CCL25	467 ± 109	274 ±81	0.386
P01135	TGFα	TGFA	295 ± 161	382 ± 83	0.724
P01137	TGFβ1	TGFB1	205 ± 57	262 ± 94	0.064
P61812	TGFβ2	TGFB2	329 ± 150	30 ± 3	1.000
P10600	TGFβ3	TGFB3	259 ± 118	130 ± 58	0.275
P40225	Thrombopoeitin	THPO	208 ± 74	159 ± 48	0.564
P35590	Tie-1	TIE1	222 ± 106	367 ± 105	1.000
Q02763	Tie-2	TEK	245 ± 174	416 ± 151	0.885
P01033	TIMP-1	TIMP1	20898 ± 4738	32175 ± 8635	0.564
P16035	TIMP-2	TIMP2	4575 ± 1545	11044 ± 3768	0.248
Q99727	TIMP-4	TIMP4	776 ± 303	1014 ± 364	1.000

P01375	TNFα	TNF	422 ± 222	332 ± 111	0.827
P01374	TNFβ	LTA	732 ± 330	183 ± 23	0.077
O14798	TRAIL R3	TNFRSF10C	399 ± 51	370 ± 91	0.773
Q9UBN6	TRAIL R4	TNFRSF10D	210 ± 38	503 ± 248	0.773
Q03405	uPAR	PLAUR	1938 ± 766	3118 ± 659	0.386
P33151	VE-Cadherin	CDH5	117 ± 54	203 ± 46	0.248
P15692	VEGF	VEGFA	286 ± 37	412 ± 140	0.248
P35968	VEGF R2	KDR	332 ± 137	415 ± 58	0.480
P35916	VEGF R3	FLT4	654 ± 251	779 ± 48	0.248
O43915	VEGF-D	FIGF	670 ± 97	893 ± 156	0.564

Data are expressed as mean ± standard error of the mean. The *P*-values for the differences between ND and T2D were calculated using a Mann-Whitney test.

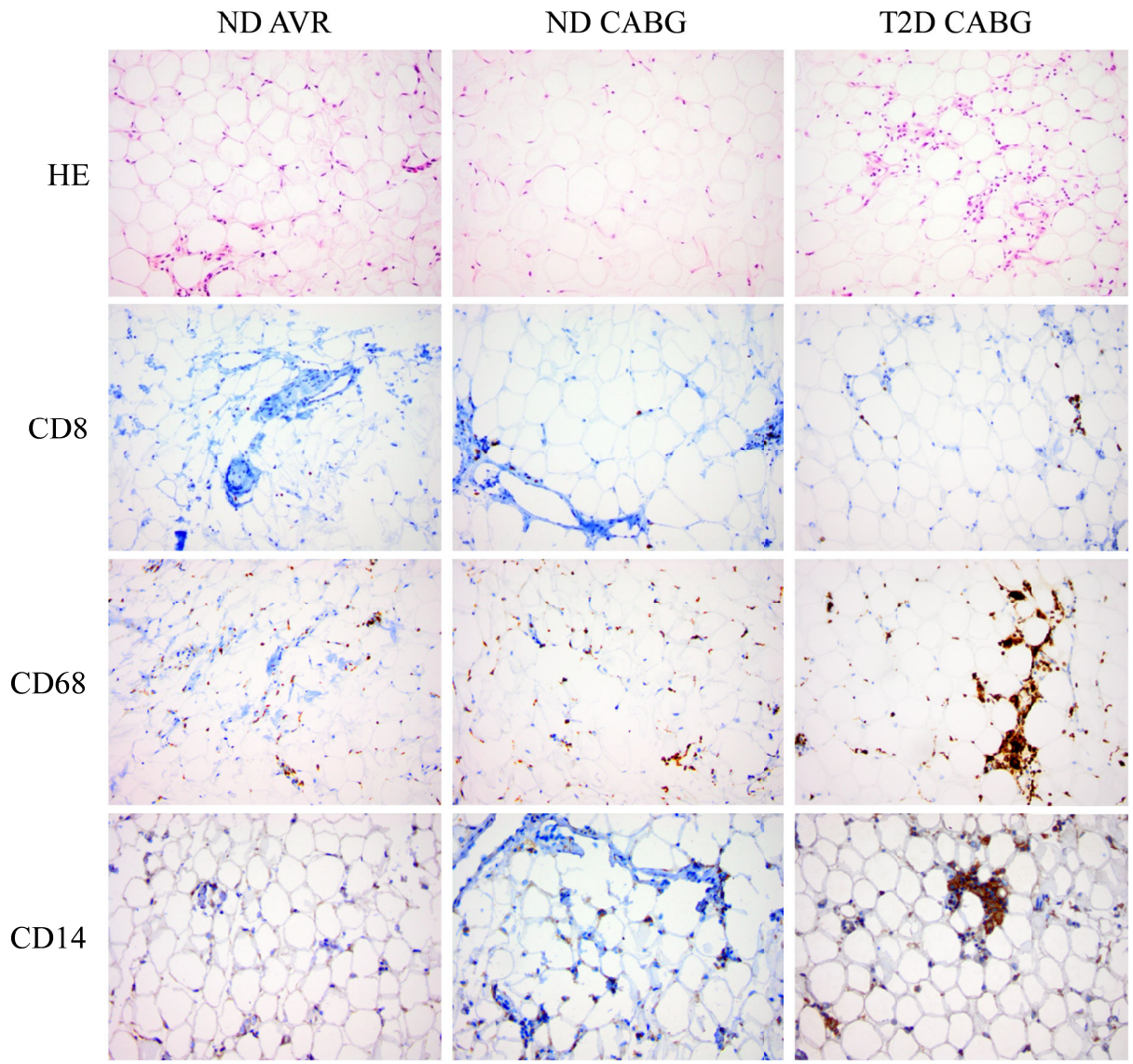

Supplementary Figure 2.1: Immunohistochemistry of epicardial adipose tissue. Epicardial adipose tissue biopsies were collected from patients undergoing aortic valve replacement (AVR) or coronary artery bypass graft surgery (CABG) and stained with haematoxylin-eosin (HE), or antibodies recognizing the cytotoxic T-cell marker CD8, the macrophage marker CD68 or CD14 followed by counterstaining with haematoxylin-eosin. The representative images presented were taken at 200x magnification from biopsies obtained from a 71 year old female patient without type 2 diabetes (ND) and a BMI of 31.2 kg/m^2 undergoing surgery for AVR, a 72 year old male ND-patient (BMI = 32.0 kg/m^2) undergoing CABG, and a 60 year old male T2D-patient (BMI = 29.4 kg/m^2) undergoing CABG.

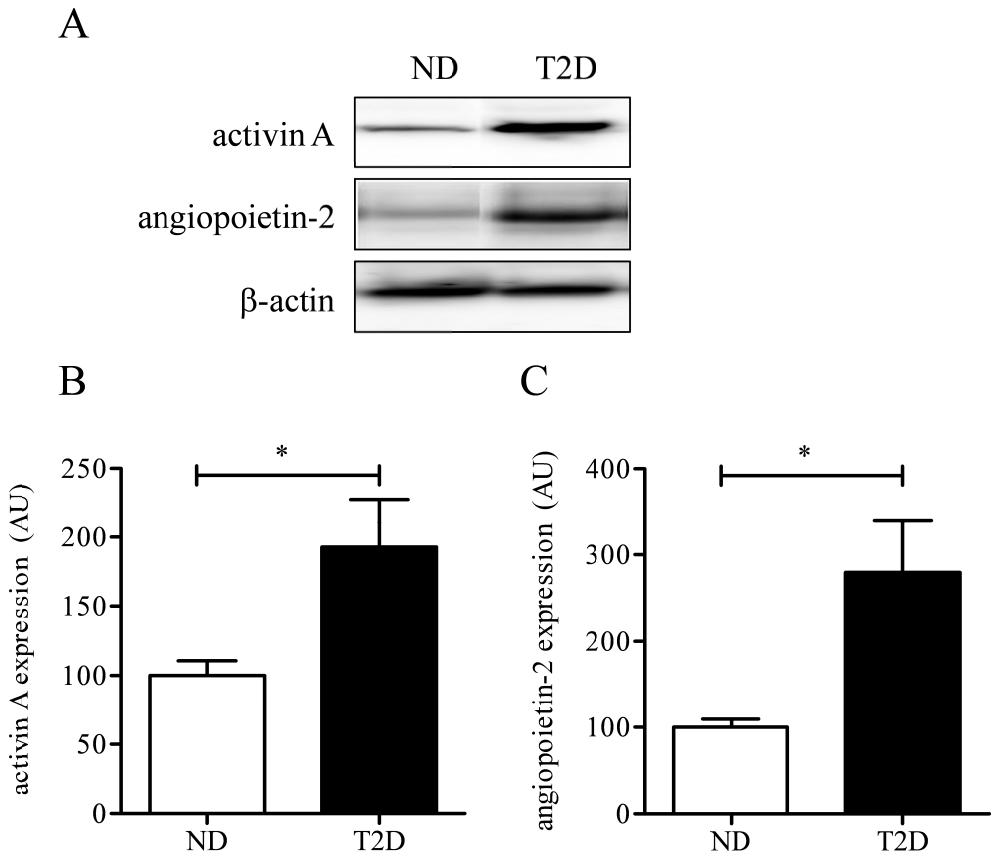

Supplementary Figure 2.2: Activin A and angiopoietin-2 expression in epicardial adipose tissue. Representative Western blots (A) and quantification of activin A (B) and angiopoietin-2 expression in epicardial adipose tissue biopsies from patients without (ND) and with type 2 diabetes (T2D). Equal protein expression was validated by reprobing the stripped filters with antibodies recognizing β-actin. Data are expressed as mean ± standard error of the mean (n=4 per group). Differences between the experimental groups were evaluated using a student's t-test, * indicates $P<0.05$ ND vs T2D.

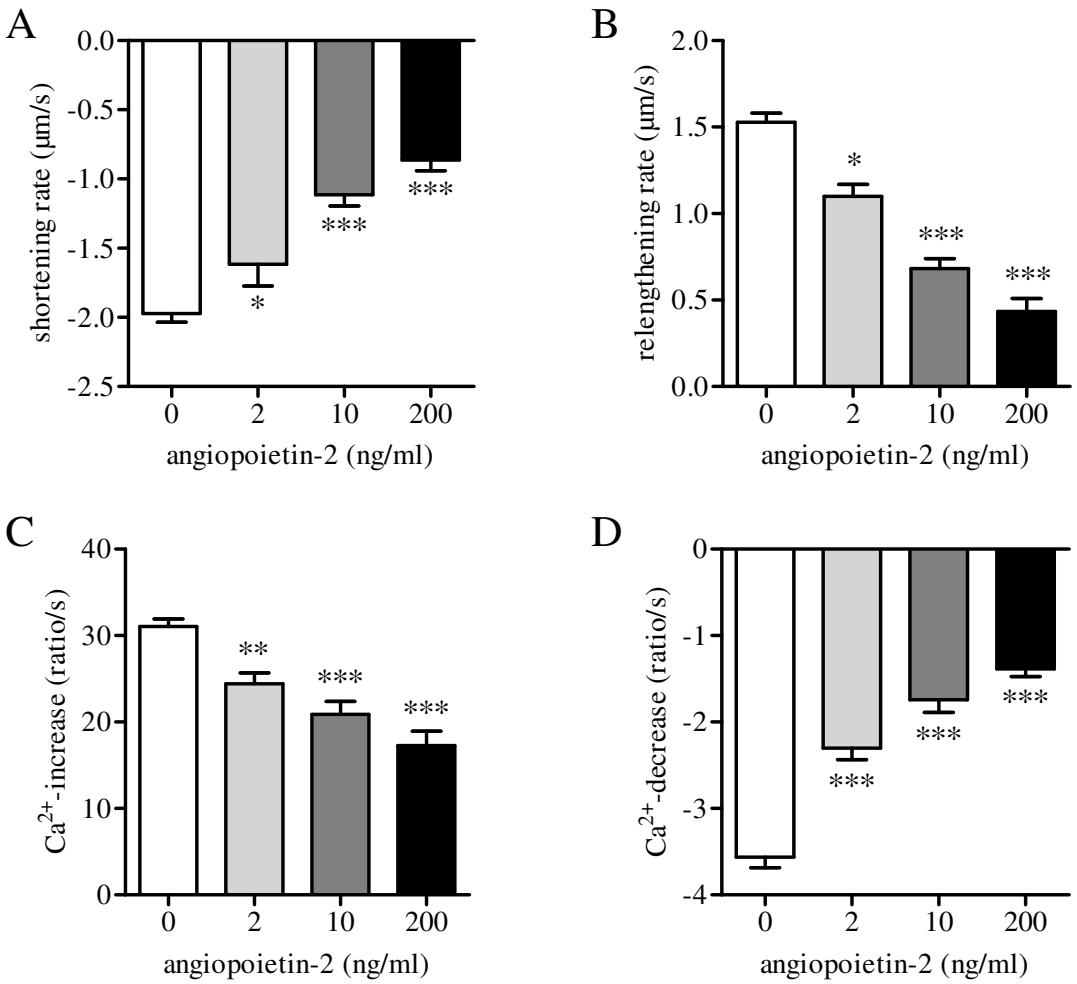

Supplementary Figure 2.3: Effect of recombinant angiopoietin-2 on contractile function and cytosolic Ca^{2+}-transients. Dose-dependent effect of a 30 min exposure of primary adult rat cardiomyocytes to angiopoietin-2 on departure velocity of contraction (A), return velocity of contraction (B), cytosolic [Ca^{2+}] increase (C), cytosolic [Ca^{2+}] decrease (D). Data were collected in four independent experiments using cardiomyocyte preparations from different rats and are expressed as mean±SEM. The effect of the various angiopoietin-2 concentrations on cardiomyocyte function was evaluated using the Kruskal-Wallis method followed by a Dunns multiple comparison test. ***P<0.001, **P<0.01, *P<0.05, vs control adipocyte medium (AM) without angiopoietin-2.

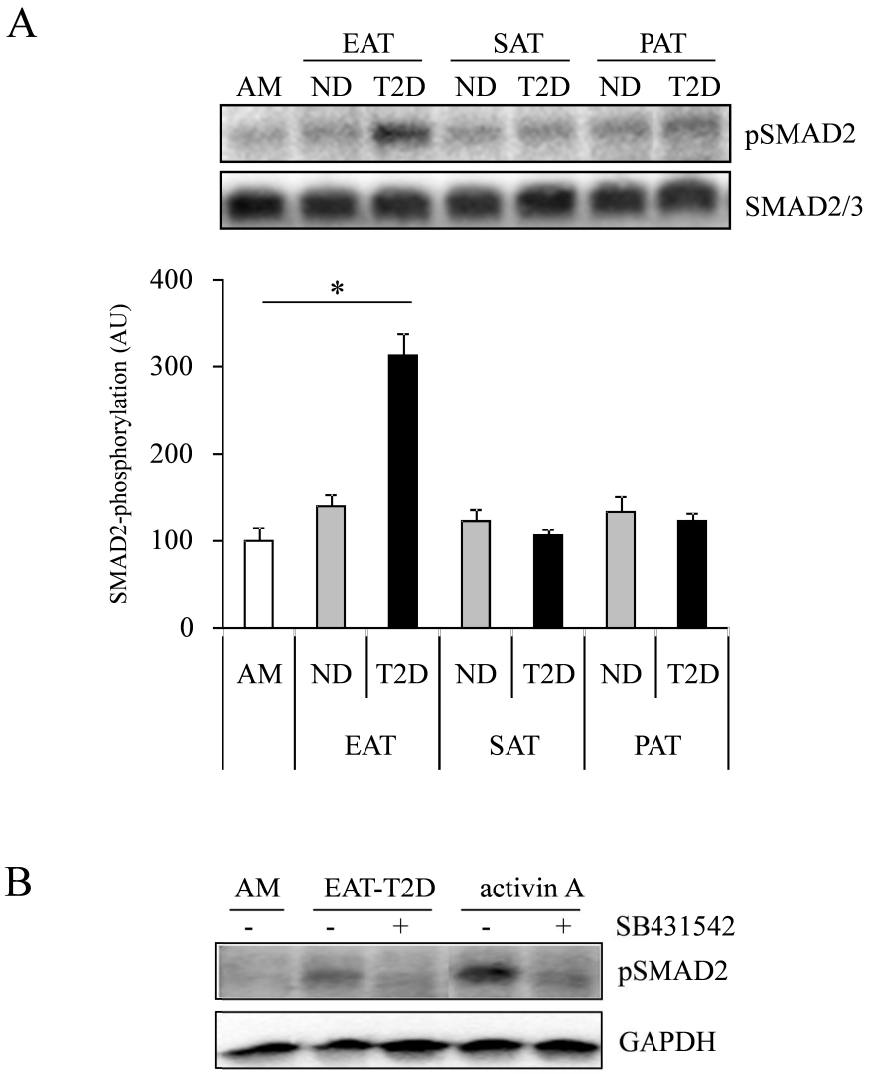

Supplementary Figure 2.4: Effect of conditioned medium on SMAD2-phosphorylation. (A) Representative Western blot and quantification of SMAD2-Ser465/Ser467-phosphorylation in primary adult rat cardiomyocytes treated with control adipocyte medium (AM) or conditioned media (CM, diluted 1:6; 24 h). Data are presented as mean±SEM of at least five independent experiments using cardiomyocytes from different rats and CM from different donors. Open bars indicate AM; gray bars, CM from ND-patients; black bars, CM from T2D-patients. Differences among the various groups were evaluated using the Kruskal-Wallis method followed by a Dunns multiple comparison test. *P<0.05 vs control adipocyte medium (AM). (B) Representative Western blot for the effect of pretreating primary adult rat cardiomyocytes with 10 µM SB431542 (1 h) on the induction of SMAD2-Ser465/Ser467-phosphorylation in response to CM-EAT-T2D or activin A (100 ng/ml) for 24 h.

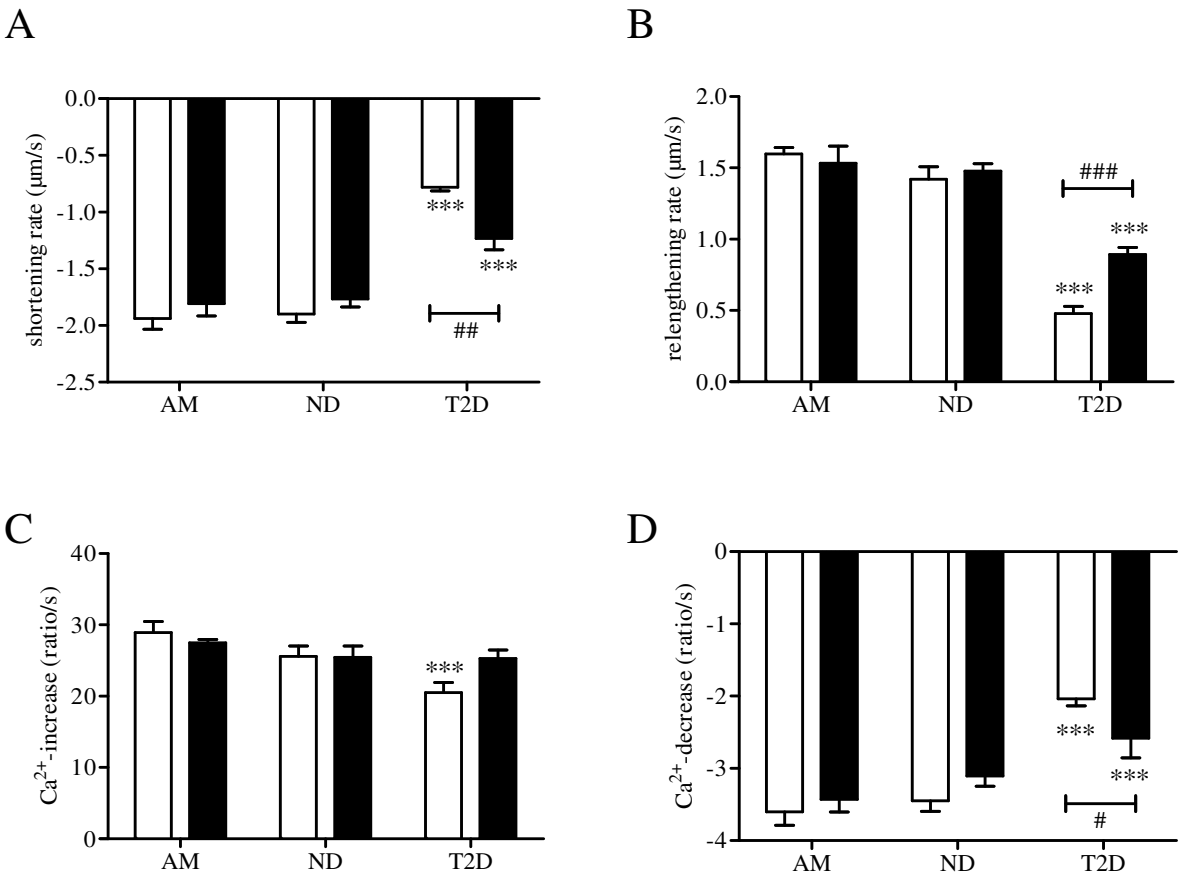

Supplementary Figure 2.5: Effect of a neutralizing activin A antibody on the detrimental effects induced by CM-EAT in cardiomyocytes. Control adipocyte medium (AM), or conditioned media (CM) from EAT of T2D- or ND-patients were pre-incubated with an activin A neutralizing antibody prior to incubation with cardiomyocytes. Effect of activin A neutralizing antibody on departure velocity of contraction (A), return velocity of contraction (B), cytosolic [Ca^{2+}] increase (C), cytosolic [Ca^{2+}] decrease (D). Data were collected in at least four independent experiments using cardiomyocyte preparations from different rats and CM from different donors are expressed as mean±SEM. Open bars, without antibody; black bars, neutralizing antibody. Differences among the groups were evaluated using the Kruskal-Wallis method followed by a Dunns multiple comparison test. ***P<0.001, vs control adipocyte medium (AM); ###P<0.001, ##P<0.01, #P<0.05 CM with or without neutralizing antibody.

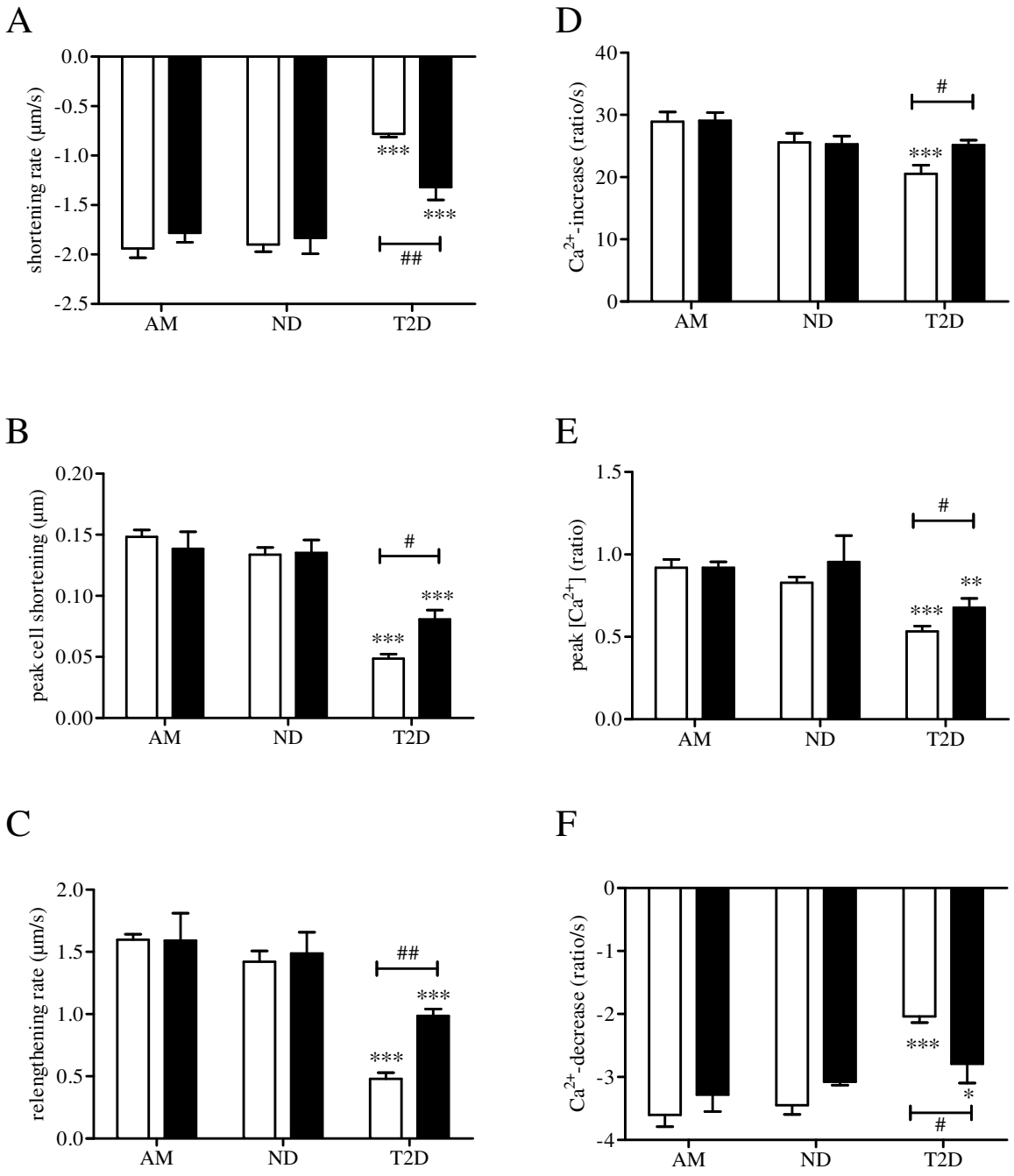

Supplementary Figure 2.6: Effect of follistatin on the detrimental effects induced by CM-EAT in cardiomyocytes. Control adipocyte medium (AM), or conditioned media (CM) from EAT of T2D- or ND-patients were pre-incubated with follistatin before incubation with cardiomyocytes. Effect of follistatin on departure velocity of contraction (A), peak sarcomere shortening (B), and return velocity of contraction (C), departure velocity of cytosolic [Ca^{2+}] increases (D), peak Fura-2 fluorescence signal (E), and cytosolic [Ca^{2+}] decreases (F). Data were collected in at least four independent experiments using cardiomyocyte preparations from different rats and CM from different donors are expressed as mean±SEM. Open bars, basal; black bars, follistatin. Differences among the groups were evaluated using the Kruskal-Wallis method followed by a Dunns multiple comparison test. ***P<0.001, **P<0.01, *P<0.05 vs control adipocyte medium (AM); ##P<0.01; #P<0.05 CM with or without follistatin.

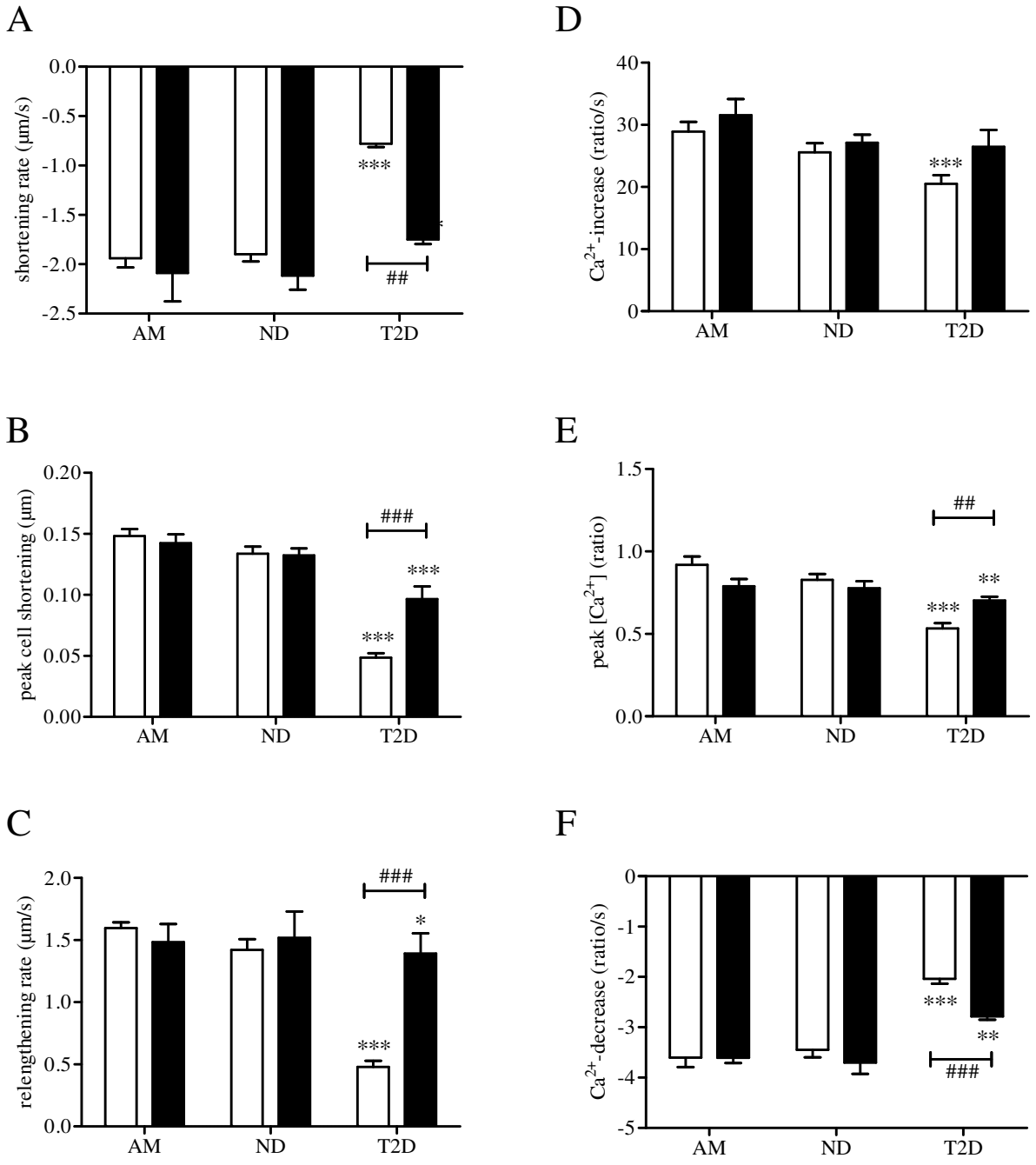

Supplementary Figure 2.7: Effect of inhibition of activin A signaling on the detrimental effects induced by CM-EAT in cardiomyocytes. Primary adult rat cardiomyocytes were pretreated with the activin A receptor-kinase inhibitor SB431542 (10 µmol/L, 1 h) and then incubated with control adipocyte medium (AM), or conditioned media from EAT of T2D- or ND-patients. Effect of SB431542 on departure velocity of contraction (A), peak sarcomere shortening (B), and return velocity of contraction (C), departure velocity of cytosolic [Ca^{2+}] increases (D), peak Fura-2 fluorescence signal (E), and cytosolic [Ca^{2+}] decreases (F). Data were collected in at least four independent experiments using cardiomyocyte preparations from different rats and CM from different donors are expressed as mean±SEM. Open bars, vehicle (DMSO); black bars, SB431542. Differences among the groups were evaluated using the Kruskal-Wallis method followed by a Dunns multiple comparison test. ***P<0.001, **P<0.01 vs control adipocyte medium (AM); ###P<0.001, ##P<0.01, CM with or without SB431542.

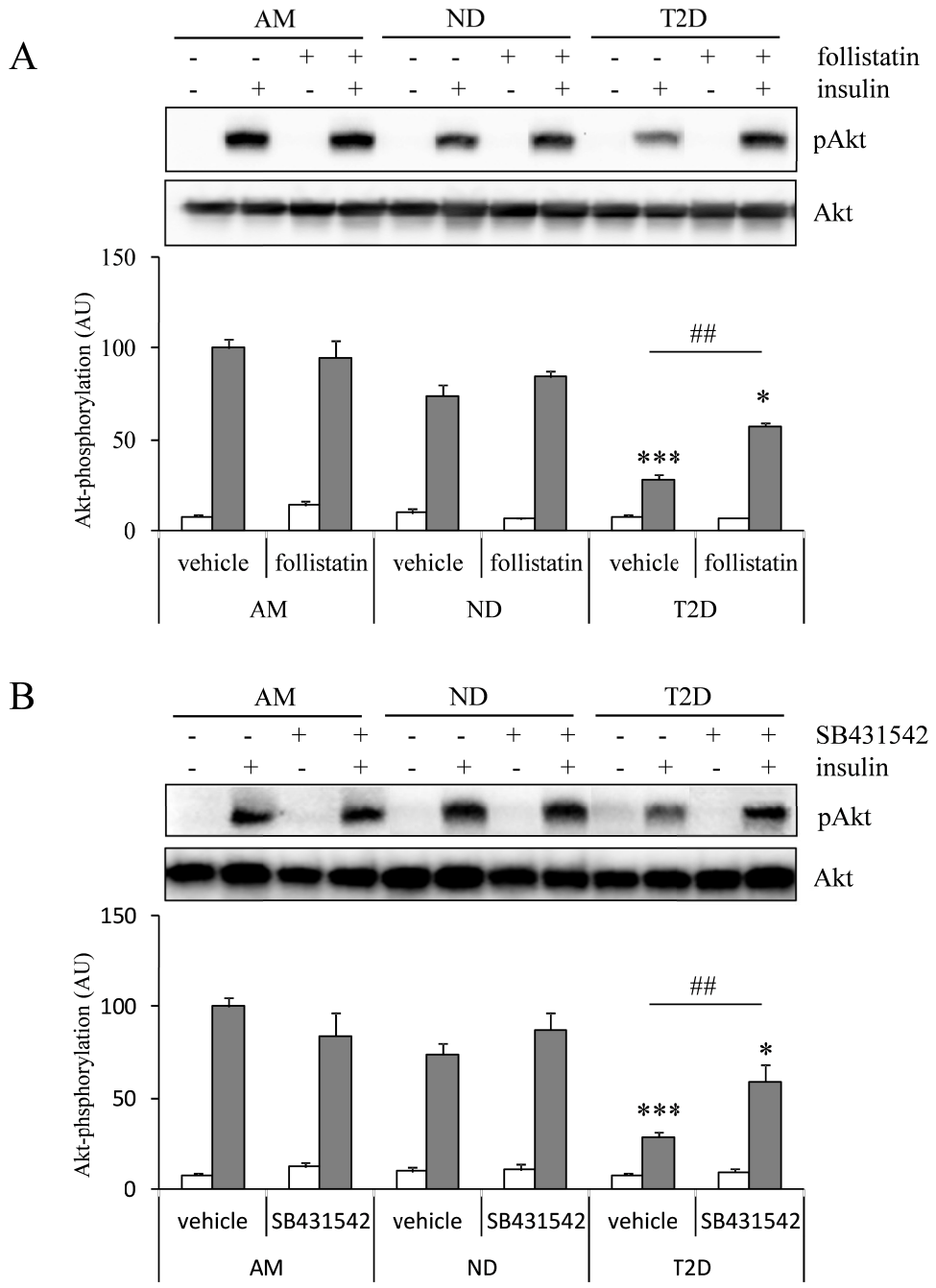

Supplementary Figure 2.8: Effect of inhibition of follistatin and SB431542 on the detrimental effects induced by CM-EAT on insulin-mediated Akt-phosphorylation in cardiomyocytes. Control adipocyte medium (AM), or conditioned media (CM) from EAT of T2D- or ND-patients were preincubated with follistatin before incubation with cardiomyocytes (A), or cardiomyocytes were pretreated with the activin A receptor-kinase inhibitor SB431542 (10 µmol/L, 1 h) and then incubated with control adipocyte medium (AM), or CM from EAT of T2D- or ND-patients (B) for 24 h. Shown are representative Western blots and quantification of insulin-induced Akt-Ser473 phosphorylation. Data were collected during at least four independent experiments using cardiomyocyte preparations from different rats and CM from different donors, and are expressed as mean±SEM. Open bars, basal; grey bars, insulin-stimulated cells (10 min; 100 nmol/L). Differences among the groups were evaluated using the Kruskal-Wallis method followed by a Dunns multiple comparison test. ***P<0.001; *P<0.05, vs AM; ##P<0.01 vehicle vs inhibitor.

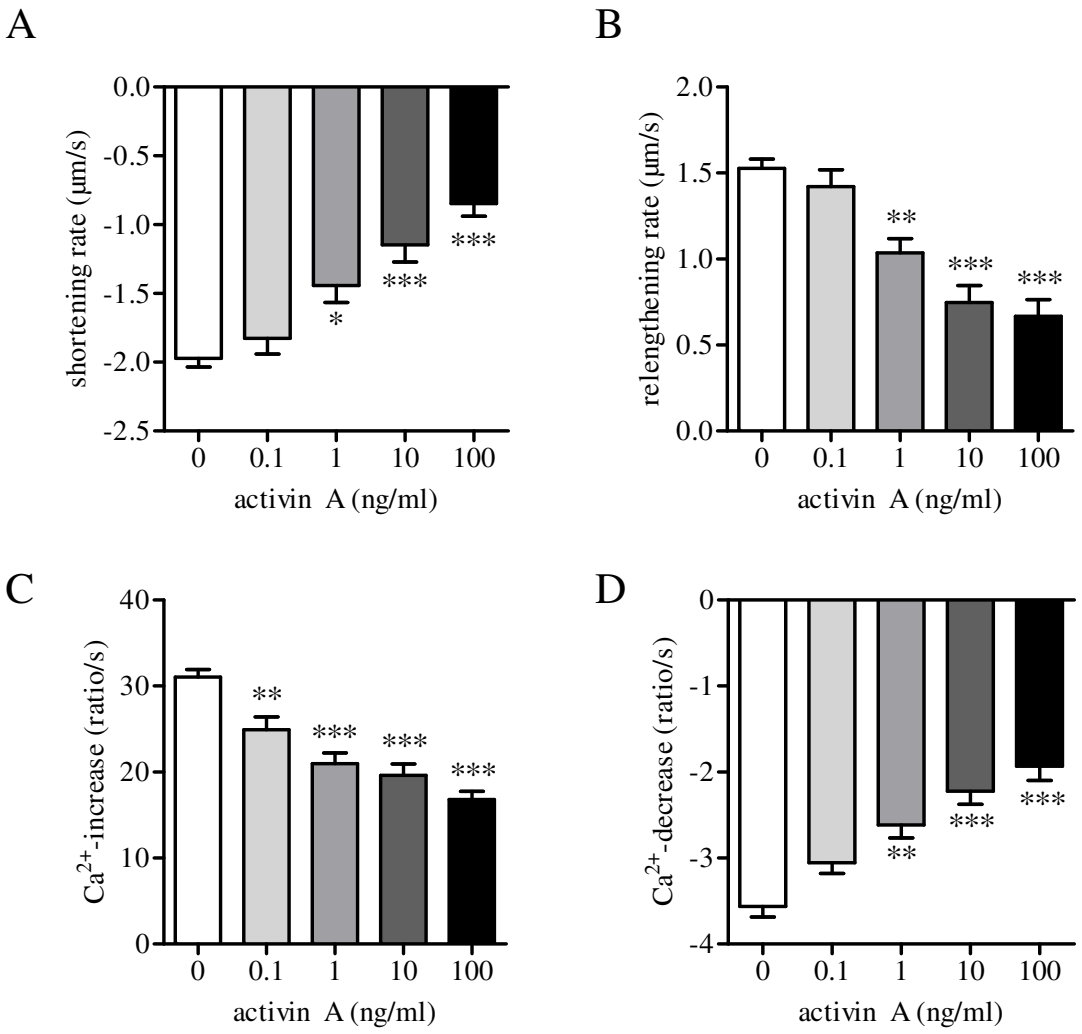

Supplementary Figure 2.9: Effect of recombinant activin A on contractile function and cytosolic Ca^{2+}-transients. Dose-dependent effect of a 30 min exposure of primary adult rat cardiomyocytes to activin A on departure velocity of contraction (A), return velocity of contraction (B), cytosolic [Ca^{2+}] increase (C), cytosolic [Ca^{2+}] decrease (D). Data were collected in four independent experiments using cardiomyocyte preparations from different rats and are expressed as mean±SEM. The effect of the various activin A concentrations on cardiomyocyte function was evaluated using the Kruskal-Wallis method followed by a Dunns multiple comparison test. ***P<0.001, **P<0.01, *P<0.05 vs control adipocyte medium (AM) without activin A.

Journal: *Circulation*

Impact factor: 15.202

Contribution: Total: 20%

Conceived / designed experiments: 10%

Performed experiments: 20%

(western blot analysis, generation of conditioned media, quantification of cytokines via enzyme-linked immunosorbent assay, preparation and isolation of rat cardiomyocytes)

Analysed data: 20%

Contributed to discussion: 20%

Wrote the manuscript: 0%

Reviewed / edited manuscript: 30%

Author: 8th author

Chapter 3

Study 2

Activin A impairs insulin action in cardiomyocytes via up-regulation of miR-143

Marcel Blumensatt[1], Sabrina Greulich[1], Daniella Herzfeld de Wiza[1], Heidi Mueller[1], Bujar Maxhera[2], Martijn. J. Rabelink[3], Rob. C. Hoeben[3], Payam Akhyari[2], Hadi Al-Hasani[1], Johannes. B. Ruige[4], and D. Margriet Ouwens[1,4]

published in Cardiovascular Research, 2013

[1]Institute for Clinical Biochemistry and Pathobiochemistry, German Diabetes Center, Duesseldorf, Germany

[2]Department of Cardiovascular Surgery, Heinrich-Heine-University, Duesseldorf, Germany

[3]Department of Molecular Cell Biology, Leiden University Medical Center, Leiden, The Netherlands

[4]Department of Endocrinology, Ghent University Hospital, Ghent, Belgium

Abbreviations

ARC – adult rat cardiomyocytes; EAT – epicardial adipose tissue; SAT – subcutaneous adipose tissue; PAT – pericardial adipose tissue; T2D – type 2 diabetes; ND – non-diabetics; CM – conditioned media; miRNA – microRNA; ORP8 – oxysterol-binding protein-related protein 8; IRS1 – insulin receptor substrate 1; PI3K – phosphatidylinositol-3'-kinase; PRAS40 – proline-rich Akt substrate of 40 kDa; PTEN – phosphatase and tensin homolog; IRβ – insulin receptor β-subunit; pre-miRNA – precursor-miRNA

Key Words

activin A, diabetic cardiomyopathy, epicardial adipose tissue, insulin resistance, miRNA

Abstract

Background

Enhanced activin A release from epicardial adipose tissue (EAT) has been linked to the development of cardiac dysfunction in type 2 diabetes (T2D). This study examined whether the inhibition of insulin action induced by epicardial adipokines in cardiomyocytes can be ascribed to alterations in miRNA-expression.

Methods and Results

Expression levels of miRNAs were assessed by real-time PCR in primary adult rat cardiomyocytes (ARC) exposed to conditioned media generated from EAT-biopsies (CM-EAT) from patients with and without T2D. CM-EAT-T2D altered the expression of eight miRNAs in ARC vs. CM-EAT from patients without T2D. Of these, only expression of the miR-143/145 cluster was affected by activin A in the same direction as CM-EAT-T2D. Accordingly, activin A neutralizing antibodies prevented the induction of the miR-143/145 cluster by CM-EAT-T2D. Subsequently, the impact of the miR-143/145 cluster on insulin action was investigated. Transfection of HL-1 cells with precursor-miR-143 (pre-miR-143), but not pre-miR-145, blunted the insulin-mediated phosphorylation of Akt and its substrate proline-rich Akt substrate of 40-kDa (PRAS40), and reduced insulin-stimulated glucose uptake. Also lentivirus-mediated expression of pre-miR-143 in ARC reduced insulin-induced Akt-phosphorylation. These effects were ascribed to down-regulation of the miR-143 target and regulator of insulin action, the oxysterol-binding protein-related protein 8 (ORP8) in both ARC and HL-1 cells. Finally, LNA-anti-miR-143 protected against the detrimental effects of CM-EAT-T2D on insulin action in ARC.

Conclusion

Activin A released from EAT-T2D inhibits insulin action via the induction of miR-143 in cardiomyocytes. This miRNA inhibits the Akt-pathway through down-regulation of the novel regulator of insulin action, ORP8.

Introduction

Diabetic cardiomyopathy is a common complication and a major cause of mortality in patients with type 2 diabetes (T2D).[1-3] Myocardial insulin resistance is closely linked to the pathophysiology of diabetic cardiomyopathy.[4, 5] Alterations in adipokine secretion by epicardial adipose tissue (EAT) have been linked to the development of cardiac dysfunction in patients with T2D.[6, 7] We previously showed that conditioned media (CM) generated from EAT from high-fat diet fed guinea pigs as well as patients with T2D induce cardiomyocyte dysfunction as illustrated by reductions in contractile function and induction of insulin resistance.[8, 9] This detrimental effect induced by CM from EAT from patients with T2D was not observed when exposing cardiomyocytes to CM from other fat depots, such as subcutaneous and pericardial adipose tissue.[8, 9] Profiling experiments could ascribe part of the cardio-depressant activity present in EAT from patients with T2D to an enhanced secretion of activin A.[8, 9] However, the molecular mechanism via which the epicardial adipokines, including activin A, impact on myocardial insulin signalling is still incompletely understood.

Accumulating evidence links microRNAs (miRNA) to the development of insulin resistance and pathogenesis of cardiometabolic diseases.[10-12] These small non-coding RNA molecules regulate the expression levels of target proteins through degradation of the mRNA encoding the protein, through repression of mRNA translation, or both.[13] Among the proteins targeted by miRNAs are components of the insulin signalling system, such as insulin receptor substrate 1 (IRS-1), as well as regulators of activity of the Akt-pathway, such as phosphatase and tensin homologue (PTEN) and oxysterol-binding protein-related protein 8 (ORP8).[10, 14-17] This study aimed at investigating whether alterations in miRNA expression participate in the induction of insulin resistance resulting from enhanced secretion of activin A from EAT from patients with T2D. Therefore, we profiled the alterations in miRNA expression in primary adult rat cardiomyocytes (ARC) that were exposed to CM generated from EAT-biopsies from patients with and without T2D. Subsequently, we analysed whether the observed alterations in miRNA expression could be ascribed to activin A. Finally, we analysed the impact of differentially regulated miRNAs on insulin action in HL-1 cells and ARC expressing precursor forms or LNA-anti-miR for the deregulated miRNA species.

Methods

An extended version of the methods applied in this study is provided in the supplement.

Conditioned media from adipose tissue

Adipose tissue biopsies collected from the epicardial, pericardial and subcutaneous adipose tissue depots were collected from patients undergoing open-heart surgery for coronary artery bypass grafting and/or valve replacement procedures after written informed consent. The procedure to obtain adipose tissue samples was approved by the ethical committee of the Heinrich-Heine-University (Duesseldorf, Germany). Biopsies were used to generate conditioned media (CM) as described.[8, 9] Activin A content in the CM was determined using a Quantikine activin A immunoassay (R&D systems, Minneapolis, MN, USA).

Isolation and culture of primary adult rat cardiomyocytes

Animal experiments were performed in accordance with the 'Principle of laboratory animal care' (NIH publication No. 85–23, revised 1996) and the current version of the German Law on the protection of animals. Cardiomyocytes were isolated from Lewis rats (Lew/Crl) as described.[8] Briefly, rats were killed following anaesthesia with ketamine (100 mg/kg; Ratiopharm, Ulm, Germany) and xylazine (Rompun, 5 mg/kg) (Bayer Healthcare, Leverkusen, Germany). The isolated heart was retrograde perfused using a Langendorff perfusion system and digested with a buffer containing collagenase (Worthington, Lakewood, NJ, USA) and hyaluronidase (Applichem, Darmstadt, Germany). Isolated cardiomyocytes were seeded and cultured on laminin-coated six-well plates before exposure to the conditioned media (CM) or control adipocyte medium (AM). When indicated, the CM were incubated for 60 min with 100 ng activin A βA subunit antibody (R&D systems, Wiesbaden-Nordenstadt, Germany) before addition to the ARC, or the ARC were incubated for 30 min with 2.5 μM of the p38 inhibitor SB203580 (Promega, Mannheim, Germany) before the addition of the CM.

Whole genome miRNA-profiling in rat cardiomyocytes

To assess the effects on miRNA expression, ARC were harvested 16h after the addition of the CM (1:4 diluted with AM). Data were collected during seven independent experiments for CM from EAT and four independent experiments for CM from the other fat depots. Total RNA was isolated from the cardiomyocytes using the miRNeasy mini kit (Qiagen, Hilden, Germany), reverse transcribed using the miScript I RT kit (Qiagen), whereafter miRNA expression levels were determined with the rat miScript Assay 384 set based on miRBase V13.0 (Qiagen) and miScript SYBR Green (Qiagen) on a StepOne Plus real-time PCR system (Applied Biosystems, Carlsbad, CA, USA). Taqman assays were used to validate miR-143 and miR-145 expression levels as described.[18]

Culture and transfection of HL-1 cells

The cardiac mouse cell line HL-1[19] was kindly provided by professor dr. W.C. Claycomb (Louisiana State University, New Orleans, LA, USA). Cells were transfected in six-well dishes with 30 nmol/l Cy3™-labeled pre-miR™ (negative control) or pre-miR™ miRNA-precursor (Ambion, Life Technologies, Darmstadt, Germany) at 70-80% confluence using Lipofectamine™ 2000 (Invitrogen, Life Technologies, Darmstadt, Germany). To silence ORP8, cells were transfected with five validated MISSION® shRNA constructs (TRCN0000105 245–249) targeting mouse ORP8 (NM175489) (Sigma Aldrich) or empty vector. Comparable data were obtained for all five distinct ORP8 shRNAs evaluated. One day after transfection, cells were serum-starved for 16h on Dulbecco's modified Eagle medium containing 5 mM glucose (Invitrogen) and supplemented with 2 mmol/l L-glutamine, 100 U/ml penicillin and 100 µg/ml streptomycin. Thereafter, the cells were stimulated with 200 nM insulin for 30 minutes or kept untreated, and harvested.

Lentiviral transduction of primary adult rat cardiomyocytes

Isolated ARC were transduced at an MOI of 5 with lentiviruses expressing pre-miR-143 or empty vector. Two days after transduction, cells were serum-starved and kept untreated or incubated for 10 min with 100 nM insulin, and harvested.

LNA-anti-miR silencing of primary adult rat cardiomyocytes

Isolated ARC were transfected with 60 nM miRCURY LNA inhibitor for miR-143 or miRCURY LNA inhibitor control (Exiqon, Vedbæk, Denmark) for 6h using lipofectamine. Then, cells were exposed to CM or AM overnight. Thereafter, the cells were stimulated with 100 nM insulin for 10 minutes or kept untreated, and harvested.

Analysis of protein expression and insulin signalling

Cells were lysed for 2h at 4°C in 50 mmol/l HEPES (pH7.4), 1% Triton X-100, supplemented with protease and phosphatase inhibitor cocktails (Complete, PhosStop; Roche Diagnostics, Mannheim, Germany) under gentle rotation. Protein content was determined using Bradford reagent (Biorad Laboratories, Munich, Germany). Effects on protein expression and insulin action were analysed via western blotting as described.[9]

Glucose uptake in HL-1 cardiomyocytes

Glucose uptake was measured in serum-starved HL-1 cells, either kept untreated or exposed for 30 min to 200 nM insulin. Then 0.12 mM deoxy-D-glucose with 0.055 µCi 2-deoxy-D-[^{3}H]glucose was added to the cells. After a 10 min incubation, incorporated glucose was measured by scintillation counting of the cell lysates.

Statistical analysis

Data are presented as mean ± standard error of the mean (SEM). Significant differences between experimental conditions were evaluated as described in the legends to the Tables and the figures using Graphpad Prism5 (GraphPad, LA Jolla, CA, USA) software. *P*-values of <0.05 were considered as statistically significant.

Results

Patient characteristics

Adipose tissue biopsies to generate CM were collected from patients with and without T2D. Pre-operative blood glucose levels were higher in T2D-patients vs. ND-patients. Age and BMI were similar between patients groups (Table 3.1). Type of surgery and medication use is listed in supplementary Table 3.1.

Effect of epicardial adipokines on miRNA expression in cardiomyocytes

In the absence of CM, 191 out of the 343 miRNAs profiled were detected in primary ARC, including the muscle-specific miR-1, miR-133 and the cardiac-specific miR-208 (Supplementary Figure 3.1 and Table 3.2).[20] Supplementary Table 3.3 lists the 152 miRNA species that were not detected in primary ARC. Of the expressed miRNAs, miR-133 was the most abundant in ARC (Supplementary Table 3.2). Furthermore, the expression of eight miRNA species was changed in ARC exposed to CM from EAT-T2D (CM-EAT-T2D) vs. CM-EAT-ND (Figure 3.1). Specifically, CM-EAT-T2D reduced the expression of miR-26a, miR-191, miR-218, and miR-425 (Figure 3.1 A-D). The levels of the miRNA cluster miR-143/145, miR-208, and of let-7c were increased in ARC exposed to CM-EAT-T2D vs. CM-EAT-ND (Figure 3.1 E-H). Exposing ARC to CM generated from subcutaneous or pericardial adipose tissue from patients with or without T2D did not alter the expression levels of these miRNAs (Figure 1).

Effect of activin A on miRNA expression in cardiomyocytes

Previously, we could ascribe an inhibition of insulin action in ARC exposed to CM-EAT-T2D to activin A.[9] The amount of activin A in CM was 1.7 ± 0.4 ng/ml in CM-EAT-T2D (n=14) vs. 0.55 ± 0.15 ng/ml in CM-EAT-ND (n=10) (P<0.02) (Supplementary Figure 3.2). Using Taqman-based assays, we showed that expression of the miR-143/145 cluster in ARC was dose-dependently increased by recombinant activin A, and that this effect became significant at 1 ng/ml (Figure 3.2 A/B). Furthermore, the response between 1 ng/ml and 10 ng/ml activin A was not significantly different. Expression levels of the other miRNAs tested were either not affected by activin A, or in the case of miR-191 alterations were observed in the opposite direction (Supplementary figure 3.3). To substantiate the involvement of activin A in the induction of the miR-143/145 cluster, neutralizing activin A antibodies were used. As

shown in Figure 3.2 C/D, pre-incubation of activin A or CM-EAT-T2D with activin A neutralizing antibodies prevented the induction of miR-143 and miR-145.

The induction of the miR-143/145 cluster is mediated by the MAP kinase p38

Activin A is a member of the transforming growth factor β family. Because the induction of the miR-143/145 cluster in response to transforming growth factor β1 involves the MAP kinase family member p38 in smooth muscle cells,[21] we examined whether p38 participates in the induction of the miR-143/145 cluster by CM-EAT-T2D in ARC. Exposure of ARC to CM-EAT-T2D increased the phosphorylation of p38 when compared with CM-EAT-ND or control medium (Figure 3.3 A). The induction of p38 phosphorylation was significantly blunted when CM-EAT-T2D was incubated with neutralizing antibodies against activin A (Figure 3.3 B). Accordingly, activin A caused a dose-dependent increase in p38 phosphorylation in ARC (Figure 3.3 C). To investigate the involvement of p38 in the induction of the miR-143/145 cluster in ARC, the pharmacological p38-inhibitor SB203580 was used. As shown in Figure 3.3 D/E, the presence of SB203580 abolished the induction of the miR-143/145 cluster by both activin A and CM-EAT-T2D.

Effect of miR-143 and miR-145 on insulin action

The mouse cardiac muscle cell line HL-1 was used to assess the impact of the miR-143/145 cluster on insulin action because of better viability following pre-miR expression when compared with primary ARC. This is particularly relevant for the quality of the glucose transport experiments, and HL-1 cells are insulin-sensitive and display the insulin-regulated glucose transporter GLUT4.[22] Transfecting HL-1 cells with pre-miR-143, reduced the insulin-mediated phosphorylations of Akt-Thr308, Akt-Ser473, and of the Akt-substrate PRAS40-Thr246 by 35%, 25%, and 20%, respectively, vs. cells transfected with pre-miR-145 or control pre-miRNA (Figure 3.4 A-C). Accordingly, insulin-mediated glucose uptake was blunted by 25% in cells expressing pre-miR-143 versus control miRNA (Figure 3.4 D). Importantly, lentivirus-mediated expression of pre-miR-143 in ARC also led to the inhibition of insulin-mediated Akt-Ser473 phosphorylation (Figure 3.4F).

The inhibition of insulin action in cells expressing pre-miR-143 could not be ascribed to alterations in the protein expression of key signalling molecules, such as the insulin receptor, IRS-1, PTEN, Akt, PRAS40, or GLUT4 (Figure 3.4 E, supplementary figure 3.4). In mice, down-regulation of the miR-143 target oxysterol-binding protein-related protein 8 (ORP8)

associates with hepatic insulin resistance.[14] Expression of pre-miR-143 reduced ORP8 protein levels in HL-1 cells and primary ARC by 20% and 25%, respectively (Figure 3.5 A/B). In contrast, control pre-miR or pre-miR-145 did not affect ORP8 abundance in HL-1 cells (Figure 3.5 A). Also exposing ARC to CM-EAT-T2D lowered ORP8 abundance when compared with cells exposed to CM-EAT-ND or control medium (Figure 3.5 C). Finally, lowering ORP8 protein levels in HL-1 cells using distinct ORP8 shRNA constructs was paralleled by reductions in insulin-stimulated Akt phosphorylation and glucose uptake vs. cells transfected with a control shRNA (Figure 3.5 D-G).

To substantiate these observations, the expression of miR-143 was silenced using LNA-anti-miR-143, which is efficiently taken up by primary ARC. In the absence of CM, LNA-anti-miR-143 increased ORP8 protein levels and enhanced insulin-mediated Akt-phosphorylation without affecting insulin receptor, PTEN, Akt and GLUT4 protein levels (Supplementary figure 3.5). Furthermore, LNA-anti-miR-143 protected against the detrimental effects of CM-EAT-T2D on insulin-mediated Akt-phosphorylation and ORP8 protein levels in ARC (Figure 3.6 A-C).

Discussion

The present study shows that CM-EAT-T2D alters the expression levels of eight miRNAs in ARC. We previously reported that CM-EAT-T2D or CM-EAT from high-fat diet fed guinea pigs induces ARC dysfunction as illustrated by reductions in contractile function and insulin action.[8, 9] These effects could be largely ascribed to an increased abundance of activin A in the CM.[8, 9] Of the miRNAs affected by CM-EAT-T2D, only the levels of miR-143 and miR-145 were affected by activin A in the same direction as CM-EAT-T2D. In addition, the induction of miR-143 and miR-145, which are processed from the same transcript under the control of the same promoter,[23, 24] was dependent on p38. Moreover, the observed up-regulation of miR-143 in response to CM-EAT-T2D or activin A, resulted in inhibition of insulin action in cardiomyocytes through the down-regulation of a recently identified miR-143 target and mediator of insulin action, ORP8.[14] Finally, the knockdown of miR-143 protected against the inhibition of insulin action and down-regulation of ORP8 in ARC exposed to CM-EAT-T2D.

A key finding of the present study is the unravelling of a novel signalling pathway via which alterations in the secretory profile of EAT may result in insulin resistance in the heart of patients with T2D. In patients with T2D, aberrant myocardial energy substrate metabolism coexists with alterations in cardiac structure and function, even in the absence of coronary artery disease or hypertension.[3, 4, 25] Whereas the healthy heart capable of switching between these substrates according to the most favourable energetic yield needed for the prevailing cardiac condition, the heart of patients with T2D displays an impaired metabolic flexibility and myocardial energy substrate metabolism is shifted toward enhanced fatty acid utilization at the expense of glucose metabolism.[4, 26, 27] Studies in humans and rodent models indicate that this metabolic inflexibility is closely associated with myocardial insulin resistance.[4, 5] In particular the insulin-stimulated phosphorylation of Akt, which mediates cardiac glucose uptake by promoting the translocation of the glucose transporter GLUT4 to the sarcolemma is impaired.[5] Importantly, the factors responsible for deregulation of this signalling pathway are largely unclear. This study reveals that an elevated secretion of activin A by EAT contributes to the inhibition of the Akt/GLUT4 pathway through up-regulation of miR-143.

Although we did not assess diabetic rat models for alterations in cardiac miR-143 expression, other studies confirmed a function for miR-143 in obesity and insulin resistance.[14, 28] Feeding mice an obesity-inducing high-fat diet increased the expression of miR-143 in adipose tissue, whereas another study reported up-regulation of both miR-143 and

miR-145 in the liver.[14, 28] Furthermore elevated miR-143 levels have been reported in the liver, heart, skeletal muscle and pancreas from *db/db*-mice and *ob/ob*-mice when compared with tissues isolated from control animals.[14, 28] In these studies, the factors responsible for the up-regulation of miR-143 remained unidentified. Here we identify activin A as regulator of miR-143 expression. We could show that the induction of this miRNA-cluster by CM-EAT-T2D is abolished upon pre-treating the CM with neutralizing activin A antibodies. Furthermore, exposing ARC to the amount of activin A present in CM-EAT-T2D increased the expression of miR-143. Finally, in line with a study examining the regulation of miR-143 expression by transforming growth factor β1 in smooth muscle cells,[21] we observed that the induction of this cluster by activin A and CM-EAT-T2D in cardiomyocytes could be abolished by inhibition of p38.

Our data further link the induction miR-143 to inhibition of insulin action. As in other target tissues for insulin action, insulin signalling in cardiomyocytes is initiated by tyrosine phosphorylation of IRS-1 by the activated insulin receptor. This facilitates the binding and activation of phosphatidylinositol-3'-kinase, thus catalysing the formation of phosphatidylinositol 3,4,5-trisphosphate and providing a platform for the binding and activation of Akt and subsequent translocation of GLUT4.[5] The phosphatase PTEN counteracts this signalling pathway by dephosphorylating phosphatidylinositol 3,4,5-trisphosphate to produce phosphatidylinositol 4,5-bisphosphate, and thereby inhibiting the activation of Akt. However, in this study the observed inhibition of insulin action in cells expressing pre-miR-143 could not be ascribed to alterations in the expression of key components of insulin action, such as the insulin receptor, IRS-1, PTEN, Akt and GLUT4. This is in accordance with a report on mice with an inducible expression of miR-143 in the liver.[14] In these animals, insulin-mediated Akt-phosphorylation is abrogated in the absence of changes in the expression of the insulin receptor, and Akt.[14] Conversely, the absence of the miR-143/145 cluster was found to protect against high-fat diet induced insulin resistance and hepatic Akt-inhibition.[14] Using proteomics-based approaches, these authors further identified ORP8 as the miR-143 target responsible for the abrogation of insulin action in the liver.[14] We extend these observations to cardiomyocytes by showing that incubation of ARC with CM-EAT-T2D as well as expression of pre-miR-143 in ARC and HL-1 cells results in a down-regulation of ORP8 expression, and that the absence of miR-143 protects against the induction of insulin resistance by CM-EAT-T2D in ARC. Furthermore, down-regulation of ORP8 expression was associated with inhibition of insulin-mediated Akt-signalling.

However, the molecular mechanism via which ORP8 regulates Akt-phosphorylation remains to be elucidated.

In contrast to miR-143, expression of pre-miR-145 had no effect on insulin action in HL-1 cells. This is in contrast to studies on colon cancer, where IRS-1 was identified as miR-145 regulated target, but in agreement with observations on mice with an inducible expression of miR-145 in the liver.[14, 29] Importantly, up-regulation of miR-145 has been reported in human samples from subjects with dilated cardiomyopathy and end-stage heart failure, thus highlighting the need for characterization of target genes regulated by miR-145.[30, 31]

Another question that remains to be addressed is the contribution of the activin A-p38-miR-143/145-ORP8 pathway in the pathophysiology of diabetic cardiomyopathy. A limitation of this study is that we could not analyse cardiac ventricular biopsies from patients with diabetic cardiomyopathy for alterations in the expression of the miR-143/145 cluster or ORP8. Furthermore, although we obtained comparable results for activin release from EAT from high-fat diet fed guinea pigs, confounding effects of medication use on adipokine release in human EAT can not be fully excluded. However, it should be noted that in a separate clinical study, activin A levels were found to be inversely associated with the myocardial metabolic rate of glucose uptake as measured using [^{18}F]-2-fluoro-2-deoxy-D-glucose during an euglycaemic-hyperinsulinaemic clamp in men with uncomplicated T2D.[32] Furthermore, activin A released from EAT has been linked to the development of atrial fibrosis.[33] Collectively, these data support of an involvement of activin A in the pathophysiology of diabetic cardiomyopathy.

In conclusion, this study identified a mechanism via which an enhanced secretion of activin A by EAT-T2D induces myocardial insulin resistance. Specifically, the p38-dependent induction of miR-143 inhibits the activation of the Akt-pathway regulating glucose uptake by insulin through down-regulation of a novel regulator of insulin action, ORP8. The elucidation of this signalling pathway may contribute to the recognition of more specific therapeutic targets for the prevention and treatment of diabetic cardiomyopathy.

Acknowledgements

We thank Dr. Robert Schwenk (DIFE, Potsdam, Germany), and Prof. Dr. Juergen Eckel (German Diabetes Centre, Duesseldorf) for helpful and critical discussions on this study.

Duality of interest

The authors have no conflicts of interest.

Funding

This work was supported by the Federal Ministry of Health, the Ministry of Innovation, Science, Research and Technology of the German State of North-Rhine Westphalia and the German Centre for Diabetes Research (Deutsches Zentrum für Diabetesforschung, DZD)

Table 3.1: Patient characteristics.

	ND	T2D	
n	10	14	
Gender	8 males, 2 females	13 males, 1 female	NS
Age	65 ± 3.7	73 ±2.5	NS
BMI, kg/m^2	29.1 ± 1.1	31.3 ±1.8	NS
Glucose before operation, mg/dl	110 ± 3.8	150 ±11	<0.001

Anthropometric characteristics are expressed as mean ± standard deviation, and differences between the disease groups were evaluated using a Mann-Whitney U-test. ND, non-diabetic; T2D, type 2 diabetes; BMI, body mass index; NS, not significant.

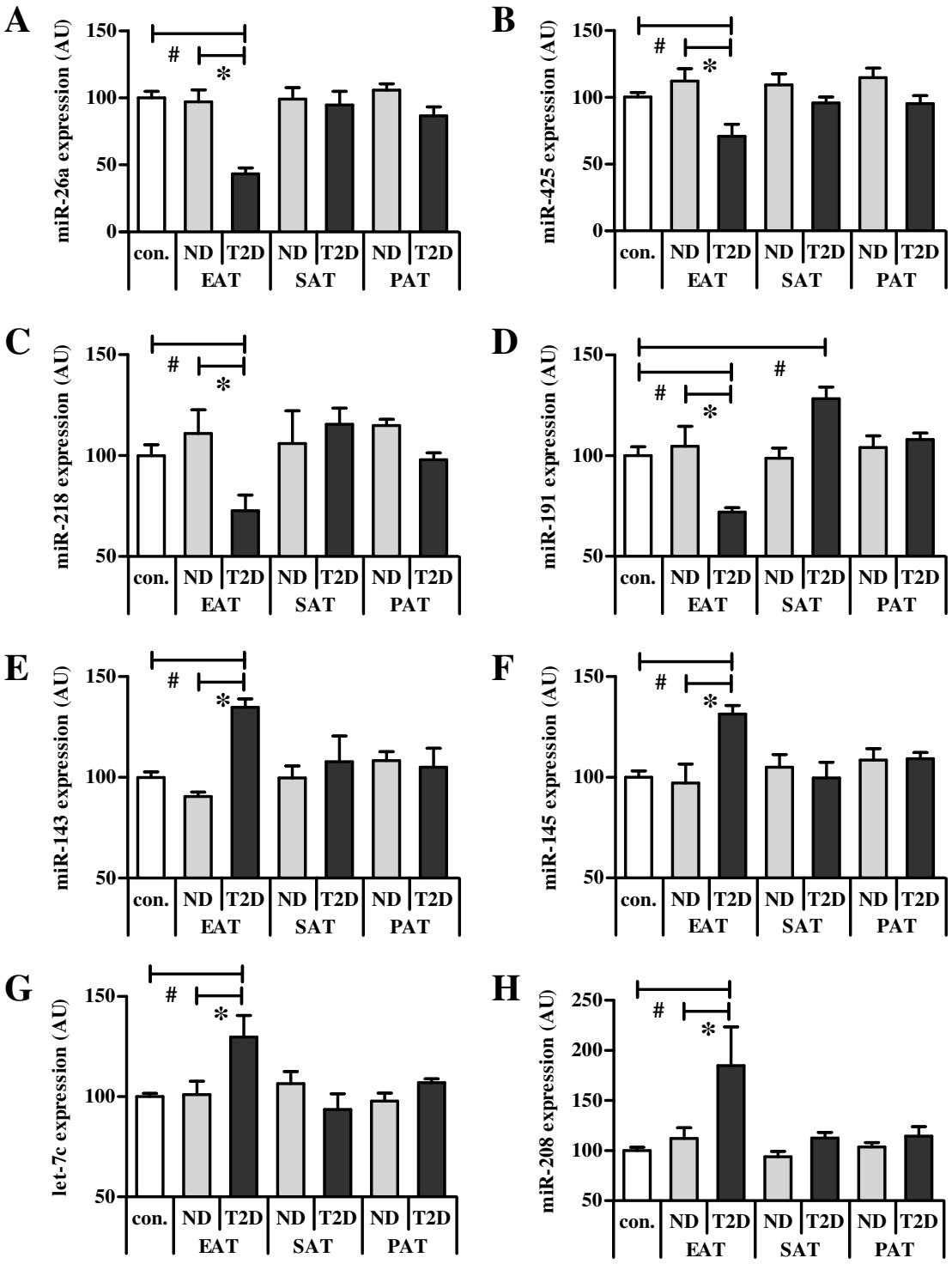

Figure 3.1: Effect of epicardial adipokines on miRNA expression in cardiomyocytes. Adult rat cardiomyocytes (ARC) were exposed to control AM (con.) or to CM (1:4 diluted) from epicardial adipose tissue (EAT), pericardial adipose tissue (PAT), and subcutaneous adipose tissue (SAT) from either patients with type 2 diabetes (T2D) or from patients without diabetes (ND). The miRNA expression in ARC exposed to control medium was set at 100. Open bars, con.; gray bars, ND; black bars, T2D. Data were collected during seven independent experiments for CM from EAT and four independent experiments for CM from PAT and SAT using ARC preparations from different rats and CM from different donors. Expression levels are expressed as mean ± SEM. Differences among the experimental groups were analysed by ANOVA followed by post-hoc Bonferroni analysis. *, $P<0.05$ ND vs. T2D.

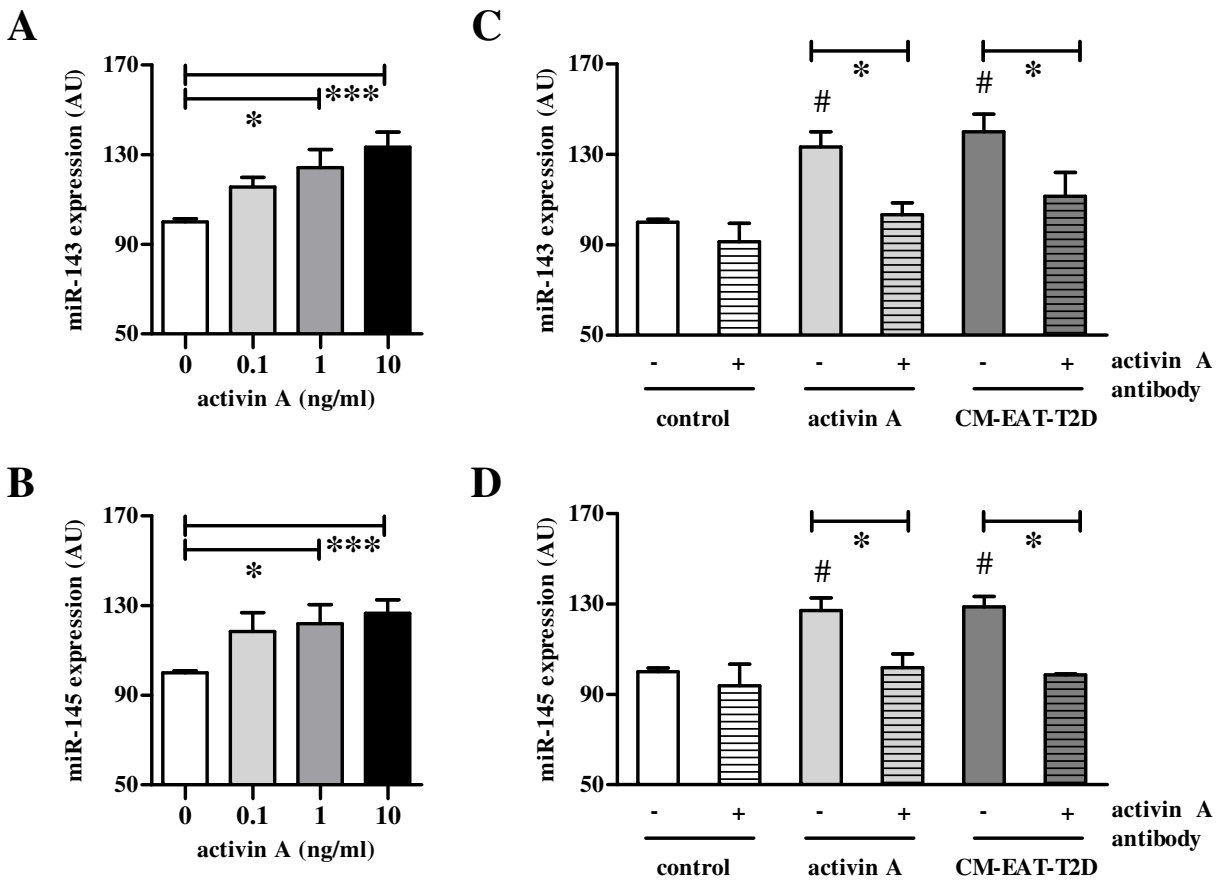

Figure 3.2: Regulation of the expression of the miR-143/145-cluster by activin A. Dose-dependent effect of a 16 h exposure of adult rat cardiomyocytes (ARC) to recombinant activin A on miR-143 (**A**) and miR-145 (**B**) expression. Experiments were performed using cardiomyocyte preparations from different rats, and are expressed as mean ± SEM (n=8). The effect of the various activin A concentrations on miRNA expression was evaluated using ANOVA followed by post-hoc Bonferroni analysis. ***, $P<0.001$; *, $P<0.05$ vs. untreated cells (0). (**C/D)** Effect of neutralizing activin A antibodies on the induction of miR-143 (**C**) and miR-145 (**D**) following a 16 h exposure of ARC to 10 ng/ml activin A or CM-EAT-T2D (1:4 diluted). Data were collected in four independent experiments using cardiomyocyte preparations from different rats and CM from different donors. #, indicates $P<0.001$ vs. control AM (control) as determined using ANOVA followed by post-hoc Bonferroni analysis; * indicates $P<0.05$ for the effect of the neutralizing activin A antibody as determined by a student's t-test.

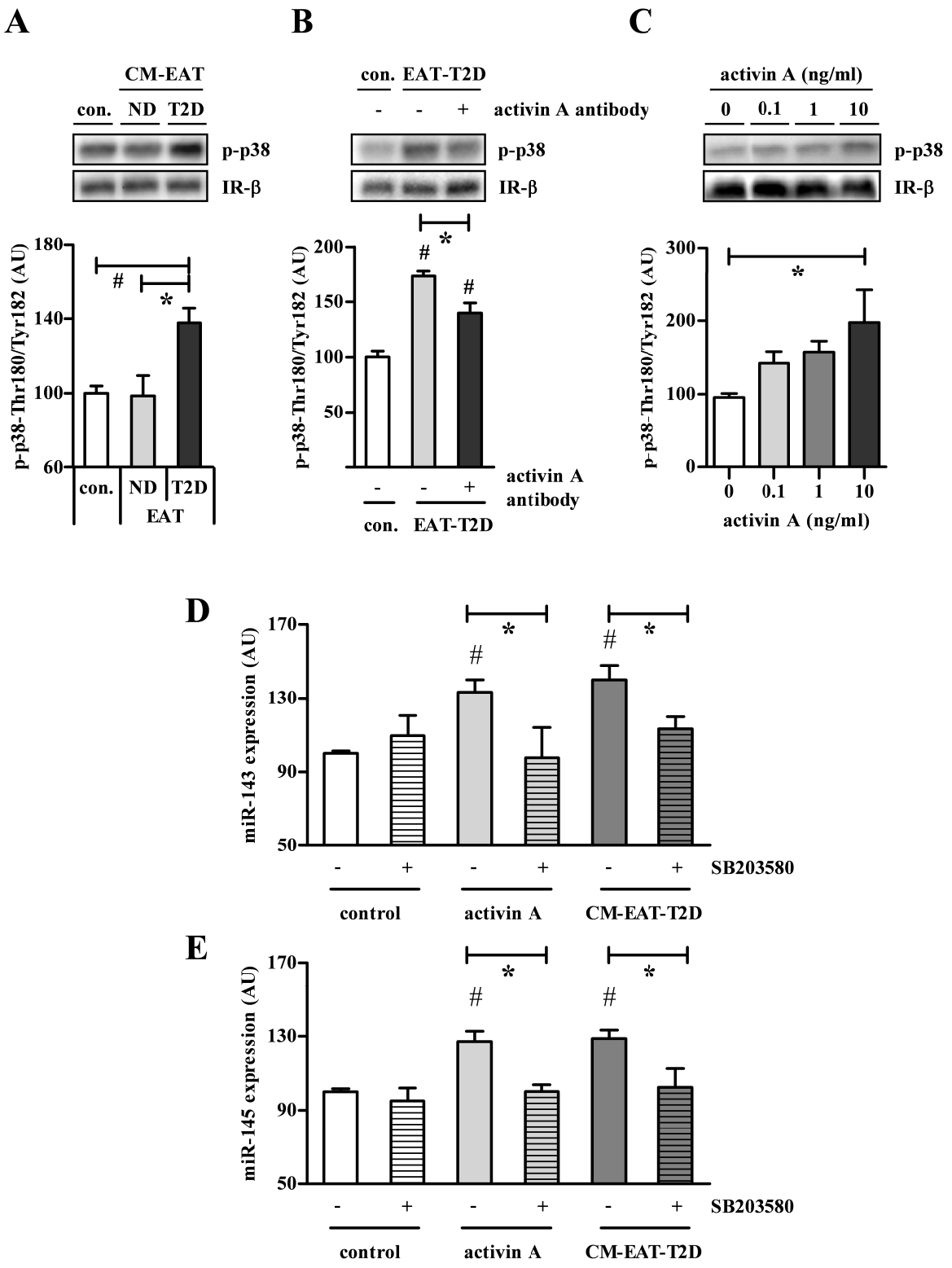

Figure 3.3: Regulation of the miR-143/145-expression by the MAP kinase p38. Phosphorylation of p38 in adult rat cardiomyocytes (ARC) exposed to CM-EAT from patients with (T2D) or without (ND) type 2 diabetes (**A**), to CM-EAT-T2D in the presence and absence of activin A neutralizing antibodies (**B**), or to increasing amounts of activin A (**C**) for 30 min. Experiments are performed using cardiomyocytes from different rats and CM from different donors. Shown are representative blots and quantifications for which the phosphorylation data

were normalized for insulin receptor β (IR-β) levels. Data are expressed as mean ± SEM (**A**: n=6, **B/C**: n=4). (**D/E)** Effect of inhibition of p38 using SB203580 on the induction of miR-143 (**D**) and miR-145 (**E**) in response to a 16 h exposure of ARC to 10 ng/ml activin A or CM-EAT-T2D. All data were collected in four independent experiments using cardiomyocytes from different rats and CM from different donors. #, indicates $P<0.001$ vs. control AM (control) as determined using ANOVA followed by post-hoc Bonferroni analysis; * indicates $P<0.05$ for the effect of the neutralizing activin A antibody as determined by a student's t-test.

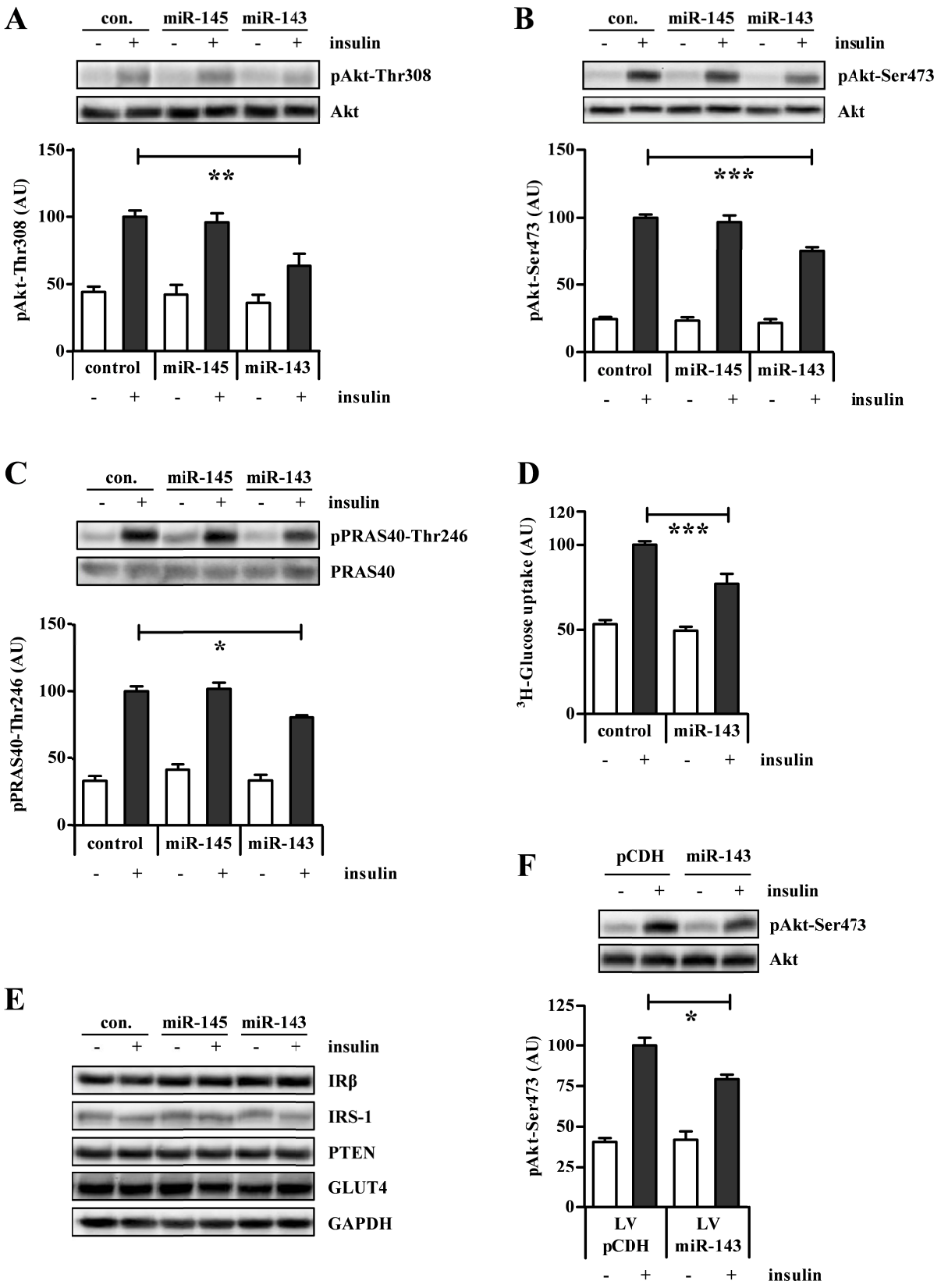

Figure 3.4: Effect of miR-143 and miR-145 on insulin action. HL-1 cells were transfected with control precursor miRNA or precursors for miR-143 or miR-145. Shown are representative blots and quantifications for the phosphorylation of Akt on Thr308 (**A**) and Ser473 (**B**), and of PRAS40 (**C**) on Thr246 in serum-starved cells (-) or following insulin stimulation (30 min; 200 nM) (+). (**D**) Rate of glucose uptake in HL-1 cells transfected

with control precursor miRNA (control) or a pre-miR-143 in serum-starved cells (-), or following insulin stimulation (30 min; 200 nM) (+). Data were collected in six independent experiments each performed in triplicate and are expressed as mean ± SEM. (**E)** Effect of miR-143 and miR-145 vs control pre-miR on the protein levels of the IRβ-subunit, IRS-1, PTEN, and GLUT4. The blot for GAPDH served as a housekeeper control for protein expression. (**F)** Representative blot and quantification of the effect of miR-143 expression on insulin-induced Akt-Ser473 phosphorylation in primary adult cardiomyocytes kept untreated (-) or following insulin stimulation (10 min; 100 nM) (+). All phosphorylation data were normalized for GAPDH levels, and expressed as mean ± SEM (**A/B**: n=8; **C**: n=5; **F:** n=6). Differences among the experimental conditions were evaluated using ANOVA followed by post-hoc Bonferroni analysis. ***, indicates $P<0.001$, **, $P<0.01$, and *, $P<0.05$.

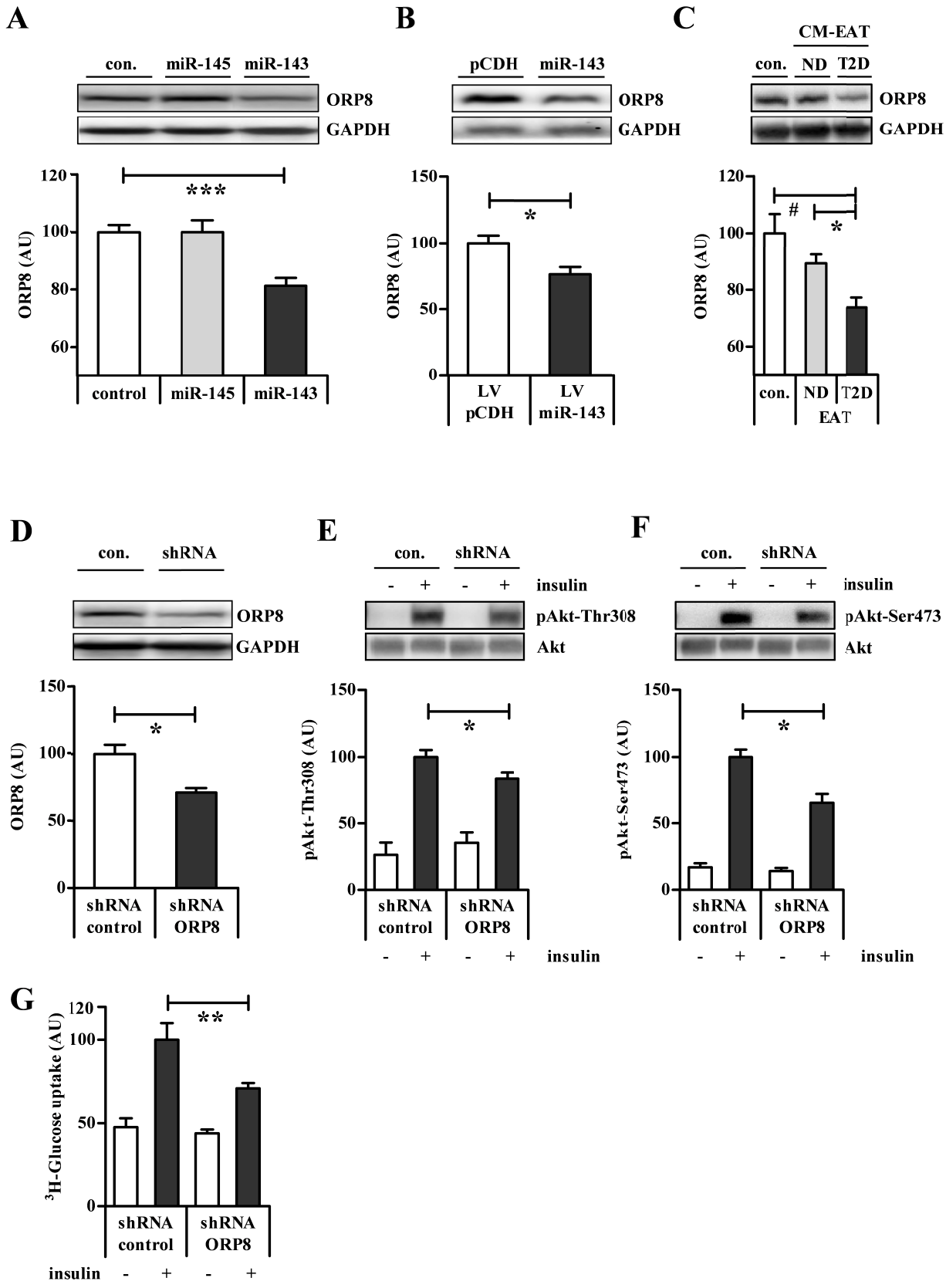
A
con.
miR-145
miR-143
ORP8
GAPDH
ORP8 (AU)
***
control
miR-145
miR-143
B
pCDH
miR-143
ORP8
GAPDH
ORP8 (AU)
*
LV pCDH
LV miR-143
C
CM-EAT
con.
ND
T2D
ORP8
GAPDH
ORP8 (AU)
#
*
con.
ND
T2D
EAT
D
con.
shRNA
ORP8
GAPDH
ORP8 (AU)
*
shRNA control
shRNA ORP8
E
con.
shRNA
insulin
pAkt-Thr308
Akt
pAkt-Thr308 (AU)
*
shRNA control
shRNA ORP8
insulin
F
con.
shRNA
insulin
pAkt-Ser473
Akt
pAkt-Ser473 (AU)
*
shRNA control
shRNA ORP8
insulin
G
3H-Glucose uptake (AU)
**
shRNA control
shRNA ORP8
insulin

Figure 3.5: Inhibition of insulin action by CM-EAT-T2D and miR-143 involves down-regulation of ORP8. Representative blots and quantification of ORP8 abundance in HL-1 cells (**A**) transfected with control precursor miRNA or precursors for miR-143 or miR-145, primary adult rat cardiomyocytes (ARC) (**B**) transduced with empty vector or vector expressing miR-143 (**B**), or ARC exposed to CM-EAT from patients with (T2D) or without (ND) type 2 diabetes (**C**). ORP8 protein levels were normalized for GAPDH expression, and expressed as mean ± SEM (**A**: n=8; **B**: n=6; **C**: n=4). Differences among the experimental conditions were evaluated using ANOVA followed by post-hoc Bonferroni analysis. *** indicates $P<0.001$; *,# $P<0.05$. (**D-F)** Effect of reduced expression of ORP8 on insulin action in HL-1 cells. HL-1 cells transfected with shRNAs for ORP8 were analysed for ORP8 expression (**D**), induction of Akt-phosphorylation (**E/F**), and glucose uptake (**G**) in untreated cells (-), and after insulin stimulation (30 min; 200 nM) (+). Signals were normalized for GAPDH (D) and Akt (E/F), respectively. Similar data were obtained with five distinct shRNA constructs. Data are expressed as mean ± SEM collected in 10 independent experiments conducted with distinct shRNA constructs. *, indicates $P<0.05$ as determined using a student's t-test.

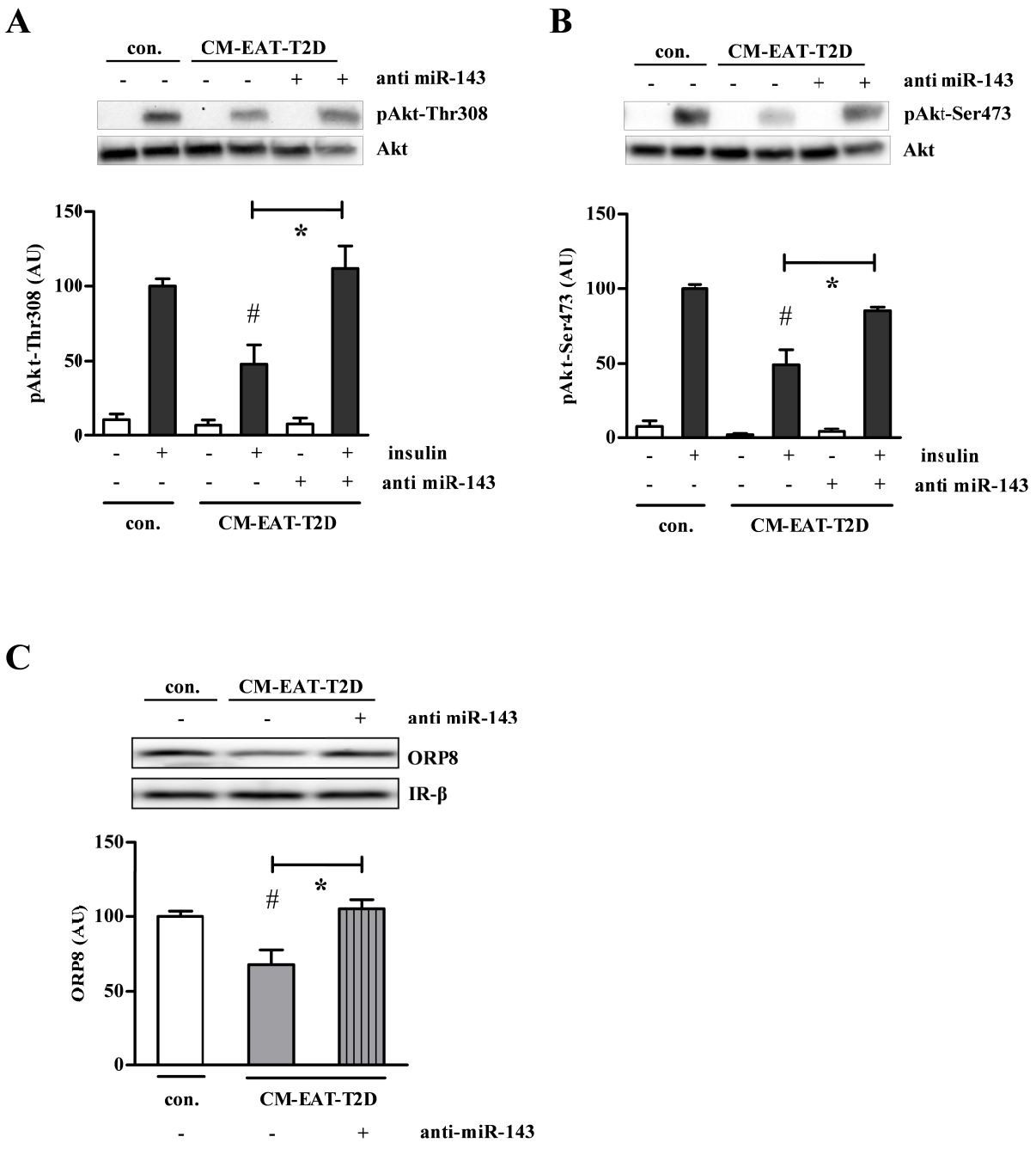

Figure 3.6: Silencing miR-143 reverses the abrogation of insulin action by CM-EAT-T2D in cardiomyocytes. Primary adult rat cardiomyocytes were transfected with LNA-anti-miR-143 (+) or LNA inhibitor control (-), and exposed to CM-EAT-T2D or control AM. Shown are representative blots and quantification for induction of Akt-Thr308 (**A**) and Akt-Ser473 (**B**) phosphorylation following insulin stimulation (10 min; 100 nM) and ORP8 expression (**C**). Signals were normalized for Akt (A/B) or IR-β (C) protein levels and are expressed as mean ± SEM from four independent experiments conducted on cardiomyocyte preparations from different rats. Data were analysed by ANOVA and Bonferroni multiple comparison analysis. # indicates $P<0.05$ for the effect of CM-EAT-T2D vs control AM; * indicates $P<0.05$ for the difference between LNA-anti-miR-143 versus LNA-inhibitor control.

References

[1] Kannel WB, McGee DL (1979) Diabetes and cardiovascular disease. The Framingham study. JAMA 241: 2035-2038

[2] Haffner SM, Lehto S, Ronnemaa T, Pyorala K, Laakso M (1998) Mortality from coronary heart disease in subjects with type 2 diabetes and in nondiabetic subjects with and without prior myocardial infarction. N.Engl.J.Med 339: 229-234

[3] Rubler S, Dlugash J, Yuceoglu YZ, Kumral T, Branwood AW, Grishman A (1972) New type of cardiomyopathy associated with diabetic glomerulosclerosis. Am.J.Cardiol. 30: 595-602

[4] Iozzo P (2010) Metabolic toxicity of the heart: insights from molecular imaging. Nutr.Metab Cardiovasc.Dis. 20: 147-156

[5] Ouwens DM, Diamant M (2007) Myocardial insulin action and the contribution of insulin resistance to the pathogenesis of diabetic cardiomyopathy. Arch.Physiol Biochem. 113: 76-86

[6] Ouwens DM, Sell H, Greulich S, Eckel J (2010) The role of epicardial and perivascular adipose tissue in the pathophysiology of cardiovascular disease. J.Cell Mol.Med. 14: 2223-2234

[7] Iozzo P (2011) Myocardial, perivascular, and epicardial fat. Diabetes Care 34 Suppl 2: S371-S379

[8] Greulich S, Herzfeld de Wiza D, Preilowski S, et al (2011) Secretory products of guinea pig epicardial fat induce insulin resistance and impair primary adult rat cardiomyocyte function. J.Cell Mol.Med. 15: 2399-2410

[9] Greulich S, Maxhera B, Vandenplas G, et al (2012) Secretory Products from Epicardial Adipose Tissue of Patients with Type 2 Diabetes Mellitus Induce Cardiomyocyte Dysfunction. Circulation 126: 2324-2410

[10] Xie H, Sun L, Lodish HF (2009) Targeting microRNAs in obesity. Expert.Opin.Ther.Targets. 13: 1227-1238

[11] Mendell JT, Olson EN (2012) MicroRNAs in stress signaling and human disease. Cell 148: 1172-1187

[12] Shantikumar S, Caporali A, Emanueli C (2012) Role of microRNAs in diabetes and its cardiovascular complications. Cardiovasc.Res. 93: 583-593

[13] Bartel DP (2009) MicroRNAs: target recognition and regulatory functions. Cell 136: 215-233

[14] Jordan SD, Kruger M, Willmes DM, et al (2011) Obesity-induced overexpression of miRNA-143 inhibits insulin-stimulated AKT activation and impairs glucose metabolism. Nat.Cell Biol. 13: 434-446

[15] Cheng Y, Zhang C (2010) MicroRNA-21 in cardiovascular disease. J.Cardiovasc.Transl.Res. 3: 251-255

[16] Ling HY, Hu B, Hu XB, et al (2012) MiRNA-21 Reverses High Glucose and High Insulin Induced Insulin Resistance in 3T3-L1 Adipocytes through Targeting Phosphatase and Tensin Homologue. Exp.Clin.Endocrinol.Diabetes 120: 553-559

[17] Liu B, Wu X, Liu B, et al (2012) MiR-26a enhances metastasis potential of lung cancer cells via AKT pathway by targeting PTEN. Biochim.Biophys.Acta 1822: 1692-1704

[18] Luo X, Zhang J, Wang H, et al (2012) PolyA RT-PCR-based quantification of microRNA by using universal TaqMan probe. Biotechnol.Lett. 34: 627-633

[19] Claycomb WC, Lanson NA, Jr., Stallworth BS, et al (1998) HL-1 cells: a cardiac muscle cell line that contracts and retains phenotypic characteristics of the adult cardiomyocyte. Proc.Natl.Acad.Sci.U.S.A 95: 2979-2984

[20] Condorelli G, Latronico MV, Dorn GW (2010) microRNAs in heart disease: putative novel therapeutic targets? Eur.Heart J. 31: 649-658

[21] Long X, Miano JM (2011) Transforming growth factor-beta1 (TGF-beta1) utilizes distinct pathways for the transcriptional activation of microRNA 143/145 in human coronary artery smooth muscle cells. J.Biol.Chem. 286: 30119-30129

[22] Schwenk RW, Dirkx E, Coumans WA, et al (2010) Requirement for distinct vesicle-associated membrane proteins in insulin- and AMP-activated protein kinase (AMPK)-induced translocation of GLUT4 and CD36 in cultured cardiomyocytes. Diabetologia 53: 2209-2219

[23] Cordes KR, Sheehy NT, White MP, et al (2009) miR-145 and miR-143 regulate smooth muscle cell fate and plasticity. Nature 460: 705-710

[24] Iio A, Nakagawa Y, Hirata I, Naoe T, Akao Y (2010) Identification of non-coding RNAs embracing microRNA-143/145 cluster. Mol.Cancer 9: 136

[25] Rijzewijk LJ, van der Meer RW, Lamb HJ, et al (2009) Altered myocardial substrate metabolism and decreased diastolic function in nonischemic human diabetic cardiomyopathy: studies with cardiac positron emission tomography and magnetic resonance imaging. J.Am.Coll.Cardiol. 54: 1524-1532

[26] Lopaschuk GD, Ussher JR, Folmes CD, Jaswal JS, Stanley WC (2010) Myocardial fatty acid metabolism in health and disease. Physiol Rev. 90: 207-258

[27] Taegtmeyer H, McNulty P, Young ME (2002) Adaptation and maladaptation of the heart in diabetes: Part I: general concepts. Circulation 105: 1727-1733

[28] Takanabe R, Ono K, Abe Y, et al (2008) Up-regulated expression of microRNA-143 in association with obesity in adipose tissue of mice fed high-fat diet. Biochem.Biophys.Res.Commun. 376: 728-732

[29] Shi B, Sepp-Lorenzino L, Prisco M, Linsley P, deAngelis T, Baserga R (2007) Micro RNA 145 targets the insulin receptor substrate-1 and inhibits the growth of colon cancer cells. J.Biol.Chem. 282: 32582-32590

[30] Ikeda S, Kong SW, Lu J, et al (2007) Altered microRNA expression in human heart disease. Physiol Genomics 31: 367-373

[31] Naga Prasad SV, Duan ZH, Gupta MK, et al (2009) Unique microRNA profile in end-stage heart failure indicates alterations in specific cardiovascular signaling networks. J.Biol.Chem. 284: 27487-27499

[32] Chen WJY, Greulich S, Rijzewijk LJ, et al (2012) Activin A is derived from human epicardial adipose tissue and associates with decreased myocardial function and glucose metabolism in human diabetic cardiomyopathy. Diabetologia 55: S495

[33] Venteclef N, Guglielmi V, Balse E, et al (2013) Human epicardial adipose tissue induces fibrosis of the atrial myocardium through the secretion of adipo-fibrokines. Eur.Heart J.

Extended version of the methods applied in this study

Adipose tissue biopsies

Patients undergoing open heart surgery for coronary artery bypass grafting and/or valve replacement procedures were enrolled in this study with written informed consent. The procedure to obtain adipose tissue samples was approved by the ethical committee of the Heinrich-Heine-University (Duesseldorf, Germany). In this study, patients with Caucasian origin were recruited and distributed into two groups, non-diabetics (ND) or T2D, on the basis of the diagnosis T2D in the medical records of the patients. Patients of other ethnic origins, diagnosed as having type 1 diabetes, HIV infection, lipodystrophy or chronic coexistent inflammatory disease were excluded from participation. Adipose tissue biopsies collected from the epicardial, pericardial and subcutaneous adipose tissue depots were used to generate conditioned media (CM) as previously described.[8, 34] Activin A content in the conditioned media was determined using a Quantikine activin A immunoassay (R&D systems, Minneapolis, MN, USA).

Isolation and culture of primary adult rat cardiomyocytes

Animal experiments were performed in accordance with the 'Principle of laboratory animal care' (NIH publication No. 85–23, revised 1996) and the current version of the German Law on the protection of animals. Cardiomyocytes were isolated from Lewis rats (Lew/Crl) as described.[8] Briefly, rats were killed following anaesthesia with ketamine (100 mg/kg; Ratiopharm, Ulm, Germany) and xylazine (Rompun, 5 mg/kg) (Bayer Healthcare, Leverkusen, Germany). The isolated heart was retrograde perfused using a Langendorff perfusion system and digested with a buffer containing collagenase (Worthington, Lakewood, NJ, USA) and hyaluronidase (Applichem, Darmstadt, Germany). Isolated cardiomyocytes were seeded and cultured on laminin-coated 6-well plates before exposure to the conditioned media (CM) or control adipocyte medium (AM). When indicated, the conditioned media were incubated for 60 min with 100 ng activin A βA subunit antibody (R&D systems, Wiesbaden-Nordenstadt, Germany) before addition to the cardiomyocytes, or the cardiomyocytes were incubated for 30 min with 2.5 μM of the p38 inhibitor SB203580 (Promega, Mannheim, Germany) before the addition of the conditioned media.

Whole genome miRNA-profiling in rat cardiomyocytes

To assess the effects on miRNA expression, cardiomyocytes were harvested 16h after the addition of the CM (1:4 diluted with AM). Data were collected during at least 7 independent experiments for CM from EAT and 4 independent experiments for CM from the other fat depots. Each independent experiment (n=1) represents treatment of fresh isolated cardiomyocyte from one animal with CM from one donor. Total RNA was isolated from the cardiomyocytes using the miRNeasy mini kit and on a Qiacube system (both from Qiagen, Hilden, Germany). Then, 500 ng total RNA was reverse transcribed using the miScript I RT kit (Qiagen), whereafter miRNA expression levels were determined with the rat miScript Assay 384 set based on miRBase V13.0 (Qiagen) and miScript SYBR Green (Qiagen) on a StepOne Plus real-time PCR system (Applied Biosystems, Carlsbad, CA, USA) with the following cycling conditions: 10‘ 95°C, followed by 40 cycles of 15‘‘ 94°C, 30‘‘ 50°C and 30‘‘ 70°C. Real-time PCR results were manually verified using the StepOne Software version 2.2.2 (Applied Biosystems), and products showing variable melting curves and/or C_t-values >37 were excluded from further analysis. For whole genome miRNA-profiling, the levels of the expressed miRNAs were normalized with the global mean method using QbasePlus software version 2.0 (Biogazelle, Ghent, Belgium).[35] Taqman assays were used to validate miR-143 and miR-145 expression levels using GoTaq® Probe qPCR Master Mix (Promega, Mannheim, Germany) and 5’- AAATCTAGGAAGTCGACCTCGGCA-3’ (Eurogentec, Seraing, Belgium) as universal probe[18] using the following cycling conditions: 2‘ 95°C, followed by 40 cycles of 15‘‘ 94°C, 1’ 60 °C. For normalization of the expression levels of selected miRNAs in subsequent (validation) experiments, the geomean of SNORA73, SNORD25 and SCARNA17 was used. These miRNAs were identified as the most stable housekeepers using the Genorm algorithm in the QbasePlus software.[36]

Lentiviral vector-based overexpression of miR-143 in adult rat cardiomyocytes

To produce an lentivirus expression vector for mature rat miR-143, the 200 nucleotide region encoding miR-143 and its up- and downstream flanking sequences was amplified using as forward primer: 5’-ACAAAGGACACGAAGATGGA-3’ and as reverse primer: 5’-GGAACCCTCTCAGAATGGA-3’. The PCR-product was cloned into pCDH-CMV-MCS-EF1-RFP (System Biosciences, Mountain View, USA), and verified by sequencing. To produce infectious virus particles, HEKT293t cells were transfected with the pCDH constructs together with helper plasmids encoding HIV-1 gag-pol, HIV-1 rev, and the VSV-G

envelope as described previously.[37] For quantification of virus yield in the harvested medium, p24 antigen levels were determined using a HIV-1 p24 antigen enzyme-linked immunosorbent assay (ELISA) kit (ZeptoMetrix Corp.,New York, NY, USA). Primary adult rat cardiomyocytes were infected with an MOI of 5 for 24 hours. Two days after transduction, cells were serum-starved and kept untreated or incubated for 10 min with 100 nM insulin, and harvested.

Culture and Transfection of HL-1 cardiomyocytes

To investigate the impact of differentially regulated miRNAs and their potential targets on insulin action, the cardiac mouse cell line HL-1 was used.[19] These cells were kindly provided by professor dr. W.C. Claycomb (Louisiana State University, New Orleans, LA, USA), and cultured at 37°C and 5% CO_2 in Claycomb medium supplemented with 10% FCS, 0.1 mmol/l noradrenaline (all from Sigma Aldrich, St. Louis, MO, USA), as well as 2 mmol/l L-glutamine, and 100 U/ml penicillin and 100 µg/ml streptomycin (Invitrogen, Life Technologies, Darmstadt, Germany). HL-1 cells were transfected in 6-well dishes with 30 nmol/l Cy3™-labeled pre-miR™ (negative control) or pre-miR™ miRNA-precursor (Ambion, Life Technologies, Darmstadt, Germany) at 70-80% confluence using Lipofectamine™ 2000 (Invitrogen, Life Technologies, Darmstadt, Germany) according to the manufacturer's instructions. Immunofluorescence inspection of the HL-1 cardiomyocytes transfected with Cy3™-labeled pre-miR™ indicate a transfection efficiency of 50-60%. To silence ORP8, cells were transfected with five validated MISSION® shRNA constructs (TRCN0000105 245 – 249) targeting mouse ORP8 (NM_175489) (Sigma Aldrich) or empty vector. Comparable data were obtained for all five distinct ORP8 shRNAs evaluated. One day after transfection, cells were serum-starved for 16h on Dulbecco's modified Eagle medium containing 5 mM glucose (Invitrogen) and supplemented with 2 mmol/l L-glutamine, 100 U/ml penicillin and 100 µg/ml streptomycin. Thereafter, the cells were stimulated with 200 nM insulin for 30 minutes or kept untreated, and harvested.

LNA-anti-miR silencing of HL-1 cells and primary rat adult cardiomyocytes

HL-1 cells were transfected as described above with 60 nM miRCURY LNA inhibitor for miR-143 or miRCURY LNA inhibitor control (Exiqon, Vedbæk, Denmark) using lipofectamine. One day after transfection, cells were serum-starved for 16h on Dulbecco's modified Eagle medium containing 5 mM glucose (Invitrogen) and supplemented with 2

mmol/l L-glutamine, 100 U/ml penicillin and 100 µg/ml streptomycin. Thereafter, the cells were stimulated with 200 nM insulin for 30 minutes or kept untreated, and harvested. Isolated primary adult rat cardiomyocytes were transfected with 60 nM miRCURY LNA inhibitor for miR-143 or miRCURY LNA inhibitor control (Exiqon, Vedbæk, Denmark) for 6h using lipofectamine. Then, cells were exposed to CM or AM overnight. Thereafter, the cells were stimulated with 100 nM insulin for 10 minutes or kept untreated, and harvested.

Analysis of protein expression and insulin signalling

Cells were lysed for 2h at 4°C in 50 mmol/l HEPES (pH7.4), 1% Triton X-100, supplemented with protease and phosphatase inhibitor cocktails (Complete, PhosStop; Roche Diagnostics, Mannheim, Germany) under gentle rotation. Protein content was determined using Bradford reagent (Biorad Laboratories, Munich, Germany). Ten microgram of protein was loaded onto SDS-Page gels, and transferred to polyvinylidene difluoride membranes (Millipore, Schwalbach, Germany). After blotting, membranes were blocked with Tris-buffered saline, containing 0.1 % Tween 20 and 5 % non fat dried milk or 5% bovine serum albumin for 1 h at room temperature and then incubated overnight at 4°C with primary antibodies for Akt, PTEN, phospho-Akt-Thr308, phospho-Akt-Ser473, phospho-p38-Thr180/Tyr182, phospho-proline rich Akt substrate of 40 kDa (PRAS40)-Thr246 (all from Cell Signaling Technology, Danvers, MA, USA), GLUT4, glyceraldehyde 3-phosphate dehydrogenase (GAPDH), ORP8 (all from Abcam, Cambridge, UK), insulin receptor β-subunit (IRβ), PRAS40 (Santa Cruz Biotechnology, Santa Cruz, CA, USA), and insulin receptor substrate 1.[38] After extensive washing, membranes were incubated with corresponding secondary horseradish peroxidase-coupled antibodies (Promega) and bound antibodies were visualized by enhanced chemiluminescence using Immobilon Western detection reagents (Millipore) on a VersaDoc 4000 MP (BioRad) work station. Images were analyzed using Quantity One analysis software (Version 4.6.7).

Glucose uptake in HL-1 cardiomyocytes

Glucose uptake was measured in serum starved cells, which were either kept untreated or exposed for 30 min to 200 nM insulin. Then 0.12 mM deoxy-D-glucose with 0.055 µCi 2-deoxy-D-[^{3}H]glucose was added to the cells. After a 10 min incubation, the cells were washed extensively with ice-cold PBS, and lysed in 1% SDS and 0,2M NaOH, whereafter incorporated glucose was measured by scintillation counting.

Statistical analysis

Data are presented as means ± standard error of the mean. Significant differences between experimental conditions were evaluated as described in the legends to the Tables and the figures using Graphpad Prism5 (GraphPad, LA Jolla, CA) software. *P*-values of <0.05 were considered as statistically significant.

Supplementary Table 3.1: Type of surgery and medication use of patients providing epicardial adipose tissue biopsies for the generation of conditioned media.

	ND	T2D	
N	10	14	
Type of operation			
Valve replacement	1	0	NS
CABG	6	9	NS
Valve replacement + CABG	3	5	NS
Medication use			
Cholesterol-lowering	5 *(5x simvastatin)*	14 *(13x simvastatin 1x atorvastatin)*	0.006
Diuretics	5 (*4x furosemide 1x hydrochlorothiazide*)	10 *(7x furosemide 1x hydrochlorothiazide 1x torasemide 1x xipamide)*	NS
Anti-coagulants	9 (*8x acetylsalicylic acid 1x phenprocoumon*)	14 (*12x acetylsalicylic acid 1x phenprocoumon 1x clopidrogel*)	NS
Anti-hypertension: β-blockers	5 *(3x bisoprolol 2x metoprolol)*	10 *(6x bisoprolol 3x metoprolol 1x nebivolol)*	NS
Anti-hypertension: angiotensin-converting-enzyme inhibitors calcium-channel blockers	5 (*4x ramipril 1x valsartan*)	11 (*7x ramipril 1x enalapril 1x lisinopril 2x amiodipine*)	NS
Glucose-lowering	0	10 (*6x metformin 1x glimepiride 3x insulin*)	0.001

Differences in medication use and type of operation were determined using a Fisher's exact test. ND, non-diabetic; T2D, type 2 diabetes; CABG, coronary artery bypass graft surgery; NS, not significant.

Supplementary Table 3.2: miRNAs expressed in adult rat cardiomyocytes and effect of conditioned media from epicardial adipose tissue (EAT) from patients with (T2D) and without type 2 diabetes (ND).

	mature miRNA	stem loop accession number	average Ct-value	Relative expression (% of miR-133)	ND	T2D
1	rno-let-7a	MI0000827/ MI0000828	22.85	14.9	103 ± 8.2	110 ± 8.5
2	rno-let-7b	MI0000829	23.79	7.81	75 ± 16.7	116 ± 10.9
3	rno-let-7b*	MI0000829	30.50	0.074	143 ± 32.6	97 ± 21.6
4	**rno-let-7c**	**MI0000830/ MI0000831**	**22.28**	22.2	**101 ± 6.7**	**130 ± 10.8**
5	rno-let-7d	MI0000601	24.11	6.23	91 ± 6.2	98 ± 3.2
6	rno-let-7d*	MI0000601	27.19	0.74	123 ± 4.4	88 ± 8.0
7	rno-let-7e	MI0000832	24.67	4.24	91 ± 10.8	130 ± 3.1
8	rno-let-7e*	MI0000832	33.15	0.012	171 ± 37.4	102 ± 23.9
9	rno-let-7f	MI0000833/ MI0000834	25.96	1.73	89 ± 15.1	98 ± 3.2
10	rno-let-7i	MI0000835	25.41	2.54	96 ± 2.9	101 ± 9.4
11	rno-let-7i*	MI0000835	34.85	0.004	106 ± 7.4	123 ± 4.6
12	rno-miR-1	MI0003489	22.13	24.6	107 ± 19.9	95 ± 16.2
13	rno-miR-1*	MI0003489	33.82	0.007	136 ± 16.3	170 ± 68.7
14	rno-miR-100	MI0000885	25.11	3.11	99 ± 9.8	95 ± 16.0
15	rno-miR-101a	MI0000886	31.70	0.032	123 ± 43.2	181 ± 94.1
16	rno-miR-101a*	MI0000886	34.19	0.006	157 ± 45.7	97 ± 6.4
17	rno-miR-101b	MI0000648	30.21	0.091	60 ± 3.0	101 ± 27.1
18	rno-miR-103/ rno-miR-107	MI0000888/ MI0000890	26.93	0.88	116 ± 8.2	102 ± 4.1
19	rno-miR-106b*	MI0000889	34.16	0.006	80 ± 13.7	90 ± 8.8
20	rno-miR-10a-5p	MI0000841	30.50	0.074	85 ± 19.1	90 ± 25.2
21	rno-miR-10b	MI0000842	33.76	0.008	71 ± 39.5	55 ± 28.5
22	rno-miR-122	MI0000891	34.75	0.004	133 ± 23.9	103 ± 31.3
23	rno-miR-125a-5p	MI0000895	24.08	6.37	103 ± 9.4	99 ± 14.1
24	rno-miR-125b*	MI0000897	30.70	0.065	108 ± 7.9	106 ± 4.1
25	rno-miR-125b-5p	MI0000896/ MI0000897	23.38	10.3	93 ± 11.6	113 ± 12.5
26	rno-miR-126	MI0000898	22.93	14.1	63 ± 14.4	74 ± 21.2
27	rno-miR-126*	MI0000898	23.80	7.72	102 ± 32.6	87 ± 30.1
28	rno-miR-127	MI0000899	33.14	0.012	114 ± 10.1	113 ± 14.0
29	rno-miR-128	MI0000900/ MI0000901	30.59	0.070	105 ± 2.8	89 ± 19.2
30	rno-miR-129*	MI0000637	30.13	0.096	194 ± 31.0	104 ± 20.0
31	rno-miR-130a	MI0000903	27.36	0.65	103 ± 2.8	88 ± 11.0
32	rno-miR-130b	MI0000904	32.58	0.018	82 ± 11.6	107 ± 6.8
33	rno-miR-132	MI0000905	30.57	0.071	80 ± 20.6	116 ± 12.8
34	rno-miR-133a/ rno-miR-133b	MI0000906/ MI0003490	20.11	100	120 ± 6.8	127 ± 4.8
35	rno-miR-135a*	MI0000908	32.90	0.014	101 ± 27.7	88 ± 6.3
36	rno-miR-138	MI0000912/ MI0000911	35.67	0.002	108 ± 53.5	169 ± 18.0
37	rno-miR-139-3p	MI0000913	32.57	0.018	128 ± 24.2	130 ± 6.7

38	rno-miR-139-5p	MI0000913	28.88	0.23	130 ± 10.8	101 ± 9.1
39	rno-miR-140	MI0000611	33.83	0.007	148 ± 46.3	139 ± 30.3
40	rno-miR-140*	MI0000611	30.46	0.076	103 ± 21.1	92 ± 17.2
41	rno-miR-141	MI0000914	34.77	0.004	102 ± 20.5	202 ± 99.5
42	rno-miR-142-3p	MI0000915	32.92	0.014	311 ± 173.4	227 ± 110.6
43	**rno-miR-143**	**MI0000916**	**26.73**	1.02	**91 ± 2.2**	**135 ± 4.2**
44	**rno-miR-145**	**MI0000918**	**23.98**	6.84	**97 ± 9.4**	**131 ± 4.3**
45	rno-miR-146a	MI0000919	27.96	0.43	80 ± 30.9	85 ± 29.4
46	rno-miR-146b	MI0006342	31.75	0.031	186 ± 32.7	125 ± 23.2
47	rno-miR-148b-3p	MI0000616	29.51	0.15	145 ± 27.9	130 ± 25.6
48	rno-miR-148b-5p	MI0000616	33.39	0.010	130 ± 23.3	100 ± 34.3
49	rno-miR-150	MI0000920	24.96	3.46	85 ± 6.5	94 ± 24.4
50	rno-miR-151	MI0000647	28.31	0.34	108 ± 6.6	106 ± 19.0
51	rno-miR-151*	MI0000647	29.21	0.18	106 ± 4.9	96 ± 14.2
52	rno-miR-152	MI0000921	27.69	0.52	103 ± 11.2	99 ± 12.4
53	rno-miR-15b	MI0000843	27.60	0.56	106 ± 9.7	114 ± 29.7
54	rno-miR-16	MI0000844	23.24	11.4	104 ± 4.3	108 ± 28.8
55	rno-miR-17-3p	MI0000845	34.19	0.006	165 ± 45.0	119 ± 18.0
56	rno-miR-17-5p	MI0006131/ MI0000845	29.82	0.12	104 ± 9.7	139 ± 15.2
57	rno-miR-181a	MI0000953/ MI0000925	27.08	0.79	105 ± 8.3	106 ± 10.2
58	rno-miR-181a*	MI0000953	34.45	0.005	107 ± 6.2	103 ± 23.9
59	rno-miR-181b	MI0000926/ MI0000927	26.84	0.94	104 ± 1.6	124 ± 17.2
60	rno-miR-181c	MI0000924	27.89	0.45	104 ± 15.8	105 ± 6.4
61	rno-miR-181d	MI0006132	26.40	1.27	94 ± 5.1	117 ± 13.3
62	rno-miR-182	MI0006133	33.80	0.008	58 ± 8.6	56 ± 5.1
63	rno-miR-183	MI0000928	34.29	0.005	72 ± 12.6	88 ± 28.2
64	rno-miR-184	MI0000929	32.30	0.021	111 ± 12.4	81 ± 9.3
65	rno-miR-185	MI0000930	29.99	0.11	95 ± 5.0	126 ± 16.5
66	rno-miR-186	MI0000931	30.29	0.086	94 ± 8.4	121 ± 9.2
67	rno-miR-190	MI0000933	30.25	0.089	90 ± 12.9	116 ± 22.8
68	rno-miR-190b	MI0006135	33.66	0.008	103 ± 39.5	85 ± 30.2
69	**rno-miR-191**	**MI0000934**	**25.24**	2.85	**105 ± 9.9**	**72 ± 2.2**
70	rno-miR-192	MI0000935	30.32	0.084	75 ± 3.4	105 ± 16.2
71	rno-miR-193	MI0000936	28.41	0.32	92 ± 6.8	131 ± 5.9
72	rno-miR-194	MI0000937/ MI0000938	31.02	0.052	146 ± 39.4	117 ± 27.5
73	rno-miR-195	MI0000939	25.90	1.80	130 ± 12.4	107 ± 11.6
74	rno-miR-196c	MI0006136	33.76	0.008	87 ± 48.1	49 ± 20.7
75	rno-miR-199a-3p	MI0000941	31.52	0.037	93 ± 31.9	95 ± 25.1
76	rno-miR-199a-5p	MI0000941	32.85	0.015	59 ± 24.2	131 ± 85.3
77	rno-miR-19a	MI0000849	32.83	0.015	78 ± 17.9	405 ± 300.0
78	rno-miR-19b	MI0000847/ MI0000848	32.65	0.017	97 ± 5.3	392 ± 238.0
79	rno-miR-200b	MI0000944	34.67	0.004	122 ± 17.8	117 ± 17.6
80	rno-miR-200c	MI0000942	31.31	0.043	81 ± 4.0	120 ± 14.7
81	rno-miR-203	MI0000945	35.51	0.002	85 ± 15.6	145 ± 23.3

82	rno-miR-206	MI0000948	24.18	5.95	71 ± 8.4	113 ± 23.5
83	**rno-miR-208**	**MI0000949**	**28.59**	0.28	**112 ± 10.7**	**185 ± 38.7**
84	rno-miR-20a	MI0000638	29.47	0.15	93 ± 24.6	139 ± 45.9
85	rno-miR-20b-3p	MI0003554	31.45	0.039	126 ± 20.8	162 ± 26.5
86	rno-miR-21	MI0000850	24.74	4.04	128 ± 14.1	120 ± 13.4
87	rno-miR-21*	MI0000850	32.12	0.024	127 ± 33.7	228 ± 54.8
88	rno-miR-210	MI0000950	28.86	0.23	99 ± 3.8	118 ± 11.3
89	rno-miR-212	MI0000952	32.97	0.013	113 ± 7.8	122 ± 40.2
90	rno-miR-214	MI0000954	28.99	0.21	79 ± 12.4	99 ± 19.4
91	rno-miR-215	MI0003482	34.88	0.004	164 ± 54.4	73 ± 24.6
92	**rno-miR-218a**	**MI0000957**	**35.68**	0.002	**111 ± 11.7**	**73 ± 7.7**
93	rno-miR-219-5p	MI0000959/ MI0000960	36.10	0.002	107 ± 16.3	97 ± 21.9
94	rno-miR-22	MI0000851	24.26	5.61	86 ± 12.2	92 ± 10.4
95	rno-miR-22*	MI0000851	27.26	0.70	105 ± 16.9	98 ± 13.2
96	rno-miR-221	MI0000961	31.76	0.031	97 ± 9.1	91 ± 5.8
97	rno-miR-223	MI0000963	35.21	0.003	160 ± 72.2	212 ± 79.4
98	rno-miR-224	MI0003483	34.94	0.003	89 ± 10.4	100 ± 55.1
99	rno-miR-23a/ rno-miR-23b	MI0000852/ MI0000853	23.12	12.4	99 ± 14.5	83 ± 7.8
100	rno-miR-24	MI0000854/ MI0000855	24.59	4.47	92 ± 9.5	105 ± 18.3
101	rno-miR-24-1*	MI0000854	30.89	0.057	102 ± 8.4	117 ± 10.2
102	rno-miR-24-2*	MI0000855	28.78	0.24	101 ± 8.5	114 ± 21.4
103	rno-miR-25	MI0000856	28.07	0.40	101 ± 3.5	111 ± 21.9
104	rno-miR-25*	MI0000856	32.09	0.025	83 ± 12.8	89 ± 15.3
105	**rno-miR-26a**	**MI0000857**	**29.40**	0.16	**97 ± 9.0**	**43 ± 4.3**
106	rno-miR-26b	MI0000858	28.07	0.40	100 ± 17.5	78 ± 16.4
107	rno-miR-26b*	MI0000858	34.83	0.004	79 ± 18.6	86 ± 17.4
108	rno-miR-27a	MI0000860	28.59	0.28	74 ± 2.6	108 ± 26.0
109	rno-miR-27b	MI0000859	25.54	2.32	81 ± 3.7	97 ± 1.1
110	rno-miR-28	MI0000861	28.72	0.26	92 ± 6.9	103 ± 6.5
111	rno-miR-28*	MI0000861	31.21	0.045	122 ± 5.0	106 ± 5.7
112	rno-miR-291a-5p	MI0000965	28.56	0.29	132 ± 14.6	112 ± 15.5
113	rno-miR-296	MI0000967	32.55	0.018	97 ± 20.0	80 ± 8.7
114	rno-miR-29a	MI0000863	22.85	14.9	108 ± 12.3	103 ± 1.2
115	rno-miR-29a*	MI0000863	31.65	0.034	118 ± 15.8	110 ± 5.8
116	rno-miR-29b	MI0000864/ MI0000862	25.79	1.95	106 ± 26.3	117 ± 11.9
117	rno-miR-29b-2*	MI0000862	35.67	0.002	120 ± 10.0	63 ± 5.0
118	rno-miR-29c	MI0000865	23.31	10.8	111 ± 21.0	116 ± 6.9
119	rno-miR-29c*	MI0000865	31.89	0.028	99 ± 10.2	100 ± 6.9
120	rno-miR-301a	MI0000593	33.76	0.008	249 ± 123.2	260 ± 132.0
121	rno-miR-301b	MI0006137	34.23	0.006	101 ± 15.4	214 ± 103.6
122	rno-miR-30a	MI0000870	23.85	7.50	106 ± 24.8	122 ± 11.3
123	rno-miR-30a*	MI0000870	26.88	0.92	108 ± 5.0	99 ± 12.5
124	rno-miR-30b-3p	MI0000868	34.40	0.005	100 ± 12.0	124 ± 5.9
125	rno-miR-30b-5p	MI0000868	26.44	1.24	108 ± 15.9	130 ± 14.5
126	rno-miR-30c	MI0000866/	22.84	15.1	92 ± 4.1	99 ± 6.6

		MI0000871				
127	rno-miR-30c-1*	MI0000866	31.43	0.039	109 ± 4.1	102 ± 7.3
128	rno-miR-30c-2*	MI0000871	31.99	0.026	118 ± 5.0	101 ± 12.4
129	rno-miR-30d	MI0000869	23.38	10.3	103 ± 9.8	113 ± 10.2
130	rno-miR-30e	MI0000867	23.99	6.79	104 ± 12.5	85 ± 11.8
131	rno-miR-30e*	MI0000867	26.70	1.04	124 ± 45.0	156 ± 38.0
132	rno-miR-320	MI0000972	26.90	0.90	81 ± 5.9	111 ± 14.2
133	rno-miR-322	MI0000589	25.56	2.28	75 ± 9.6	81 ± 11.7
134	rno-miR-323	MI0000591	30.50	0.074	112 ± 41.5	106 ± 31.1
135	rno-miR-324-5p	MI0000594	30.20	0.091	85 ± 8.0	114 ± 2.0
136	rno-miR-325-3p	MI0000596	36.34	0.001	99 ± 10.5	119 ± 10.2
137	rno-miR-325-5p	MI0000596	34.17	0.006	77 ± 27.0	119 ± 5.8
138	rno-miR-328	MI0000602	26.45	1.23	77 ± 17.9	80 ± 10.1
139	rno-miR-331	MI0000608	32.21	0.023	84 ± 4.9	138 ± 15.1
140	rno-miR-335	MI0000612	33.71	0.008	101 ± 32.1	140 ± 15.8
141	rno-miR-338	MI0000618	33.43	0.010	54 ± 31.6	66 ± 15.1
142	rno-miR-339-3p	MI0000620	32.16	0.023	89 ± 10.9	107 ± 10.6
143	rno-miR-339-5p	MI0000620	29.58	0.14	67 ± 11.2	96 ± 4.4
144	rno-miR-340-3p	MI0000622	33.81	0.008	88 ± 13.1	71 ± 13.7
145	rno-miR-342-5p	MI0000626	34.50	0.005	93 ± 0.5	76 ± 18.0
146	rno-miR-345-5p	MI0000631	28.46	0.31	76 ± 2.9	88 ± 5.1
147	rno-miR-34a	MI0000877	29.65	0.13	98 ± 4.5	115 ± 11.4
148	rno-miR-34c	MI0000876	34.35	0.005	156 ± 86.8	147 ± 10.4
149	rno-miR-350	MI0000639	33.95	0.007	127 ± 34.5	100 ± 9.3
150	rno-miR-352	MI0000644	24.59	4.48	102 ± 10.9	90 ± 13.2
151	rno-miR-361	MI0003481	33.90	0.007	125 ± 12.2	92 ± 4.5
152	rno-miR-365	MI0001656	31.70	0.032	90 ± 9.6	84 ± 8.3
153	rno-miR-370	MI0003486	25.02	3.32	73 ± 10.6	117 ± 16.1
154	rno-miR-374	MI0003552	28.09	0.40	96 ± 17.5	97 ± 21.0
155	rno-miR-378	MI0003719	25.59	2.24	121 ± 18.1	102 ± 10.8
156	rno-miR-378*	MI0003719	28.72	0.26	74 ± 10.0	137 ± 20.3
157	rno-miR-384-5p	MI0006142	35.98	0.002	86 ± 29.0	79 ± 21.9
158	rno-miR-423	MI0006145	22.13	24.6	69 ± 30.0	76 ± 4.8
159	**rno-miR-425**	**MI0006146**	**28.43**	0.31	**112 ± 9.2**	**71 ± 9.2**
160	rno-miR-450a	MI0001654	31.28	0.043	90 ± 7.6	71 ± 20.9
161	rno-miR-451	MI0001731	32.05	0.025	125 ± 31.5	91 ± 15.8
162	rno-miR-455	MI0006148	33.49	0.009	146 ± 18.4	76 ± 12.9
163	rno-miR-484	MI0006151	28.06	0.40	129 ± 34.5	75 ± 4.8
164	rno-miR-497	MI0003724	29.15	0.19	104 ± 17.7	84 ± 8.6
165	rno-miR-499	MI0003721	27.12	0.77	115 ± 23.0	62 ± 3.6
166	rno-miR-505	MI0003720	29.17	0.19	94 ± 4.0	89 ± 4.5
167	rno-miR-532-3p	MI0006154	29.52	0.15	105 ± 26.1	84 ± 15.0
168	rno-miR-532-5p	MI0006154	34.29	0.005	116 ± 29.9	111 ± 16.7
169	rno-miR-542-3p	MI0003528	32.52	0.018	110 ± 11.1	101 ± 23.1
170	rno-miR-542-5p	MI0003528	32.86	0.014	116 ± 24.7	107 ± 18.7
171	rno-miR-598-3p	MI0006155	32.66	0.017	106 ± 7.1	76 ± 23.9
172	rno-miR-652	MI0006169	29.06	0.20	80 ± 7.6	116 ± 16.9

173	rno-miR-664	MI0003722/ MI0003723	27.56	0.57	134 ± 6.0	119 ± 15.0
174	rno-miR-671	MI0006156	29.09	0.20	93 ± 20.1	103 ± 20.7
175	rno-miR-674-3p	MI0006159	31.48	0.038	101 ± 25.3	68 ± 14.3
176	rno-miR-674-5p	MI0006159	32.00	0.026	98 ± 24.8	90 ± 5.8
177	rno-miR-742	MI0006161	34.07	0.006	138 ± 20.3	103 ± 7.9
178	rno-miR-770	MI0006165	26.47	1.22	101 ± 9.2	83 ± 8.3
179	rno-miR-7a	MI0000641/ MI0000836	28.75	0.25	91 ± 14.7	63 ± 13.7
180	rno-miR-7a*	MI0000641/ MI0000836	32.62	0.017	100 ± 18.0	96 ± 6.1
181	rno-miR-7b	MI0000837	34.56	0.004	86 ± 14.4	70 ± 3.7
182	rno-miR-872	MI0006117	30.94	0.055	108 ± 14.3	83 ± 17.1
183	rno-miR-872*	MI0006117	35.28	0.003	172 ± 23.6	130 ± 15.7
184	rno-miR-92a	MI0000878/ MI0000879	27.33	0.67	135 ± 5.1	137 ± 13.6
185	rno-miR-92b	MI0006167	28.28	0.35	104 ± 7.9	104 ± 21.4
186	rno-miR-93	MI0000880	28.92	0.22	102 ± 6.6	127 ± 17.7
187	rno-miR-96	MI0000881	34.08	0.006	107 ± 47.7	141 ± 48.2
188	rno-miR-98	MI0000882	30.73	0.063	101 ± 15.8	95 ± 5.3
189	rno-miR-99a	MI0000883	24.34	5.32	96 ± 8.4	86 ± 10.6
190	rno-miR-99a*	MI0000883	33.01	0.013	112 ± 6.9	116 ± 26.0
191	rno-miR-99b	MI0000884	27.07	0.80	96 ± 18.7	95 ± 2.0

Supplementary Table 3.3: miRNAs not detected in adult rat cardiomyocytes.

	mature miRNA	stem loop accession number
1	rno-miR-106b	MI0000889
2	rno-miR-10a-3p	MI0000841
3	rno-miR-124	MI0000892/MI0000893/MI0000894
4	rno-miR-124*	MI0000892/MI0000893/MI0000894
5	rno-miR-125a-3p	MI0000895
6	rno-miR-125b-3p	MI0000896
7	rno-miR-129	MI0000902
8	rno-miR-134	MI0000907
9	rno-miR-135a	MI0000908
10	rno-miR-135b	MI0000645
11	rno-miR-136	MI0000909
12	rno-miR-136*	MI0000909
13	rno-miR-137	MI0000910
14	rno-miR-138*	MI0000912
15	rno-miR-142-5p	MI0000915
16	rno-miR-147	MI0006130
17	rno-miR-153	MI0000922
18	rno-miR-154	MI0000923
19	rno-miR-187	MI0000932
20	rno-miR-188	MI0006134
21	rno-miR-18a	MI0000846
22	rno-miR-193*	MI0000936
23	rno-miR-196a	MI0000940
24	rno-miR-196a*	MI0000940
25	rno-miR-196b	MI0001152
26	rno-miR-200a	MI0000943
27	rno-miR-204	MI0000946
28	rno-miR-204*	MI0000946
29	rno-miR-205	MI0000947
30	rno-miR-207	MI0003479
31	rno-miR-20a*	MI0000638
32	rno-miR-20b-5p	MI0003554
33	rno-miR-211	MI0000951
34	rno-miR-216a	MI0000955
35	rno-miR-217	MI0000956
36	rno-miR-218a-2*	MI0000957
37	rno-miR-219-1-3p	MI0000959
38	rno-miR-219-2-3p	MI0000960
39	rno-miR-222	MI0000962
40	rno-miR-23a*	MI0000852
41	rno-miR-27a*	MI0000860
42	rno-miR-290	MI0000964
43	rno-miR-291a-3p	MI0000965
44	rno-miR-292-3p	MI0000966

45	rno-miR-292-5p	MI0000966
46	rno-miR-296*	MI0000967
47	rno-miR-297	MI0000968
48	rno-miR-298	MI0000969
49	rno-miR-299	MI0000970
50	rno-miR-29b-1*	MI0000864
51	rno-miR-300-3p	MI0000971
52	rno-miR-300-5p	MI0000971
53	rno-miR-30d*	MI0000869
54	rno-miR-31	MI0000872
55	rno-miR-32	MI0000873
56	rno-miR-322*	MI0000589
57	rno-miR-323*	MI0000591
58	rno-miR-324-3p	MI0000594
59	rno-miR-326	MI0000599
60	rno-miR-327	MI0000600
61	rno-miR-329	MI0000604
62	rno-miR-33	MI0000874
63	rno-miR-330	MI0000606
64	rno-miR-330*	MI0000606
65	rno-miR-336	MI0000613
66	rno-miR-337	MI0000614
67	rno-miR-338*	MI0000618
68	rno-miR-340-5p	MI0000622
69	rno-miR-341	MI0000624
70	rno-miR-342-3p	MI0000626
71	rno-miR-343	MI0000628
72	rno-miR-344-3p	MI0000629
73	rno-miR-344-5p	MI0000629
74	rno-miR-345-3p	MI0000631
75	rno-miR-346	MI0000633
76	rno-miR-347	MI0000635
77	rno-miR-349	MI0000636
78	rno-miR-34b	MI0000875
79	rno-miR-34c*	MI0000876
80	rno-miR-351	MI0000642
81	rno-miR-363	MI0003553
82	rno-miR-363*	MI0003553
83	rno-miR-369-3p	MI0003551
84	rno-miR-369-5p	MI0003551
85	rno-miR-375	MI0006140
86	rno-miR-376a	MI0003545
87	rno-miR-376a*	MI0003545
88	rno-miR-376b-3p	MI0003544
89	rno-miR-376b-5p	MI0003544
90	rno-miR-376c	MI0003543
91	rno-miR-377	MI0003487

92	rno-miR-379	MI0003541
93	rno-miR-379*	MI0003541
94	rno-miR-380	MI0006141
95	rno-miR-381	MI0003546
96	rno-miR-382	MI0003548
97	rno-miR-382*	MI0003548
98	rno-miR-383	MI0003478
99	rno-miR-384-3p	MI0006142
100	rno-miR-409-3p	MI0003550
101	rno-miR-409-5p	MI0003550
102	rno-miR-410	MI0006143
103	rno-miR-411	MI0006144
104	rno-miR-412	MI0003488
105	rno-miR-421	MI0001423
106	rno-miR-429	MI0001643
107	rno-miR-431	MI0001722
108	rno-miR-433	MI0001724
109	rno-miR-434	MI0006147
110	rno-miR-448	MI0001639
111	rno-miR-449a	MI0001650
112	rno-miR-463	MI0006149
113	rno-miR-466c	MI0006114
114	rno-miR-471	MI0006150
115	rno-miR-483	MI0003485
116	rno-miR-485	MI0003549
117	rno-miR-487b	MI0003547
118	rno-miR-488	MI0006168
119	rno-miR-489	MI0003477
120	rno-miR-493	MI0003540
121	rno-miR-494	MI0003542
122	rno-miR-495	MI0006152
123	rno-miR-500	MI0006153
124	rno-miR-501	MI0003480
125	rno-miR-503	MI0003555
126	rno-miR-539	MI0003526
127	rno-miR-540	MI0003524
128	rno-miR-541	MI0003527
129	rno-miR-543	MI0003525
130	rno-miR-543*	MI0003525
131	rno-miR-551b	MI0006343
132	rno-miR-598-5p	MI0006155
133	rno-miR-672	MI0006157
134	rno-miR-673	MI0006158
135	rno-miR-708	MI0006160
136	rno-miR-708*	MI0006160
137	rno-miR-743a	MI0006162
138	rno-miR-743b	MI0006115

139	rno-miR-758	MI0006163
140	rno-miR-760-3p	MI0006164
141	rno-miR-760-5p	MI0006164
142	rno-miR-871	MI0006116
143	rno-miR-873	MI0006166
144	rno-miR-877	MI0006119
145	rno-miR-878	MI0006120
146	rno-miR-879	MI0006121
147	rno-miR-880	MI0006122
148	rno-miR-881	MI0006123
149	rno-miR-883	MI0006126
150	rno-miR-9	MI0000838/MI0000840
151	rno-miR-9*	MI0000838/MI0000840
152	rno-miR-99b*	MI0000884

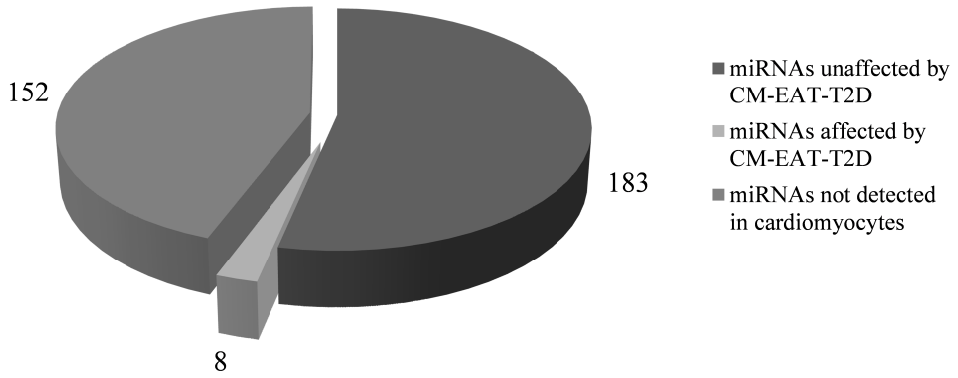

Supplementary Figure 3.1: miRNA expression in primary rat cardiomyocytes. Expression of 343 miRNAs was profiled by real-time PCR using the miRBase V13.0 library. miRNAs displaying a Ct-value over 37, and products showing variable melting curves were considered as not expressed. Collectively, expression of 152 miRNAs could not be detected in cardiomyocytes whereas abundance of 191 miRNAs was quantified by real-time PCR. Expression of eight microRNA species of the expressed 191 was affected by conditioned media from epicardial adipose tissue from patients with type 2 diabetes (CM-EAT-T2D).

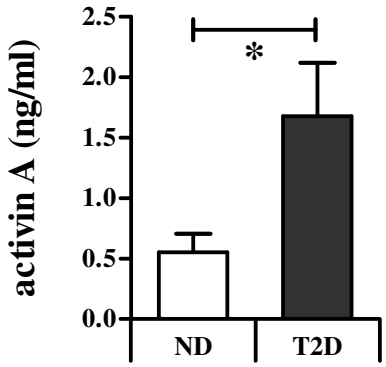

Supplementary Figure 3.2: Activin A levels in conditioned media form epicardial adipose tissue from patients without type 2 diabetes (ND) and with type 2 diabetes (T2D). Activin A levels were determined using enzyme-linked immunoabsorbent assays. Values are expressed as mean ± standard error of the mean (ND: n=10; T2D: n=14). Differences between ND and T2D were assessed using a student's t-test. * indicates $P<0.05$.

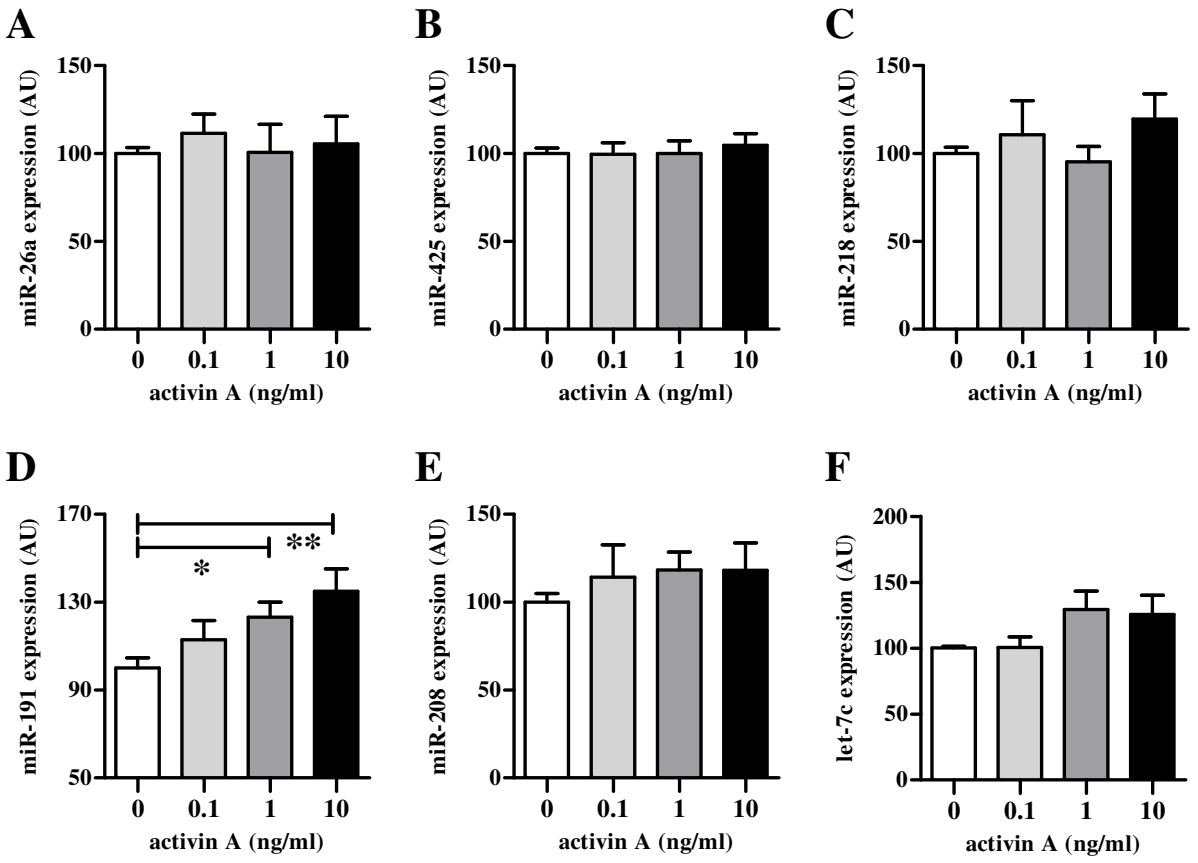

Supplementary Figure 3.3: Effect of activin A on the expression of miRNAs in adult rat cardiomyocytes. Dose dependent effect of a 16 h exposure of primary adult rat cardiomyocytes to recombinant activin A on (**A**) miR-26a, (**B**) miR-425, (**C**) miR-218, (**D**) miR-191, (**E**) miR-208 and (**F**) let-7c expression. Data were collected in 5 independent experiments using cardiomyocyte preparations from different rats, and are expressed as mean ± standard error of the mean. The effect of the various activin A concentrations on miRNA expression was evaluated using ANOVA followed by a Bonferroni analysis for multiple comparisons. $^{**}P<0.01$, $^{*}P<0.05$ vs untreated cardiomyocytes.

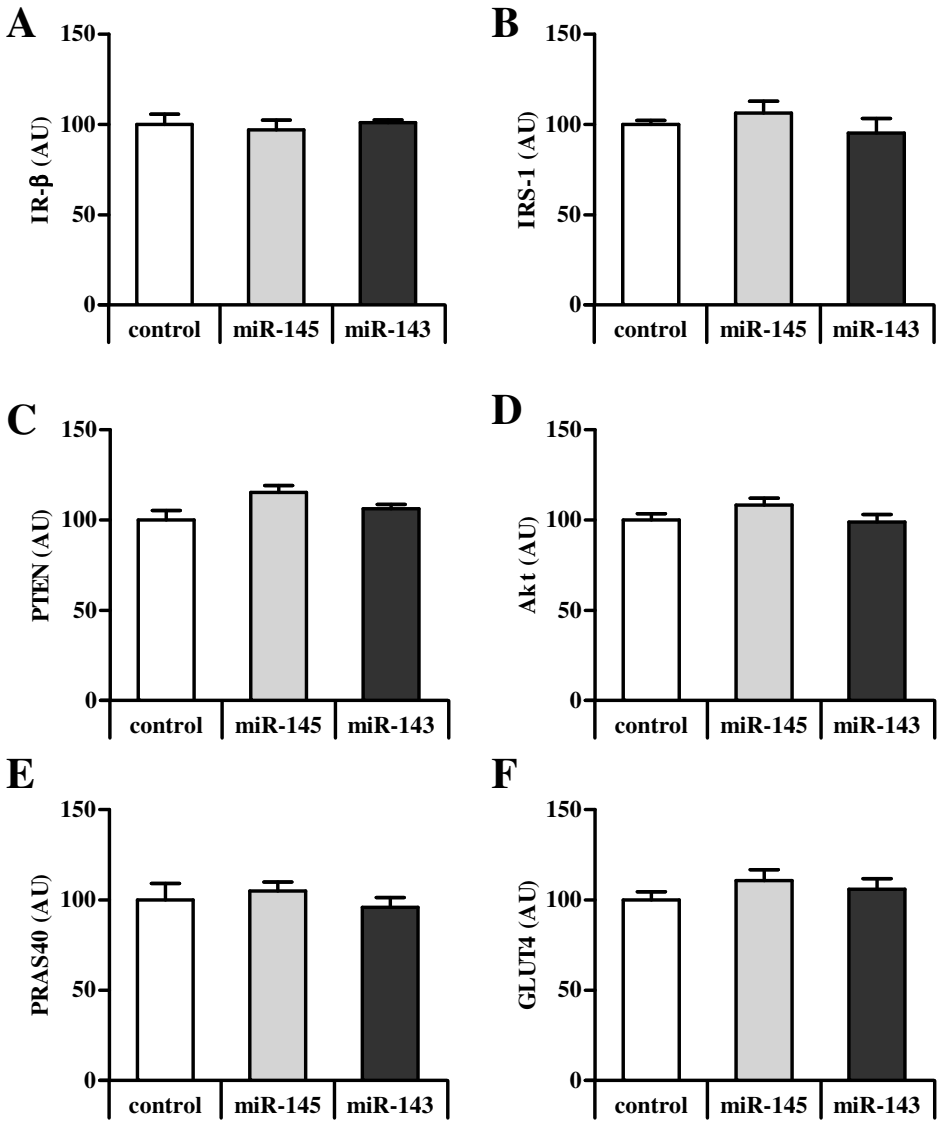

Supplementary Figure 3.4: Effect of miR-143 and miR-145 on protein expression of components of the insulin signalling pathway. Shown are quantifications for the protein expression of the insulin receptor β subunit (IRβ) (**A**), insulin receptor substrate 1 (IRS-1) (**B**), phosphatase and tensin homolog (PTEN) (**C**), Akt (**D**), the proline-rich Akt substrate of 40-kDa (PRAS40) (**E**), and the glucose transporter GLUT4 (**F**). Data are expressed as mean ± standard error of the mean of 4 independent experiments.

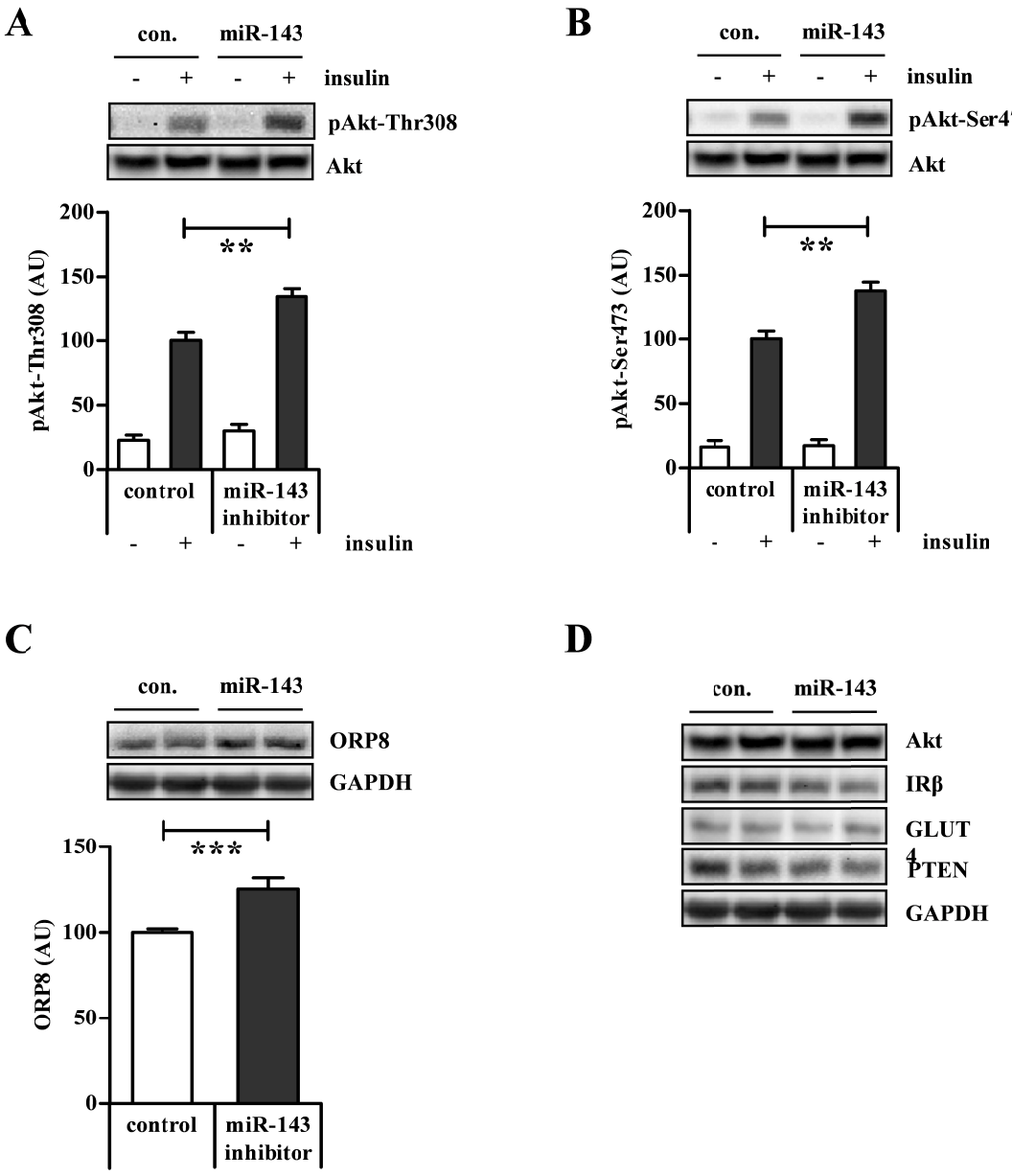

Supplementary Figure 3.5: Silencing miR-143 enhances insulin action in HL-1 cells. HL-1 cells were transfected with LNA-anti-miR-143 or LNA inhibitor control using lipofectamine. The following day, cells were serum starved for 16h and exposed to insulin (30 min; 200 nM) or kept untreated. Shown are representative blots and quantification for induction of Akt-Thr308 (**A**) and Akt-Ser473 (**B**) phosphorylation following insulin stimulation (10 min; 100 nM) and ORP8 expression (**C**). Signals were normalized for GAPDH protein levels and are expressed as mean ± standard error of the mean from 4 independent experiments. **, indicates $P<0.01$ and ***, indicates $P<0.001$ for differences between LNA-anti-miR-143 versus LNA-inhibitor control. **D.** Representative blots for the effect of LNA-anti-miR-143 versus or LNA inhibitor control on protein levels of Akt, the insulin receptor β-subunit, GLUT4, PTEN and GAPDH.

Journal: *Cardiovascular Research*

Impact factor: 5.940

Contribution: Total: 90%

Conceived / designed experiments: 90%

Performed experiments: 100%

(western blot analysis, generation of conditioned media, quantification of cytokines via enzyme-linked immunosorbent assay, preparation and isolation of rat cardiomyocytes, isolation of RNA and quantitative real-time PCR, cell culture techniques including transfection of HL-1 cardiomyocytes and lentiviral transduction of rat cardiomyocytes, silencing of miRNAs, glucose uptake in HL-1 cardiomyocytes)

Analysed data: 90%

Contributed to discussion: 90%

Wrote the manuscript: 90%

Reviewed / edited manuscript: 80%

Author: 1st author

Chapter 4

Study 3

Adipocyte-derived factors impair insulin signaling in differentiated human vascular smooth muscle cells via the up-regulation of miR-143

Marcel Blumensatt[1*], Nina Wronkowitz[2*], Claudia Wiza[1], Andrea Cramer[2], Heidi Mueller[1], Martijn J. Rabelink[3], Rob C. Hoeben[3], Juergen Eckel[2], Henrike Sell[2] and D. Margriet Ouwens[1,4]

submitted to Biochimica et Biophysica Acta – Molecular Basis of Disease, 2013

* shared first authorship

[1]Institute for Clinical Biochemistry and Pathobiochemistry, German Diabetes Center, Duesseldorf, Germany

[2]Paul-Langerhans-Group for Integrative Physiology, German Diabetes Center, Duesseldorf, Germany

[3]Department of Molecular Cell Biology, Leiden University Medical Center, Leiden, The Netherlands

[4]Department of Endocrinology, Ghent University Hospital, Ghent, Belgium

Highlights

- adipocyte-derived factors impair insulin action in vascular smooth muscle cells
- adipocyte-derived factors induce miR-143 in vascular smooth muscle cells
- miR-143 impairs insulin action via down-regulation of ORP8

Key Words

vascular smooth muscle cells, insulin signaling, p38, adipokines, miRNA

Abstract

Cardiovascular complications are common in patients with type 2 diabetes. Adipokines have been implicated in the induction of proliferative and pro-atherogenic alterations in human vascular smooth muscle cells (hVSMC). Other reports demonstrated the importance of the miRNA cluster miR-143/145 in the regulation of VSMC homeostasis and insulin sensitivity. Here we investigated whether the detrimental effects of adipokines on hVSMC function could be ascribed to alterations in miR-143/145 expression. Exposure of hVSMC to conditioned media (CM) from primary human subcutaneous adipocytes increased the expression of smooth muscle α-actin (SMA), and the miR-143/145 cluster, but markedly impaired the insulin-mediated phosphorylation of Akt and its substrate endothelial nitric oxide synthase (eNOS). Furthermore, CM promoted the phosphorylation of SMAD2 and p38, which have both been linked to miR-143/145 induction. Accordingly, the induction of miR-143/145 as well as the inhibition of insulin-mediated Akt- and eNOS-phosphorylation was prevented when hVSMC were treated with pharmacological inhibitors for Alk-4/5/7 and p38 before the addition of CM. Transfection of hVSMC with precursor miR-143, but not with precursor miR-145, resulted in impaired insulin-mediated phosphorylation of Akt and eNOS. This inhibition of insulin signaling by CM and miR-143 is associated with a reduction in the expression of the oxysterol-binding protein-related protein 8 (ORP8). Finally, knock-down of ORP8 resulted in impaired insulin-mediated phosphorylation of Akt in hVSMC. Thus, the detrimental effects of adipocyte-derived conditioned media on insulin action in primary hVSMC can be ascribed to the Alk- and p38-dependent induction of miR-143 and subsequent down-regulation of ORP8.

Introduction

Cardiovascular complications are common in patients with type 2 diabetes and a major cause of mortality.[1] Accumulating evidence shows that adipose tissue secreted factors, termed adipokines, may participate in the development of cardiovascular complications in patients with type 2 diabetes by affecting the function of amongst others cardiomyocytes and smooth muscle cells (SMC).[2-4]

Vascular endothelial cells and SMC represent the major cell types of the artery wall preserving vessel wall homeostasis. SMC are highly plastic and modulate their phenotype in response to physiological and pathological cues. Differentiated SMC are quiescent and contractile. In response to vascular injury or growth factor signaling, SMC de-differentiate and adopt a proliferative, migratory phenotype that contributes to vascular occlusion in a variety of disorders, including atherosclerosis.[5] Vascular insulin resistance may also participate in the development of cardiovascular dysfunction in type 2 diabetes. The insulin-mediated activation of phosphatidylinositol 3'-kinase (PI3K) results in the activation of Akt, which on its turn promotes the phosphorylation of endothelial nitric oxide synthase (eNOS). This results in activation of eNOS and an increase in bioavailable nitric oxide (NO) thereby promoting vasodilation. Under conditions of insulin resistance, activation of the PI3K/Akt/eNOS-pathway is impaired. Intriguingly, this is paralleled by an overactivation of the mitogen activated protein kinase (MAPK) pathway, which promotes proliferation of vascular cells. Studies on mouse models with selective disruption of the insulin receptor in either endothelial or vascular smooth muscle cells have further highlighted the importance of vascular insulin action *in vivo*.[6]

Previously we showed that conditioned media (CM) prepared from human adipocytes induces pro-atherogenic changes in primary human vascular smooth muscle cells (hVSMC) with an increase in proliferation and migration, thus indicating an involvement of adipokines in the development of atherosclerosis.[2, 3] However, until now the underlying mechanism, which are responsible for hVSMC dysfunction induced by adipokines remains incompletely understood. In cardiomyocytes, we observed that conditioned media generated from epicardial adipose tissue from patients with type 2 diabetes induce cardiomyocyte dysfunction as illustrated by contractile dysfunction and insulin resistance.[4] Furthermore, we found that the induction of insulin resistance in cardiomyocytes could be ascribed to the increases in miR-143 expression.[7] Also in other tissues, such as the liver and adipose tissue, induction of miR-143 is associated with obesity and insulin resistance.[8, 9] Interestingly, studies on SMC

linked the miR-143/145-cluster to the regulation of SMC plasticity differentiation.[10] Therefore the aim of this study is to examine the role of the miR-143/145-cluster in primary human vascular smooth muscle cells (hVSMC) in more detail by studying the effects of CM on the expression of the miR-143/145-cluster, and whether these effects associate with alterations in insulin action.

Material and Methods

Cell culture and differentiation of smooth muscle cells

Primary human coronary artery smooth muscle cells (hVSMC) from two different donors (Caucasian, female, 55 and 56 years old) were purchased from tebu-bio (Offenbach, Germany) and Lonza (Basel, Switzerland). The hVSMCs were supplied as proliferating cells and cultured according to the manufacturers' instructions. For experiments, differentiation was induced culturing the subconfluent cells of passage 3 for 14 days in smooth muscle cell differentiation medium (tebu-bio, Offenbach, Germany). Differentiation of the hVSMC was assessed by morphological criteria and by immunostaining with smooth muscle α-actin. Following differentiation, hVSMC were incubated for 24 hours in adipocyte-derived conditioned media or maintained in SMC serum-free basal medium (PromoCell, Heidelberg Germany). When indicated cells were treated for 1 hour with 10 µM SB431542 (Sigma Aldrich, St. Louis, MO) or 2.5 µM SB203580 (Promega, Mannheim, Germany) prior to the addition of the media. For insulin signaling, the cultures were stimulated for 10 min with 100 nM insulin.

Adipocyte isolation, culture and generating of conditioned media

Conditioned media (CM) were generated from mature subcutaneous adipocytes that were differentiated from pre-adipocytes isolated from subcutaneous adipose tissue obtained from lean or moderately overweight women (n= 13, body mass index 28.1 ± 1.3, and aged 39.0 ± 3.9 years) undergoing plastic surgery. The procedure was approved by the ethical committee of the Heinrich-Heine-University (Düsseldorf, Germany). All patients were healthy, free of medication and had no evidence of metabolic diseases according to routine laboratory tests. Pre-adipocytes were isolated by collagenase digestion of adipose tissue as described.[11] Isolated pre-adipocytes were resuspended in Dulbecco's modified Eagles/Hams F12 (DMEM/F12) medium supplemented with 10% FCS, seeded in 75 cm^2 culture flasks and maintained at 37°C with 5% CO2. After overnight incubation, cultures were washed and further incubated in an adipocyte differentiation medium (DMEM/F12, 33 µmol/l biotin, 17 µmol/l d-panthothenic-acid, 66 nM insulin, 1 nM triiodo-L-thyronine, 100 nM cortisol, 10 µg/ml apo-transferrin, 50 µg/µl gentamycin, 15 mmol/l HEPES, 14 nmol/l $NaHCO_3$, pH 7.4) for 15 days with medium change every 2–3 days and addition of 5 µM troglitazone for the first 3 days. For the collection of CM, differentiated adipocytes were maintained for 48 hrs in

SMC serum free basal medium (PromoCell) with addition of 50 ng/ml fungizone and 50 µg/ml gentamycin. Then CM was collected and stored as aliquots at -80°C until further use.

Analysis of protein expression

For analysis of protein expression and phosphorylation, hVSMC were lysed in 50 mM HEPES, pH 7.4, 1% TritonX100 supplemented with protease and phosphatase inhibitor cocktails (Complete, PhosStop; Roche Diagnostics, Mannheim, Germany). After incubation for 2 hrs at 4°C on a rotation shaker, the suspension was centrifuged at 10,000g for 15 min, and protein content was determined using Bradford reagent (Biorad Laboratories, Munich, Germany). Thereafter, five microgram of protein was separated by SDS-PAGE and transferred to polyvenylidene fluorid membranes (Millipore, Schwalbach, Germany) in a semi-dry blotting apparatus.[12] Membranes were blocked with Tris-buffered saline containing 0.1% Tween and 5% non-fat dry milk and subsequently incubated overnight at 4°C with primary antibodies for Akt, phospho-Akt-Ser473, phospho-Akt-Thr308, phospho-p38-Thr180/Tyr182, phospho-SMAD2-Ser465/467 (all from Cell Signaling Technology, Danvers, MA, USA), glyceraldehyde 3-phosphate dehydrogenase (GAPDH), oxysterol-binding protein-related protein 8 (ORP-8) (abcam Cambridge, UK), smooth muscle α-actin (Sigma Aldrich), α-tubulin (Calbiochem Merck Biosciences, Schwalbach, Germany) insulin receptor β-subunit (IRβ), and phospho-eNOS-Ser1177 (Santa Cruz Biotechnology, Santa Cruz, CA, USA). After washing, membranes were incubated with corresponding secondary HRP-coupled antibody (Promega). Bound conjugate was detected using enhanced chemiluminescence using Immobilon HRP substrate (Millipore, Billerica, MA, USA). Signals were visualized and quantitated on a Versadoc work station (VersaDoc 4000 MP; BioRad, Munich, Germany) using Quantity One software (BioRad, version 4.6.7).

RNA isolation, cDNA synthesis and qRT-PCR

For analysis of miRNA- and mRNA expression, total RNA was extracted using a miRNeasy mini kit (Qiagen, Hilden, Germany) and reverse transcribed using the miScript RT kit (Qiagen). Then miRNA expression levels were determined with miScript Primer Assays (Qiagen) using miScript SYBR Green (Qiagen) on a StepOne Plus real-time PCR system (Applied Biosystems, Carlsbad, CA, USA). MCP-1 and PAI-1 mRNA expression levels (QuantiTect Primer Assays, Qiagen) were determined after cDNA synthesis using GoScript™ Reverse Transcription System (Promega) and GoTaq® qPCR Master Mix (Promega).

Transfection of hVSMC with miRNA-precursor

To investigate the impact of differentially regulated miRNAs and their potential targets on insulin action, differentiated hVSMCs were transfected in 6-well dishes with 30 nmol/l Cy3™-labeled pre-miR™ (negative control) or pre-miR™ miRNA-precursor (Ambion, Life Technologies, Darmstadt, Germany) using Hiperfect (Qiagen) as transfection reagent. 48h after transfection in SMC serum free basal medium (PromoCell) cells are stimulated with insulin and lysed for protein isolation and western blot analysis.

Lentiviral vector-based Silencing of ORP8

To silence ORP8, three validated MISSION® shRNA constructs (TRCN000014 -6765, -7289 -7487) targeting human ORP8 (NM_020841) (Sigma Aldrich) or empty vector were used to produce infectious virus particles (LV). Therefore, HEK293t were transfected with the shRNA constructs together with helper plasmids encoding HIV-1 gag-pol, HIV-1 rev, and the VSV-G envelope as described previously.[13] For quantification of virus yield in the harvested medium, p24 antigen levels were determined using a HIV-1 p24 antigen enzyme-linked immunosorbent assay (ELISA) kit (ZeptoMetrix Corp., New York, NY, USA). hVSMCs are transduced with a MOI of 2 for 24 hours. Two days after transduction of hVSMCs in serum free basal medium (PromoCell), cells were stimulated with 100 nM insulin for 10 minutes or kept untreated, and harvested.

Statistical analysis

Data are presented as means ± standard error of the mean. Significant differences between experimental conditions were evaluated as described in the legends to the tables and the figures using GraphPad Prism 6 for Mac OS X (GraphPad, LA Jolla, CA) software. *P*-values of <0.05 were considered as statistically significant.

Results

Effects of adipocyte-derived factors on primary human vascular smooth muscle cells

Exposure of hVSMC to CM increased the expression of the miR-143/145 cluster by 1.3-fold ($P<0.001$) as compared to cells kept in control medium (Figure 4.1 A/B). Furthermore, CM increased the mRNA levels of SMA by 2.6-fold, and of the pro-inflammatory cytokines PAI-1 and MCP-1 by 3.1- and 2.8-fold, respectively (all $P<0.001$) (Figure 4.1 C/E). Exposing hVSMC to CM inhibited the insulin-mediated phosphorylation of Akt on Thr308 and Ser473, and its substrate eNOS on Ser1177 by 53%, 44%, and 37%, respectively versus cells kept in control medium (all $P<0.001$) (Figure 4.2). Incubation with CM did not affect the basal phosphorylation levels of these proteins (Figure 4.2).

Effect of inhibition of TGFβ receptor- and p38-signaling on the CM-induced expression of miR-143/145 and inhibition of insulin action in hVSMC

A previous report ascribed the induction of the miR-143/145 cluster in hVSMC to the activation of the p38-signaling pathway by transforming growth factor β (TGFβ).[14] Figure 4.3 A/B shows that the phosphorylation of SMAD2, a component of the TGFβ receptor signaling pathway, as well as the phosphorylation of p38 were increased by 3.9- and 5.1-fold, respectively in hVSMC exposed to CM versus cells kept in control medium. To examine whether the TGFβ receptor- and p38-signaling pathway(s) participate in the induction of the miR-143/145 cluster, pharmacological inhibitors were used. Pretreating the hVSMC with either SB431542, which inhibits the TGFβ type I receptors 'Activin Receptor-Like Kinase' (ALK) 4, 5 and -7, or with the p38 inhibitor SB203580, completely abolished the induction the miR-143/145-cluster by CM in hVSMC (Figure 4.3 C/D). Furthermore, the inhibition of insulin-induced phosphorylation of Akt-Thr308, Akt-Ser473, and eNOS-Ser1177 by CM was prevented in hVSMC incubated with SB431542 or SB203580 before exposure to CM (Figure 4.4). In contrast to the effects on the miRNA-143/145 cluster and insulin action, the inhibitors did not or only partially prevent the induction of SMA, PAI-1 and MCP-1 in hVSMC by CM (Supplementary Figure 4.1).

Effect of miR-143 and miR-145 overexpression on insulin signaling

To investigate the impact of the miR-143/145 cluster on insulin action, hVSMC were transfected with precursors for miR-143 and miR-145, respectively. In line with a previous report,[10] SMA protein abundance was increased in cells transfected with pre-miR-143 and pre-miR-145 by 9.0- and 2.0-fold respectively versus cells transfected with control pre-miR (P<0.05) (Figure 4.5A). Insulin-stimulated phosphorylation of Akt-Thr308, Akt-Ser473, and eNOS-Ser1177 were reduced by 42%, 44%, and 39%, respectively, in cells transfected with pre-miR-143 versus cells transfected with control pre-miR (Figure 4.5 B-D). In contrast, transfection with pre-miR-145 did not affect insulin action (Figure 4.5 B-D).

Several reports have linked miR-143 to regulation of insulin resistance through down-regulation of ORP8. As shown in Figure 4.6 A, transfection of hVSMC with pre-miR-143 reduced ORP8 protein levels by 25% (P<0.01) versus cells transfected with either control pre-miR or pre-miR-145. Also exposure to CM lowered ORP8 levels by 30% (P<0.01) versus cells kept in control medium, and this reduction in ORP8 abundance was not observed in hVSMC treated with either SB431542 or SB203580 prior to exposure to the CM (Figure 4.6 B). To examine whether the down-regulation of ORP8 results in insulin resistance in hVSMC, cells were transduced with lentiviruses encoding control shRNA or shRNA for ORP8. A 30% decrease in ORP8 abundance, which is comparable to that achieved by expression of miR-143 or exposure to CM, was found to impair insulin-mediated Akt-Ser473 phosphorylation by 25% (Figure 4.6 C/D).

Discussion

The present study shows that adipocyte-derived factors impair insulin signaling in hVSMC. Exposing the hVSMC to adipocyte-derived conditioned media was found to increase the expression of miR-143. The resulting decrease in the expression of the validated miR-143 target ORP8 resulted in inhibition of the insulin-mediated phosphorylation of Akt/eNOS-signaling pathway. Furthermore, the activation of the miR-143/ORP8 pathway by CM was sensitive to inhibition of Alk4/5/7 and p38-signaling. In contrast, the induction of the inflammatory markers PAI-1 and MCP-1 by CM as well as the induction of SMA by CM was not fully reversed by Alk4/5/7- and p38-inhibition, indicating that these effects involve at least in part different pathways.

In contrast to classical target tissue for insulin action, like liver fat and muscle, the function of proper insulin action in the vasculature is less well understood. Nevertheless, vascular smooth muscle cell function is impaired in patients with type 2 diabetes,[15] and studies using a vascular insulin receptor knock-out mouse illustrate the importance of activation of the Akt/eNOS-pathway by insulin for vasodilation.[6, 16] Whether the inhibition of insulin action in SMC also has detrimental effects on the progression of atherosclerosis is less well understood. One study reported that the presence of high palmitate induces a “selective” insulin resistance in hVSMC with a profound inhibition of the insulin induced PI3K-signaling, whereas the activation of the MAPK-pathway is enhanced.[17] Additionally this study showed that increased activation of MAPK-signaling by insulin is involved in hVSMC proliferation, migration, and inflammation.[17] Alternatively, in advanced plaque progression, inflammation and insulin resistance may promote apoptosis of SMC and therefore thinning of fibrous cap and causing plaque rupture.[18] Finally, insulin-stimulated eNOS-derived NO production has important anti-inflammatory and anti-thrombotic properties through inhibition of leucocyte adhesion, and limiting platelet adhesion and aggregation, and reduced expression of plasminogen activator inhibitor-1 (PAI-1), a prothrombotic protein.[19] Furthermore, NO has been shown to inhibit DNA synthesis, mitogenesis, and proliferation of vascular smooth muscle cells.[20-22] Therefore, impaired insulin signaling with reduced bioavailable NO may predispose vasculature to hyper-inflammatory and thrombotic states.

The present study shows that CM directly impairs insulin action in hVSMC via induction of miR-143 and subsequent down-regulation of ORP8. Although the mechanism via which ORP8 regulates insulin action remains unclear, the induction of miR-143 is closely associated with obesity and insulin resistance. Feeding mice a high-fat diet increased the

levels of miR-143 in adipose tissue,[9] while both miR-143 and miR-145 are up-regulated in the liver of mice fed a high-fat diet.[8] Moreover in the liver, heart, skeletal muscle and pancreas from *db/db*-mice, expression of miR-143 was increased as compared to tissues isolated from wild type control animals. Liver specific knock out of the miR-143/145-cluster protects against high-fat diet induced insulin resistance and hepatic Akt-inhibition.[8] The authors of that study further identified ORP8 as a direct miR-143 target, and showed that a decrease in ORP8 protein abundance is responsible for the abrogation of insulin action in the liver.[8] Finally, in cardiomyocytes we recently reported that the induction of miR-143 by activin A secreted from epicardial adipose tissue promotes insulin resistance via ORP8, and that silencing miR-143 expression protects cardiomyocytes against the induction of insulin resistance.[7]

The strong association of miR-143 with insulin resistance in multiple tissues seems in contrast to the function ascribed to this miRNA in SMC. In SMC, an anti-proliferative function has been reported for the miR-143/145-cluster,[10, 14] and especially miR-145 has been found to promote the differentiation to the quiescent contractile phenotype of SMC.[14] Accordingly, CM also induced the expression of miR-145 in quiescent differentiated hVSMC, which was accompanied with the induction of SMA. In mice, miR-145 overexpression reduces neo-intima formation after vascular injury, but paradoxically miR-145 deficient mice show similar effects.[23, 24] In humans, levels of miR-145 are elevated in atherosclerotic plaques,[25, 26] and were found to correlate with an unstable plaque phenotype.[26] Collectively, these findings point toward an important dual role for the miR-143/145 in SMC homeostasis, but also indicate that further studies toward the underlying mechanism(s) are clearly needed, such as comparing the impact of CM on differentiated versus undifferentiated SMC and elucidation of the targets regulated by the miR-143/145-cluster.

A limitation of the present study is that we could not identify the factor in CM responsible for the induction of the miR-143/145-cluster. In line with previous reports, the induction of miR-143/145 was sensitive to inhibition of Alk4/5/7- and p38-signaling.[7, 14] However, while these studies identified TGFβ and activin A as inducers of miR-143/145, levels of these factors were below the limit of detection in the CM used in the present study. Consequently, one may speculate that other members of the TGFβ family elicit the effects observed here. Alternatively, we recently reported that CM itself induces the expression of activin A in SMC,[27] thereby raising the possibility that an autocrine action of activin A on hVSMC induced by CM promotes the induction of the miR-143/145-cluster.

Conclusion

The present report shows for the first time that adipocyte-derived factors impair insulin signaling in hVSMC. The inhibition of insulin signaling can be ascribed to the Alk4/5/7- and p38-dependent induction of miR-143 (Figure 4.7). This miRNA plays a pivotal role in the CM-induced impairment of insulin-induced Akt/eNOS-signaling via down-regulation of ORP8. These data further highlight the involvement of adipokines in the pathogenesis of cardiovascular complications in type 2 diabetes.

Acknowledgments

This work was supported by the Federal Ministry of Health, the Ministry of Innovation, Science, Research and Technology of the German State of North-Rhine Westphalia, the Deutsche Forschungsgesellschaft (SE-1922/2-1) and the German Center for Diabetes Research (Deutsches Zentrum für Diabetesforschung, DZD). The authors further thank professor Dr. Christoph Andree and Dr. Mazen Hagouan (both Sana Hospital, Duesseldorf-Gerresheim, Germany) for their continuous and invaluable support in the collection of adipose tissue samples for adipocyte isolation.

Duality of interest

The authors have no conflicts of interest.

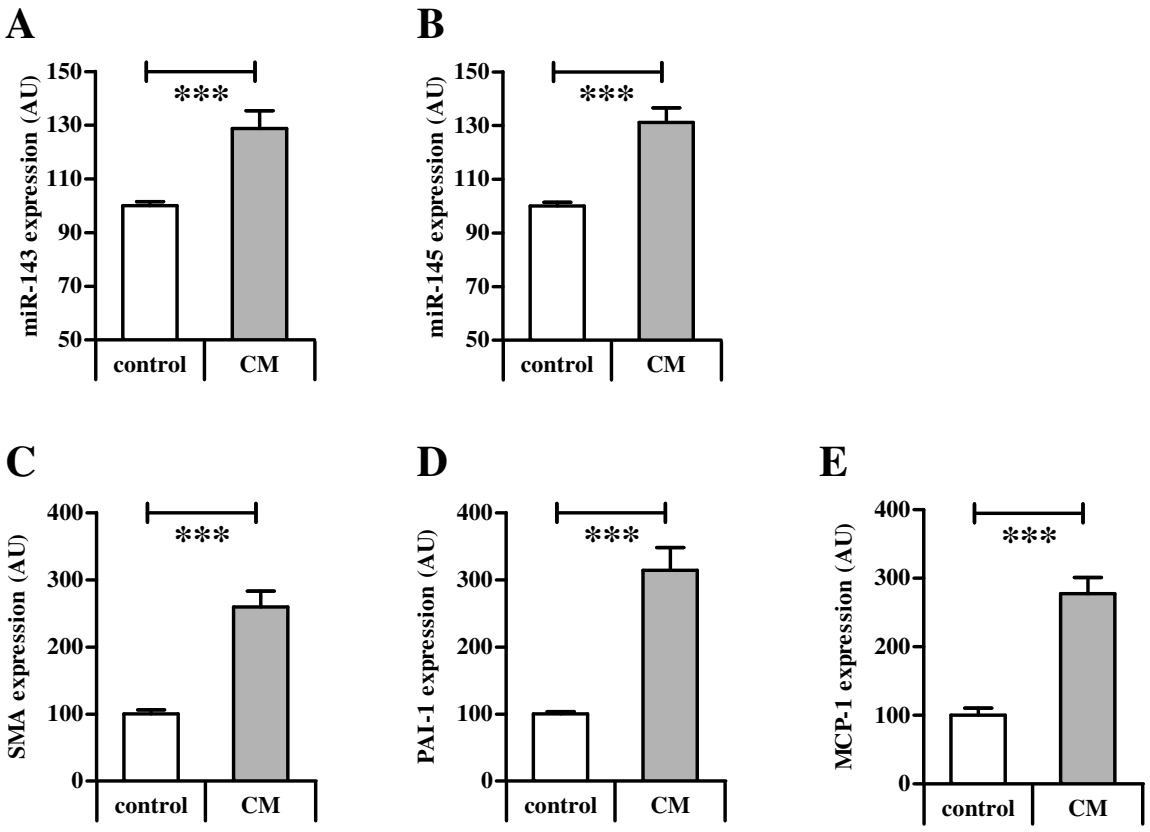

Figure 4.1: Effect of conditioned media on miRNA and gene expression in primary human vascular smooth muscle cells. Cells were exposed to control media or conditioned media (CM) for 24h and levels of miR-143 (A), miR-145 (B), smooth muscle actin (SMA) (C), PAI-1 (D), and MCP-1 (E) were quantified by real-time PCR. Data were collected in 16 independent experiments using 2 different donors and CM from 8 different preparations, and are expressed as mean ± standard error of the mean. Differences between the groups were evaluated using student's t-test. ***, indicates $P<0.001$ versus control medium.

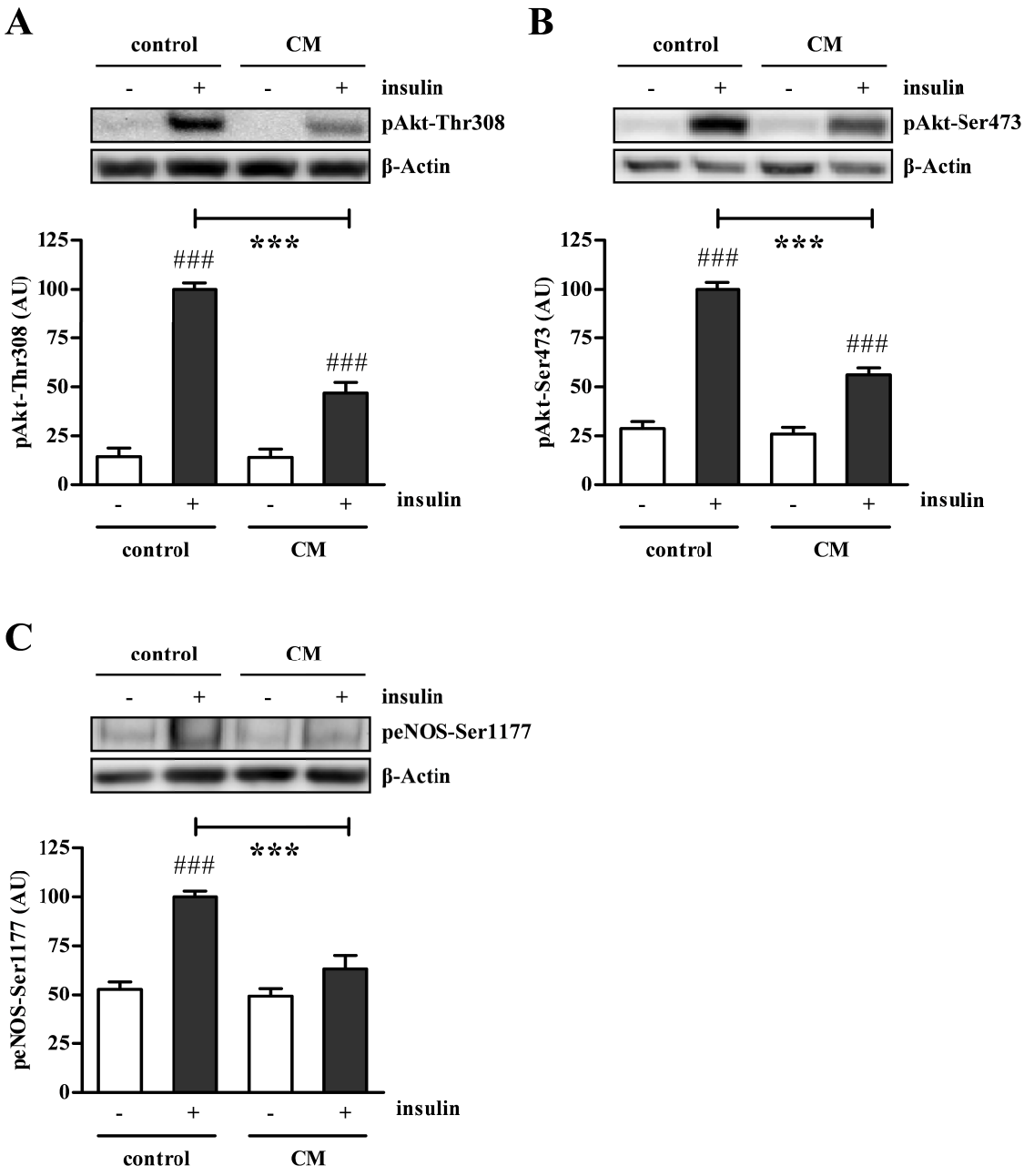

Figure 4.2: Effect of conditioned media on insulin action in primary human vascular smooth muscle cells. Cells were exposed to control media or conditioned media (CM) for 24h and kept untreated (-) or stimulated for 10 min with 100 nM insulin (+). Shown are representative Western blots and quantifications for the phosphorylation levels of Akt-Thr308 (A), Akt-Ser-473 (B), and eNOS-Ser1177 (C). Phosphorylation levels normalized for β-actin are expressed as mean ± standard error of the mean of at least 8 independent experiments using cells from 2 different donors and CM from 8 different preparations. Differences among the experimental conditions were evaluated using two-way ANOVA. ###, indicates $P<0.001$ for the effect of insulin versus untreated cells; *** indicates $P<0.001$ for the effect of CM versus control medium.

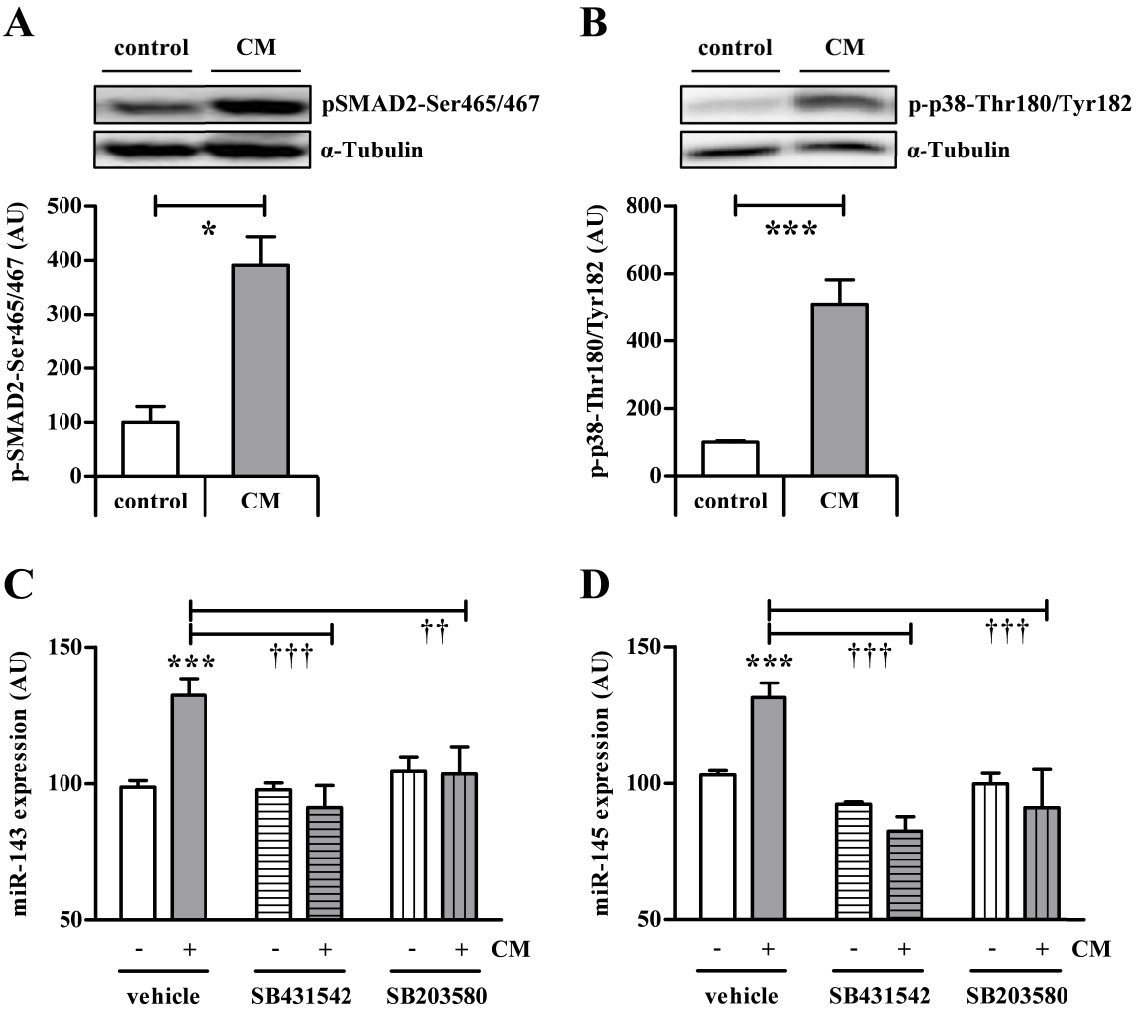

Figure 4.3: Involvement of TGFβ receptor- and p38-signaling in the induction of the miR-143/145 cluster in primary human vascular smooth muscle cells. Cells were exposed to control media or conditioned media (CM) for 24h. Shown are representative Western blots and quantifications for the phosphorylation levels of SMAD2-Ser465/467 (A), and p38-Thr180/Tyr182 (B). Phosphorylation levels normalized for α-tubulin are expressed as mean ± standard error of the mean of 14 independent experiments using cells from 2 distinct donors and CM from 7 different preparations. Differences between the groups were evaluated using student's t-test. ***, indicates $P<0.001$; *, $P<0.05$ versus control medium. C/D. Cells were exposed to DMSO (vehicle), or pharmacological inhibitors for Alk4/5/7 (SB431542), or p38 (SB203580) for 1 h prior to the addition of control medium (-) or CM (+), whereafter expression of miR-143 (C), and miR-145 (D) were determined via real-time PCR. Data are expressed as mean ± standard error of the mean of least 8 independent experiments using cells from 2 different donors and CM from 8 different preparations. Differences among the groups were analyzed using two-way ANOVA and Bonferroni multiple comparison analysis. ***, indicates P<0.001 for CM versus control medium; †††, $P<0.001$; ††, $P<0.01$ for CM only versus inhibitors.

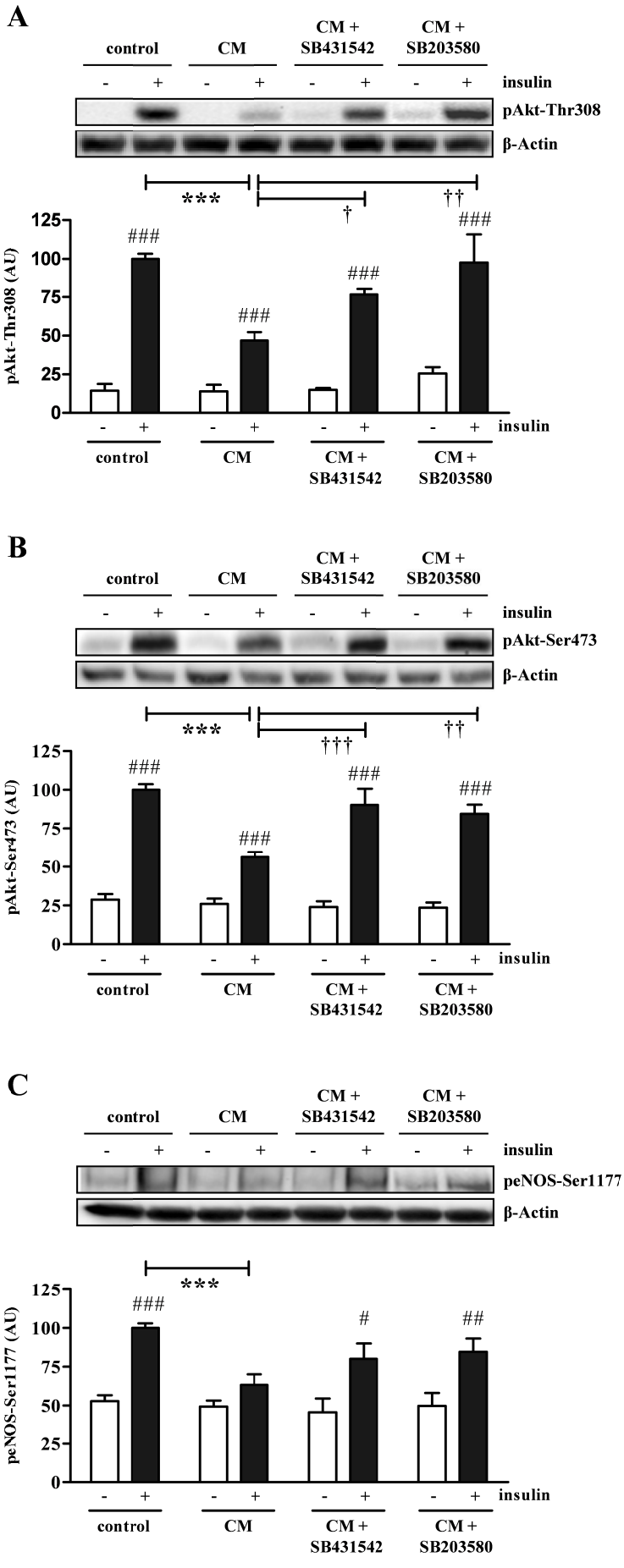
A
control
CM
CM + SB431542
CM + SB203580
insulin
pAkt-Thr308
β-Actin
***
†
††
###
pAkt-Thr308 (AU)
B
pAkt-Ser473
†††
pAkt-Ser473 (AU)
C
peNOS-Ser1177
peNOS-Ser1177 (AU)
#
##

Figure 4.4: Involvement of TGFβ receptor- and p38-signalling in insulin action in primary human vascular smooth muscle cells. Cells were exposed to DMSO (vehicle), or pharmacological inhibitors for Alk4/5/7 (SB431542), or p38 (SB203580) for 1 h prior to the addition of control medium (-) or conditioned media CM, +). Shown are representative Western blots and quantifications for the phosphorylation levels of Akt-Thr308 (A), Akt-Ser-473 (B), and eNOS-Ser1177 (C). Phosphorylation levels normalized for β-actin are expressed as mean ± standard error of the mean of at least 4 independent experiments using cells from two distinct donors and CM from 4 different preparations. Differences among the experimental conditions were evaluated using two-way ANOVA. ###, indicates $P<0.001$ for the effect of insulin versus untreated cells; *** indicates $P<0.001$ for the effect of CM versus control medium; †††, $P<0.001$; ††, $P<0.01$; †, $P<0.05$ for CM only versus CM + inhibitors.

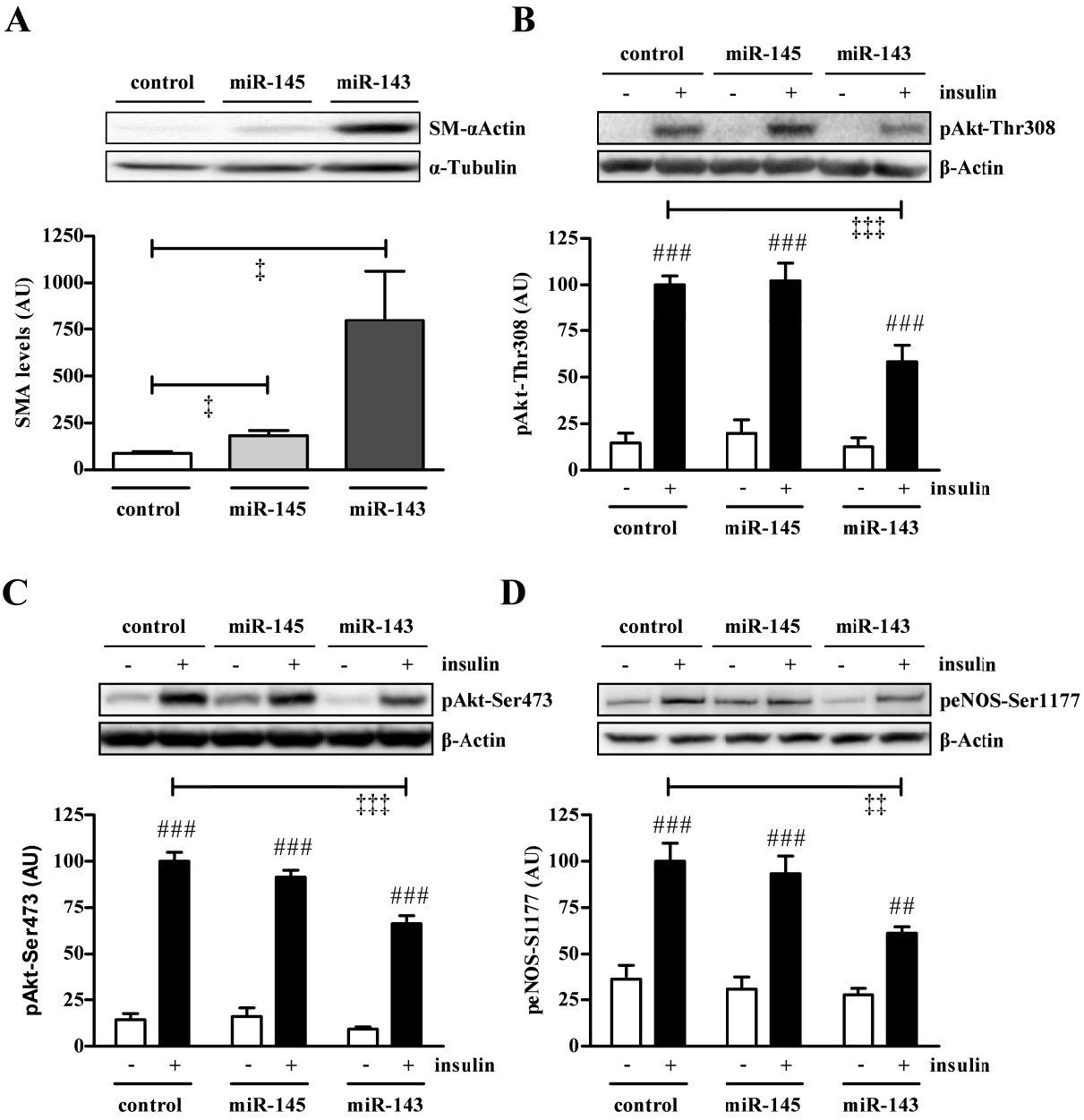

Figure 4.5: Effect of miR-143 and miR-145 expression on insulin action in primary human vascular smooth muscle cells. Cells were transfected with control precursor miRNA or precursors for miR-143 or miR-145, respectively. Shown are representative blots and quantifications for the protein abundance of smooth muscle α-actin (A), and the phosphorylation levels of Akt-Thr308 (B), Akt-Ser-473 (C), and eNOS-Ser1177 (D). Signal normalized for tubulin (A) or β-actin (B-D) are expressed as mean ± standard error of the mean of 8 independent experiments performed on cells from two different donors. Differences among the experimental conditions were evaluated using ANOVA (A) or two-way ANOVA (B-D) followed by Bonferroni multiple comparison analysis. ###, indicates $P<0.001$ for the effect of insulin versus untreated cells; ‡‡‡, $P<0.001$; ‡‡, $P<0.01$; ‡, $P<0.05$ for miR-143 or miR-145 versus control pre-miR.

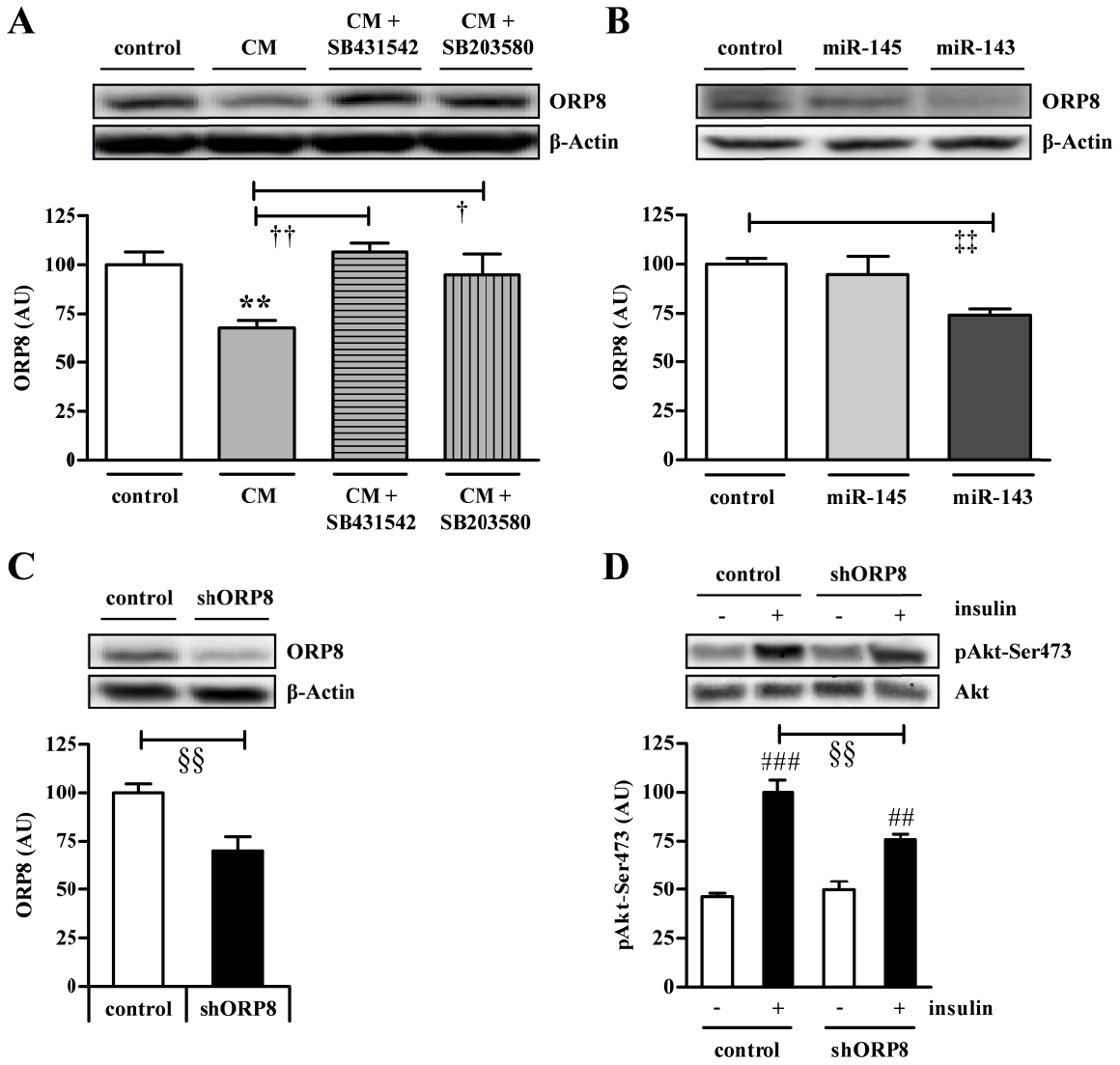

Figure 4.6: Inhibition of insulin action by conditioned media involves down-regulation of the miR-143 target ORP8. Primary human vascular smooth muscle cells were transfected with control precursor miRNA or precursors for miR-143 or miR-145 (A), or exposed to conditioned media (CM) in the presence or absence of SB431542 or SB203580 (B) whereafter protein levels of ORP8 were examined via Western blot analysis. Shown are representative blots and quantifications. ORP8 abundance normalized for β-actin is expressed as mean ± standard error of the mean of 16 independent experiments using cells from 2 distinct donors and CM from 8 different preparations. Differences among the experimental conditions were evaluated using ANOVA followed by Bonferroni multiple comparison analysis. **, indicates P<0.01 for the effect of CM versus control medium; ††, *P*<0.01; †, *P*<0.05 for CM only versus CM + inhibitors; ; ‡‡, *P*<0.05 for miR-143 or miR-145 versus control pre-miR. C/D. Impact of silencing ORP expression in primary human vascular smooth muscle cells. Lysates from cells transduced with lentiviruses coding for control shRNA or ORP8 shRNA were analyzed for ORP8 protein abundance (C) and insulin-mediated phosphorylation of Akt-Ser473 (D) under untreated conditions (-) or following stimulation with insulin (10 min; 100 nM). Signals were normalized for β-actin (C) or Akt (D) respectively, and expressed as mean ± standard error of the mean of 8 independent experiments using cells from two different donors and 4 distinct shRNA constructs. ### indicates *P*<0.001; ##, *P*<0.01 for the effect of insulin versus untreated cells; §§, *P*<0.01 for the effect of ORP8 shRNA versus control shRNA.

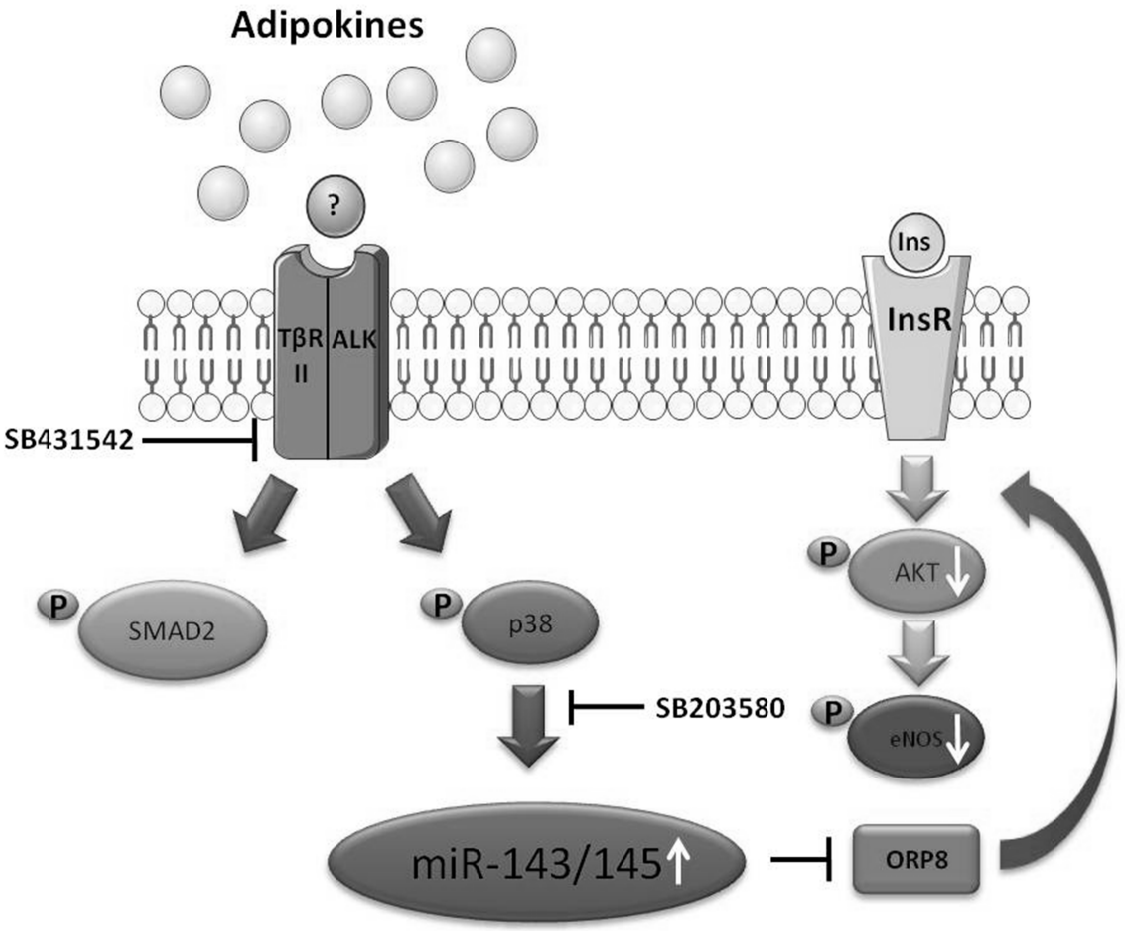

Figure 4.7: Possible mechanism for CM-induced insulin resistance in hVSMC. Adipocyte-derived factors belonging to the TGFβ-superfamily and binding to ALK induce SMAD2 and p38 phosphorylation. Especially the SMAD-independent pathway via p38 leads to an up-regulation of the miRNA 143/145 cluster. miR-143 is able to reduce the expression of ORP8 resulting in impaired insulin-stimulated Akt and eNOS phosphorylation. ALK: activin receptor-like kinases, Ins: insulin, InsR: insulin receptor, TβR II: transforming growth factor β receptor 2, ORP8: oxysterol-binding protein-related protein 8

References

[1] Grundy SM (2004) Obesity, metabolic syndrome, and cardiovascular disease. J.Clin.Endocrinol.Metab 89: 2595-2600

[2] Schlich R, Willems M, Greulich S, et al (2013) VEGF in the Crosstalk between Human Adipocytes and Smooth Muscle Cells: Depot-Specific Release from Visceral and Perivascular Adipose Tissue. Mediators.Inflamm. 2013: 982458

[3] Lamers D, Schlich R, Greulich S, Sasson S, Sell H, Eckel J (2011) Oleic acid and adipokines synergize in inducing proliferation and inflammatory signalling in human vascular smooth muscle cells. J.Cell Mol.Med. 15: 1177-1188

[4] Greulich S, Maxhera B, Vandenplas G, et al (2012) Secretory products from epicardial adipose tissue of patients with type 2 diabetes mellitus induce cardiomyocyte dysfunction. Circulation 126: 2324-2334

[5] Owens GK (1995) Regulation of differentiation of vascular smooth muscle cells. Physiol Rev. 75: 487-517

[6] Fulton DJ (2009) Mechanisms of vascular insulin resistance: a substitute Akt? Circ.Res. 104: 1035-1037

[7] Blumensatt M, Greulich S, Herzfeld de WD, et al (2013) Activin A impairs insulin action in cardiomyocytes via up-regulation of miR-143. Cardiovasc.Res.

[8] Jordan SD, Kruger M, Willmes DM, et al (2011) Obesity-induced overexpression of miRNA-143 inhibits insulin-stimulated AKT activation and impairs glucose metabolism. Nat.Cell Biol. 13: 434-446

[9] Takanabe R, Ono K, Abe Y, et al (2008) Up-regulated expression of microRNA-143 in association with obesity in adipose tissue of mice fed high-fat diet. Biochem.Biophys.Res.Commun. 376: 728-732

[10] Cordes KR, Sheehy NT, White MP, et al (2009) miR-145 and miR-143 regulate smooth muscle cell fate and plasticity. Nature 460: 705-710

[11] Hauner H, Petruschke T, Russ M, Rohrig K, Eckel J (1995) Effects of tumour necrosis factor alpha (TNF alpha) on glucose transport and lipid metabolism of newly-differentiated human fat cells in cell culture. Diabetologia 38: 764-771

[12] Wichelhaus A, Russ M, Petersen S, Eckel J (1994) G protein expression and adenylate cyclase regulation in ventricular cardiomyocytes from STZ-diabetic rats. Am.J.Physiol 267: H548-H555

[13] Carlotti F, Bazuine M, Kekarainen T, et al (2004) Lentiviral vectors efficiently transduce quiescent mature 3T3-L1 adipocytes. Mol.Ther. 9: 209-217

[14] Long X, Miano JM (2011) Transforming growth factor-beta1 (TGF-beta1) utilizes distinct pathways for the transcriptional activation of microRNA 143/145 in human coronary artery smooth muscle cells. J.Biol.Chem. 286: 30119-30129

[15] Montero D, Walther G, Perez-Martin A, Vicente-Salar N, Roche E, Vinet A (2013) Vascular smooth muscle function in type 2 diabetes mellitus: a systematic review and meta-analysis. Diabetologia 56: 2122-2133

[16] Symons JD, McMillin SL, Riehle C, et al (2009) Contribution of insulin and Akt1 signaling to endothelial nitric oxide synthase in the regulation of endothelial function and blood pressure. Circ.Res. 104: 1085-1094

[17] Cersosimo E, Xu X, Musi N (2012) Potential role of insulin signaling on vascular smooth muscle cell migration, proliferation, and inflammation pathways. Am.J.Physiol Cell Physiol 302: C652-C657

[18] Bornfeldt KE, Tabas I (2011) Insulin resistance, hyperglycemia, and atherosclerosis. Cell Metab 14: 575-585

[19] Landmesser U, Hornig B, Drexler H (2004) Endothelial function: a critical determinant in atherosclerosis? Circulation 109: II27-II33

[20] Garg UC, Hassid A (1989) Nitric oxide-generating vasodilators and 8-bromo-cyclic guanosine monophosphate inhibit mitogenesis and proliferation of cultured rat vascular smooth muscle cells. J.Clin.Invest 83: 1774-1777

[21] Nakaki T, Nakayama M, Kato R (1990) Inhibition by nitric oxide and nitric oxide-producing vasodilators of DNA synthesis in vascular smooth muscle cells. Eur.J.Pharmacol. 189: 347-353

[22] Nunokawa Y, Tanaka S (1992) Interferon-gamma inhibits proliferation of rat vascular smooth muscle cells by nitric oxide generation. Biochem.Biophys.Res.Commun. 188: 409-415

[23] Cheng Y, Liu X, Yang J, et al (2009) MicroRNA-145, a novel smooth muscle cell phenotypic marker and modulator, controls vascular neointimal lesion formation. Circ.Res. 105: 158-166

[24] Xin M, Small EM, Sutherland LB, et al (2009) MicroRNAs miR-143 and miR-145 modulate cytoskeletal dynamics and responsiveness of smooth muscle cells to injury. Genes Dev. 23: 2166-2178

[25] Santovito D, Mezzetti A, Cipollone F (2012) MicroRNAs and atherosclerosis: new actors for an old movie. Nutr.Metab Cardiovasc.Dis. 22: 937-943

[26] Cipollone F, Felicioni L, Sarzani R, et al (2011) A unique microRNA signature associated with plaque instability in humans. Stroke 42: 2556-2563

[27] Lamers D, Schlich R, Horrighs A, Cramer A, Sell H, Eckel J (2012) Differential impact of oleate, palmitate, and adipokines on expression of NF-kappaB target genes in human vascular smooth muscle cells. Mol.Cell Endocrinol. 362: 194-201

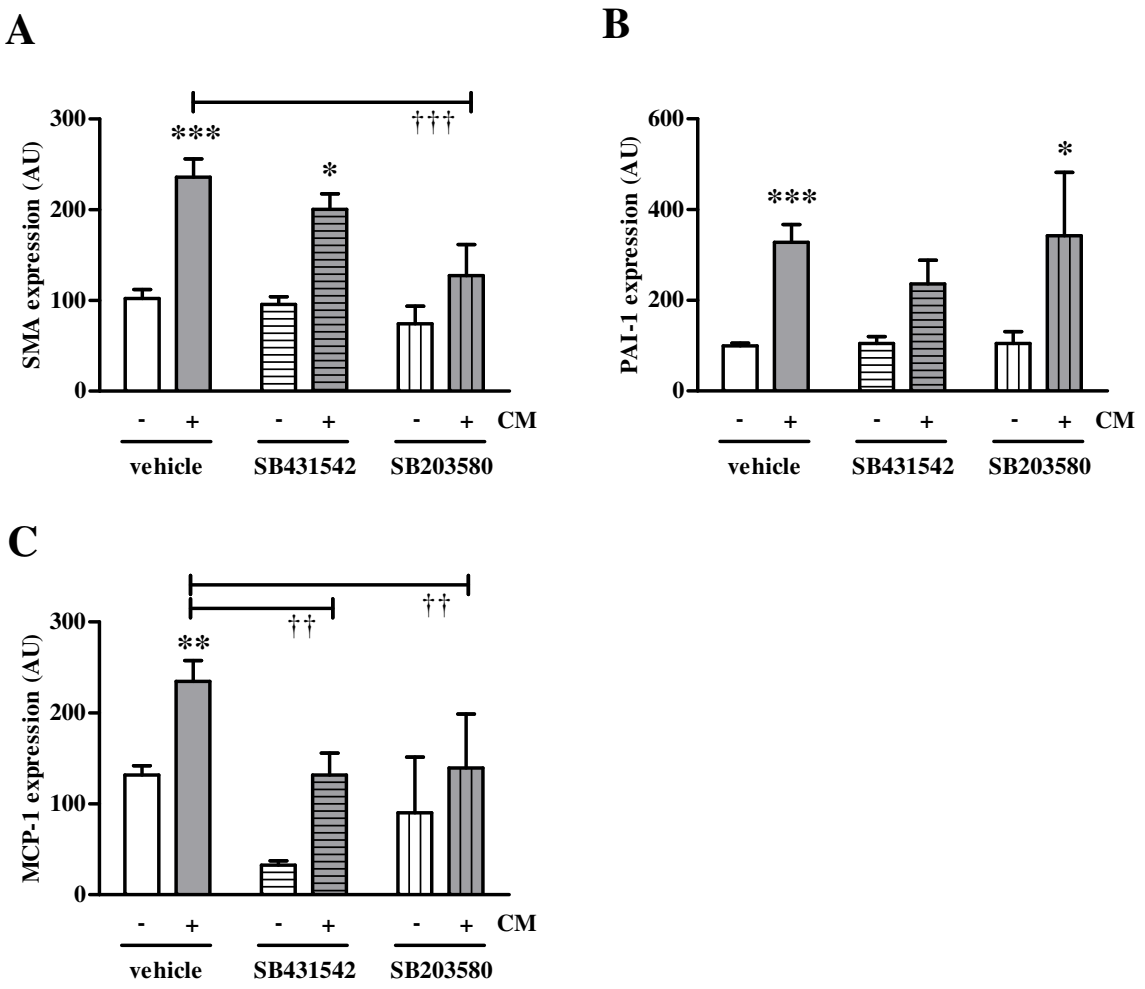

Supplementary Figure 4.1: Effect of inhibition of TGFβ receptor- and p38-signalling on the induction of gene expression by conditioned media in primary human vascular smooth muscle cells. Cells were exposed DMSO (vehicle), or pharmacological inhibitors for Alk4/5/7 (SB431542), or p38 (SB203580) for 1 h prior to the addition of control medium (-) or conditioned media CM (+) for 24 h. Then expression levels of smooth muscle α-actin (SMA), PAI-1, and MCP-1 were determined via real-time PCR. Data are expressed as mean ± standard error of the mean of least 8 independent experiments using cells from 2 different donors and conditioned media from 8 different preparations. Differences among groups the groups were analyzed using two-way ANOVA and Bonferroni multiple comparison analysis. ***, indicates $P<0.001$; **, $P<0.01$; *, $P<0.05$ for CM versus control medium; †††, $P<0.001$; ††, $P<0.01$ for CM only versus inhibitors.

Journal: *Biochimica et Biophysica Acta – Molecular Basis of Disease*

Impact factor: 4.910

Contribution: Total: 50%

Conceived / designed experiments: 60%

Performed experiments: 30%

(western blot analysis, isolation of RNA and quantitative real-time PCR, cell culture techniques including transfection and lentiviral transduction of hVSMC)

Analysed data: 60%

Contributed to discussion: 40%

Wrote the manuscript: 50%

Reviewed / edited manuscript: 60%

Author: 1st author (shared)

Chapter 5

General Discussion

5. General Discussion

The present studies have demonstrated that secreted factors from adipose tissue or adipocytes have severe consequences on the physiology of cardiomyocytes and smooth muscle cells, respectively. Specifically, epicardial adipose tissue from patients with T2D induced contractile dysfunction, a diminished insulin signaling and an altered expression of miRNAs in cardiomyocytes. Particularly, contractile dysfunction and reduced sensitivity to insulin as well as expression of the miR-143/145 cluster in cardiomyocytes could be ascribed to an increased secretion of activin A from epicardial adipose tissue from patients with T2D compared to patients without diabetes or to other fat depots. Moreover, adipocyte-derived conditioned media induced expression of miR-143/145 in smooth muscle cells. In both cell types, cardiomyocytes and smooth muscle cells, a disturbed insulin action could be ascribed to higher levels of miR-143. Collectively, these findings provide new insights how adipose tissue contributes to the pathophysiology of cardiovascular complications in diabetes.

5.1. Adipose tissue and cardiovascular complications

5.1.1. Difference between epicardial adipose tissue and other fat depots

Using the explant technology described in chapter 2, we have generated conditioned media (CM) from visceral fat depots, the epicardial (EAT) and pericardial adipose tissue (PAT) and from a non-visceral fat depot, the subcutaneous adipose tissue (SAT) either from patients with T2D or without diabetes (ND). Using antibody arrays, we first determined the distinct secretion profile from EAT compared to the other fat depots. Importantly, we were able to make a difference between the adipokine secretion pattern of EAT from patients with T2D and without diabetes (chapter 2). In table 5.1, identified factors are listed which have shown an altered secretion between EAT and the other fat depots, irrespective of the patients having diabetes or not.

Table 5.1: Difference of released adipose tissue-derived factors between EAT, SAT or PAT.

adipose tissue-derived factor	EAT vs. SAT	EAT vs. PAT
adiponectin	=	↓
activin A	↑	↑
angiopoietin-2	↑	↑
cardiotrophin-1	=	↑
endoglin	=	↑
E-selectin	↓	↓
omentin	↑	↑
TIMP-2	↑	↑

Listed are selected proteins measured in the conditioned media generated from adipose tissue. Shown are differences in the abundance of the mentioned proteins between the epicardial (EAT), subcutaneous (SAT) or pericardial (PAT) adipose tissue.

Normally, adipose tissue functions as a storage depot when food intake exceeds the energy demand of the body. Since obesity and its metabolic consequences have now been recognized, it is important to understand the pathogenic potential of adipose tissue and how enlarged adipose tissue leads to severe metabolic consequences. The pathogenic potential of adipose tissue significantly depends on its location and therefore it becomes important where the excess fat is stored.[169] Obese and metabolic healthy subjects often have less visceral adipose tissue than obese patients with metabolic diseases.[170, 171] In addition, patients with

metabolic complications and normal weight exhibit more visceral adipose tissue than individuals of similar weight but with normal metabolism.[171] Obviously, the location of a visceral fat depot itself might explain the detrimental effects of its enlargement. For instance, there is no boundary like a fascia between EAT and the myocardium. While secreted factors from the subcutaneous adipose tissue have to act through the circulation of the body, EAT can directly affect the underlying cardiomyocytes.[44]

Like in other fat depots the selective expression and secretion of several adipokines could be demonstrated for EAT.[172] Even though some studies have investigated the expression of adipokines in EAT with quantitative real-time PCR (qRT-PCR), microarray analysis or antibody arrays, only a few studies have confirmed the secretion of selected factors from EAT such as IL-1β, IL-6, MCP-1 and TNF-α.[173] Nevertheless, the expression data highlight that there is a fat depot specific expression of adipokines, which further distinguishes EAT from other fat depots.[44] By analysing conditioned media with antibody arrays, we were able to extend the knowledge about the differences regarding the secretome between EAT and SAT and even between EAT and the visceral PAT (see chapter 2 and table 5.1). Using cytometric bead arrays and ELISA, Venteclef and colleagues have found that EAT secrets angiogenic factors and matrix metalloproteinases more abundantly than SAT. In line with our findings, they have confirmed that activin A is released in higher amounts from EAT compared to SAT. The authors of the same study have also described that EAT, but not SAT, induces atrial fibrosis as illustrated by enhanced accumulation of collagen fibres between myocytes.[174] Interestingly, pathological states, such as coronary artery disease (CAD) or the metabolic syndrome, are clearly associated with an altered expression of secreted proteins in EAT.[173] It has been reported that EAT from patients suffering from CAD expresses pro-inflammatory markers in higher doses compared to SAT.[173] Moreover IL-6, leptin, resistin and TNF-α have been found to be expressed more abundantly in EAT of patients with CAD compared to control subjects.[175, 176]

However, the question why the secretion profile of the same depot differs between patients with and without T2D still has to be answered. Typically, the cellular content of adipose tissue consists of adipocytes, fibroblasts, endothelial cells, macrophages and preadipocytes, which can all release a variety of pro-inflammatory chemo-, cytokines and other factors.[177, 178] According to previous reports, infiltration of immune cells attracted by a pro-inflammatory milieu in EAT from patients with CAD occurs.[173, 179-181] In this work, we have extended these observations by showing a dramatic increase in macrophage and monocyte infiltration in EAT-TD2 versus EAT-ND (chapter 2), which could be responsible

for the altered secretion profile. In physiological conditions, fat cells serve as lipid storage cells, leading to an enlargement of adipocyte cell size. In obesity and T2D, hypertrophic enlargement of adipocytes triggers low-grade inflammation and infiltration of immune cells into the adipose tissue. Moreover, increased storage of lipids optimally occurs by differentiation of new adipocytes from preadipocytes, a process called adipogenesis. A decreased expression of adipogenic genes has been shown to be associated with metabolic diseases and T2D.[182] Increased cell size and number results in increased fat mass, which needs an accurate and sufficient blood supply. Impaired angiogenesis leading to hypoxic conditions in adipose tissue exacerbates adipocyte metabolic dysfunction and causes a pro-inflammatory response and metabolic diseases.[183] Morbidly hypertrophic and lipid-overloaded adipocytes as well as accumulated immune cells cause a disturbed secretion profile and therefore link pathogenic enlargement of adipose tissue to low-grade inflammation in T2D and obesity.

Besides the specific localisation and the intrinsic characteristics of a fat depot, the degree of oxidative stress is another aspect which should be noted here. Proteomic analysis has revealed that proteins responsible for oxidative stress are expressed more abundantly in EAT than in SAT from patients with cardiovascular disease.[184] Accordingly, generation of reactive oxygen species (ROS), which are known to be associated with inflammation and cardiovascular diseases, was higher in EAT than in SAT.[184] Hence, an increased level of ROS may also contribute to the alterations of the secretory profile of EAT.

5.1.2. Epicardial adipose tissue-derived factors impair cardiomyocyte physiology

The heart failure introduced by Rubler and referred to as diabetic cardiomyopathy commonly occurs during diabetes and is characterised by cardiac fibrosis, left ventricular hypertrophy, altered substrate utilization and an impaired calcium signaling followed by disturbed cardiac performance.[46, 49] In particular, diabetic cardiomyopathy is characterised by diastolic dysfunction due to an inadequate relaxation of the left ventricle.[58, 59]

In chapters 2 and 3, we investigated the potential of epicardial adipose tissue to impair contractility and the insulin signaling pathway of isolated adult rat cardiomyocytes (ARC). One key finding in respect to the physiology of cardiomyocytes was reduced sarcomere shortening and intracellular Ca^{2+}-fluxes in cells treated with CM-EAT-T2D. In line with a previous study, we have suggested a reduced performance of Serca2a, which is responsible

for the disturbed Ca^{2+}-homeostasis.[185] This assumption is supported by the reduced protein level of Serca2a, even after short time exposure for 30 min of ARC to the CM-EAT-T2D. Very fast removal of Ca^{2+} into the sarcoplasmic reticulum or the extracellular lumen is essential for cardiac relaxation.[186] This process is facilitated during diastole mainly by Serca2a and to a lesser extent by the sarcolemmal Na^{+}/Ca^{2+}-exchanger.[187] In addition, a reduced Serca2a protein abundance has also been reported in diabetes-related heart failure.[188-190] Nevertheless, due to the relativly short incubation time of ARCs with CM, we also assume that posttranscriptional modifications such as phosphorylations and de-phosphorylations play a pivotal role in the CM-induced effects. In this context, CM-dependent phosphorylation of phospholamban (PLB) seems to be very interesting. De-phosphorylated PLB acts as an inhibitor of Serca2a and phosphorylation of PLB by proteinkinase A or calmodulin-dependent protein kinase releases inhibition and induces a substantial increase of sarcoplasmic Ca^{2+}-uptake via Serca2a.[189] Notably, we have also observed weaker effects on contractile function with CM-SAT-T2D compared to CM-EAT-T2D, which agrees with other studies where subcutaneous adipose tissue induced contractile dysfunction.[191-193] However, to the best of our knowledge, we have reported here for the first time direct detrimental effects of the EAT-derived secretome from patients with T2D and that these effects are stronger compared to either other fat depots from the same patient or to EAT from patients without T2D. Within the CM, we have identified two proteins, namely activin A and angiopoietin-2, which alone mimic the effects of CM-EAT-T2D, but so far we cannot exclude other factors modulating contraction.

Moreover, we have described in chapters 2 and 3 that EAT-derived factors abrogate insulin-stimulated Akt phosphorylation in cardiomyocytes, which is partially due to activin A, but not angiopoetin-2 (see section 5.1.3 and 5.1.4). In contrast to the CM-induced contractile dysfunction, we have only observed a significant inhibitory effect on insulin signaling if we prolonged the incubation time of ARCs with CM. Therefore, we speculate that the insulin signaling cascade is affected by a different pathway compared to the contractility of the cardiomyocytes. This is consistent with our results in chapter 3, where we describe the involvement of miRNA expression in the CM-induced insulin resistance of cardiomyocytes (see section 5.2.2). Many studies have also confirmed, that adipocyte-derived factors alter insulin signaling in adipocytes, skeletal muscle and cardiomyocytes and it is generally accepted that obesity correlates with insulin resistance.[194, 195] Furthermore, factors derived from epididymal adipose tissue from diabetic rats abrogate insulin action in cardiomyocytes, which is paralleled by a reduced insulin stimulated glucose uptake.[195] The effects of EAT on

energy substrate metabolism have not been examined in cardiomyocytes so far. Nevertheless, to the best of our knowledge, we have proven for the first time that EAT-derived factors alter insulin-stimulated Akt phosphorylation (chapter 2). Moreover, we have identified the induction of miR-143 expression as a crucial factor for CM-induced insulin resistance and except for CM-EAT-T2D none of the used CM had the ability to induce the respective miRNA (see section 5.2.2).

5.1.3. Activin A as an epicardial adipokine highly secreted from patients with type 2 diabetes

In chapter 2, we identified activin A as an epicardial adipokine secreted in higher amounts from patients with T2D. Moreover, we have characterised in chapters 2 and 3 the detrimental effect of activin A on contractility and insulin action in ARC. Using neutralizing antibodies for activin A, we were able to partially block the detrimental CM-induced effects on the physiology of cardiomyocytes. We have also shown that activin A activates at least two pathways, due to the activation of SMAD- and p38MAPK-signaling, and that activin A induces the expression of the miR-143/145-cluster.

Activin A is produced by nearly all tissues including the adipose tissue and it was discovered as a circulating protein within the blood.[196] In addition, activin A has also been implicated in several immune processes.[197, 198] After inflammatory stimulus with lipopolysaccharides (LPS), increased circulating levels of activin A could be detected.[199] This was paralleled by TNF-α as one of the first pro-inflammatory cytokines released into the circulation during inflammation.[199] Interestingly, it could be shown that activin A is secreted from monocytes and bone marrow stromal fibroblasts by cognate interaction with activated T cells, indicating macrophages as a potential source for activin A release during T2D.[200]

However, several studies have reported that activin A serum levels are not elevated in systemic circulation of humans with a chronic inflammatory disease such as T2D or adiposity.[201-203] In contrast to that, the amount of circulating levels of activin A positively correlates with high glucose and insulin levels as well as with insulin resistance in subjects with T2D and it could be shown that T2D patients had higher activin A levels in the intracoronary sinus than the patients without T2D.[202, 204] Indeed, we suggest that activin A secreted from EAT does not influence the myocardium via circulation but rather in a paracrine and direct way. This is supported by the lack of fascia-like boundaries between the heart and EAT.[43] Consistent with our findings, activin A released from EAT is associated

with decreased myocardial function and glucose metabolism in human diabetic cardiomyopathy.[204] Cardiac fibrosis is also common in diabetic cardiomyopathy and EAT-derived activin A promotes myocardial fibrosis, which underlines the pro-fibrotic effects of activin A.[46, 174, 205-207]

Activin A belongs to a diversified family of signaling proteins, namely the TGF-β-superfamily including the TGF-β-isoforms, bone morphogenetic proteins (BMPs), growth and differentiation factors (GDFs) and activins (Acts), inhibins (Inhs) as well as Müllerian inhibiting substance (MCS). Even though the subgroups of this family have diverging functions *in vivo*, they all share the same dimeric structure.[208] Members of the activins consists of activin β-subunits. Activin A, as the best characterised member of this family, is a homodimer of two activin β_A-subunits whereas activin B or activin AB consists of two activin β_B-subunits or one of each, respectively.[197] Like other members of the TGF-β-superfamily, activins transduce their signals by binding and bringing together two transmembrane receptor kinases, namely TGF-β type 1 (TβR-1) and type 2 receptors (TβR-2).[208-210] Both receptors, TβR-1 and TβR-2, contain a cytoplasmic serine-threonine kinase domain and after assembly of the heterodimer, TβR-2 phosphorylates and activates TβR-1, which propagates a phosphorylation cascade to intracellular effectors.[211] Activins are further distinguished from the other members of the superfamily by the use of at least two different type 1 receptors (ActRI-b/Alk4 or TβR-1/Alk5) and two different type 2 receptors (ActR-II or ActR-IIb).[208] Upon binding to its receptors, activin A induces the canonical receptor-mediated activation of SMAD-dependent signal transduction, which was also supported by our findings in Chapter 2.[212] Here, CM-EAT-T2D increased the phosphorylation of SMAD2 without any changes on total SMAD2 protein expression in ARC. An inhibitor for the receptors Alk4 and Alk5 completely diminished CM-induced SMAD2 phosphorylation. Since other members of the TGF-β-superfamily induce the activation of SMAD2, it is also plausible, that further factors besides activin A induce contractile dysfunction via SMAD2 phosphorylation. In contrast to that, we are able to link CM-induced contractile dysfunction to activin A by using neutralizing antibodies for activin A, recombinant follistatin, as a physiological inhibitor of activins, and the inhibitor of its receptors (Alk4 and Alk5) in combination with CM-EAT-T2D. Our results indicate activin A to be a prominent cardiodepressant factor due to activation of SMAD2-signaling within cardiomyocytes.

Furthermore, TGFβ-signaling also activates SMAD-independent downstream targets like p38 and it was shown that activin A accelerates p38-signaling at least in erythroid cells.[213-215] To the best of our knowledge, we have shown here for the first time, that activin A

has the ability to induce p38 phosphorylation in a dose dependent manner in cardiomyocytes (chapter 3). In contrast to SMAD2 activation, we could link activin A-dependent activation of p38 to an increased expression of both mature miR-143 and miR-145 and to a decreased insulin action (chapter 3). Previously, Long and colleagues have demonstrated that TGFβ1 induces the expression of miR-143/145 via p38 in smooth muscle cells, which is consistent with our findings in chapters 3 and 4.[214]

Besides our findings, *in vitro* studies have also suggested that p38 promotes cardiac growth and hypertrophy.[216] Inhibition of the p38-pathway diminishes cardiomyocyte growth in response to hypertrophic stimuli and over-activation of the same pathway induces hypertrophic changes *in vitro*.[217-220] Interestingly, transgenic overexpression of the p38-activators, MKK3 and MKK6, results in cardiac interstitial fibrosis, ventricular wall thinning, and death due to heart failure.[221, 222] Conversely *in vivo* studies have shown contradictory results regarding p38-induced hypertrophic growth. However, all studies have in common, that p38 induction is more closely related to pathological forms of hypertrophy than to physiological compensation. In line with our results, p38 is also activated in cardiomyocytes by pro-inflammatory cytokines, including TGF-β. In this kind of activation, p38 is associated with cardiac remodelling and myocardial infarction.[223] Moreover, p38-activation itself seems to play a role in cardiac cytokine production and release. These cytokines lead to recruitment and proliferation of fibroblasts and inflammatory cells, resulting in fibrosis and remodelling.[216] As discussed previously, we have linked activin A-induced p38-activation with miR-143 expression and insulin resistance in cardiomyocytes. To what extent CM-induced p38-activation leads to hypertrophic growth or cardiac fibrosis has to be further elucidated.

5.1.4. Potential functions of selective factors showing a deregulated release by EAT-T2D

In chapter 2 and in a separate study, we have reported that omentin-1 is highly expressed in and secreted from EAT compared to other fat depots such as PAT and SAT (Table 5.1).[224] However, secretion and expression of omentin from EAT from subjects with T2D is markedly reduced compared to EAT-ND.[224] Previously, omentin has been identified to be secreted by visceral but not by SAT. Here, cells from the stromavascular fraction rather than adipocytes are the main source of omentin protein expression and it could also be demonstrated that omentin has beneficial effects on insulin-stimulated glucose uptake in

adipocytes.[225] In addition, omentin protein and mRNA levels are decreased in adipose tissue in obesity, T2D and in subjects with CAD.[226-228] Plasma omentin levels also inversely correlate with BMI, fasting plasma glucose, insulin and HbA1c and positively associate with insulin sensitivity, adiponectin and HDL-cholesterol in patients with T2D.[224] In addition, recombinant omentin-1 partially abolishes the detrimental effects of CM-EAT-T2D on insulin action in cardiomyocytes, underlining the beneficial effects of omentin on glucose metabolism.[224] Since omentin negatively correlates with heart rate and positively associates with diastolic parameters such as early peak filling rate and early deceleration peak, omentin seems to be a cardioprotective adipose tissue-derived factor.[224] This was supported by the ability of recombinant omentin to protect cardiomyocytes against the harmful effects of CM-EAT-T2D.[224]

Like activin A, angiopoietin-2 (ang2) was highly abundant in CM-EAT-T2D and had also detrimental effects on contractility but did not influence insulin action (chapter 2). Serca2a, a key regulator involved in the electromechanical coupling in cardiomyocytes, is reduced in CM-EAT-T2D and by ang2, which might explain the decreased cardiac performance. The Framingham study has revealed that ang2 is higher in patients with the metabolic syndrome and its circulating levels are positively related to diabetes.[229] Besides ang2, there are three other members of the angiopoietin family, ang1, ang3 and ang4.[230] Ang1 is an agonist of the transmembrane receptor tyrosine kinase Tie2, which is mainly expressed in endothelium cells.[231] Upon binding to Tie2, ang1 induces migration, inhibits apoptotic pathways and reduces endothelium leakage, causing migration of leucocytes into the underlying tissues.[230] Generally, ang1 exerts anti-inflammatory effects as illustrated by suppressed up-regulation of E-selectin, ICAM-1 and VCAM-1.[232, 233] In contrast, ang2 is primarily released during inflammation. High concentrations of ang2 competitively inhibit endothelial ang1-signaling through Tie2, especially in inflammation and angiogenesis.[234] Nevertheless, we have described in chapter 2 for the first time that ang2 released by EAT also influences cardiomyocyte physiology. Both, the exact pathway of ang2 in cardiomyocytes and the consequences of EAT-derived ang2 to coronary arteries should be object of further investigations.

Besides ang2 and activin A, soluble CD14 (sCD14) is highly enriched in CM-EAT-T2D, which is consistent with higher serum levels found in obese individuals and subjects with T2D.[235] Furthermore, serum levels of sCD14 seem to be elevated in patients with chronic heart failure.[236] This protein is mainly expressed by monocytes and positioned by a glycophosphatidylinositol (GPI)-anchor at the plasma membrane, where it acts as a coreceptor

for bacterial lipopolysaccharides (LPS) and triggers activation of the innate immune system via toll-like receptor 4.[237] The soluble and circulating form is released by shredding the protein from the GPI-anchor.[238] Although it is not endogenously expressed in other cell types, sCD14 also plays a crucial role in the LPS-recognition and -response of at least endothelial cells. In this cell type, it is important for LPS-induced expression of VCAM-1 and ICAM-1 as well as for secretion of inflammatory cytokines IL-6 and IL-8.[239, 240] However, little is known about the role of sCD14 in the pathogenesis of diabetes-related heart failure. The fact that sCD14 is mainly expressed and released by monocytes, could be another indicator for increased migration of monocytes to EAT-T2D compared to EAT-ND which, may contribute to the low grade inflammation of adipose tissue in T2D.

5.1.5. Adipocyte-derived factors induce vascular insulin resistance

In chapter 4 we have investigated the influence of adipocyte-derived factors on insulin action in human vascular smooth muscle cells (hVSMC). We have observed that CM generated from human adipocytes diminishes nsulin-stimulated Akt-phosphorylation, which results in a reduced insulin-stimulated phosphorylation of the Akt-substrate endothelial nitric oxide synthetase (eNOS).

For many years it has been known that low-grade inflammation during obesity and insulin resistance is closely linked to the development of T2D and atherosclerotic cardiovascular disease.[241] It has thoroughly been established that insulin resistance is an independent risk factor for development of CAD and atherosclerosis.[242] During progression of obesity-associated inflammation, release of pro-inflammatory adipokines occurs. One of the most established adipose tissue-derived factors is TNF-α, which is increased in circulation in obese and even in insulin-resistant and atherogenic states.[243, 244]

With regard to endothelial cells, it seems that insulin signaling induces a number of athero-protective processes. For instance, in a mouse model, where the insulin receptor is conditionally deleted in endothelial cells, atherosclerotic lesion size was 2-fold higher than in control animals, even though blood pressure, plasma lipids, systemic insulin sensitivity and glucose tolerance remained equal between the IR-deficient and control mice. In addition, endothelial VCAM-1 expression was elevated in mice lacking insulin action, causing increased adhesion of immune cells to the endothelium. This coexisted with a reduced eNOS-activity and decreased NO-induced vasodilation. Altogether, mice with impaired endothelial insulin signaling exhibit initial steps in the progression of atherosclerosis.[245] However, in T2D and states of insulin resistance compensatory mechanism lead to systemic hyperinsulinemia

and it is assumed, that higher levels of insulin lead to a selective insulin resistance in SMC with decreased PI3K- and increased MAPK-signaling.[246] Here, an increased insulin-stimulated activation of the MAPK-pathway could promote the proliferative and migrative phenotype of SMC during early events of atherosclerosis. Indeed, a previous study has highlighted the proliferative effects of adipocyte-derived CM, which we also have used in chapter 4 on hVSMC.[247] The authors of this study have suggested, that the CM-induced proliferation of hVSMC could be maintained by at least two pathways, including a NFκB-dependent and a p38-dependent pathway. Our results in chapter 4 indicate that p38-activity is also crucial for the reduced insulin-stimulated Akt- and eNOS-phosphorylation. To which extent the CM-induced effects on insulin signaling coincide with a higher rate of proliferation of hVSMC has to be further elucidated. Conversely, data from other investigators have suggested that disturbed Akt-signaling leads to higher rates of apoptosis due to the lack of cell-survival signaling in endothelial cells, smooth muscle cells and macrophages.[248] Higher rates of apoptosis of SMC can promote end-stage atherosclerosis, as plaque become instable due to decreased production of extracellular matrix, causing thinning of the fibrous cap and cap rupture.[246]

Even though we have not shown that adipocyte-derived factors induce release of bioactive MCP-1, we did see an up-regulation of MCP-1 mRNA-expression in hVSMC treated with adipocyte-derived CM. Many studies have supported the hypothesis that MCP-1 sustains recruiting of monocytes into early atherosclerotic lesions.[249] Interestingly, MCP-1 is present in macrophage-rich atherosclerotic plaques in humans, due to its expression within SMC, amongst others.[250] Cushing and colleagues have demonstrated that oxidized LDLs, but not native LDLs, induce MCP-1 expression in endothelial cell and SMC.[251] Thus, CM-induced expression of MCP-1 in SMC has emerged as a possible molecular link between oxidized LDL and foam cell recruitment within the vessel wall.

5.2. The role of microRNAs in cardiovascular disease

5.2.1. Profiling of miRNA-expression in cardiomyocytes and smooth muscle cells

In chapter 3, we have compared miRNA-expression in ARC exposed to CM-EAT-T2D to ARC treated with CM-EAT-ND, using a quantitative real time (qRT)-PCR- and targeted-based approach. Deregulated miRNA-species have additionally been validated in cardiomyocytes treated with CM from other fat depots, in order to identify those miRNA-species, which are specifically induced by the epicardial secretome. We have expanded our results by profiling miRNA expression in rat arterial smooth muscle cells (RASMC), which have been treated with either CM-PVAT-T2D or CM-PVAT-ND (Figure 5.1). Perivascular adipose tissue (PVAT) is closely related to epicardial adipose tissue, however it differs in its localization as it surrounds blood vessels.[44]

In general, profiling miRNA expression is helpful for identifying specific miRNAs, which participate in organismal development and maintain tissue differentiation.[252] For instance, microarray analysis has revealed that up to 71 miRNAs are expressed in significantly different levels in adipose tissue of ob/ob mice compared to wild type mice.[253] Today, a number of high throughput methods for profiling miRNA expression either in body fluids, tissues or cells are available, such as qRT-PCR-, microarray- or deep-sequencing-techniques. This has led to the consideration of miRNAs as biomarkers for diverse molecular diagnostic applications.[254] Notably, it is possible to identify various kinds of cancer and their differentiation status via measuring selected miRNAs. The importance and appreciation of studies including miRNA expression profiles becomes obvious by the immensely rising numbers of publications related to this topic. The search term “miRNA profiling” in the “pubmed”-database results in 1031 counts in the year 2012 whereas only 1 publication is found in 2001.

As in other tissues, there is a specific miRNA-expression signature of fetal and adult heart. During development, several miRNAs are precisely regulated in their spatial and temporal expression levels, with the purpose to control protein expression levels. In addition, cardiac miRNA concentrations vary widely in human and during experimental heart disease.[255-257] So far, the growing list of heart failure-associated miRNAs has identified a

subset of specific miRNAs involved in cardiac hypertrophy, fibrosis, electrophysiological remodeling and alterations in calcium handling.[258] For instance, several miRNAs have been found to regulate cardiac fibrosis, including miR-21, miR-29, miR-30, miR-133, miR-101 and miR-24.[258] Particularly, miR-21, as one of the strongest up-regulated miRNA in the failing human heart, seems to be a crucial player in the progression of cardiac fibrosis. Thum and colleagues have demonstrated that stress-induced expression of miR-21 within the heart is mainly due to increased levels of the same miRNA in fibroblasts and that inhibition of miR-21 protects against stress-induced structural and functional deteriorations.[259] Generally, miR-21 has also been associated with fibrosis in other tissues and pathological states such as diabetic nephropathy, which further underlines the widely accepted role of miR-21 during fibrosis.[260] Interestingly, it could be shown that miRNA expression is not only regulated on a transcriptional level but also during processing of the pri-miRNA. For instance, TGF-β1 promotes a rapid increase of the mature miR-21 by regulating he posttranscriptional processing of pri-miRNA by Drosha.[261] Since the expression of miR-21 is connected to TGF-β-signaling, it is worthwhile to investigate the influence of CM-EAT-T2D and especially of activin A on miR-21 expression in cardiac fibroblasts.[174, 262]

In chapter 3, we have identified eight differentially expressed miRNAs in ARC treated with CM-EAT-T2D. Except for activin A (section 5.1.3), we have not investigated other epicardial adipokines and their potential to alter expression level of these deregulated miRNAs. However, we could explain the detrimental effects of CM-EAT-T2D on insulin signaling due to a higher expression of miR-143 in cardiomyocytes. Accordingly, either miR-143 or miR-145 has been found to be up-regulated in human heart failure.[263-265] Using neutralizing antibodies against activin A, we have been able to completely block the induction of miR-143 and miR-145 by CM-EAT-T2D indicating that only activin A within the CM is responsible for the elevated expression of miR-143 and miR-145. Nevertheless, the influence of further deregulated adipokines on the expression levels of other miRNAs and how these miRNA affect cardiomyocyte function, should be investigated in the future. We have additionally profiled the expression of miRNAs in rat atrial SMCs (RASMC) treated with either PVAT from patients with T2D or without (ND). In this context, we have found eight miRNAs to be affected by CM-PVAT-T2D (Figure 5.1), while they are either not or less affected by CM-PVAT-ND. In addition, miR-29c has been observed to be decreased in cells treated with CM-PVAT-ND. Most of the deregulated miRNAs are supposed to be involved in cancer progression, but miR-217 is also associated with endothelial dysfunction by targeting Sirtuin 1 (SIRT1) in human atherosclerotic plaques.[266] In vasculature of rodents, SIRT1

mediates vasodilatation via release of endothelial nitric oxide synthase-derived nitric oxide. Deletion of SIRT1 has been shown to interfere with crucial steps of endothelial activation and atherogenesis by promoting NFκB-signaling.[267, 268] The exact role of Sirt1 in SMC has not been clarified so far, but its expression is down-regulated in SMC of streptozotocin-induced diabetic rats.[269]

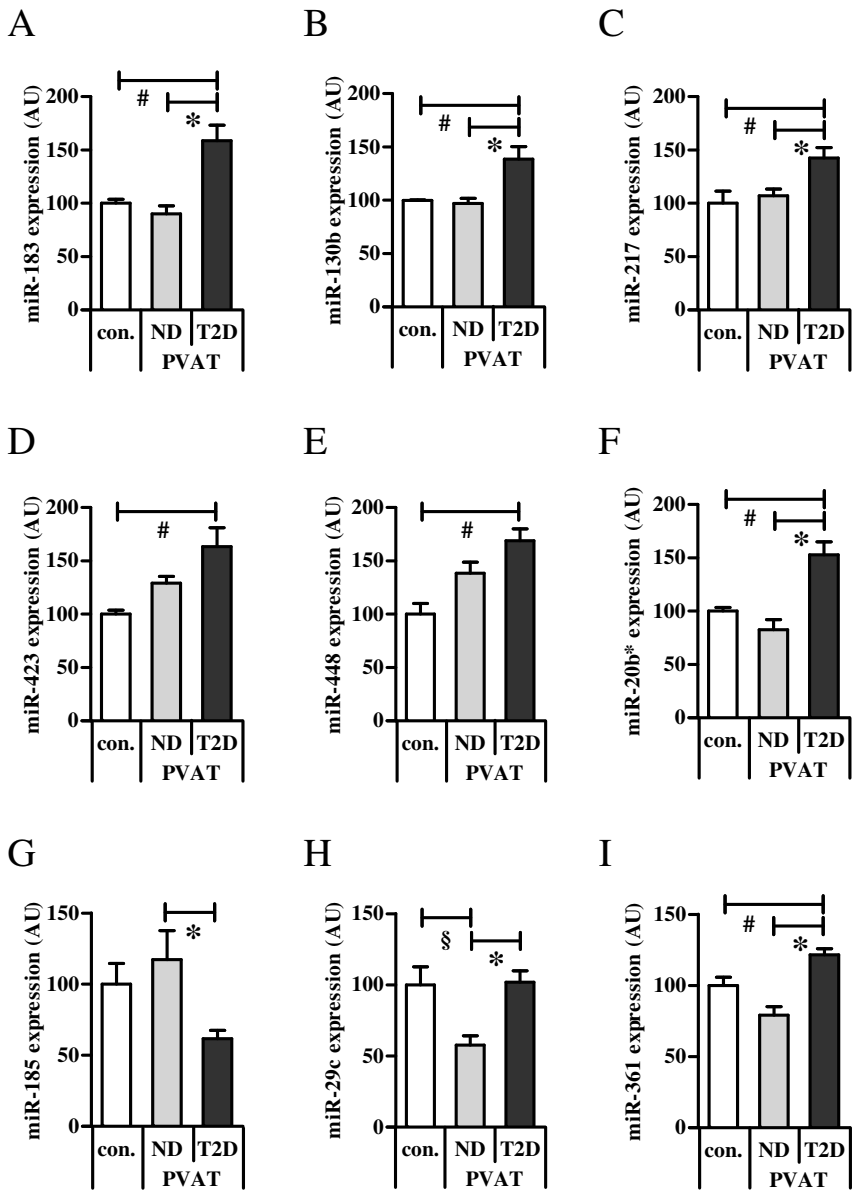

Figure 5.1: Effect of perivascular adipokines on miRNA expression in smooth muscle cells. Rat smooth muscle cells (RASMC) were exposed to control media (con.) or to CM (diluted 1:4) from perivascular adipose tissue (PVAT) either from patients with type 2 diabetes (T2D) or from patients without diabetes (ND). The miRNA expression of RASMC exposed to control medium was set at 100. Open bars, con.; gray bars, ND; black bars, T2D. Data were collected during eight independent experiments. Expression levels are expressed as mean ± SEM. Differences among experimental groups were analysed by ANOVA followed by post-hoc Bonferroni analysis. *, $P<0.05$ ND vs. T2D; §, $P<0.05$ control vs. ND; and #, $P<0.05$ control vs. T2D

The extent to which all altered miRNAs influence the physiology of cardiomyocytes and SMCs has to be further investigated. It still is an immense challenge to link a distinct miRNA-expression pattern to the phenotype of diseases like T2D. Due to the capacity of miRNAs to alter hundreds of targets, the discovery of targets responsible for a pathological state is still exciting. In addition, one target can also be influenced by several miRNAs, which increase the complexity of miRNA-research. Today, several computational based approaches try to predict target sites of a distinct miRNA in mRNAs, but the probability of a false positive is quite high.[135] Otherwise, a more stringent prediction of each site could eliminate some biological targets without eliminating all false positives.[135] Other aspects in the context of target-prediction are the regulatory processes counteracting miRNA-directed regulation of potential targets. For instance, Sandberg and colleagues have reported an alternative cleavage and polyadenylation of target-mRNAs in proliferating cells, causing elimination of conserved miRNA-binding sites.[270] Even in one cell type, miRNA-mediated repression can be modulated by RNA-binding proteins. This has been shown by the stress-induced binding of a particular protein to a 3'UTR of a mRNA, which in turn increased the miR-122-directed repression.[271] In other cases, binding of a protein can block binding of a miRNA to its complementary sequence within its target-mRNA.[272] Altogether, predicting targets of a specific miRNA, which is altered in cells treated with CM, could be helpful but not sufficient to find novel miRNA-regulated proteins.

Usually, studies concerning miRNA-profiles also use microarray- or proteomic-based approaches to find altered targets between two distinct conditions. Comparison of altered miRNAs with altered protein levels can help to correlate one miRNA to the expression of one or several proteins. Using a proteomic-based approach, we are planning to analyse alterations of protein expression in RASMC treated with CM-PVAT-T2D compared to CM-PVAT-ND to find potential novel targets for the deregulated miRNAs shown in Figure 5.1.

5.2.2. The miR-143/145 cluster and its role in cardiovascular disease

Both miRNAs, miR-143 and miR-145, have been up-regulated in cardiomyocytes due to EAT-derived factors from patients with T2D (chapter 3). Here, activin A plays a pivotal role. Besides cardiomyocytes, we have shown that adipocyte-derived CM also induces the expression of miR-143 and miR-145 in human vascular smooth muscle cells (hVSMC) (chapter 4). In both cell types miR-143 impairs insulin action as illustrated by reduced insulin-stimulated Akt phosphorylation.

Both miRNAs are present in nearly every murine and human tissue with the strongest expression in cervix, uterus, colon, prostate and stomach of humans, while they are also detected in heart, muscle and adipose tissue of humans and mice.[163, 273-276] Expression profiles of miRNAs have been used for classification, diagnosis and progression of malignancies and hence several distinct and so-called onco-miRNAs, involved in tumor initiation and progression, have been identified. Thus, miR-143 and miR-145 have been found to be down-regulated in many cancers or cancer cells lines like colon and gastric cancers, chronic lymphocytic leukemias, B cell lymphomas as well as bladder, cervical, colorectal and prostate cancers and are therefore considered as tumorsupressors.[277-284] Functional analysis has highlighted target genes *ERK5* and *KRAS* for miR-143 and *IRS-1* and *c-myc* for miR-145, which all play a role in tumorgenesis.[285-288] In humans and mice, genomic localizations of the highly conserved miRNAs are very close to each other, which leads to the assumption that they have a common pri-miRNA. Indeed, the mature miRNAs are processed by the same 11-kb long non-coding RNA, suggesting that miR-143 and miR-145 are transcribed as a bicistronic unit with common regulatory elements. Accordingly, they are also referred to as the miR-143/145 cluster.[274, 289] Even though the expression is under control of the same regulatory elements, some studies have reported that there is a slight difference in their expression levels, which is potentially due to different rates of posttranscriptional processing by Dicer or Drosha. In line with this, expression levels of miR-145 seem to be higher than those of miR-143 in cardiomyocytes (chapter 3) and smooth muscle cells (chapter 4), respectively.

Nevertheless, work from Cordes and colleagues has also uncovered the well-controlled expression of both miRNAs by a cardiac specific enhancer during cardiogenesis. This enhancer leads to an increased and robust expression of the reporter gene LacZ in the endo- and myocardium during embryogenesis, whereas it is notably absent in the aorta and the pulmonary arteries. Postnatally, the pattern is reversed with high expression levels in SMCs of the aorta or coronary arteries and low expression levels in ventricular myocardium. The identified enhancer includes binding sites for the transcription factors serum response factor (SRF) and Nkx2-5. Moreover, it could be shown *in vivo*, that SRF-binding sites are important for miRNA expression in SMC and that mutation of Nkx2-5 binding sites diminish activity of the enhancer within the heart.[289] The observation that SRF in combination with myocardin can induce miR-143/145 expression has been extended by Long and colleagues. They have reported a TGF-β1-dependent activation of p38 for human coronary artery SMCs, which in turn leads to an induction of SRF and myocardin. Moreover, they have identified SMAD-

binding elements within the upstream region of the miR-143/145 gene and they have proven TGF-β1 to induce expression of miR-143/145 via the p38/SRF-pathway and via a SMAD-dependent pathway.[214] With regard to cardiomyocytes, we have extended this observation in chapter 3 where pharmacological inhibition of p38 prevented induction of both miR-143 and miR-145. However, so far we cannot exclude that activin A-dependent activation of SMAD-signaling influences miRNA expression as well. With regard to SMC, we have also demonstrated that adipocyte-derived factors activate p38 and SMAD2 and that at least p38 was crucial for induction of the miR-143/145 cluster. The extent to which CM-EAT-T2D or activin A in cardiomyocytes or adipocyte-derived factors in SMC induce expression of SRF and/or myocardin still has to be examined. In addition, it remains to be investigated whether CM-EAT-T2D-induced expression of miR-143/145 involves Nkx2-5.

In T2D, a reduced IRS-1 abundance is often associated with the progression of insulin resistance.[290] Moreover, it has been reported that both miR-143 and miR-145 influence the protein levels of IRS-1 and of insulin growth factor-receptor in cancer cells and hence inhibit growth factor-induced growth and proliferation.[291, 292] Even though we have observed a reduced insulin-stimulated Akt-phosphorylation in the atrial mouse cell line HL-1 transfected with precursors of miR-143, we did not see any alterations in the expression of either IRS-1 or the β-chain of the insulin receptor (chapter 3). This was also the case for cells transfected with precursor of miR-145 where we also see no difference in the expression and activation of key components of the insulin signaling cascade. These results indicate that both miRNAs do not alter IRS-1 protein expression in cardiomyocytes, which is further supported by results shown in Figure 5.2. Here, IRS-1 protein concentrations did not change in ARC exposed to CM-EAT-T2D.

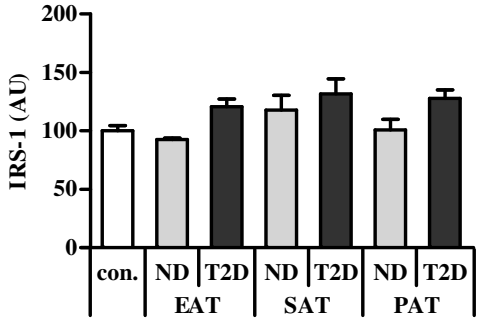

Figure 5.2: Effect of epicardial adipokines on the protein expression of IRS-1 in ARC. Primary adult rat cardiomyocytes (ARC) were exposed to control adipocyte medium (con.) or to conditioned media (CM, diluted 1:4) from epicardial adipose tissue (EAT), pericardial adipose tissue (PAT) and subcutaneous adipose tissue (SAT) from either patients with type 2 diabetes (T2D) or from patients without diabetes (ND) and IRS-1 protein expression was determined by Western Blot analysis. IRS-1 in ARC exposed to control medium was set at 100. Open bars, con.; gray bars, ND; black bars, T2D.

Importantly, miR-143 function is also related to adipose tissue biology. Comparative expression analysis has revealed higher levels of miR-143 in differentiated adipocytes compared to pre-adipocytes *in vivo* and *in vitro*.[253] Conversely, inhibition of miR-143 leads to a reduced expression of adipogenic genes and triglyceride accumulation, indicating a prominent role of miR-143 in adipocyte differentiation.[163] Intriguingly, miR-143 expression is reduced in adipose tissue from ob/ob mice compared to wild type mice.[253] In contrast, another study has reported that miR-143 is up-regulated in adipose tissue of mice fed a HFD compared to control conditions.[164] The participation of miR-143 in pathogenic growth of adipocytes in T2D has not been investigated so far, but it would be interesting to examine how impaired levels of miR-143 lead to hypertrophy and inflammation of adipose tissue in T2D.

Amongst cardiovascular cells, vascular (V)SMCs are uniquely plastic because they can oscillate between a differentiated and a more proliferative state, which is associated with changes in morphology and migration rates.[289, 293, 294] The transition of VSMC from the differentiated to the proliferative phenotype, a process known as phenotype switching, plays a critical role in the pathogenesis of cardiovascular diseases such as hypertension, vascular injury and atherosclerosis.[295] Many studies have described the involvement of miR-143/145 in directing the phenotype of VSMCs towards the differentiated and non-proliferative phenotype.[289, 296] In detail, miR-143 and miR-145 modulate actin remodeling, contractility of VSMCs, migration, proliferation, and differentiation.[293, 297] Accordingly, differentiation markers such as smooth muscle alpha actin, calponin and SM-myosin are increased in VSMC with higher expression levels of miR-143/145. These effects are stronger for miR-145 compared to miR-143.[289] Myocardin, as a co-factor for SFR, is a master regulator of smooth muscle phenotype due to up-regulation of miR-143/145 and it could be shown that miR-145 activity is required for myocardin-dependent conversion of fibroblasts to VSMCs.[289, 296] In addition, miR-143/145 knockout mice had arterial hypotension, reduced diastolic and systolic blood pressure as well as reduced cardiac and left ventricular mass.[294] However, during progression of atherosclerosis, miR-143 and miR-145 seem to be down-regulated, indicating that smooth muscle cells have lost their ability to maintain the contractile phenotype.

We have shown that both miR-143 and miR-145 are up-regulated in cardiomyocytes (chapter 3) and human vascular smooth muscle cells (chapter 4) in response to adipocyte-derived factors. Higher levels of miR-143 lead to reduced insulin signaling, which is further supported by a study from Jordan and colleagues.[166] Here, mice fed a high fat diet have higher levels of miR-143/145 in the liver which causes hepatic insulin resistance *in vivo*.[166] The fact

that miR-143 is important for glucose metabolism is further supported by its ability to regulate hexokinase-2 and hence inhibit glycolysis.[298]

5.2.3. Oxysterol binding protein-like 8 – a new modulator of insulin action and a target of miR-143

In chapters 3 and 4, we have described that protein levels of oxysterol binding protein-like 8 (ORP8) are posttranscriptionally regulated by miR-143 in the atrial mouse cell line HL-1, in adult rat cardiomyocytes and in human vascular smooth muscle cells. Furthermore, we have shown that ORP8 is involved in the insulin signaling cascade. However, the exact mechanism how ORP8 regulates insulin action is not known and remains to be clarified.

In humans, ORP8 belongs to a family of 12 proteins. This family consists of oxysterol binding protein (OSBP) and OSBP-related proteins (ORP), whose expression has recently been described throughout the eukaryotic kingdom.[299] Accordingly, mRNA expression of ORP8 in humans has been measured in several tissues like heart, kidney, lungs and liver with the highest mRNA expression in brain and testis.[299] The most abundant protein level of ORP8 in mice has been shown in liver, spleen, kidney and brain with lower expression in skeletal muscle, heart and adipose tissue.[166, 300] OSBP is a cytoplasmic protein with an affinity to several oxysterols, which acts as a sterol-dependent scaffold protein that regulates signal transduction pathways.[301] Moreover, it is responsible for trafficking ceramides from the endoplasmic reticulum (ER) to the golgi apparatus for sphingomyelin synthesis.[302]

All members of the OSBP-family have a carboxyterminal OSBP-related ligand binding domain (ORD) in common, which has been shown to bind oxysterol and cholesterol. Those members of the protein family, including ORP8, which contain a PH-domain interact with phosphatidylinositol phosphates (PIP) at the plasma membrane and are designated long(L)ORPs, whereas ORPs lacking a PH-domain are called short(S)ORPs. In general, all members are located at the ER, either with their phenyl-alanines in an acidic tract (FFAT)-motif associated with VAMP-associated proteins (VAP) within the membrane of the ER, or with their aminoterminal transmembrane domain, such as ORP8 and ORP5.[303] In most cases, ORPs are present in membrane contact sites (MCS) between the ER and other organelles, like endosomes, lysosomes, lipid droplets, golgi apparatus and particularly between the plasma membrane, where the PH-domain can bind PIPs. MCS are locations where a non-vesicle based exchange between lipids, other molecules or signals occurs.[304] For instance, in yeast it

could be shown that homologues proteins of ORPs, namely Osh proteins, can bind sterols and exchange them between liposomes.[305]

In line with the report from Jordan and colleagues, we have identified ORP8 as a modulator of insulin action as well as a target of miR-143 in rat cardiomyocytes (chapter 3) and human smooth muscle cells (chapter 4).[166] Based on our results, we suggest that ORP8 does not affect the expression levels of key components of the signaling cascade, such as the insulin receptor, Akt, IRS-1, PTEN or GLUT-4, but rather acts on the insulin-mediated phosphorylation cascade. Interestingly, Osh proteins have been found to be involved in phosphoinositide metabolism in yeast. Here, Osh proteins regulate the activity of the integral ER membrane protein and phosphatidylinositol phosphatase Sac1.[306] Within MCS, Sac1 is able to alter PIP levels in the plasma membrane although it is anchored in the ER.[307, 308] It could also be shown that at least the human ORP9S and ORP10 can bind several phosphoinositides and specifically PIP3, respectively. How ORP8 may influence PIP3-levels at the plasma membrane is unclear, but a regulatory influence on the insulin-stimulated increase of PIP3 could be a good explanation for the involvement of ORP8 in the insulin-mediated signal transduction cascade.

A second phosphatase anchored in the ER, the phospho tyrosine phosphatase 1B (PTP1B), has been suggested to bind signaling substrates at the plasma membrane, including the insulin receptor.[309, 310] Several studies have demonstrated that PTP1B-activity promotes the development of insulin resistance in T2D due to dephosphorylation-events of important signaling molecules like the insulin receptor.[311, 312] PTP1B carries out its function at MCS, where it may becomes accessible for ORPs. However, the extent to which a miR-143-mediated reduction of ORP8 protein levels leads to a higher activity of PTP1B and therefore to a diminished insulin-signaling has to be elucidated in the future.

ORP8 protein expression has also been observed in human coronary artery atherosclerotic lesions and mRNA levels of ORP8 have been shown to be elevated in advanced atherosclerotic lesions compared to a healthy artery wall. Moreover, co-localization analysis of ORP8 and the monocyte/macrophage-marker CD68 within the coronary artery wall indicates that ORP8-expression is more restricted to macrophages in advanced lesions compared to healthy parts of the artery wall. Therefore, the authors of this study have assumed that elevated levels of mRNA-expression of ORP8 in advanced lesions are limited to macrophages and not to smooth muscle or endothelial cells. Unfortunately, the authors did not assess the role of ORP8 in smooth muscle cells during the formation of advanced lesions, but they could demonstrate that decreased ORP8 expression leads to transcriptional activation of

the ATP binding cassette transporter A1 (ABCA1) and to higher cholesterol efflux of macrophages.[300] In chapter 4, we have shown that smooth muscle cells exposed to adipocyte-derived CM exhibit a reduced expression of ORP8, which resulted in a decreased insulin-stimulated Akt phosphorylation. However, Nagao and colleagues have linked a decreased PI3K/Akt-activation in smooth muscle cells to an altered expression of ABCA1 and cholesterol efflux indicating that miR-143-induced reduction of ORP8 may play a role in cholesterol efflux of hVSMC.[313]

5.2.4. EAT-derived factors up-regulate cardiac specific miR-208a

In chapter 3, we have described the miRNA-expression patterns of primary adult rat cardiomyocytes exposed to CM generated from epicardial, pericardial and subcutaneous adipose tissue either from patients with or without T2D. Among the altered miRNAs in cardiomyocytes exposed to CM-EAT-T2D, miR-208 is the most affected miRNA with a total increase of approximately 80% compared to control conditions. The results of chapter 3 and unpublished data also underline that miR-208 expression in rat cardiomyocytes is not driven by activin A or by p38. This indicates that a different pathway is involved in the regulation of this miRNA as compared to miR-143 and miR-145.

Recently, the expression of miR-208b has also been described in humans, mice and rats. At the time of establishing the expression profile of miRNAs within cardiomyocytes (chapter 3), miR-208b was not included in the commercially available and used primer library based on miRBase database. Today, the previously described miR-208, which has been measured in chapter 3, is also referred to as miR-208a.[314] Both miRNAs, miR-208a and miR-208b, exhibit almost identical sequences and therefore assemble the cardiac enriched miR-208 miRNA family, which is completed by miR-499 as a third member of this family. Expression of miR-208a is restricted to the adult heart and is encoded by an intron of the α-cardiac muscle myosin heavy chain gene *Myh6*, whereas miR-208b is expressed in the embryonic heart with predominant expression in skeletal muscle from an intron of the β-cardiac muscle myosin heavy chain gene *Myh7*.[315, 316] However, miR-499 exhibits a similar seed sequence but differs in the 3'region from miR-208a and miR-208b, is located within the not well studied myosin gene *Myh7b* and is expressed in adult heart as well as in skeletal muscle.[316]

The gene products of Myh6 and Myh7, α-MHC and β-MHC, respectively, are major contractile proteins of cardiomyocytes, with β-MHC containing a relatively slow adenosine triphosphatase (ATPase) and α-MHC a fast ATPase. Therefore, the isoforms differ primarily in their ability to convert ATP to mechanical work and thus affect contractility of the cardiac

sarcomeres due to their different expression ratios.[317, 318] In various forms of cardiac stress and cardiac hypertrophy as well as during diabetes, a shift from α-MHC to β-MHC occurs with consequent diminution of cardiac performance. Down-regulation of α-MHC and up-regulation of β-MHC are common features of cardiac injury regardless of the species.[65, 319-321] In chapter 2, we have reported a markedly impaired cardiac performance of adult rat cardiomyocytes exposed to CM-EAT-T2D for 30 minutes as characterized by reductions in departure velocity of contraction, peak sarcomere shortening and return velocity of contraction due to impaired Ca^{2+}-uptake and -release from the sarcoplasmic reticulum. Moreover, long time incubation of ARC with CM-EAT-T2D for 24h led to an increased level of Myh7-mRNA with simultaneously constant levels of Myh6-mRNA, indicating a change in expression ratios of the myosin isoforms (Figure 5.3). Since up-regulation of β-MHC is a marker of hypertrophy, heart failure and cardiac remodelling the findings shown in figure 5.3 further underline the detrimental effects of CM-EAT-T2D on the physiology of cardiomyocytes. Interestingly, miR-208a is thought to be a regulator of cardiac hypertrophy due to controlling the protein levels of α-MHC and β-MHC. Cardiomyocyte-specific overexpression of miR-208a in mice leads to significantly increased left ventricular mass, higher β-MHC protein concentrations, enlarged cardiomyocyte cell size and decreased fractional shortening. All of these promote the assumption that higher levels of miR-208a induce hypertrophic cardiac growth and cardiac dysfunction.[315] Accordingly, overexpression of miR-208a increases expression of Myh7-mRNA and decreases expression of Myh6-mRNA (Figure 5.4) in ARC, which further supports our hypothesis that secreted factors from EAT of T2D-patients induce cardiac remodelling by up-regulation of miR-208a. Moreover, increased levels of miR-208a have been associated with arrhythmia by regulating cardiac conduction and fibrosis, whereas a reduced level of miR-208a prevents pathological cardiac remodelling in mice. Hearts from miR-208 knockout mice seem to be resistant against stress-induced cardiac remodelling, and fibrosis without any changes of the β-MHC-concentrations.[314, 316, 322] Importantly, miR-208a is proposed to be a strong predictor of cardiac death and heart failure in humans.[323] In this study by Satoh and colleagues, a positive correlation between miR-208a and Myh7-mRNA and a negative correlation between miR-208a and Myh6-mRNA levels have been found in biopsies from patients with dilated cardiomyopathy.[323] Moreover, the authors have also described that miR-208a positively correlates with the increased collagen volume fraction and negatively correlates with left ventricular ejection fraction in patients suffering from dilated cardiomyopathy.[323] Interestingly, miR-208a tends to be higher in the circulation of subjects with acute CAD.[324]

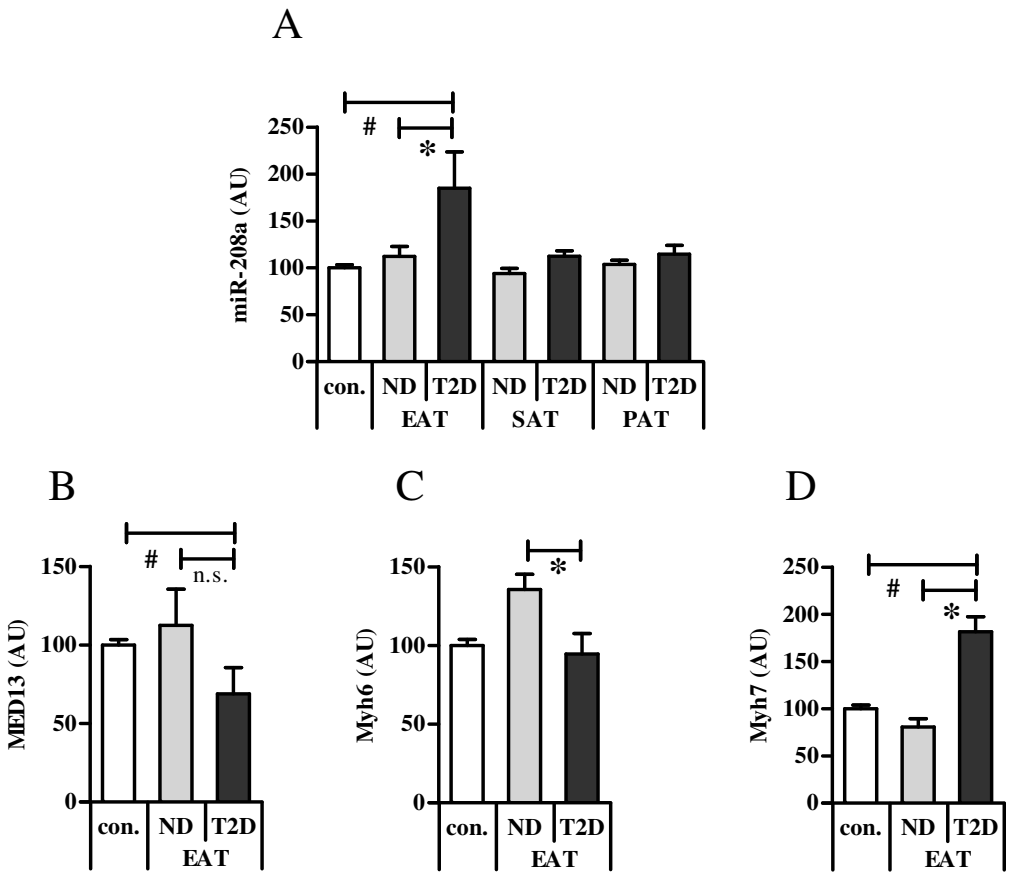

Figure 5.3: Effect of epicardial adipokines on the expression of miR-208a, MED13, Myh6 and Myh7. Primary adult rat cardiomyocytes (ARC) were exposed to control adipocyte medium (con.) or to conditioned media (CM, diluted 1:4) from epicardial adipose tissue (EAT), pericardial adipose tissue (PAT) and subcutaneous adipose tissue (SAT) either from patients with type 2 diabetes (T2D) or from patients without diabetes (ND). The (A) miR-208a or mRNA expression of (B) MED13, (C) Myh6, (D) Myh7 in ARC were measured by qRT-PCR and expression of ARC exposed to control medium was set at 100. Open bars, con.; gray bars, ND; black bars, T2D. Expression data of miRNA were collected during 7 independent experiments for CM from EAT and 4 independent experiments for CM from PAT and SAT using ARC preparations from different rats and CM from different donors. Expression data of mRNA were collected during 4 independent experiments. Expression levels are expressed as mean ± SEM. Differences among experimental groups were analyzed by ANOVA followed by post-hoc Bonferroni analysis. *, $P<0.05$ ND versus T2D and #, $P<0.05$ T2D versus control.

A confirmed target of miR-208a in mice is mediator complex subunit 13 (MED13) and we have also observed that mRNA expression of MED13 is significantly down-regulated in ARC exposed to CM-EAT-T2D compared to control conditions (Figure 5.3), and that overexpression of miR-208a in ARC leads to a slight but not yet significantly (p=0.05) decreased MED13 mRNA concentration (Figure 5.4). It is well known that miRNAs often decrease protein levels without any measurable changes in mRNA levels, therefore the

changes on MED13 expression levels in genetically modified ARC and cells exposed to CM further have to be confirmed on protein expression. Grueter and colleagues have reported that inhibition of miR-208a increases MED13 levels within the heart and transgenic overexpression of MED13 in the heart protects mice against high fed died (HFD)-induced obesity.[325] This study has reported that pharmacological inhibition of miR-208a with locked nucleic acid (LNA)-modified antisense oligonucleotides leads to a reduced HFD-induced weight gain, primarily due to significantly decreased amounts of visceral white adipose tissue, illustrated by reduced fat mass and adipocyte size. Moreover, serum triglycerides and cholesterol levels are reduced and the progression of hepatic steatosis is blunted in mice treated with LNA-miR-208a. However, cardiac-specific inhibition of miR-208a improves HFD-induced insulin resistance as illustrated by improved glucose tolerance and reduced fasting insulin levels. The authors of this study could also demonstrate that cardiac overexpression of the miR-208a-target, MED13, displays similar results compared to mice treated with LNA-miR-208a. Notably, mice with higher levels of MED13 protein within their heart seem to be resistant against HFD-induced weight gain, although there was no difference in food consumption or physical activity compared to wild type mice. MED13 is a component and negative regulator of the Mediator complex, a modulator of gene transcription. There are reports indicating MED13 as a transcriptional regulator of genes involved in metabolic pathways.[325] Interestingly, application of LNA-miR-208a not only improves metabolic parameters, but also protects rats against hypertension-induced heart failure. In particular, inhibition of cardiac miR-208a prevents pathological myosin switching and remodelling while improving cardiac function.[326]

In chapter 2, we have reported that elevated secretion of activin A and angiopoietin-2 from EAT-T2D is responsible for the reduced cardiac performance described in chapter 2, but we have also demonstrated that activin A does not influence the expression of miR-208. So far, little is known about the transcriptional regulation of miR-208a but we have demonstrated here for the first time that secreted factors from adipose tissue increase the expression of miR-208a within cardiomyocytes. This may cause cardiac remodelling, hypertrophy and pathological metabolic changes as well as systemic alterations, such as a disturbed glucose tolerance, insulin sensitivity and fat mass expansion.

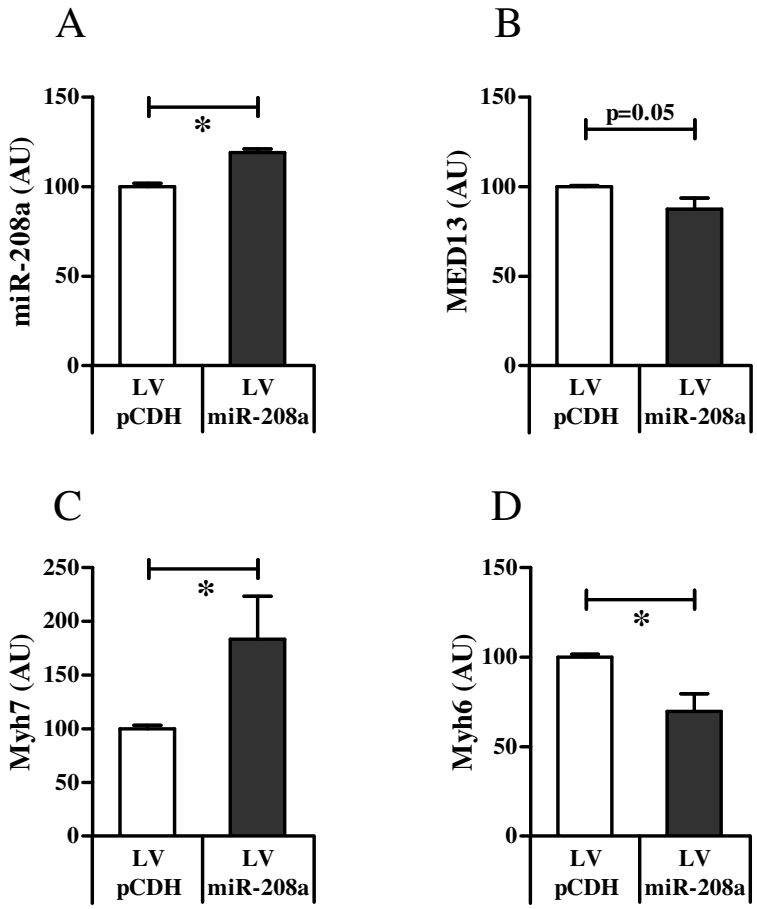

Figure 5.4: Overexpression of miR-208a in adult rat cardiomyocytes. Primary adult rat cardiomyocytes (ARC) were infected with lentivirus particles including a construct for the expression of miR-208a (LV miR-208a) or empty vector (LV pCDH) with a MOI of 2. The (A) miR-208a or mRNA expression of (B) MED13, (C) Myh6, or (D) Myh7 was measured by qRT-PCR and expression in ARC infected with LV pCDH was set at 100. Open bars, LV pCDH.; black bars, LV miR-208a. Data were collected during 4 independent experiments. Expression levels are expressed as mean ± SEM. Differences among experimental groups were analyzed by student's t-test. *, $P<0.05$ LV pCDH versus LV miR-208a.

5.3. Conclusions and Perspectives

In patients with T2D, adipose tissue is characterized by a chronic state of low grade inflammation, which is causally linked with an altered secretion of adipokines. In this context, increased visceral adipose tissue is associated with progression of T2D and insulin resistance of peripheral tissues. Moreover, insulin resistance is an independent risk factor for the development of cardiovascular diseases such as diabetic cardiomyopathy or atherosclerosis.

The present work reports the contribution of released factors from adipose tissue or from adipocytes to myocardial dysfunction and to alterations in the homeostasis of smooth muscle cells, which are involved in initial events of atherosclerosis. Altogether, the reported results support the assumption that factors secreted from adipose tissue or adipocytes have detrimental effects on cardiomyocytes and on smooth muscle cells, hence underlining the causal link between inflamed adipose tissue in T2D and progression of cardiovascular diseases. Specifically, we have shown that heart-specific visceral adipose tissue, the epicardial adipose tissue (EAT), from patients with T2D secretes a different subset of proteins compared to other fat depots. We have also demonstrated that EAT-T2D has a higher rate of macrophage infiltration, indicating a pro-inflammatory milieu within EAT of patients suffering from T2D. Nevertheless, the exact underlying reasons why EAT becomes inflamed during diabetes and why EAT-T2D is characterized by a different secretome compared to EAT-ND has to be elucidated in the future. However, due to the limited capacity of the antibody arrays used to analyse CM-EAT, we suggest further, not yet identified, adipokines released from EAT. This is supported by the results of activin A and angiopoietin-2. Both proteins were able to mimic some but not all effects of CM-EAT-T2D, indicating other proteins to be involved in the cross talk between EAT and cardiomyocytes. The present work demonstrates that exposing cardiomyocytes to CM-EAT-T2D leads to contractile dysfunction and insulin resistance. These effects could be ascribed to selective accumulation of activin A and angiopoietin-2 in the CM. Collectively, these data show that inflammation of EAT-T2D is associated with alterations in adipokine secretion, which may contribute to the pathogenesis of type 2 diabetes–related heart diseases. Moreover, EAT-derived factors from patients with T2D induce an altered and unique miRNA expression signature in cardiomyocytes characterized by eight deregulated miRNAs, including the miR-143/145 cluster and heart specific miR-208a. This is in line with previous reports where a specific miRNA expression signature could be associated with distinct states of disease progression such as cardiovascular diseases and diabetes. In particular, the CM-promoted expression of miR-143/145 could be

assigned to the release of activin A by EAT. Investigations regarding the functional consequences of up-regulated miR-143 in cardiomyocytes have illustrated its contribution to the progression of insulin resistance by reducing the novel modulator of insulin action, ORP8. The reduced ability of insulin to mediate glucose uptake within cardiomyocytes is a major hallmark of diabetic cardiomyopathy and represents an indicator for the metabolic inflexibility in the heart of patients with T2D. In order to extend and strengthen the *in vitro* experiments presented in this work, expression of miR-143 should also be measured in heart biopsies from patients with T2D. This may raise the potential of miR-143 as a pharmaceutical target to prevent insulin resistance of the human diabetic heart.

Furthermore, incubation of human vascular smooth muscle cells (hVSMC) with adipocyte-derived factors from human subcutaneous adipose tissue also increases expression of miR-143/145, which is paralleled by a significant reduction of insulin-mediated phosphorylation of Akt and its target eNOS, thus contributing to the progression of atherosclerosis. Since we have used human SMC, we could extend our own observation that miR-143 abrogates insulin action in rat cardiomyocytes *in vitro* as well as previous reports showing that miR-143 induces hepatic insulin resistance in mice. It is worthwhile to investigate the contribution of miR-143 to insulin resistance in other tissues like the skeletal muscle as a primary organ responsible for glucose clearance.

In addition, miR-208a is up-regulated, amongst others, in cardiomyocytes by epicardial adipokines and represents a promising candidate for further investigations. This cardiac-specific miRNA is associated with hypertrophy, cardiac remodeling and metabolic changes, similar to symptoms of patients suffering from diabetic-related heart failure. In particular, involvement of miR-208a expression in lipid metabolism by influencing expression of MED13 in cardiomyocytes should be analysed in detail. In this context, further key experiments have to investigate CM-mediated alterations in parameters of lipid metabolism such as uptake and oxidation of fatty acids and whether these effects can be ascribed to miR-208a expression in cardiomyocytes.

Collectively, the present work provides new insights into the potential contribution of adipose tissue from patients suffering from type 2 diabetes to the pathogenesis of cardiovascular complications. Specifically, the relevance of epicardial adipokines and miRNAs for the progression of contractile dysfunction and cardiac insulin resistance is emphasized. Furthermore, the importance of miR-143 for insulin action in cardiomyocytes and smooth muscle cells is highlighted.

Bibliography

[1] Leonid Poretsky (2009) Principles of diabetes mellitus. 2 edn. Springer,

[2] American Diabetes Association (2004) Diagnosis and classification of diabetes mellitus. Diabetes Care 27 Suppl 1: S5-S10

[3] Schneider S, Bock C, Wetzel M, Maul H, Loerbroks A (2012) The prevalence of gestational diabetes in advanced economies. J.Perinat.Med. 40: 511-520

[4] Akerblom HK, Vaarala O, Hyoty H, Ilonen J, Knip M (2002) Environmental factors in the etiology of type 1 diabetes. Am.J.Med.Genet. 115: 18-29

[5] Bluestone JA, Herold K, Eisenbarth G (2010) Genetics, pathogenesis and clinical interventions in type 1 diabetes. Nature 464: 1293-1300

[6] DiLorenzo TP, Serreze DV (2005) The good turned ugly: immunopathogenic basis for diabetogenic CD8+ T cells in NOD mice. Immunol.Rev. 204: 250-263

[7] Serreze DV, Fleming SA, Chapman HD, Richard SD, Leiter EH, Tisch RM (1998) B lymphocytes are critical antigen-presenting cells for the initiation of T cell-mediated autoimmune diabetes in nonobese diabetic mice. J.Immunol. 161: 3912-3918

[8] Zipris D, Lien E, Nair A, et al (2007) TLR9-signaling pathways are involved in Kilham rat virus-induced autoimmune diabetes in the biobreeding diabetes-resistant rat. J.Immunol. 178: 693-701

[9] Mehers KL, Gillespie KM (2008) The genetic basis for type 1 diabetes. Br.Med.Bull. 88: 115-129

[10] Zimmet P, Alberti KG, Shaw J (2001) Global and societal implications of the diabetes epidemic. Nature 414: 782-787

[11] Tripathy D, Chavez AO (2010) Defects in insulin secretion and action in the pathogenesis of type 2 diabetes mellitus. Curr.Diab.Rep. 10: 184-191

[12] American Diabetes Association (2010) Diagnosis and classification of diabetes mellitus. Diabetes Care 33: 62-69

[13] Zimmet P, Magliano D, Matsuzawa Y, Alberti G, Shaw J (2005) The metabolic syndrome: a global public health problem and a new definition. J.Atheroscler.Thromb. 12: 295-300

[14] Alberti KG, Zimmet P, Shaw J (2005) The metabolic syndrome--a new worldwide definition. Lancet 366: 1059-1062

[15] Leroith D (2012) Pathophysiology of the metabolic syndrome: implications for the cardiometabolic risks associated with type 2 diabetes. Am.J.Med.Sci. 343: 13-16

[16] Duvnjak L, Duvnjak M (2009) The metabolic syndrome - an ongoing story. J.Physiol Pharmacol. 60 Suppl 7: 19-24

[17] Alberti KG, Eckel RH, Grundy SM, et al (2009) Harmonizing the metabolic syndrome: a joint interim statement of the International Diabetes Federation Task Force on Epidemiology and Prevention; National Heart, Lung, and Blood Institute; American Heart Association; World Heart Federation; International Atherosclerosis Society; and International Association for the Study of Obesity. Circulation 120: 1640-1645

[18] Klein S, Sheard NF, Pi-Sunyer X, et al (2004) Weight management through lifestyle modification for the prevention and management of type 2 diabetes: rationale and strategies: a statement of the American Diabetes Association, the North American Association for the Study of Obesity, and the American Society for Clinical Nutrition. Diabetes Care 27: 2067-2073

[19] Mokdad AH, Ford ES, Bowman BA, et al (2003) Prevalence of obesity, diabetes, and obesity-related health risk factors, 2001. JAMA 289: 76-79

[20] Field AE, Coakley EH, Must A, et al (2001) Impact of overweight on the risk of developing common chronic diseases during a 10-year period. Arch.Intern.Med. 161: 1581-1586

[21] Carey VJ, Walters EE, Colditz GA, et al (1997) Body fat distribution and risk of non-insulin-dependent diabetes mellitus in women. The Nurses' Health Study. Am.J.Epidemiol. 145: 614-619

[22] Bray GA, Clearfield MB, Fintel DJ, Nelinson DS (2009) Overweight and obesity: the pathogenesis of cardiometabolic risk. Clin.Cornerstone. 9: 30-40

[23] Rexrode KM, Carey VJ, Hennekens CH, et al (1998) Abdominal adiposity and coronary heart disease in women. JAMA 280: 1843-1848

[24] Despres JP, Lemieux I, Bergeron J, et al (2008) Abdominal obesity and the metabolic syndrome: contribution to global cardiometabolic risk. Arterioscler.Thromb.Vasc.Biol. 28: 1039-1049

[25] Zeyda M, Stulnig TM (2009) Obesity, inflammation, and insulin resistance--a mini-review. Gerontology 55: 379-386

[26] Lehr S, Hartwig S, Lamers D, et al (2012) Identification and validation of novel adipokines released from primary human adipocytes. Mol.Cell Proteomics. 11: M111

[27] Scherer PE (2006) Adipose tissue: from lipid storage compartment to endocrine organ. Diabetes 55: 1537-1545

[28] Kershaw EE, Flier JS (2004) Adipose tissue as an endocrine organ. J.Clin.Endocrinol.Metab 89: 2548-2556

[29] Breitling R (2009) Robust signaling networks of the adipose secretome. Trends Endocrinol.Metab 20: 1-7

[30] Sell H, Eckel J (2009) Chemotactic cytokines, obesity and type 2 diabetes: in vivo and in vitro evidence for a possible causal correlation? Proc.Nutr.Soc. 68: 378-384

[31] Tchkonia T, Lenburg M, Thomou T, et al (2007) Identification of depot-specific human fat cell progenitors through distinct expression profiles and developmental gene patterns. Am.J.Physiol Endocrinol.Metab 292: E298-E307

[32] Dusserre E, Moulin P, Vidal H (2000) Differences in mRNA expression of the proteins secreted by the adipocytes in human subcutaneous and visceral adipose tissues. Biochim.Biophys.Acta 1500: 88-96

[33] Cinti S, Mitchell G, Barbatelli G, et al (2005) Adipocyte death defines macrophage localization and function in adipose tissue of obese mice and humans. J.Lipid Res. 46: 2347-2355

[34] Coppack SW (2005) Adipose tissue changes in obesity. Biochem.Soc.Trans. 33: 1049-1052

[35] Sell H, Laurencikiene J, Taube A, et al (2009) Chemerin is a novel adipocyte-derived factor inducing insulin resistance in primary human skeletal muscle cells. Diabetes 58: 2731-2740

[36] Sell H, Divoux A, Poitou C, et al (2010) Chemerin correlates with markers for fatty liver in morbidly obese patients and strongly decreases after weight loss induced by bariatric surgery. J.Clin.Endocrinol.Metab 95: 2892-2896

[37] Sacks HS, Fain JN (2007) Human epicardial adipose tissue: a review. Am.Heart J. 153: 907-917

[38] Rabkin SW (2007) Epicardial fat: properties, function and relationship to obesity. Obes.Rev. 8: 253-261

[39] Iacobellis G, Willens HJ (2009) Echocardiographic epicardial fat: a review of research and clinical applications. J.Am.Soc.Echocardiogr. 22: 1311-1319

[40] Katsiki N, Mikhailidis DP, Wierzbicki AS (2013) Epicardial fat and vascular risk: a narrative review. Curr.Opin.Cardiol. 28: 458-463

[41] Cikim AS, Topal E, Harputluoglu M, et al (2007) Epicardial adipose tissue, hepatic steatosis and obesity. J.Endocrinol.Invest 30: 459-464

[42] Kankaanpaa M, Lehto HR, Parkka JP, et al (2006) Myocardial triglyceride content and epicardial fat mass in human obesity: relationship to left ventricular function and serum free fatty acid levels. J.Clin.Endocrinol.Metab 91: 4689-4695

[43] Iacobellis G, Corradi D, Sharma AM (2005) Epicardial adipose tissue: anatomic, biomolecular and clinical relationships with the heart. Nat.Clin.Pract.Cardiovasc.Med. 2: 536-543

[44] Ouwens DM, Sell H, Greulich S, Eckel J (2010) The role of epicardial and perivascular adipose tissue in the pathophysiology of cardiovascular disease. J.Cell Mol.Med 14: 2223-2234

[45] Ernande L, Derumeaux G (2012) Diabetic cardiomyopathy: myth or reality? Arch.Cardiovasc.Dis. 105: 218-225

[46] Rubler S, Dlugash J, Yuceoglu YZ, Kumral T, Branwood AW, Grishman A (1972) New type of cardiomyopathy associated with diabetic glomerulosclerosis. Am.J.Cardiol. 30: 595-602

[47] Kannel WB, Hjortland M, Castelli WP (1974) Role of diabetes in congestive heart failure: the Framingham study. Am.J.Cardiol. 34: 29-34

[48] Gottdiener JS, Arnold AM, Aurigemma GP, et al (2000) Predictors of congestive heart failure in the elderly: the Cardiovascular Health Study. J.Am.Coll.Cardiol. 35: 1628-1637

[49] Boudina S, Abel ED (2010) Diabetic cardiomyopathy, causes and effects. Rev.Endocr.Metab Disord. 11: 31-39

[50] Devereux RB, Roman MJ, Paranicas M, et al (2000) Impact of diabetes on cardiac structure and function: the strong heart study. Circulation 101: 2271-2276

[51] Xu FP, Chen MS, Wang YZ, et al (2004) Leptin induces hypertrophy via endothelin-1-reactive oxygen species pathway in cultured neonatal rat cardiomyocytes. Circulation 110: 1269-1275

[52] Kim M, Oh JK, Sakata S, et al (2008) Role of resistin in cardiac contractility and hypertrophy. J.Mol.Cell Cardiol. 45: 270-280

[53] Cook SA, Varela-Carver A, Mongillo M, et al (2010) Abnormal myocardial insulin signalling in type 2 diabetes and left-ventricular dysfunction. Eur.Heart J. 31: 100-111

[54] Karason K, Sjostrom L, Wallentin I, Peltonen M (2003) Impact of blood pressure and insulin on the relationship between body fat and left ventricular structure. Eur.Heart J. 24: 1500-1505

[55] Belke DD, Betuing S, Tuttle MJ, et al (2002) Insulin signaling coordinately regulates cardiac size, metabolism, and contractile protein isoform expression. J.Clin.Invest 109: 629-639

[56] Shimizu M, Umeda K, Sugihara N, et al (1993) Collagen remodelling in myocardia of patients with diabetes. J.Clin.Pathol. 46: 32-36

[57] McQueen AP, Zhang D, Hu P, et al (2005) Contractile dysfunction in hypertrophied hearts with deficient insulin receptor signaling: possible role of reduced capillary density. J.Mol.Cell Cardiol. 39: 882-892

[58] Brooks BA, Franjic B, Ban CR, et al (2008) Diastolic dysfunction and abnormalities of the microcirculation in type 2 diabetes. Diabetes Obes.Metab 10: 739-746

[59] Shivalkar B, Dhondt D, Goovaerts I, et al (2006) Flow mediated dilatation and cardiac function in type 1 diabetes mellitus. Am.J.Cardiol. 97: 77-82

[60] Semeniuk LM, Kryski AJ, Severson DL (2002) Echocardiographic assessment of cardiac function in diabetic db/db and transgenic db/db-hGLUT4 mice. Am.J.Physiol Heart Circ.Physiol 283: H976-H982

[61] Van den Bergh A, Vanderper A, Vangheluwe P, et al (2008) Dyslipidaemia in type II diabetic mice does not aggravate contractile impairment but increases ventricular stiffness. Cardiovasc.Res. 77: 371-379

[62] Dong F, Zhang X, Yang X, et al (2006) Impaired cardiac contractile function in ventricular myocytes from leptin-deficient ob/ob obese mice. J.Endocrinol. 188: 25-36

[63] Stolen TO, Hoydal MA, Kemi OJ, et al (2009) Interval training normalizes cardiomyocyte function, diastolic Ca2+ control, and SR Ca2+ release synchronicity in a mouse model of diabetic cardiomyopathy. Circ.Res. 105: 527-536

[64] Haghighi K, Gregory KN, Kranias EG (2004) Sarcoplasmic reticulum Ca-ATPase-phospholamban interactions and dilated cardiomyopathy. Biochem.Biophys.Res.Commun. 322: 1214-1222

[65] Dhalla NS, Liu X, Panagia V, Takeda N (1998) Subcellular remodeling and heart dysfunction in chronic diabetes. Cardiovasc.Res. 40: 239-247

[66] Taniguchi CM, Emanuelli B, Kahn CR (2006) Critical nodes in signalling pathways: insights into insulin action. Nat.Rev.Mol.Cell Biol. 7: 85-96

[67] Fang ZY, Prins JB, Marwick TH (2004) Diabetic cardiomyopathy: evidence, mechanisms, and therapeutic implications. Endocr.Rev. 25: 543-567

[68] Bertrand L, Horman S, Beauloye C, Vanoverschelde JL (2008) Insulin signalling in the heart. Cardiovasc.Res. 79: 238-248

[69] Young ME, McNulty P, Taegtmeyer H (2002) Adaptation and maladaptation of the heart in diabetes: Part II: potential mechanisms. Circulation 105: 1861-1870

[70] Fraze E, Donner CC, Swislocki AL, Chiou YA, Chen YD, Reaven GM (1985) Ambient plasma free fatty acid concentrations in noninsulin-dependent diabetes mellitus: evidence for insulin resistance. J.Clin.Endocrinol.Metab 61: 807-811

[71] Lopaschuk GD (2002) Metabolic abnormalities in the diabetic heart. Heart Fail.Rev. 7: 149-159

[72] RANDLE PJ, GARLAND PB, HALES CN, NEWSHOLME EA (1963) The glucose fatty-acid cycle. Its role in insulin sensitivity and the metabolic disturbances of diabetes mellitus. Lancet 1: 785-789

[73] Ramalingam L, Oh E, Thurmond DC (2012) Novel roles for insulin receptor (IR) in adipocytes and skeletal muscle cells via new and unexpected substrates. Cell Mol.Life Sci.

[74] White MF, Shoelson SE, Keutmann H, Kahn CR (1988) A cascade of tyrosine autophosphorylation in the beta-subunit activates the phosphotransferase of the insulin receptor. J.Biol.Chem. 263: 2969-2980

[75] Nystrom FH, Quon MJ (1999) Insulin signalling: metabolic pathways and mechanisms for specificity. Cell Signal. 11: 563-574

[76] Muniyappa R, Montagnani M, Koh KK, Quon MJ (2007) Cardiovascular actions of insulin. Endocr.Rev. 28: 463-491

[77] Ouwens DM, Diamant M (2007) Myocardial insulin action and the contribution of insulin resistance to the pathogenesis of diabetic cardiomyopathy. Arch Physiol Biochem. 113: 76-86

[78] Cantley LC (2002) The phosphoinositide 3-kinase pathway. Science 296: 1655-1657

[79] Leevers SJ, Vanhaesebroeck B, Waterfield MD (1999) Signalling through phosphoinositide 3-kinases: the lipids take centre stage. Curr.Opin.Cell Biol. 11: 219-225

[80] Songyang Z, Shoelson SE, Chaudhuri M, et al (1993) SH2 domains recognize specific phosphopeptide sequences. Cell 72: 767-778

[81] Sarbassov DD, Guertin DA, Ali SM, Sabatini DM (2005) Phosphorylation and regulation of Akt/PKB by the rictor-mTOR complex. Science 307: 1098-1101

[82] Tschopp O, Yang ZZ, Brodbeck D, et al (2005) Essential role of protein kinase B gamma (PKB gamma/Akt3) in postnatal brain development but not in glucose homeostasis. Development 132: 2943-2954

[83] Cho H, Thorvaldsen JL, Chu Q, Feng F, Birnbaum MJ (2001) Akt1/PKBalpha is required for normal growth but dispensable for maintenance of glucose homeostasis in mice. J.Biol.Chem. 276: 38349-38352

[84] Cho H, Thorvaldsen JL, Chu Q, Feng F, Birnbaum MJ (2001) Akt1/PKBalpha is required for normal growth but dispensable for maintenance of glucose homeostasis in mice. J.Biol.Chem. 276: 38349-38352

[85] Chaanine AH, Hajjar RJ (2011) AKT signalling in the failing heart. Eur.J.Heart Fail. 13: 825-829

[86] DeBosch B, Treskov I, Lupu TS, et al (2006) Akt1 is required for physiological cardiac growth. Circulation 113: 2097-2104

[87] Cho H, Mu J, Kim JK, et al (2001) Insulin resistance and a diabetes mellitus-like syndrome in mice lacking the protein kinase Akt2 (PKB beta). Science 292: 1728-1731

[88] Frame S, Cohen P (2001) GSK3 takes centre stage more than 20 years after its discovery. Biochem.J. 359: 1-16

[89] Egert S, Nguyen N, Brosius FC, III, Schwaiger M (1997) Effects of wortmannin on insulin- and ischemia-induced stimulation of GLUT4 translocation and FDG uptake in perfused rat hearts. Cardiovasc.Res. 35: 283-293

[90] Kessler A, Tomas E, Immler D, Meyer HE, Zorzano A, Eckel J (2000) Rab11 is associated with GLUT4-containing vesicles and redistributes in response to insulin. Diabetologia 43: 1518-1527

[91] Miinea CP, Sano H, Kane S, et al (2005) AS160, the Akt substrate regulating GLUT4 translocation, has a functional Rab GTPase-activating protein domain. Biochem.J. 391: 87-93

[92] Uphues I, Kolter T, Goud B, Eckel J (1994) Insulin-induced translocation of the glucose transporter GLUT4 in cardiac muscle: studies on the role of small-molecular-mass GTP-binding proteins. Biochem.J. 301 (Pt 1): 177-182

[93] Kane S, Sano H, Liu SC, et al (2002) A method to identify serine kinase substrates. Akt phosphorylates a novel adipocyte protein with a Rab GTPase-activating protein (GAP) domain. J.Biol.Chem. 277: 22115-22118

[94] Eguez L, Lee A, Chavez JA, et al (2005) Full intracellular retention of GLUT4 requires AS160 Rab GTPase activating protein. Cell Metab 2: 263-272

[95] Larance M, Ramm G, Stockli J, et al (2005) Characterization of the role of the Rab GTPase-activating protein AS160 in insulin-regulated GLUT4 trafficking. J.Biol.Chem. 280: 37803-37813

[96] Stone S, Abkevich V, Russell DL, et al (2006) TBC1D1 is a candidate for a severe obesity gene and evidence for a gene/gene interaction in obesity predisposition. Hum.Mol.Genet. 15: 2709-2720

[97] Chadt A, Leicht K, Deshmukh A, et al (2008) Tbc1d1 mutation in lean mouse strain confers leanness and protects from diet-induced obesity. Nat.Genet. 40: 1354-1359

[98] Dokas J, Chadt A, Nolden T, et al (2013) Conventional knockout of Tbc1d1 in mice impairs insulin- and AICAR-stimulated glucose uptake in skeletal muscle. Endocrinology

[99] Pozuelo RM, Peggie M, Wong BH, Morrice N, MacKintosh C (2003) 14-3-3s regulate fructose-2,6-bisphosphate levels by binding to PKB-phosphorylated cardiac fructose-2,6-bisphosphate kinase/phosphatase. EMBO J. 22: 3514-3523

[100] Luiken JJ, Koonen DP, Willems J, et al (2002) Insulin stimulates long-chain fatty acid utilization by rat cardiac myocytes through cellular redistribution of FAT/CD36. Diabetes 51: 3113-3119

[101] Coort SL, Hasselbaink DM, Koonen DP, et al (2004) Enhanced sarcolemmal FAT/CD36 content and triacylglycerol storage in cardiac myocytes from obese zucker rats. Diabetes 53: 1655-1663

[102] Christoffersen C, Bollano E, Lindegaard ML, et al (2003) Cardiac lipid accumulation associated with diastolic dysfunction in obese mice. Endocrinology 144: 3483-3490

[103] Horio T, Suzuki M, Takamisawa I, et al (2005) Pioglitazone-induced insulin sensitization improves vascular endothelial function in nondiabetic patients with essential hypertension. Am.J.Hypertens. 18: 1626-1630

[104] Ouwens DM, Boer C, Fodor M, et al (2005) Cardiac dysfunction induced by high-fat diet is associated with altered myocardial insulin signalling in rats. Diabetologia 48: 1229-1237

[105] Go AS, Mozaffarian D, Roger VL, et al (2013) Heart disease and stroke statistics--2013 update: a report from the American Heart Association. Circulation 127: e6-e245

[106] Kenchaiah S, Evans JC, Levy D, et al (2002) Obesity and the risk of heart failure. N.Engl.J.Med. 347: 305-313

[107] Lakka HM, Lakka TA, Tuomilehto J, Salonen JT (2002) Abdominal obesity is associated with increased risk of acute coronary events in men. Eur.Heart J. 23: 706-713

[108] Ross R (1999) Atherosclerosis--an inflammatory disease. N.Engl.J.Med. 340: 115-126

[109] Hansson GK, Robertson AK, Soderberg-Naucler C (2006) Inflammation and atherosclerosis. Annu.Rev.Pathol. 1: 297-329

[110] Glass CK, Witztum JL (2001) Atherosclerosis. the road ahead. Cell 104: 503-516

[111] Skalen K, Gustafsson M, Rydberg EK, et al (2002) Subendothelial retention of atherogenic lipoproteins in early atherosclerosis. Nature 417: 750-754

[112] Kume N, Cybulsky MI, Gimbrone MA, Jr. (1992) Lysophosphatidylcholine, a component of atherogenic lipoproteins, induces mononuclear leukocyte adhesion molecules in cultured human and rabbit arterial endothelial cells. J.Clin.Invest 90: 1138-1144

[113] Witztum JL, Steinberg D (1991) Role of oxidized low density lipoprotein in atherogenesis. J.Clin.Invest 88: 1785-1792

[114] Libby P (2002) Inflammation in atherosclerosis. Nature 420: 868-874

[115] Galis ZS, Sukhova GK, Lark MW, Libby P (1994) Increased expression of matrix metalloproteinases and matrix degrading activity in vulnerable regions of human atherosclerotic plaques. J.Clin.Invest 94: 2493-2503

[116] Fleming I, Busse R (2003) Molecular mechanisms involved in the regulation of the endothelial nitric oxide synthase. Am.J.Physiol Regul.Integr.Comp Physiol 284: R1-12

[117] Fulton D, Gratton JP, McCabe TJ, et al (1999) Regulation of endothelium-derived nitric oxide production by the protein kinase Akt. Nature 399: 597-601

[118] Rudic RD, Shesely EG, Maeda N, Smithies O, Segal SS, Sessa WC (1998) Direct evidence for the importance of endothelium-derived nitric oxide in vascular remodeling. J.Clin.Invest 101: 731-736

[119] Murohara T, Asahara T, Silver M, et al (1998) Nitric oxide synthase modulates angiogenesis in response to tissue ischemia. J.Clin.Invest 101: 2567-2578

[120] Trovati M, Massucco P, Mattiello L, et al (1999) Human vascular smooth muscle cells express a constitutive nitric oxide synthase that insulin rapidly activates, thus increasing guanosine 3':5'-cyclic monophosphate and adenosine 3':5'-cyclic monophosphate concentrations. Diabetologia 42: 831-839

[121] Buchwalow IB, Podzuweit T, Bocker W, et al (2002) Vascular smooth muscle and nitric oxide synthase. FASEB J. 16: 500-508

[122] Kahn AM, Husid A, Allen JC, Seidel CL, Song T (1997) Insulin acutely inhibits cultured vascular smooth muscle cell contraction by a nitric oxide synthase-dependent pathway. Hypertension 30: 928-933

[123] Lee JH, Ragolia L (2006) AKT phosphorylation is essential for insulin-induced relaxation of rat vascular smooth muscle cells. Am.J.Physiol Cell Physiol 291: C1355-C1365

[124] Touyz RM, Tolloczko B, Schiffrin EL (1994) Insulin attenuates agonist-evoked calcium transients in vascular smooth muscle cells. Hypertension 23: I25-I28

[125] Kim YC, Zemel MB (1993) Insulin increases vascular smooth muscle recovery from intracellular calcium loads. Hypertension 22: 74-77

[126] Lee RC, Feinbaum RL, Ambros V (1993) The C. elegans heterochronic gene lin-4 encodes small RNAs with antisense complementarity to lin-14. Cell 75: 843-854

[127] Wightman B, Ha I, Ruvkun G (1993) Posttranscriptional regulation of the heterochronic gene lin-14 by lin-4 mediates temporal pattern formation in C. elegans. Cell 75: 855-862

[128] Bartel DP (2004) MicroRNAs: genomics, biogenesis, mechanism, and function. Cell 116: 281-297

[129] Reinhart BJ, Slack FJ, Basson M, et al (2000) The 21-nucleotide let-7 RNA regulates developmental timing in Caenorhabditis elegans. Nature 403: 901-906

[130] Pasquinelli AE, Reinhart BJ, Slack F, et al (2000) Conservation of the sequence and temporal expression of let-7 heterochronic regulatory RNA. Nature 408: 86-89

[131] Lagos-Quintana M, Rauhut R, Lendeckel W, Tuschl T (2001) Identification of novel genes coding for small expressed RNAs. Science 294: 853-858

[132] Lee RC, Ambros V (2001) An extensive class of small RNAs in Caenorhabditis elegans. Science 294: 862-864

[133] Lau NC, Lim LP, Weinstein EG, Bartel DP (2001) An abundant class of tiny RNAs with probable regulatory roles in Caenorhabditis elegans. Science 294: 858-862

[134] Inui M, Martello G, Piccolo S (2010) MicroRNA control of signal transduction. Nat.Rev.Mol.Cell Biol. 11: 252-263

[135] Bartel DP (2009) MicroRNAs: target recognition and regulatory functions. Cell 136: 215-233

[136] Kim VN, Han J, Siomi MC (2009) Biogenesis of small RNAs in animals. Nat.Rev.Mol.Cell Biol. 10: 126-139

[137] Lee Y, Kim M, Han J, et al (2004) MicroRNA genes are transcribed by RNA polymerase II. EMBO J. 23: 4051-4060

[138] Cai X, Hagedorn CH, Cullen BR (2004) Human microRNAs are processed from capped, polyadenylated transcripts that can also function as mRNAs. RNA. 10: 1957-1966

[139] Altuvia Y, Landgraf P, Lithwick G, et al (2005) Clustering and conservation patterns of human microRNAs. Nucleic Acids Res. 33: 2697-2706

[140] Tam W (2001) Identification and characterization of human BIC, a gene on chromosome 21 that encodes a noncoding RNA. Gene 274: 157-167

[141] Calin GA, Dumitru CD, Shimizu M, et al (2002) Frequent deletions and down-regulation of micro- RNA genes miR15 and miR16 at 13q14 in chronic lymphocytic leukemia. Proc.Natl.Acad.Sci.U.S.A 99: 15524-15529

[142] Lee Y, Jeon K, Lee JT, Kim S, Kim VN (2002) MicroRNA maturation: stepwise processing and subcellular localization. EMBO J. 21: 4663-4670

[143] Lee Y, Ahn C, Han J, et al (2003) The nuclear RNase III Drosha initiates microRNA processing. Nature 425: 415-419

[144] Yeom KH, Lee Y, Han J, Suh MR, Kim VN (2006) Characterization of DGCR8/Pasha, the essential cofactor for Drosha in primary miRNA processing. Nucleic Acids Res. 34: 4622-4629

[145] Kim VN (2004) MicroRNA precursors in motion: exportin-5 mediates their nuclear export. Trends Cell Biol. 14: 156-159

[146] Filipowicz W, Bhattacharyya SN, Sonenberg N (2008) Mechanisms of post-transcriptional regulation by microRNAs: are the answers in sight? Nat.Rev.Genet. 9: 102-114

[147] Breving K, Esquela-Kerscher A (2010) The complexities of microRNA regulation: mirandering around the rules. Int.J.Biochem.Cell Biol. 42: 1316-1329

[148] Blow MJ, Grocock RJ, van DS, et al (2006) RNA editing of human microRNAs. Genome Biol. 7: R27

[149] Kawahara Y, Zinshteyn B, Sethupathy P, Iizasa H, Hatzigeorgiou AG, Nishikura K (2007) Redirection of silencing targets by adenosine-to-inosine editing of miRNAs. Science 315: 1137-1140

[150] Hutvagner G, Zamore PD (2002) A microRNA in a multiple-turnover RNAi enzyme complex. Science 297: 2056-2060

[151] Song JJ, Smith SK, Hannon GJ, Joshua-Tor L (2004) Crystal structure of Argonaute and its implications for RISC slicer activity. Science 305: 1434-1437

[152] Yekta S, Shih IH, Bartel DP (2004) MicroRNA-directed cleavage of HOXB8 mRNA. Science 304: 594-596

[153] Lewis BP, Burge CB, Bartel DP (2005) Conserved seed pairing, often flanked by adenosines, indicates that thousands of human genes are microRNA targets. Cell 120: 15-20

[154] Brennecke J, Stark A, Russell RB, Cohen SM (2005) Principles of microRNA-target recognition. PLoS.Biol. 3: e85

[155] Grimson A, Farh KK, Johnston WK, Garrett-Engele P, Lim LP, Bartel DP (2007) MicroRNA targeting specificity in mammals: determinants beyond seed pairing. Mol.Cell 27: 91-105

[156] Lytle JR, Yario TA, Steitz JA (2007) Target mRNAs are repressed as efficiently by microRNA-binding sites in the 5' UTR as in the 3' UTR. Proc.Natl.Acad.Sci.U.S.A 104: 9667-9672

[157] Kertesz M, Iovino N, Unnerstall U, Gaul U, Segal E (2007) The role of site accessibility in microRNA target recognition. Nat.Genet. 39: 1278-1284

[158] Kiriakidou M, Tan GS, Lamprinaki S, De Planell-Saguer M, Nelson PT, Mourelatos Z (2007) An mRNA m7G cap binding-like motif within human Ago2 represses translation. Cell 129: 1141-1151

[159] Parker R, Sheth U (2007) P bodies and the control of mRNA translation and degradation. Mol.Cell 25: 635-646

[160] Poy MN, Eliasson L, Krutzfeldt J, et al (2004) A pancreatic islet-specific microRNA regulates insulin secretion. Nature 432: 226-230

[161] Poy MN, Hausser J, Trajkovski M, et al (2009) miR-375 maintains normal pancreatic alpha- and beta-cell mass. Proc.Natl.Acad.Sci.U.S.A 106: 5813-5818

[162] Williams MD, Mitchell GM (2012) MicroRNAs in insulin resistance and obesity. Exp.Diabetes Res. 2012: 484696

[163] Esau C, Kang X, Peralta E, et al (2004) MicroRNA-143 regulates adipocyte differentiation. J.Biol.Chem. 279: 52361-52365

[164] Takanabe R, Ono K, Abe Y, et al (2008) Up-regulated expression of microRNA-143 in association with obesity in adipose tissue of mice fed high-fat diet. Biochem.Biophys.Res.Commun. 376: 728-732

[165] Kloting N, Berthold S, Kovacs P, et al (2009) MicroRNA expression in human omental and subcutaneous adipose tissue. PLoS.One. 4: e4699

[166] Jordan SD, Kruger M, Willmes DM, et al (2011) Obesity-induced overexpression of miRNA-143 inhibits insulin-stimulated AKT activation and impairs glucose metabolism. Nat.Cell Biol. 13: 434-446

[167] Kornfeld JW, Baitzel C, Konner AC, et al (2013) Obesity-induced overexpression of miR-802 impairs glucose metabolism through silencing of Hnf1b. Nature 494: 111-115

[168] Krutzfeldt J, Rajewsky N, Braich R, et al (2005) Silencing of microRNAs in vivo with 'antagomirs'. Nature 438: 685-689

[169] Lebovitz HE, Banerji MA (2005) Point: visceral adiposity is causally related to insulin resistance. Diabetes Care 28: 2322-2325

[170] Sims EA (2001) Are there persons who are obese, but metabolically healthy? Metabolism 50: 1499-1504

[171] Karelis AD, St-Pierre DH, Conus F, Rabasa-Lhoret R, Poehlman ET (2004) Metabolic and body composition factors in subgroups of obesity: what do we know? J.Clin.Endocrinol.Metab 89: 2569-2575

[172] Iacobellis G, Barbaro G (2008) The double role of epicardial adipose tissue as pro- and anti-inflammatory organ. Horm.Metab Res. 40: 442-445

[173] Mazurek T, Zhang L, Zalewski A, et al (2003) Human epicardial adipose tissue is a source of inflammatory mediators. Circulation 108: 2460-2466

[174] Venteclef N, Guglielmi V, Balse E, et al (2013) Human epicardial adipose tissue induces fibrosis of the atrial myocardium through the secretion of adipo-fibrokines. Eur.Heart J.

[175] Baker AR, Silva NF, Quinn DW, et al (2006) Human epicardial adipose tissue expresses a pathogenic profile of adipocytokines in patients with cardiovascular disease. Cardiovasc.Diabetol. 5: 1

[176] Eiras S, Teijeira-Fernandez E, Shamagian LG, Fernandez AL, Vazquez-Boquete A, Gonzalez-Juanatey JR (2008) Extension of coronary artery disease is associated with increased IL-6 and decreased adiponectin gene expression in epicardial adipose tissue. Cytokine 43: 174-180

[177] Bourlier V, Bouloumie A (2009) Role of macrophage tissue infiltration in obesity and insulin resistance. Diabetes Metab 35: 251-260

[178] Olefsky JM, Glass CK (2010) Macrophages, inflammation, and insulin resistance. Annu.Rev.Physiol 72: 219-246

[179] Hirata Y, Tabata M, Kurobe H, et al (2011) Coronary atherosclerosis is associated with macrophage polarization in epicardial adipose tissue. J.Am.Coll.Cardiol. 58: 248-255

[180] Hirata Y, Kurobe H, Akaike M, et al (2011) Enhanced inflammation in epicardial fat in patients with coronary artery disease. Int.Heart J. 52: 139-142

[181] Zhou Y, Wei Y, Wang L, et al (2011) Decreased adiponectin and increased inflammation expression in epicardial adipose tissue in coronary artery disease. Cardiovasc.Diabetol. 10: 2

[182] Nadler ST, Stoehr JP, Schueler KL, Tanimoto G, Yandell BS, Attie AD (2000) The expression of adipogenic genes is decreased in obesity and diabetes mellitus. Proc.Natl.Acad.Sci.U.S.A 97: 11371-11376

[183] Ye J, Gao Z, Yin J, He Q (2007) Hypoxia is a potential risk factor for chronic inflammation and adiponectin reduction in adipose tissue of ob/ob and dietary obese mice. Am.J.Physiol Endocrinol.Metab 293: E1118-E1128

[184] Salgado-Somoza A, Teijeira-Fernandez E, Fernandez AL, Gonzalez-Juanatey JR, Eiras S (2010) Proteomic analysis of epicardial and subcutaneous adipose tissue reveals differences in proteins involved in oxidative stress. Am.J.Physiol Heart Circ.Physiol 299: H202-H209

[185] Greulich S, De Wiza DH, Preilowksi S, et al (2011) Secretory products of guinea pig epicardial fat induce insulin resistance and impair primary adult rat cardiomyocyte function. J.Cell Mol.Med 15: 2399-2410

[186] Frank KF, Bolck B, Erdmann E, Schwinger RH (2003) Sarcoplasmic reticulum Ca2+-ATPase modulates cardiac contraction and relaxation. Cardiovasc.Res. 57: 20-27

[187] Bers DM, Bassani JW, Bassani RA (1996) Na-Ca exchange and Ca fluxes during contraction and relaxation in mammalian ventricular muscle. Ann.N.Y.Acad.Sci. 779: 430-442

[188] Poornima IG, Parikh P, Shannon RP (2006) Diabetic cardiomyopathy: the search for a unifying hypothesis. Circ.Res. 98: 596-605

[189] Periasamy M, Bhupathy P, Babu GJ (2008) Regulation of sarcoplasmic reticulum Ca2+ ATPase pump expression and its relevance to cardiac muscle physiology and pathology. Cardiovasc.Res. 77: 265-273

[190] Choi KM, Zhong Y, Hoit BD, et al (2002) Defective intracellular Ca(2+) signaling contributes to cardiomyopathy in Type 1 diabetic rats. Am.J.Physiol Heart Circ.Physiol 283: H1398-H1408

[191] Look C, Morano I, Ehrhart-Bornstein M, Bornstein SR, Lamounier-Zepter V (2011) Adipocyte-derived factors suppress heart contraction. Int.J.Obes.(Lond) 35: 84-90

[192] Look C, Morano I, Lamounier-Zepter V (2008) Human adipocyte-derived factors directly inhibit cardiac contraction. J.Muscle Res.Cell Motil. 29: 181-184

[193] Lamounier-Zepter V, Look C, Alvarez J, et al (2009) Adipocyte fatty acid-binding protein suppresses cardiomyocyte contraction: a new link between obesity and heart disease. Circ.Res. 105: 326-334

[194] Sell H, Eckel J, Dietze-Schroeder D (2006) Pathways leading to muscle insulin resistance--the muscle--fat connection. Arch.Physiol Biochem. 112: 105-113

[195] Palanivel R, Vu V, Park M, Fang X, Sweeney G (2008) Differential impact of adipokines derived from primary adipocytes of wild-type versus streptozotocin-induced diabetic rats on glucose and fatty acid metabolism in cardiomyocytes. J.Endocrinol. 199: 389-397

[196] Vejda S, Cranfield M, Peter B, et al (2002) Expression and dimerization of the rat activin subunits betaC and betaE: evidence for the ormation of novel activin dimers. J.Mol.Endocrinol. 28: 137-148

[197] Phillips DJ, de Kretser DM, Hedger MP (2009) Activin and related proteins in inflammation: not just interested bystanders. Cytokine Growth Factor Rev. 20: 153-164

[198] Phillips DJ, Jones KL, Scheerlinck JY, Hedger MP, de Kretser DM (2001) Evidence for activin A and follistatin involvement in the systemic inflammatory response. Mol.Cell Endocrinol. 180: 155-162

[199] Jones KL, Brauman JN, Groome NP, de Kretser DM, Phillips DJ (2000) Activin A release into the circulation is an early event in systemic inflammation and precedes the release of follistatin. Endocrinology 141: 1905-1908

[200] Abe M, Shintani Y, Eto Y, Harada K, Kosaka M, Matsumoto T (2002) Potent induction of activin A secretion from monocytes and bone marrow stromal fibroblasts by cognate interaction with activated T cells. J.Leukoc.Biol. 72: 347-352

[201] Weigert J, Neumeier M, Wanninger J, et al (2009) Adiponectin upregulates monocytic activin A but systemic levels are not altered in obesity or type 2 diabetes. Cytokine 45: 86-91

[202] Wu H, Wu M, Chen Y, Allan CA, Phillips DJ, Hedger MP (2012) Correlation between blood activin levels and clinical parameters of type 2 diabetes. Exp.Diabetes Res. 2012: 410579

[203] Andersen GO, Ueland T, Knudsen EC, et al (2011) Activin A levels are associated with abnormal glucose regulation in patients with myocardial infarction: potential counteracting effects of activin A on inflammation. Diabetes 60: 1544-1551

[204] Chen W, Greulich S, Rijzewijk l, van der Meer R, Bekaert M, Lamb H (2012) Activin A is derived from human epicardial adipose tissue and associates with decreased myocardial function and glucose metabolism in human diabetic cardiomyopathy. Diabetologia 55: 495

[205] Sulyok S, Wankell M, Alzheimer C, Werner S (2004) Activin: an important regulator of wound repair, fibrosis, and neuroprotection. Mol.Cell Endocrinol. 225: 127-132

[206] Werner S, Alzheimer C (2006) Roles of activin in tissue repair, fibrosis, and inflammatory disease. Cytokine Growth Factor Rev. 17: 157-171

[207] Matsuse T, Ikegami A, Ohga E, et al (1996) Expression of immunoreactive activin A protein in remodeling lesions associated with interstitial pulmonary fibrosis. Am.J.Pathol. 148: 707-713

[208] Hinck AP (2012) Structural studies of the TGF-betas and their receptors - insights into evolution of the TGF-beta superfamily. FEBS Lett. 586: 1860-1870

[209] Yamashita H, ten DP, Franzen P, Miyazono K, Heldin CH (1994) Formation of hetero-oligomeric complexes of type I and type II receptors for transforming growth factor-beta. J.Biol.Chem. 269: 20172-20178

[210] Wrana JL, Attisano L, Carcamo J, et al (1992) TGF beta signals through a heteromeric protein kinase receptor complex. Cell 71: 1003-1014

[211] Wrana JL, Attisano L, Wieser R, Ventura F, Massague J (1994) Mechanism of activation of the TGF-beta receptor. Nature 370: 341-347

[212] ten Dijke P, Arthur HM (2007) Extracellular control of TGFbeta signalling in vascular development and disease. Nat.Rev.Mol.Cell Biol. 8: 857-869

[213] Bakin AV, Rinehart C, Tomlinson AK, Arteaga CL (2002) p38 mitogen-activated protein kinase is required for TGFbeta-mediated fibroblastic transdifferentiation and cell migration. J.Cell Sci. 115: 3193-3206

[214] Long X, Miano JM (2011) Transforming growth factor-beta1 (TGF-beta1) utilizes distinct pathways for the transcriptional activation of microRNA 143/145 in human coronary artery smooth muscle cells. J.Biol.Chem. 286: 30119-30129

[215] Huang HM, Li YC, Chung MH (2010) Activin A induction of erythroid differentiation through MKK6-p38alpha/p38beta pathway is inhibited by follistatin. J.Cell Physiol 223: 687-694

[216] Rose BA, Force T, Wang Y (2010) Mitogen-activated protein kinase signaling in the heart: angels versus demons in a heart-breaking tale. Physiol Rev. 90: 1507-1546

[217] Nemoto S, Sheng Z, Lin A (1998) Opposing effects of Jun kinase and p38 mitogen-activated protein kinases on cardiomyocyte hypertrophy. Mol.Cell Biol. 18: 3518-3526

[218] Liang Q, Molkentin JD (2003) Redefining the roles of p38 and JNK signaling in cardiac hypertrophy: dichotomy between cultured myocytes and animal models. J.Mol.Cell Cardiol. 35: 1385-1394

[219] Zechner D, Thuerauf DJ, Hanford DS, McDonough PM, Glembotski CC (1997) A role for the p38 mitogen-activated protein kinase pathway in myocardial cell

growth, sarcomeric organization, and cardiac-specific gene expression. J.Cell Biol. 139: 115-127

[220] Wang Y, Huang S, Sah VP, et al (1998) Cardiac muscle cell hypertrophy and apoptosis induced by distinct members of the p38 mitogen-activated protein kinase family. J.Biol.Chem. 273: 2161-2168

[221] Liao P, Georgakopoulos D, Kovacs A, et al (2001) The in vivo role of p38 MAP kinases in cardiac remodeling and restrictive cardiomyopathy. Proc.Natl.Acad.Sci.U.S.A 98: 12283-12288

[222] Klein G, Schaefer A, Hilfiker-Kleiner D, et al (2005) Increased collagen deposition and diastolic dysfunction but preserved myocardial hypertrophy after pressure overload in mice lacking PKCepsilon. Circ.Res. 96: 748-755

[223] Matsumoto-Ida M, Takimoto Y, Aoyama T, Akao M, Takeda T, Kita T (2006) Activation of TGF-beta1-TAK1-p38 MAPK pathway in spared cardiomyocytes is involved in left ventricular remodeling after myocardial infarction in rats. Am.J.Physiol Heart Circ.Physiol 290: H709-H715

[224] Greulich S, Chen WJ, Maxhera B, et al (2013) Cardioprotective properties of omentin-1 in type 2 diabetes: evidence from clinical and in vitro studies. PLoS.One. 8: e59697

[225] Yang RZ, Lee MJ, Hu H, et al (2006) Identification of omentin as a novel depot-specific adipokine in human adipose tissue: possible role in modulating insulin action. Am.J.Physiol Endocrinol.Metab 290: E1253-E1261

[226] de Souza Batista CM, Yang RZ, Lee MJ, et al (2007) Omentin plasma levels and gene expression are decreased in obesity. Diabetes 56: 1655-1661

[227] Tan BK, Adya R, Farhatullah S, et al (2008) Omentin-1, a novel adipokine, is decreased in overweight insulin-resistant women with polycystic ovary syndrome: ex vivo and in vivo regulation of omentin-1 by insulin and glucose. Diabetes 57: 801-808

[228] Zhong X, Zhang HY, Tan H, et al (2011) Association of serum omentin-1 levels with coronary artery disease. Acta Pharmacol.Sin. 32: 873-878

[229] Lieb W, Zachariah JP, Xanthakis V, et al (2010) Clinical and genetic correlates of circulating angiopoietin-2 and soluble Tie-2 in the community. Circ.Cardiovasc.Genet. 3: 300-306

[230] Moss A (2013) The angiopoietin:Tie 2 interaction: A potential target for future therapies in human vascular disease. Cytokine Growth Factor Rev.

[231] Davis S, Aldrich TH, Jones PF, et al (1996) Isolation of angiopoietin-1, a ligand for the TIE2 receptor, by secretion-trap expression cloning. Cell 87: 1161-1169

[232] Kim I, Moon SO, Park SK, Chae SW, Koh GY (2001) Angiopoietin-1 reduces VEGF-stimulated leukocyte adhesion to endothelial cells by reducing ICAM-1, VCAM-1, and E-selectin expression. Circ.Res. 89: 477-479

[233] Gamble JR, Drew J, Trezise L, et al (2000) Angiopoietin-1 is an antipermeability and anti-inflammatory agent in vitro and targets cell junctions. Circ.Res. 87: 603-607

[234] Yuan HT, Khankin EV, Karumanchi SA, Parikh SM (2009) Angiopoietin 2 is a partial agonist/antagonist of Tie2 signaling in the endothelium. Mol.Cell Biol. 29: 2011-2022

[235] Mo H, Liu S, Zhou Z, et al (2010) Change of serum soluble CD14 level in newly diagnosed Type 2 diabetes and its significance. Zhong.Nan.Da.Xue.Xue.Bao.Yi.Xue.Ban. 35: 699-704

[236] Wu L, Xu DL, Deng LH, Ye TC, Deng H, Li Y (2008) Variation of serum soluble CD14 levels in patients with chronic heart failure. Nan.Fang Yi.Ke.Da.Xue.Xue.Bao. 28: 1237-1239

[237] Simmons DL, Tan S, Tenen DG, Nicholson-Weller A, Seed B (1989) Monocyte antigen CD14 is a phospholipid anchored membrane protein. Blood 73: 284-289

[238] Kirkland TN, Viriyakosol S (1998) Structure-function analysis of soluble and membrane-bound CD14. Prog.Clin.Biol.Res. 397: 79-87

[239] Frey EA, Miller DS, Jahr TG, et al (1992) Soluble CD14 participates in the response of cells to lipopolysaccharide. J.Exp.Med. 176: 1665-1671

[240] Pugin J, Schurer-Maly CC, Leturcq D, Moriarty A, Ulevitch RJ, Tobias PS (1993) Lipopolysaccharide activation of human endothelial and epithelial cells is mediated by lipopolysaccharide-binding protein and soluble CD14. Proc.Natl.Acad.Sci.U.S.A 90: 2744-2748

[241] Shah A, Mehta N, Reilly MP (2008) Adipose inflammation, insulin resistance, and cardiovascular disease. JPEN J.Parenter.Enteral Nutr. 32: 638-644

[242] DeFronzo RA (2010) Insulin resistance, lipotoxicity, type 2 diabetes and atherosclerosis: the missing links. The Claude Bernard Lecture 2009. Diabetologia 53: 1270-1287

[243] Hotamisligil GS, Arner P, Caro JF, Atkinson RL, Spiegelman BM (1995) Increased adipose tissue expression of tumor necrosis factor-alpha in human obesity and insulin resistance. J.Clin.Invest 95: 2409-2415

[244] Winkler G, Salamon F, Harmos G, et al (1998) Elevated serum tumor necrosis factor-alpha concentrations and bioactivity in Type 2 diabetics and patients with android type obesity. Diabetes Res.Clin.Pract. 42: 169-174

[245] Rask-Madsen C, Li Q, Freund B, et al (2010) Loss of insulin signaling in vascular endothelial cells accelerates atherosclerosis in apolipoprotein E null mice. Cell Metab 11: 379-389

[246] Bornfeldt KE, Tabas I (2011) Insulin resistance, hyperglycemia, and atherosclerosis. Cell Metab 14: 575-585

[247] Lamers D, Schlich R, Greulich S, Sasson S, Sell H, Eckel J (2011) Oleic acid and adipokines synergize in inducing proliferation and inflammatory signalling in human vascular smooth muscle cells. J.Cell Mol.Med. 15: 1177-1188

[248] Fernandez-Hernando C, Ackah E, Yu J, et al (2007) Loss of Akt1 leads to severe atherosclerosis and occlusive coronary artery disease. Cell Metab 6: 446-457

[249] Charo IF, Taubman MB (2004) Chemokines in the pathogenesis of vascular disease. Circ.Res. 95: 858-866

[250] Nelken NA, Coughlin SR, Gordon D, Wilcox JN (1991) Monocyte chemoattractant protein-1 in human atheromatous plaques. J.Clin.Invest 88: 1121-1127

[251] Cushing SD, Berliner JA, Valente AJ, et al (1990) Minimally modified low density lipoprotein induces monocyte chemotactic protein 1 in human endothelial cells and smooth muscle cells. Proc.Natl.Acad.Sci.U.S.A 87: 5134-5138

[252] Alvarez-Garcia I, Miska EA (2005) MicroRNA functions in animal development and human disease. Development 132: 4653-4662

[253] Xie H, Lim B, Lodish HF (2009) MicroRNAs induced during adipogenesis that accelerate fat cell development are downregulated in obesity. Diabetes 58: 1050-1057

[254] Pritchard CC, Cheng HH, Tewari M (2012) MicroRNA profiling: approaches and considerations. Nat.Rev.Genet. 13: 358-369

[255] Dorn GW (2012) Decoding the cardiac message: the 2011 Thomas W. Smith Memorial Lecture. Circ.Res. 110: 755-763

[256] van RE, Sutherland LB, Liu N, et al (2006) A signature pattern of stress-responsive microRNAs that can evoke cardiac hypertrophy and heart failure. Proc.Natl.Acad.Sci.U.S.A 103: 18255-18260

[257] Thum T, Galuppo P, Wolf C, et al (2007) MicroRNAs in the human heart: a clue to fetal gene reprogramming in heart failure. Circulation 116: 258-267

[258] Elzenaar I, Pinto YM, van Oort RJ (2013) MicroRNAs in Heart Failure: New targets in disease management. Clin.Pharmacol.Ther.

[259] Thum T, Gross C, Fiedler J, et al (2008) MicroRNA-21 contributes to myocardial disease by stimulating MAP kinase signalling in fibroblasts. Nature 456: 980-984

[260] Wang J, Gao Y, Ma M, et al (2013) Effect of miR-21 on Renal Fibrosis by Regulating MMP-9 and TIMP1 in kk-ay Diabetic Nephropathy Mice. Cell Biochem.Biophys.

[261] Davis BN, Hilyard AC, Lagna G, Hata A (2008) SMAD proteins control DROSHA-mediated microRNA maturation. Nature 454: 56-61

[262] Zhu H, Luo H, Li Y, et al (2013) MicroRNA-21 in Scleroderma Fibrosis and its Function in TGF-beta- Regulated Fibrosis-Related Genes Expression. J.Clin.Immunol. 33: 1100-1109

[263] Ikeda S, Kong SW, Lu J, et al (2007) Altered microRNA expression in human heart disease. Physiol Genomics 31: 367-373

[264] Matkovich SJ, Van Booven DJ, Youker KA, et al (2009) Reciprocal regulation of myocardial microRNAs and messenger RNA in human cardiomyopathy and reversal of the microRNA signature by biomechanical support. Circulation 119: 1263-1271

[265] Naga Prasad SV, Duan ZH, Gupta MK, et al (2009) Unique microRNA profile in end-stage heart failure indicates alterations in specific cardiovascular signaling networks. J.Biol.Chem. 284: 27487-27499

[266] Menghini R, Casagrande V, Cardellini M, et al (2009) MicroRNA 217 modulates endothelial cell senescence via silent information regulator 1. Circulation 120: 1524-1532

[267] Stein S, Lohmann C, Schafer N, et al (2010) SIRT1 decreases Lox-1-mediated foam cell formation in atherogenesis. Eur.Heart J. 31: 2301-2309

[268] Winnik S, Stein S, Matter CM (2012) SIRT1 - an anti-inflammatory pathway at the crossroads between metabolic disease and atherosclerosis. Curr.Vasc.Pharmacol. 10: 693-696

[269] Toniolo A, Warden EA, Nassi A, Cignarella A, Bolego C (2013) Regulation of SIRT1 in Vascular Smooth Muscle Cells from Streptozotocin-Diabetic Rats. PLoS.One. 8: e65666

[270] Sandberg R, Neilson JR, Sarma A, Sharp PA, Burge CB (2008) Proliferating cells express mRNAs with shortened 3' untranslated regions and fewer microRNA target sites. Science 320: 1643-1647

[271] Bhattacharyya SN, Habermacher R, Martine U, Closs EI, Filipowicz W (2006) Stress-induced reversal of microRNA repression and mRNA P-body localization in human cells. Cold Spring Harb.Symp.Quant.Biol. 71: 513-521

[272] Mishima Y, Giraldez AJ, Takeda Y, et al (2006) Differential regulation of germline mRNAs in soma and germ cells by zebrafish miR-430. Curr.Biol. 16: 2135-2142

[273] Kopp F, Schnoedt M, Haase R, Wagner E, Roidl A, Ogris M (2013) De-targeting by miR-143 decreases unwanted transgene expression in non-tumorigenic cells. Gene Ther.

[274] Iio A, Nakagawa Y, Hirata I, Naoe T, Akao Y (2010) Identification of non-coding RNAs embracing microRNA-143/145 cluster. Mol.Cancer 9: 136

[275] Sempere LF, Freemantle S, Pitha-Rowe I, Moss E, Dmitrovsky E, Ambros V (2004) Expression profiling of mammalian microRNAs uncovers a subset of brain-

expressed microRNAs with possible roles in murine and human neuronal differentiation. Genome Biol. 5: R13

[276] Elia L, Quintavalle M, Zhang J, et al (2009) The knockout of miR-143 and -145 alters smooth muscle cell maintenance and vascular homeostasis in mice: correlates with human disease. Cell Death.Differ. 16: 1590-1598

[277] Akao Y, Nakagawa Y, Naoe T (2006) MicroRNAs 143 and 145 are possible common onco-microRNAs in human cancers. Oncol.Rep. 16: 845-850

[278] Akao Y, Nakagawa Y, Naoe T (2007) MicroRNA-143 and -145 in colon cancer. DNA Cell Biol. 26: 311-320

[279] Akao Y, Nakagawa Y, Kitade Y, Kinoshita T, Naoe T (2007) Downregulation of microRNAs-143 and -145 in B-cell malignancies. Cancer Sci. 98: 1914-1920

[280] Takagi T, Iio A, Nakagawa Y, Naoe T, Tanigawa N, Akao Y (2009) Decreased expression of microRNA-143 and -145 in human gastric cancers. Oncology 77: 12-21

[281] Lin T, Dong W, Huang J, et al (2009) MicroRNA-143 as a tumor suppressor for bladder cancer. J.Urol. 181: 1372-1380

[282] Wang X, Tang S, Le SY, et al (2008) Aberrant expression of oncogenic and tumor-suppressive microRNAs in cervical cancer is required for cancer cell growth. PLoS.One. 3: e2557

[283] Michael MZ, O' Connor SM, van Holst Pellekaan NG, Young GP, James RJ (2003) Reduced accumulation of specific microRNAs in colorectal neoplasia. Mol.Cancer Res. 1: 882-891

[284] Wang CJ, Zhou ZG, Wang L, et al (2009) Clinicopathological significance of microRNA-31, -143 and -145 expression in colorectal cancer. Dis.Markers 26: 27-34

[285] Chen X, Guo X, Zhang H, et al (2009) Role of miR-143 targeting KRAS in colorectal tumorigenesis. Oncogene 28: 1385-1392

[286] Sachdeva M, Zhu S, Wu F, et al (2009) p53 represses c-Myc through induction of the tumor suppressor miR-145. Proc.Natl.Acad.Sci.U.S.A 106: 3207-3212

[287] Akao Y, Nakagawa Y, Iio A, Naoe T (2009) Role of microRNA-143 in Fas-mediated apoptosis in human T-cell leukemia Jurkat cells. Leuk.Res. 33: 1530-1538

[288] Shi B, Sepp-Lorenzino L, Prisco M, Linsley P, deAngelis T, Baserga R (2007) Micro RNA 145 targets the insulin receptor substrate-1 and inhibits the growth of colon cancer cells. J.Biol.Chem. 282: 32582-32590

[289] Cordes KR, Sheehy NT, White MP, et al (2009) miR-145 and miR-143 regulate smooth muscle cell fate and plasticity. Nature 460: 705-710

[290] Pulakat L, Aroor AR, Gul R, Sowers JR (2012) Cardiac insulin resistance and microRNA modulators. Exp.Diabetes Res. 2012: 654904

[291] He J, Qian X, Carpenter R, et al (2013) Repression of miR-143 Mediates Cr (VI)-Induced Tumor Angiogenesis via IGF-IR/IRS1/ERK/IL-8 Pathway. Toxicol.Sci. 134: 26-38

[292] Pekow JR, Dougherty U, Mustafi R, et al (2012) miR-143 and miR-145 are downregulated in ulcerative colitis: putative regulators of inflammation and protooncogenes. Inflamm.Bowel.Dis. 18: 94-100

[293] Rangrez AY, Massy ZA, Metzinger-Le M, V, Metzinger L (2011) miR-143 and miR-145: molecular keys to switch the phenotype of vascular smooth muscle cells. Circ.Cardiovasc.Genet. 4: 197-205

[294] Xin M, Small EM, Sutherland LB, et al (2009) MicroRNAs miR-143 and miR-145 modulate cytoskeletal dynamics and responsiveness of smooth muscle cells to injury. Genes Dev. 23: 2166-2178

[295] Rensen SS, Doevendans PA, van Eys GJ (2007) Regulation and characteristics of vascular smooth muscle cell phenotypic diversity. Neth.Heart J. 15: 100-108

[296] Cheng Y, Liu X, Yang J, et al (2009) MicroRNA-145, a novel smooth muscle cell phenotypic marker and modulator, controls vascular neointimal lesion formation. Circ.Res. 105: 158-166

[297] Boettger T, Beetz N, Kostin S, et al (2009) Acquisition of the contractile phenotype by murine arterial smooth muscle cells depends on the Mir143/145 gene cluster. J.Clin.Invest 119: 2634-2647

[298] Zhao S, Liu H, Liu Y, et al (2013) miR-143 inhibits glycolysis and depletes stemness of glioblastoma stem-like cells. Cancer Lett. 333: 253-260

[299] Jaworski CJ, Moreira E, Li A, Lee R, Rodriguez IR (2001) A family of 12 human genes containing oxysterol-binding domains. Genomics 78: 185-196

[300] Yan D, Mayranpaa MI, Wong J, et al (2008) OSBP-related protein 8 (ORP8) suppresses ABCA1 expression and cholesterol efflux from macrophages. J.Biol.Chem. 283: 332-340

[301] Wang PY, Weng J, Anderson RG (2005) OSBP is a cholesterol-regulated scaffolding protein in control of ERK 1/2 activation. Science 307: 1472-1476

[302] Perry RJ, Ridgway ND (2006) Oxysterol-binding protein and vesicle-associated membrane protein-associated protein are required for sterol-dependent activation of the ceramide transport protein. Mol.Biol.Cell 17: 2604-2616

[303] Weber-Boyvat M, Zhong W, Yan D, Olkkonen VM (2013) Oxysterol-binding proteins: Functions in cell regulation beyond lipid metabolism. Biochem.Pharmacol.

[304] Toulmay A, Prinz WA (2011) Lipid transfer and signaling at organelle contact sites: the tip of the iceberg. Curr.Opin.Cell Biol. 23: 458-463

[305] Schulz TA, Choi MG, Raychaudhuri S, et al (2009) Lipid-regulated sterol transfer between closely apposed membranes by oxysterol-binding protein homologues. J.Cell Biol. 187: 889-903

[306] Stefan CJ, Manford AG, Baird D, Yamada-Hanff J, Mao Y, Emr SD (2011) Osh proteins regulate phosphoinositide metabolism at ER-plasma membrane contact sites. Cell 144: 389-401

[307] Baird D, Stefan C, Audhya A, Weys S, Emr SD (2008) Assembly of the PtdIns 4-kinase Stt4 complex at the plasma membrane requires Ypp1 and Efr3. J.Cell Biol. 183: 1061-1074

[308] Foti M, Audhya A, Emr SD (2001) Sac1 lipid phosphatase and Stt4 phosphatidylinositol 4-kinase regulate a pool of phosphatidylinositol 4-phosphate that functions in the control of the actin cytoskeleton and vacuole morphology. Mol.Biol.Cell 12: 2396-2411

[309] Flint AJ, Tiganis T, Barford D, Tonks NK (1997) Development of "substrate-trapping" mutants to identify physiological substrates of protein tyrosine phosphatases. Proc.Natl.Acad.Sci.U.S.A 94: 1680-1685

[310] Anderie I, Schulz I, Schmid A (2007) Direct interaction between ER membrane-bound PTP1B and its plasma membrane-anchored targets. Cell Signal. 19: 582-592

[311] de LC, Greco A, Fiorentino TV, Mannino GC, Hribal ML (2013) Variants of insulin-signaling inhibitor genes in type 2 diabetes and related metabolic abnormalities. Int.J.Genomics 2013: 376454

[312] Vakili S, Ebrahimi SS, Sadeghi A, et al (2012) Hydrodynamic-based delivery of PTP1B shRNA reduces plasma glucose levels in diabetic mice. Mol.Med.Rep.

[313] Nagao S, Murao K, Imachi H, et al (2006) Platelet derived growth factor regulates ABCA1 expression in vascular smooth muscle cells. FEBS Lett. 580: 4371-4376

[314] Oliveira-Carvalho V, Carvalho VO, Bocchi EA (2013) The emerging role of miR-208a in the heart. DNA Cell Biol. 32: 8-12

[315] Callis TE, Pandya K, Seok HY, et al (2009) MicroRNA-208a is a regulator of cardiac hypertrophy and conduction in mice. J.Clin.Invest 119: 2772-2786

[316] van RE, Quiat D, Johnson BA, et al (2009) A family of microRNAs encoded by myosin genes governs myosin expression and muscle performance. Dev.Cell 17: 662-673

[317] Weiss A, Leinwand LA (1996) The mammalian myosin heavy chain gene family. Annu.Rev.Cell Dev.Biol. 12: 417-439

[318] VanBuren P, Harris DE, Alpert NR, Warshaw DM (1995) Cardiac V1 and V3 myosins differ in their hydrolytic and mechanical activities in vitro. Circ.Res. 77: 439-444

[319] Gupta MP (2007) Factors controlling cardiac myosin-isoform shift during hypertrophy and heart failure. J.Mol.Cell Cardiol. 43: 388-403

[320] Krenz M, Robbins J (2004) Impact of beta-myosin heavy chain expression on cardiac function during stress. J.Am.Coll.Cardiol. 44: 2390-2397

[321] Rupp H, Elimban V, Dhalla NS (1989) Diabetes-like action of intermittent fasting on sarcoplasmic reticulum Ca2+-pump ATPase and myosin isoenzymes can be prevented by sucrose. Biochem.Biophys.Res.Commun. 164: 319-325

[322] van RE, Sutherland LB, Qi X, Richardson JA, Hill J, Olson EN (2007) Control of stress-dependent cardiac growth and gene expression by a microRNA. Science 316: 575-579

[323] Satoh M, Minami Y, Takahashi Y, Tabuchi T, Nakamura M (2010) Expression of microRNA-208 is associated with adverse clinical outcomes in human dilated cardiomyopathy. J.Card Fail. 16: 404-410

[324] Fichtlscherer S, De RS, Fox H, et al (2010) Circulating microRNAs in patients with coronary artery disease. Circ.Res. 107: 677-684

[325] Grueter CE, van RE, Johnson BA, et al (2012) A cardiac microRNA governs systemic energy homeostasis by regulation of MED13. Cell 149: 671-683

[326] Montgomery RL, Hullinger TG, Semus HM, et al (2011) Therapeutic inhibition of miR-208a improves cardiac function and survival during heart failure. Circulation 124: 1537-1547

Danksagung

Bei meinem Doktorvater Herrn Prof. Hadi Al-Hasani möchte ich mich für seine Tipps und Diskussionsbeiträge bedanken sowie für die Begutachtung dieser Arbeit.

Herrn Prof. Michael Feldbrügge danke ich für die Übernahme des Korreferats und das Interesse an meiner Arbeit.

Ein besonderes Wort der Dankbarkeit gilt meiner Betreuerin Frau Prof. Margriet Ouwens für die Überlassung des interessanten und herausfordernden Themas, sowie für das Korrekturlesen dieser Arbeit. Besonders möchte ich mich aber auch für die Freiheiten bedanken, die für meine Entwicklung zum eigenverantwortlichen Denken und Arbeiten unerlässlich waren.

Auch möchte ich mich bei allen aktuellen und ehemaligen Mitgliedern der AG Biochemie sowie der Paul-Langerhans-Gruppe bedanken, die mich während meiner Arbeit begleitet haben. Insbesondere danke ich Annika, die für den letzten Schliff dieser Arbeit gesorgt hat.

Bei Daniella und Heidi bedanke ich mich für die tatkräftige Unterstützung im Laboralltag. Ohne die zahllosen PCRs und unendlichen aber immer amüsanten Stunden zum Wochenbeginn im Tierlabor wäre diese Arbeit nicht möglich gewesen. Durch eure offene und stets hilfsbereite Art haltet ihr den Laden zusammen!

Allen weiteren Mitgliedern der AG Ouwens sei an dieser Stelle gedankt. Sabrina, dir danke ich für die gute und erfolgreiche Zusammenarbeit und dafür, dass du mich beim „Schnippeln“ stets bei Laune gehalten hast. „Dönerstag“ solltest du dir patentieren lassen! Ein ganz besonders großes Dankeschön geht an die Western Blot-Queen Claudia, die meine Tischnachbarin, Leidensgenossin und großer Sheldon-Fan ist. Vielen Dank für die zahlreichen Diskussion und Ideen, die bei der Verwirklichung meiner Arbeit sehr hilfreich waren. Auch danke ich dir für deine Freundschaft, deine aufmunternde Art und dafür, dass ich dich beim Squash immer besiegen durfte.

Meiner Familie gilt ein besonders großes Dankeschön! Meinen Eltern danke ich von ganzem Herzen! Ohne eure ununterbrochene und aufrichtige Unterstützung in allen Bereichen meines Lebens wäre das Alles nicht möglich gewesen. Vielen Dank, dass ihr mir meinen Weg geebnet habt und mich zu dem gemacht habt was ich bin. Vielen, vielen Dank auch an meine Geschwister, meinen Bruder Carsten und meine Schwester Sarah. Schön, dass ihr immer für mich da seid und danke, dass es euch gibt.

Meine letzten tausend Dankeschöns gehen an meine Katharina. Ohne dich wäre diese Arbeit wohl nie in dieser Art und Weise zustande gekommen. Selbst an Tagen an denen es nicht so gut lief hast du mich wieder aufgebaut und mich an das Wesentliche des Lebens erinnert. Für deinen Rückhalt und dein Verständnis, deine Geduld und deine Art mir Mut zuzusprechen bin ich dir unendlich und für immer dankbar.

Eidesstattliche Erklärung

Ich versichere an Eides Statt, dass die Dissertation von mir selbständig und ohne unzulässige fremde Hilfe unter Beachtung der „Grundsätze zur Sicherung guter wissenschaftlicher Praxis an der Heinrich-Heine-Universität Düsseldorf“ erstellt worden ist. Die Dissertation wurde in der vorgelegten oder in ähnlicher Form noch bei keiner anderen Institution eingereicht. Ich habe bisher keine erfolglosen Promotionsversuche unternommen.

Düsseldorf, den 25.09.2013

Marcel Blumensatt